UNIVERSIDADE FEDERAL DO CEARÁ
CENTRO DE CIÊNCIAS
PROGRAMA DE PÓS-GRADUAÇÃO EM GEOLOGIA

FRANCISCO IRINEUDO BEZERRA DE OLIVEIRA

ASPECTOS TAFONÔMICOS E PALEOECOLÓGICOS DAS PALEOENTOMOFAUNAE DAS FORMAÇÕES CRATO E FONSECA

FORTALEZA
2023

FRANCISCO IRINEUDO BEZERRA DE OLIVEIRA

ASPECTOS TAFONÔMICOS E PALEOECOLÓGICOS DAS PALEOENTOMOFAUNAE DAS FORMAÇÕES CRATO E FONSECA

Tese apresentada ao Programa de Pós-Graduação em Geologia da Universidade Federal do Ceará, como requisito parcial à obtenção do título de doutor em Geologia.

Orientador: Prof. Dr. Márcio Mendes.

FORTALEZA
2023

Dados Internacionais de Catalogação na Publicação
Universidade Federal do Ceará
Sistema de Bibliotecas
Gerada automaticamente pelo módulo Catalog, mediante os dados fornecidos pelo(a) autor(a)

O47a Oliveira, Francisco Irineudo Bezerra de.
Aspectos tafonômicos e paleoecológicos das paleoentomofaunae das formações Crato e Fonseca / Francisco Irineudo Bezerra de Oliveira. – 2023.
231 f. : il. color.

Tese (doutorado) – Universidade Federal do Ceará, Centro de Ciências, Programa de Pós-Graduação em Geologia, Fortaleza, 2023.
Orientação: Prof. Dr. Márcio Mendes.

1. Querogenização. 2. Piritização. 3. Telodiagênese. 4. Lagerstätten. I. Título.

CDD 551

FRANCISCO IRINEUDO BEZERRA DE OLIVEIRA

ASPECTOS TAFONÔMICOS E PALEOECOLÓGICOS DAS PALEOENTOMOFAUNAE DAS FORMAÇÕES CRATO E FONSECA

Tese apresentada ao Programa de Pós-Graduação em Geologia da Universidade Federal do Ceará, como requisito parcial à obtenção do título de doutor em Geologia.

Aprovada em: 29/09/2023.

BANCA EXAMINADORA

_____
Prof. Dr. Márcio Mendes (Orientador)
Universidade Federal do Ceará (UFC)

_____
Prof. Dr. Wellington Ferreira da Silva Filho
Universidade Federal do Ceará (UFC)

_____
Prof. Dr. Daniel Rodrigues do Nascimento Júnior
Universidade Federal do Ceará (UFC)

_____
Prof. Dr. José de Araújo Nogueira Neto
Universidade Federal de Goiás (UFG)

_____
Prof. Dr. João Kerensky Rufino Moreira
Secretária Municipal de Fortaleza (SME)

_____
Prof. Dr. Felipe Antônio de Lima Toledo
Universidade de São Paulo (USP)

A todos que pretenderam, mas não tiveram oportunidade.

AGRADECIMENTOS

Este trabalho teve o apoio da Coordenação de Aperfeiçoamento de Pessoal de Nível Superior (CAPES), que concedeu suporte financeiro por meio de uma bolsa de doutoramento, processo 88882.454892/2019-01.

. Sou profundamente grato ao meu orientador, professor Dr. Márcio Mendes. Muito desse trabalho, e do que aprendi ao longo dos anos, não teria acontecido sem os seus ensinamentos, seu apoio e sua dedicação como mentor.

Como é para quase todo trabalho científico, os resultados apresentados aqui são frutos de uma intensa e produtiva colaboração científica que eu tive a oportunidade de realizar com diversos ótimos cientistas. Particularmente, essa pesquisa não teria logrado nenhum êxito sem a contribuição dos professores Dr. João Hermínio da Silva (Física/UFCA); Dr. Paulo de Tarso Cavalcante Freire (Dpto de Física/UFC) e Dr. Alexandre Rocha Paschoal (Dpto de Física/UFC). Estes colaboradores sempre ajudaram na elaboração das hipóteses e discussões propostas, além de fornecerem a infraestrutura necessária para as análises apresentadas no corpo deste trabalho.

Também é crucial demonstrar um franco agradecimento pela proeminente colaboração da Dra Mónica Morayma Solórzano-Kraemer (*Senckenberg Research Institute*), cujo auxílio, incentivo e criticismo foram basilares para as interpretações pronunciadas aqui. Ao Dr. Peter Vršanský (*Slovak Academy of Sciences*) por gentilmente compartilhar seu conhecimento sobre Sistemática.

Meus sinceros agradecimentos a todos os professores e colaboradores do Programa de Pós-Graduação em Geologia (PPGG) da UFC que dividiram parte de seu conhecimento comigo, seja dentro de uma sala de aula ou fora dela. Em especial, gostaria de destacar o professor Dr. Daniel Costa Fortier (PPGG/UFPI) por cortesmente me incentivar a estudar Evolução e o professor Dr. Roberto Iannuzzi (PPGG/UFRGS), cujo ensinamento mudou minha visão sobre ciência.

Gostaria de demonstrar minha gratidão a todos aqueles que ajudaram direta ou indiretamente, na obtenção, tratamento ou discussão dos dados discutidos nesta tese, a mencionar os MSc. Joel Pedrosa Sousa (PPGG/UFC) e MSc. Inácio Ocinai de Lima Neto (PPGG/UFC) pelo suporte na fase de preparação das amostras. Os MSc. Wemerson José Alencar (Física/UFC) e MSc. José Avelar de Sousa da Silva (Física/UFC) pela contribuição na obtenção de dados espectroscopia Raman e Infravermelho. O Dr. Enzo Victorino Hernández Agressot (Instituto Federal do Paraná) e a Dra Anupama Gosh (PUC-Rio) pelo

auxílio na aquisição dos dados de MEV-EDS. A Dra Charlotte Willians por atenciosamente revisar os textos escritos em língua inglesa.

Agradeço minha família, meus pais Antônio Nilo e Maria Ivete pelo apoio e ensinamentos fundamentais na construção de meu caráter. Em especial, ao meu irmão Ivanilo Bezerra pelos constantes incentivos e acompanhamentos ao longo da vida.

Não menos importante, gostaria de agradecer os amigos de caminhada pelas discussões estimulantes, companherismo e momentos de descontração: MSc. Saulo Limaverde Saraiva (Biologia/UFC); MSc. Vitor Azevedo (Geology/Trinity College); MSc. Dayme Cavalcante (Geologia/UFC); MSc. Leonardo Corecco (Geologia/UFRGS); MSc. Iure Teixeira (Geociências/USP); MSc. Mateus Miranda (Geologia/Unicamp); Dr. Felipe Holanda dos Santos (Geologia/UFC); MSc. Milagros Cardona (Geologia/UFC); MSc. Aerson Barreto Jr (Geologia/UFPE); Dr. Felipe Peixoto (Geografia/UERN); BSc. Gabrielle de Melo Alberto (Biologia/UECE); MSc. Wemerson Alencar (Física/UFC), e muitos outros que, mesmo não estando citados, compartilharam dessa jornada.

Agradeço as instituições que forneceram a infraestrutura necessária para o desenvolvimento deste trabalho, incluindo: o Laboratório de Paleontologia (LP) do Departamento de Geologia da UFC; a Central Analítica da UFC/CT-INFRA/MCTI-SISANO/Pró-equipamentos CAPES pelo suporte nas análises de Microscopia Eletrônica de Varredura (MEV). Agradeço imensamente o apoio do Laboratório de Microscopia e Espectroscopia Vibracional (Levm) do Departamento de Física da UFC pelas análises espectroscópicas. Agradeço também o laboratório de laminação (LAMIN) e Preparação de Amostras (LPA) do Departamento de Geologia da UFC.

"*I am, somehow, less interested in the weight and convolutions of Einstein's brain than in the near certainty that people of equal talent have lived and died in cotton fields and sweatshops*." (Stephen Jay Gould, The Panda's Thumb: More Reflections in Natural History, 1980).

RESUMO

Nos últimos anos, o avanço da tecnologia tem disponibilizado uma variedade de ferramentas analíticas que permitem os geocientistas investigarem, de forma detalhada, o passado do nosso planeta. No centro desse processo, a Paleobiologia, a Paleoecologia e a Tafonomia são disciplinas que têm se beneficiado de métodos, desenvolvidos para outros fins, para realizarem descobertas cada vez mais minuciosas relativas à história biológica e geológica de organismos e ecossistemas pretéritos. Neste contexto, os depósitos do tipo *Lagerstätten* estiveram no núcleo das discussões referentes aos inúmeros achados envolvendo a preservação excepcional de fósseis com tecidos moles. O objetivo desta tese é lançar luz sobre os processos tafonômicos e paleoecológicos envolvidos na preservação das paleoentomofaunas das formações Crato (Cretáceo Inferior do Ceará) e Fonseca (Eoceno-Oligoceno de Minas Gerais). Técnicas como Microscopia Eletrônica de Varredura (MEV), Espectroscopia por Energia Dispersiva de Raios-X (EDS), Espectroscopia Raman por transformada de Fourier (FT Raman), Espectroscopia por Infravermelho próximo por transformada de Fourier (FTIR) e diversos procedimentos estatísticos foram empregados a fim de caracterizar o grau de articulação dos indivíduos, a fidelidade de preservação dos tecidos cuticulares, a mineralogia e a composição química dos espécimes em escalas macro e micrométricas. Os resultados aqui apresentados detêm o primeiro estudo tafonômico realizado na paleoentomofauna da Formação Fonseca. Ao contrário da ainda pouco conhecida paleoentomofauna da Formação Fonseca, a paleoentomofauna da Formação Crato é mundialmente famosa pela beleza e abundância de seus fósseis. Aqui, atestou-se que os insetos piritizados (mineralizados) da Fm. Crato aparecem com um grau de preservação maior do que os insetos querogenizados. Tal achado difere dos dados de pesquisas similares disponíveis na literatura, pois as carcaças piritizadas são caracterizadas, em geral, por passarem longos períodos na zona de respiração bacteriana anaeróbica (Redução de Sulfato) que é menos favorável a preservação fiel de tecidos lábeis do que a zona de metanogênese. Os insetos da Fm. Crato apresentam diferentes aspectos referentes a fatores pós-diagenéticos, sendo os insetos mineralizados mais afetados por processos telodiagenéticos. Verificou-se que os insetos mineralizados menos articulados são preferencialmente preservados por goethita, enquanto que os insetos mineralizados mais articulados são preferenciamente preservados por hematita. Neste estudo, foram analisados 1.135 insetos fósseis, incluídos em 55 famílias diferentes, oriundos dos calcários claros e azulados da Fm. Crato, a fim de mensurar sua relevância ecológica (abundância, distribuição) e bioestratinômica (interação com o

paleoambiente). A análise sugere maior incidência de insetos aquáticos e semiaquáticos preservados em posição dorsoventral nos calcários claros. Em contraste, os calcários azulados registram essencialmente insetos terrestres, proporcionalmente mais desarticulados do que os indivíduos preservados nos calcários claros, indicando que esses insetos sofreram maior grau de retrabalhamento na fase bioestratinômica. Comparada com outras paleoentomofaunas do Cretáceo Inferior, a literatura taxonômica da paleoentomofauna da Fm. Crato apresenta diferenças bem marcantes. Enquanto outras paleoentomofaunas preservadas nas formações Yixian (China) e Zaza (Rússia) são dominadas por espécies de Coleoptera e Hymenoptera, a Fm. Crato registra relativamente menos espécies desses grupos e é relativamente mais rica em espécies de Paleoptera (Odonata).

Palavras-chave: querogenização; piritização; telodiagênese; *lagerstätten*; Eoceno-Oligoceno; Aptiano.

ABSTRACT

In the past few years, the development of technology has made a variety of analytical tools available. Geoscientists have taken advantage of these innovations to expand our knowledge of the planet's past. At the core of this progress, disciplines such as Paleobiology, Paleoecology and Taphonomy have benefited from these advances to conceive new discoveries regarding the biological and geological history of past organisms and ecosystems. In this context, *Lagerstätten*-type deposits played a prominent role in discussions regarding new findings involving the preservation of soft tissues in the fossil record. The aim of this thesis is to shed light on the taphonomic and paleoecological processes involved in the preservation of paleoenthomofauna from the Crato (Lower Cretaceous of Ceará) and Fonseca (Eocene-Oligocene of Minas Gerais) formations. For this purpose, a combination of techniques were employed such as Scanning Electron Microscopy (SEM), Energy Dispersive X-Ray Spectroscopy (EDS), Fourier Transform Raman Spectroscopy (FT Raman), Near Infrared Spectroscopy by Transform Fourier (FTIR) and various statistical procedures. These tools were used to characterize the articulation of the individuals, the preservation fidelity of the cuticular tissues, the mineralogy and the chemical composition of the specimens in macro and micrometric scales. Here, the results represent the first taphonomic study carried out on the paleoentomofauna of the Fonseca Formation. In contrast to the still little-known paleoentomofauna of the Fonseca Formation, the paleoentomofauna of the Crato Formation is world famous for the beauty and abundance of its fossils. This document attested that the pyritized (mineralized) insects of Crato Fm. appear with a higher degree of preservation than the kerogenized ones. This data differs from other similar studies available in the literature. In general, pyritized carcasses spend much more time within the zone of anaerobic bacterial respiration (sulfate reduction) which is less favorable for preservation of labile tissues than the methanogenesis zone. Crato insects show different aspects related to post-diagenetic aspects since mineralized insects are more affected by telodiagenetic processes. Mineralized and partially articulated insects are preferentially preserved by goethite. In contrast, mineralized and articulated insects are preferentially preserved by hematite. In this study, 1.135 insects from the pale and bluish limestones of Crato Fm. were analyzed, included in 55 different families, to measure their ecological (abundance, distribution) and biostratinomic (interaction with the paleoenvironment) relevance. This study shows a higher number of aquatic and semi-aquatic insects preserved in a dorsoventral position in pale limestones. In contrast, the bluish limestones mostly record terrestrial insects, where individuals are proportionately more

disarticulated than the insects preserved in pale limestones. This finding indicates that insects from bluish limestones underwent more rework in the biostratinomic phase. Compared to other Early Cretaceous paleoentomofaunae, the taxonomic literature for Crato paleoentomofauna is markedly different. While other preserved paleoentomofaunae in the Yixian (China) and Zaza (Russia) formations are dominated by Coleoptera and Hymenoptera species, Crato Fm. records relatively fewer species from these groups and is relatively richer in Paleoptera (Odonata) species.

Keywords: kerogenization; pyritization; telodiagenesis; *lagerstätten*; Eocene-Oligocene; Aptian.

LISTA DE FIGURAS

SUMÁRIO

1 INTRODUÇÃO GERAL

1.1 Bacias do Fonseca e Araripe

1.1.1 Localização

A Bacia de Fonseca encontra-se localizada na porção centro-leste do estado de Minas Gerais (Figura 1), sudeste brasileiro, situada a leste da região denominada Quadrilátero Ferrífero próxima à Serra do Caraça. As localidades fossilíferas afloram próximas à drenagem de córregos subsidiários do Rio Piracicaba, distante 2 km do distrito de Fonseca (43°15´–43°20´ O e 20°09´–20°10´ S) que pertence ao município de Alvinópolis, em uma área rural privada pertencente à empresa de reflorestamento industrial de eucaliptos Cenibra (Nipo Brasileira Cenibra Celulose S.A).

Figura 1 – Localização da área de estudo

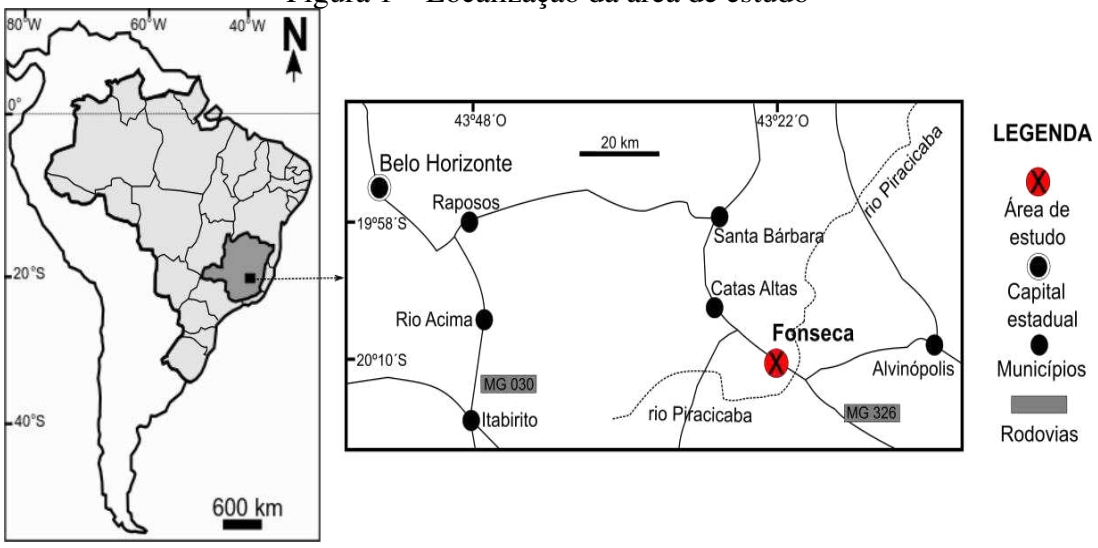

Fonte: o autor.

A Bacia do Araripe fica localizada no interior do Nordeste brasileiro, mais precisamente no sul do estado do Ceará, que também recobre áreas dos estados de Pernambuco, Piauí e Paraíba. A bacia é limitada pelas seguintes coordenadas 38°30´–40°60´ O e 7°07´–7º49´ S (Figura 2).

Figura 2 – Localização da área de estudo

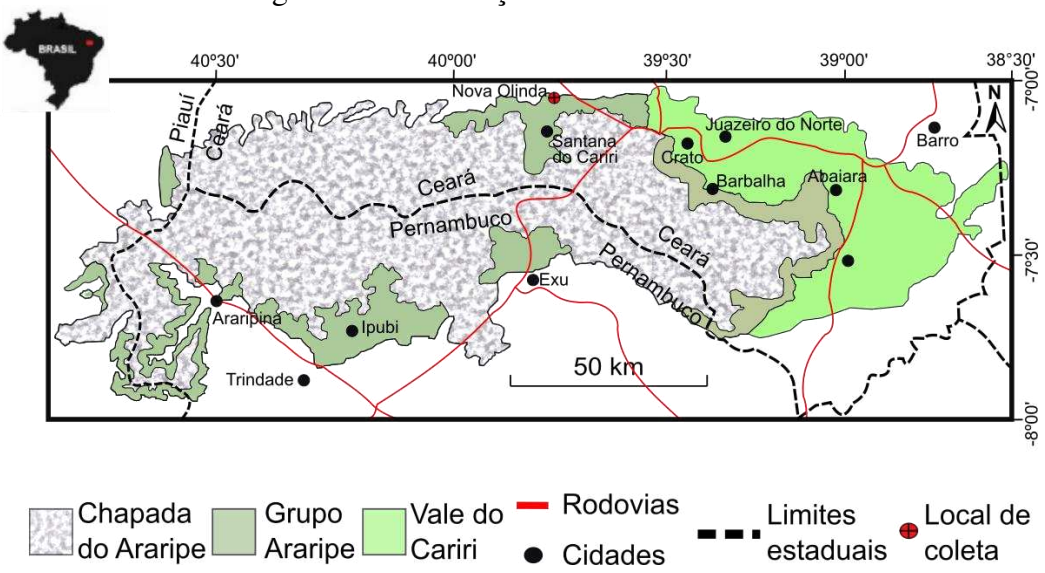

Fonte: o autor.

A coleta do material fóssil utilizado nesse trabalho foi realizada em pedreiras na localidade de Triunfo, município de Nova Olinda, Ceará. O afloramento se caracteriza como uma frente de lavra a céu aberto, distante cerca de 3 km da sede de Nova Olinda. A pedreira é uma das principais produtoras regionais de placas de calcários destinadas à construção civil. Essas placas são a principal fonte de renda da região, comercialmente chamadas de PEDRA CARIRI.

1.1.2 Contexto geotectônico

Bacia de Fonseca

A Bacia de Fonseca representa um gráben cenozóico encravado no extremo leste do Quadrilátero Ferrífero (Figura 3). O termo “Quadrilátero Ferrífero” se refere aos inúmeros depósitos de minério de ferro relacionados às sequências sedimentar-exalativas do Supergrupo Minas, limitado aproximadamente pelas linhas que unem as cidades de Itaúna, Mariana, Congonhas do Campo e Itabira (DORR, 1969).

Figura 3 – Localização da Bacia de Fonseca no contexto regional do Quadrilátero Ferrífero, Minas Gerais: A – Sinclinal Moeda; B, Sinclinal Dom Bosco; C, Sinclinal Gandarela; D, Sinclinal Serra do Curral; E, Falhas transcorrentes; F, Falhas reversas

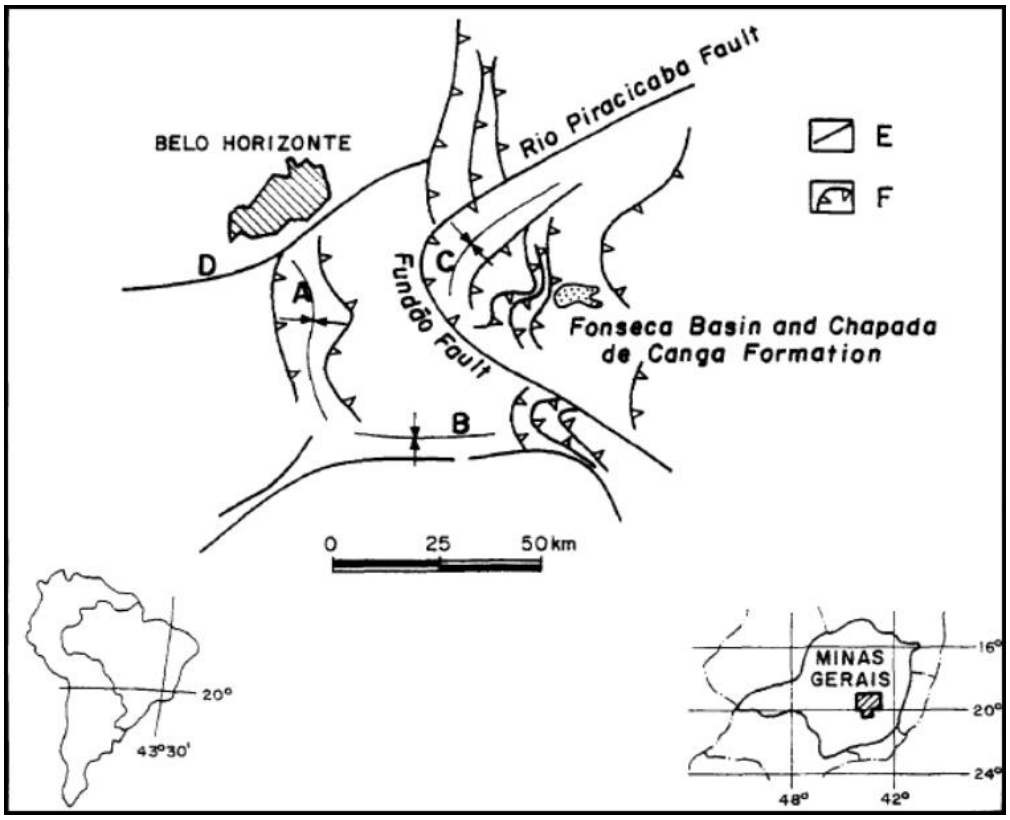

Fonte: Sant´Anna et al. (1997).

A origem da Bacia de Fonseca está relacionada com o neotectonismo distensivo e soerguimento crustal ocorridos em pulsos, durante o Paleógeno e Neógeno. Após a ruptura do Gondwana, que resultou na separação entre o Brasil e o continente africano, a crosta continental da plataforma sul-americana voltou a sofrer processos distencionais no final do Paleoceno e início do Eoceno, com a geração de novas calhas tectônicas no sudeste do Brasil. Este evento distencional atuou sobre um grande planalto quebrando-o e formando montanhas (Serras da Mantiqueira e do Mar) separadas entre si por pequenos grábens continentais (ZALÁN, 2004). Este processo levou à formação de inúmeras pequenas bacias, cujo conjunto foi denominado por Almeida (1976) de Sistema de Riftes da Serra do Mar e por Riccomini (1989) de Rifte Continental do Sudeste do Brasil. Este sistema extensional é observado nos registros sedimentares das bacias continentais de São Paulo (SP), Taubaté (SP), Bonfim (SP), Itaboraí (RJ), Resende (RJ), Formação São Domingos (MG), depósitos sedimentares de São João del Rei (MG), bacias do Rio Doce (MG), Gandarela (MG) e Fonseca (MG) (Figura 4).

Figura 4 – Localização das principais bacias continentais paleógenas do SE brasileiro

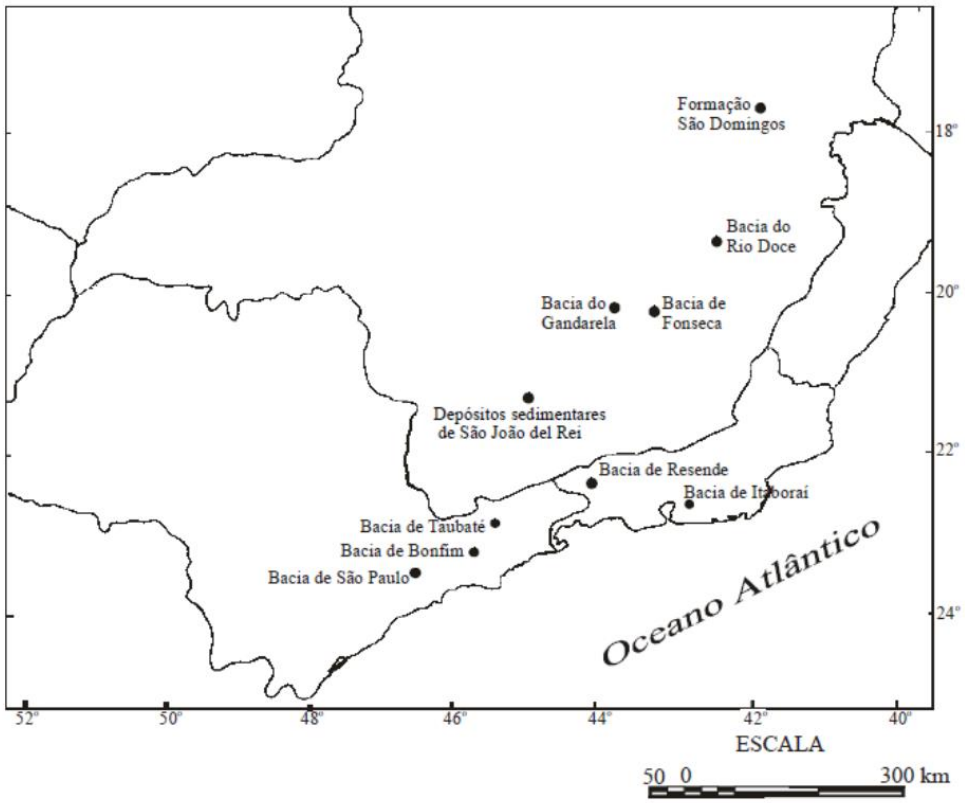

Fonte: Maizatto (2001).

Segundo Riccomini (1989), a tectônica cenozóica na região sudeste gerou diversos *hemi-grabens* responsáveis pelo acúmulo expressivo de sedimentos, chegando a alcançar espessuras de 500 m de preenchimento sedimentar na bacia de Taubaté (HASUI e PONÇANO, 1978). No intervalo Eoceno-Oligoceno, verificam-se depósitos sedimentares gerados por sistema de leques aluviais associados à planície aluvial de rios entrelaçados. A formação desses depósitos ocorre em resposta ao campo de esforços extensionais imposto pela bacia de Santos (RICCOMINI, 1989). Durante esta etapa, ocorre uma intensa atividade de falhas normais, predominantemente de direção NE-SW, associada a um soerguimento regional e vinculada aos processos de abertura do Atlântico (HASUI, 1998).

Segundo Saad *et al*. (2005), o soerguimento do Brasil oriental teria ocorrido em pulsos, reativando lineamentos e suturas nos intervalos Eoceno–Oligoceno (35–33 Ma), Mioceno (16–13 Ma), Mioceno–Plioceno (7–5 Ma) e Pleistoceno (1 Ma). De acordo com esse autor, a Bacia de Fonseca está inserida no setor morfossedimentar constituído pelos planaltos do Quadrilátero Ferrífero, representado pelas serras do Caraça, dos Pinhos e pela Cadeia do Espinhaço. Durante os dois primeiros pulsos, a região Sudeste foi marcada por um soerguimento epirogenético concomitante a uma fase tectônica distensiva e

consequentemente, expressiva sedimentação em bacias tanto no Quadrilátero Ferrífero (por exemplo, Fonseca e Gandarela) quanto no rifte continental do sudeste (SAAD *et al*., 2005).

A partir de uma análise neotectônica de depósitos cenozóicos exibindo fácies típicas de paleoambientes deposicionais fluviais (bacias intermontanas) do Quadrilátero Ferrífero, Lipski (2002) identificou três eventos principais: um no Oligoceno, relacionado à geração dos grábens e dois no Plioceno, relacionados com a reativação de estruturas pre-existentes. Varajão *et al*. (2009) consideraram as taxas de erosão e da pedogênese, e propuseram que a atual paisagem do Quadrilátero Ferrífero é produto de um processo erosivo constante, associado a um intenso soerguimento epirogenético.

Bacia do Araripe

A Bacia do Araripe está inserida no interior da Província Borborema, que compreende uma região tectônica localizada no Nordeste do Brasil com aproximadamente 450.000 km^2. Esta província se formou pela convergência dos crátons: Amazônico, Oeste Africano – São Luís e São Francisco – Congo, que ocorreu durante a formação do Gondwana (~600 Ma), consistindo de gnaisses e migmatitos de idade paleoproterozoica e arqueanas, e coberturas metassedimentares e metavulcânicas de idade neoproterozoica (Toniano e Criogeniano) (BRITO NEVES *et al.,* 2000). A Província Borborema foi afetada pelos eventos: Transamazônico (~2.0 a 2.2 Ga); Cariris Velhos (1000 Ma – 920 Ma) e Brasiliano (750 – 500 Ma) (NEVES *et al.,* 2006; SANTOS *et al.,* 2010). A Província Borborema é usualmente dividida em domínio norte (setentrional), central (zona transversal) e sul (meridional) demarcados pelas zonas de cisalhamento Patos e Pernambuco (BRITO NEVES *et al.,* 2000). A Bacia intracontinental do Araripe ocupa a Zona Transversal da Borborema, ou seja, está situada entre as zonas de cisalhamento Patos (limite norte) e Pernambuco (limite sul) (Figura 5).

Figura 5 – Bacia do Araripe dentro do contexto geotectônico da Província Borborema

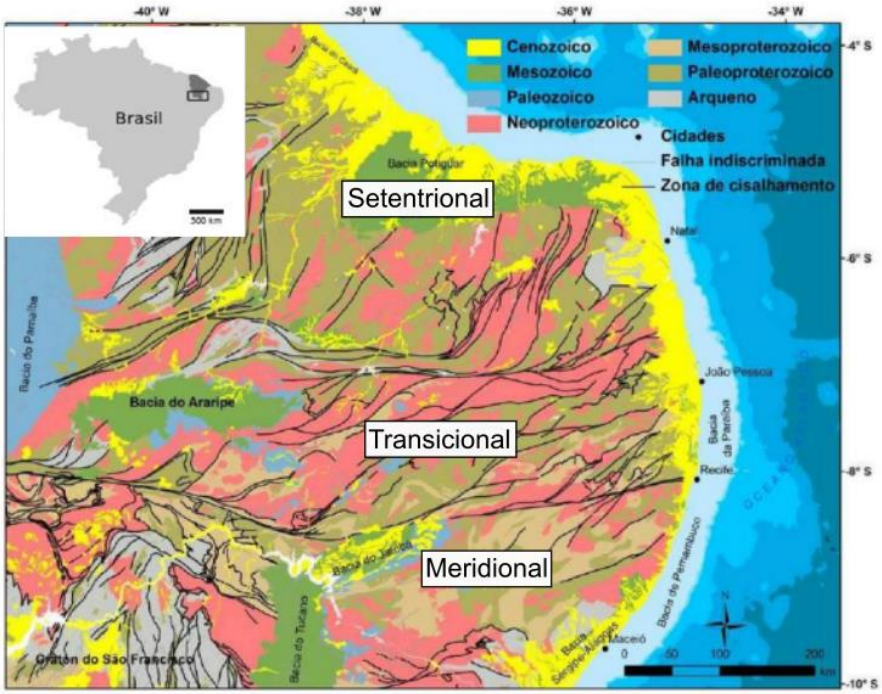

Fonte: Miranda (2015, com modificações).

Internamente, a Bacia do Araripe está dividida em duas sub-bacias, denominadas de Cariri (a leste), e Feira Nova ou Feitoria (a oeste), separadas pelo *horst* de Dom Leme (PONTE e PONTE FILHO, 1996). Em 1983, Rand realizou o primeiro levantamento gravimétrico e magnetométrico da bacia e observou que as anomalias gravimétricas estabeleceram os limites e profundidades aproximadas, 2400 e 2000 m, dos depocentros Leste e Oeste, respectivamente. Rand (1983) propôs um mapa Bouguer para essa bacia, o qual foi baseado em 800 estações gravimétricas distribuídas em malha irregular pela bacia, apresentado em escala de 1:250.000. Castro e Castelo Branco (1999) confirmaram a estruturação já proposta por Rand e Manso (1984) para a Bacia do Araripe, usando como base modelagem gravimétrica 3D. A modelagem proposta por esses autores sugeriu a existência de profundidades de até 1600 m.

Chang *et al.* (1988) propuseram a existência de três episódios principais de rifteamento, que foram chamados de Sin-rifte I (Jurássico Superior), Sin-rifte II (Neocomiano) e Sin-rifte III (Barremiano). Durante o estágio Sin-rifte II foi desenvolvido o *trend* Cariri-Potiguar que destaca o alinhamento de formação das bacias intracratônicas: Araripe, Rio do Peixe, Iguatu, Malhada Vermelha, Lima Campos, Icó e Potiguar (MATOS, 1992, 1999). Essas bacias interiores representam um sistema de riftes abortados, associados à separação, de sul para norte, da América do Sul e da África (MATOS, 1999). A geometria

dessas bacias foi controlada por zonas de cisalhamento proterozoicas de direção NE-SW, produzidas durante a orogenia do Ciclo Brasiliano (MATOS, 1999). Esta distensão geral teria reativado segmentos da Zona de Cisalhamento Patos originando todas as bacias interiores, inclusive a Bacia do Araripe.

Alguns trabalhos recentes têm sugerido novos aspectos da evolução tectônica da Bacia do Araripe. Miranda *et al.* (2014), sugeriram que a bacia experimentou uma fase de evolução tectônica inicial do tipo *pull apart*, baseado em aspectos geométricos e cinemáticos observados hoje no arcabouço da bacia. Marques *et al.* (2014) propuseram que a bacia passou por processo de inversão tectônica, possivelmente levado a efeito por causa de deformações crustais tardias, que fizeram com que as antigas estruturas pré-cambrianas atuassem como falhas inversas. Recentemente, Richetti *et al*. (2022) compararam os cenários existentes de inversão da Bacia do Araripe, e propuseram um modelo alternativo envolvendo compressão oblíqua associada ao desenvolvimento de falhas reversas de baixo ângulo.

1.1.3 Arcabouço Estratigráfico

Bacia de Fonseca

A Bacia de Fonseca ocupa uma área de cerca de 2 km^2, delimitada por falhamentos normais com direções NE e NO (FANTON, 2013). O Embasamento no qual a bacia se encontra assentada é constituído por rochas granito-gnáissicas (Associação TTG) e rochas metaultramáficas, metavulcanossedimentares e ortoquartzitos do Supergrupo Rio das Velhas (*greenstone belt*), dentro do contexto regional do Quadrilátero Ferrífero (Figura 6).

Figura 6 – Contexto geológico do Quadrilátero Ferrífero e o mapa geológico da Bacia de Fonseca

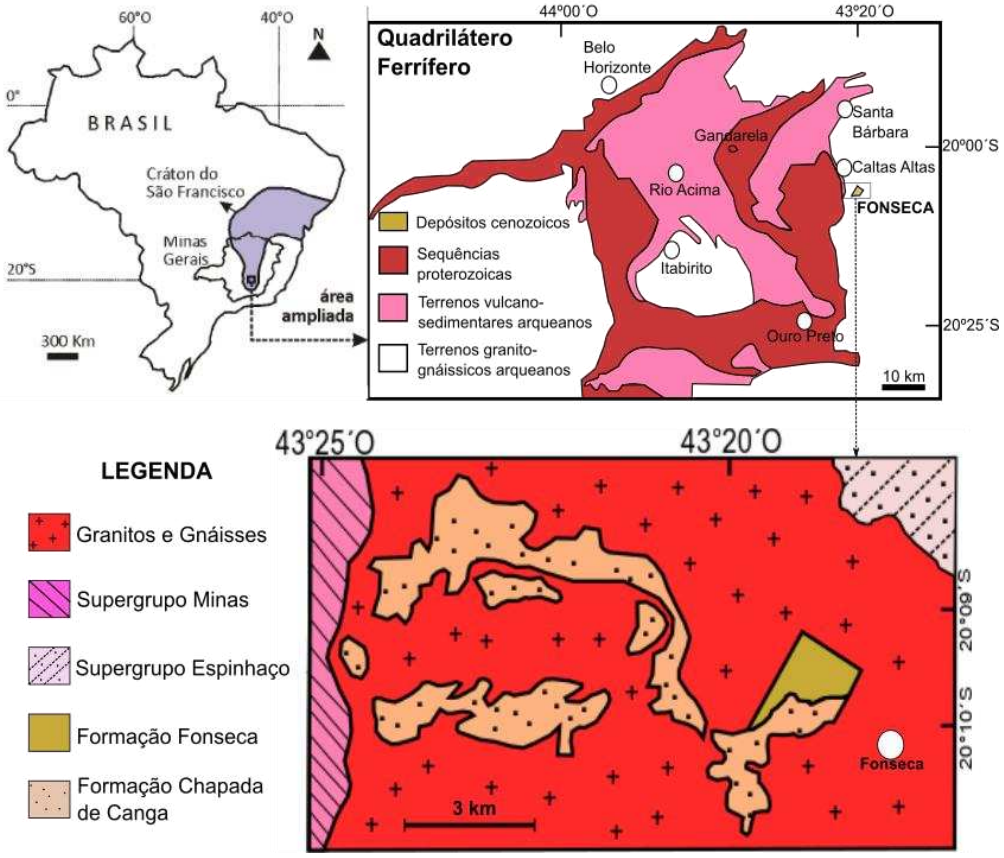

Fonte: Fanton (2013, com modificações).

As cercanias da bacia são compostas por quartzitos e itabiritos do Supergrupo Minas (incluindo minérios de ferro) e quartzitos do Supergrupo Espinhaço (serras do Caraça e dos Pinhos) de idade proterozoica (DORR, 1969). Esses terrenos atuaram como as principais áreas-fonte de sedimentos responsáveis pelo preenchimento da Bacia de Fonseca (SANT´ANNA e SCHORSCHER, 1997).

A Bacia de Fonseca se caracteriza por rochas argiloarenosas e linhitos de origem lacustre e fluvial correspondentes à Formação Fonseca (MAIZATTO, 2001). Na primeira tentativa de organização litoestratigráfica da bacia, proposta por Maxwell (1972), o preenchimento desta unidade incluía, além da Formação Fonseca, a cobertura de canga ferruginosa denominada de Formação Chapada de Canga no topo. No entanto, Sant´Anna e Schorscher (1997) redefiniram a litoestratigrafia da Bacia de Fonseca, dissociando a Formação Fonseca da Formação Chapada de Canga. Portanto, o preenchimento da bacia é restrito à Formação Fonseca, cuja seção colunar tipo foi formalizada por Sant´Anna e Schorscher (1997) a oeste do distrito de Fonseca, ao lado de um subsidiário do rio Piracicaba

(Figura 7).

Figura 7 – Seção colunar tipo da Formação Fonseca levantada por Sant´Anna e Schorscher (1997)

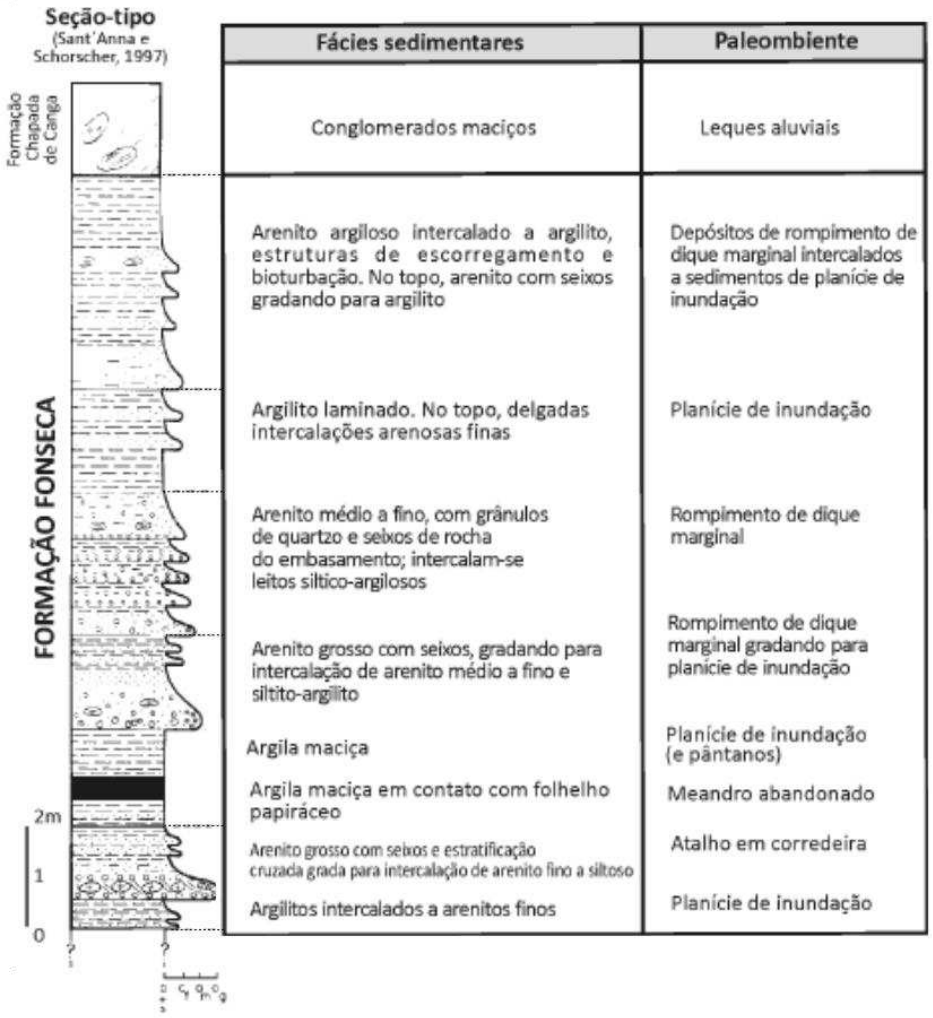

Fonte: Fanton (2013).

Bacia do Araripe

A Bacia do Araripe faz parte de um conjunto de pequenas bacias situadas entre as bacias de Tucano-Jatobá e Parnaíba, as bacias interiores (Figura 8). A maioria destas bacias (inclusive a Bacia do Araripe) possuem registro de rochas de idades paleozóicas que são correlatas às formações Tacaratu e Serra Grande, bacias do Parnaíba e Jatobá, respectivamente (ASSINE, 1992). As unidades paleozóicas destas bacias foram consideradas basais e posicionadas no intervalo Ordoviciano Superior/Devoniano Inferior (ASSINE, 1992, 2007; PONTE e PONTE FILHO, 1996). Estas ocorrências foram uma das principais evidências para Cordani *et al.* (1984) considerar que todas as bacias interiores representam fragmentos de uma

única bacia no interior do Nordeste. Porém, mais tarde, entendeu-se que suas evoluções tectônicas e estratigráficas são particulares, indicando histórias evolutivas diferentes (ASSINE, 1994).

Figura 8 – Mapa de localização das bacias interiores do nordeste do Brasil

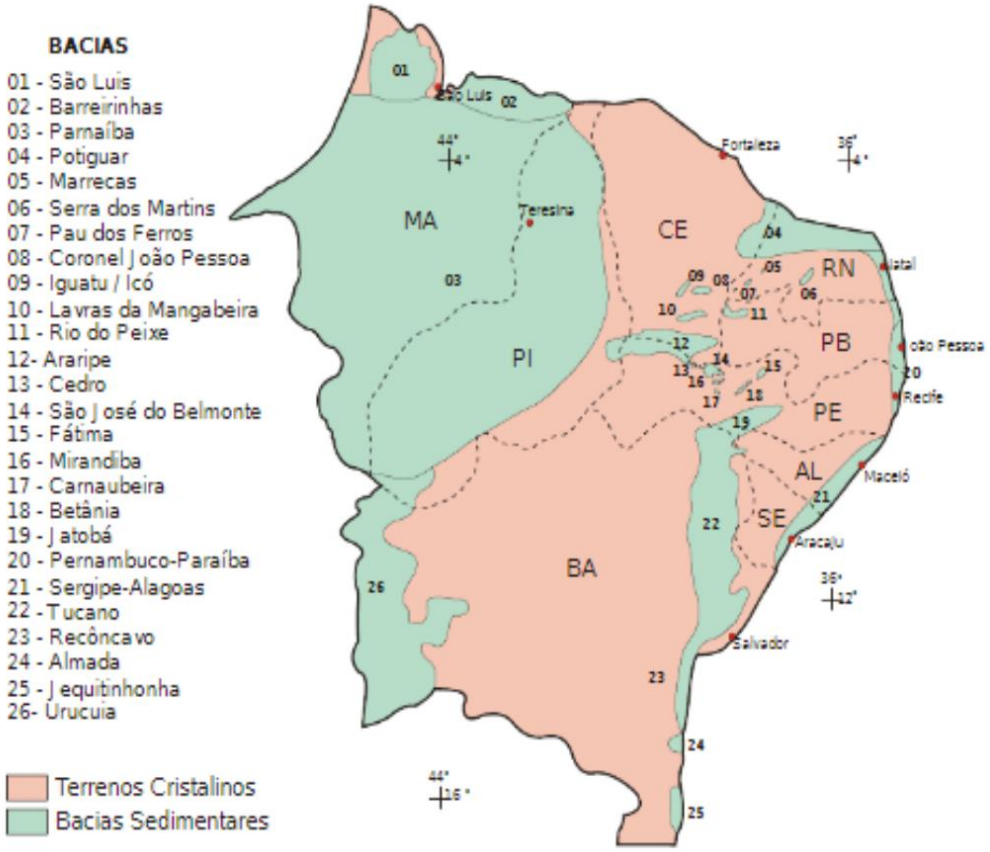

Fonte: Aguiar et al. (2010).

Apesar do registro paleozóico, a maior parte do desenvolvimento estrutural das bacias interiores do Nordeste está relacionada a um processo de rifteamento influenciado pela abertura do oceano Atlântico Sul, durante o Mesozóico. A cobertura sedimentar da Bacia do Araripe é representada por discordâncias regionais e hiatos deposicionais (ASSINE, 1992; PONTE e PONTE FILHO, 1996; ASSINE *et al*., 2014). Considerando a complexidade tectônica e estratigráfica, várias cartas estratigráficas foram propostas e modificadas ao longo da evolução dos conhecimentos sobre a bacia (Figura 9). Ponte e Ponte Filho (1996) dividiram a evolução mesozóica das bacias interiores do Nordeste em cinco tectono-sequências, que foram chamadas de: a) Beta (Neo-ordoviciano - Siluriano), representada pela Formação Cariri/Mauriti na Bacia do Araripe; b) Pré-Rifte (Neojurássico - Eocretáceo), correspondente a Sin-rifte I, representada pelas formações Brejo Santo e Missão Velha; c)

Sin-rifte (Neocominiano), que corresponde a Sin-rifte II, representada pela Formação Abaiara; d) Pós-rifte (Aptiano-Albiano), correspondente a Sin-rifte III, representada pelo Grupo Santana (formações Rio da Batateira, Crato, Ipubi, Romualdo e Arajara) e a Formação Exu; e e) Zeta (Cenozoica) representada por coberturas eluvionares, coluvionares e aluvionares.

Figura 9 – Resumo das principais propostas estratigráficas da Bacia do Araripe

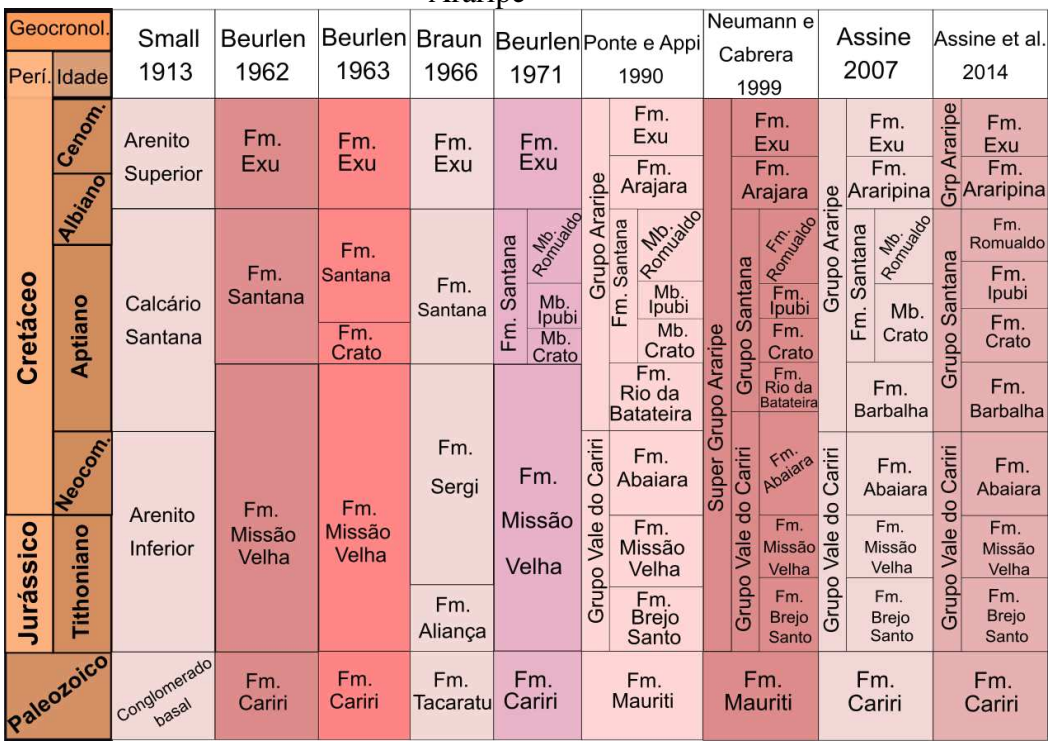

Fonte: o autor.

Posteriormente, Assine (2007) dividiu a coluna estratigráfica da Bacia do Araripe em quatro grandes unidades, limitadas por discordâncias: Sequência Paleozóica, correspondente à unidade litoestratigráfica basal da bacia, de idade paleozóica, representada pela Formação Cariri; Sequência Pré-Rifte, representada pelas formações Brejo Santo e Missão Velha, andar Dom João do Jurássico Superior; Sin-Rifte, representada pela Formação Abaiara, andar Rio da Serra de idade neocomiana; Sequência Pós-Rifte I, representada pela Formação Barbalha e Formação Santana, andar Alagoas de idade aptiana–albiana; e Sequência Pós-Rifte II, equivalente às formações Araripina e Exu de idade cenomaniana. Mais tarde, Assine *et al*. (2014) apresentaram uma nova proposta de revisão a tectono-sequência Pos-Rifte I, onde se unificou o empilhamento sedimentar do Grupo Santana na seguinte ordem: Formação Barbalha, Formação Crato, Formação Ipubi e Formação Romualdo (Figura 10).

Figura 10 – Perfil estratigráfico esquemático da Bacia do Araripe, de acordo com a classificação proposta por Assine *et al.* (2014)

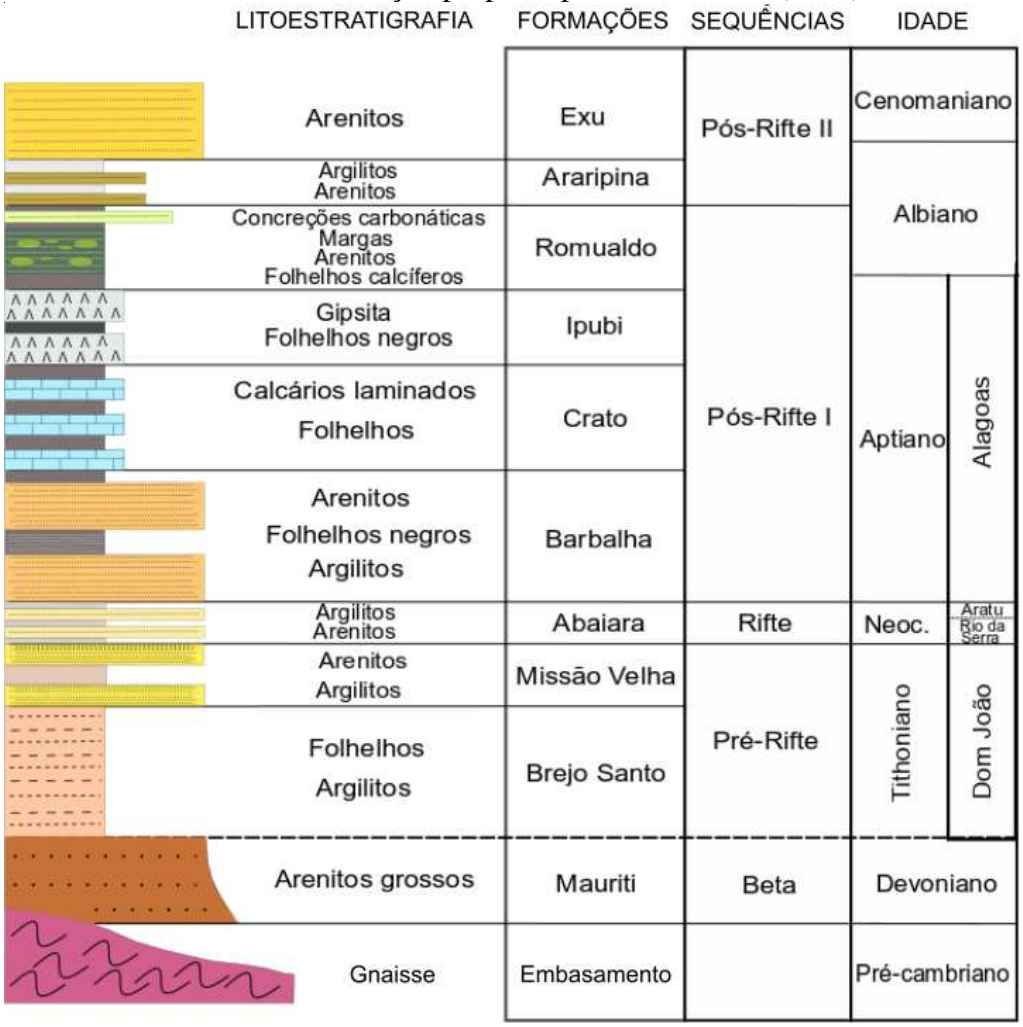

Fonte: Assine et al. (2014, com modificações).

1.2 Histórico de estudos paleontológicos nas bacias de Fonseca e do Araripe

Bacia de Fonseca

Baseado na literatura disponível, as folhas são os macrofósseis mais abundantes na Bacia de Fonseca, sendo incomuns flores e frutos, ou mesmo lenho fóssil. O primeiro a reportar material paleobotânico nessa unidade foi o francês Claude-Henri Gorceix (1842-1919). Segundo este autor, os fitofósseis do tipo compressão e impressão são comumente encontrados em intercalações milimétricas de siltito nos linhitos e folhelhos da Formação Fonseca. Os trabalhos de Gorceix trouxeram a tona morfoespécies relacionadas à Fabaceae, Melastomataceae e possíveis monocotiledôneas. Gorceix também reportou um dos raros exemplares de pteridófita e impressões de uma gramínea (GORCEIX, 1876, 1884).

Em meados da primeira métade do Século XX, Hollick e Berry (1924), Berry (1935) e Dolianiti (1949) descreveram muitas espécies novas de vegetais oriundos da Fm. Fonseca. As pesquisas destes autores revelaram a presença de representantes de Bignoniaceae, Combretaceae, Euphorbiaceae, Fabaceae, Malpighiaceae, Meliaceae, Primulaceae, Siparunaceae e Sapotaceae. A partir destes trabalhos, começou-se a perceber o tamanho da diversidade florística destes depositos. Em 1955, Curvello apresentou a descrição de um lenho de Fabaceae, um dos poucos encontrados na Bacia de Fonseca. Na segunda metade do Século XX, os pesquisadores Duarte e Oliveira-e-Silva também revelaram morfoespécies associadas à Combretaceae, Fabaceae, Myrtaceae e Vochysiaceae na Fm. Fonseca (DUARTE, 1974; OLIVEIRA-E-SILVA, 1982). Durante esse período, em especial, ocorre a descoberta notável de *Eriotheca prima* Duarte, 1974 (Malvaceae), marcando o que viria ser o primeiro registro de uma flor no Cenozóico do Brasil. Depois dos anos 2000, poucas novas espécies de folhas foram descritas como *Terminalia palaeopubescens* Fanton *et al*. (2012). Em 2013, Fanton *et al*. (2013) contabilizou 33 morfoespécies de dicotiledôneas, excluindo as ocorrências informais, distribuídas em 18 famílias na Bacia de Fonseca. Particularmente, a paleoflora de Fonseca chamou a atenção de Burnham e Johnson (2004), que relataram uma alta diversidade de espécies para uma paleoflora pouco estudada.

Sommer e Lima (1967) foram os primeiros a realizar uma análise sobre a diversidade microflorística da Bacia de Fonseca. Neste trabalho, os pesquisadores citaram ocorrências de Begoniaceae, Leguminosae, Combretaceae, Menispermaceae e Podocarpaceae. Lima e Salard-Cheboldaeff (1981) desenvolveram um estudo palinológico mais completo, identificando uma grande variedade de esporos e grãos-de-pólen, e atribuíram uma idade

eocênica para os depósitos da bacia, sendo a primeira datação bioestratigráfica nesta unidade. Mais tarde, em 1999, Maizatto e Porfiro propuseram a criação da biozona *Retibrevitricolpites triangulatus*, a qual denota uma idade neoeocênica. Maizatto *et al*. (2000) estabeleceram uma segunda biozona na Bacia de Fonseca, *Dacrydiumites florinii* considerada de idade oligocênica. Logo depois, em 2001, Maizatto apresenta uma pesquisa palinológica integrando dados com outras bacias continentais do SE do Brasil. Os resultados de Maizatto (2001) culminaram na criação de uma nova biozona na região, *Crassoretitriletes vanraadshooveni*, correspondendo ao Mioceno Inferior, definida na Bacia de Gandarela também situada no contexto regional do Quadrilátero Ferrífero. Maizatto *et al*. (2008) também conduziram um extenso estudo palinológico em linhitos e siltitos da Bacia de Fonseca, com o objetivo de refinar seu arcabouço biocronoestratigráfico.

Com relação à paleofauna, Costa Lima foi o primeiro autor a apresentar um inseto fóssil proviniente da Bacia de Fonseca em 1944. Porém, a primeira espécie de inseto, formalmente descrita, *Spargotermes costalimai*, é proposta por Emerson em 1965. Outras espécies de insetos só viriam a ser propostas após um longo intervalo, em 2001-2002, os pesquisadores Márcio Mendes, Irajá Pinto e Martins-Neto descreveram mais cinco espécies de insetos nesta unidade. Somente no ano de 2015, Mendes e colaboradores formalizaram mais duas espécies de Hymenoptera. Por fim, Bezerra *et al*. (2020a) propôs uma segunda espécie de cupim primitivo (Mastotermitiidae) como representante da paleoentomofauna de Fonseca.

Bacia do Araripe

Os estudos paleontológicos na Bacia do Araripe começam de fato em meados do século XIX, quando a arquiduquesa Maria Leopoldina Josefa Carolina chega ao Rio de Janeiro em 1817, trazendo naturalistas em sua comitiva. No entanto, entre o final do século XVIII e início do XIX, João da Sylva Feijó (1760-1824), sargento-mor das milícias da capitania do Ceará, já havia reportado coleta de peixes fósseis com estilo de preservação incomum, durante suas expedições pelo interior do território do Ceará à procura de depósitos de salitre (NOBRE, 1978; CARVALHO *et al*., 2021). Entre os anos de 1817 e 1820, os naturalistas alemães Johann Baptist von Spix e Karl Friedrich Philipp von Martius realizaram uma viagem pelos territórios dos atuais estados da Bahia, Maranhão, Pernambuco e Piauí. Os resultados desta expedição foram publicados na obra de três volumes *Reise in Brasilien* (Viagem pelo Brasil). Embora os naturalistas não chegarem à Bacia do Araripe, deve-se a eles

a primeira ilustração de um peixe fóssil preservado numa concreção carbonática oriundo desta unidade, provavelmente um *Rhacolepis buccalis* (CARVALHO e SANTOS, 2005).

Nos anos seguintes foram realizadas várias expedições de naturalistas, principalmente, franceses e britânicos. Entre anos de 1838 e 1839, o botânico escocês George Gardner visitou o interior do Ceará, coletando diversos exemplares de peixes fósseis que seriam posteriormente repassados ao ictiólogo suíço Louis Agassiz. Em 1841, o criacionista Agassiz apresentou à comunidade científica as primeiras espécies (peixes fósseis) descritas da Bacia do Araripe (AGASSIZ, 1841). Baseado na paleoictiofauna coletada por Gardner, Agassiz (1844) datou as rochas da região como sendo de idade cretácea. Isso acabou sendo um marco para geologia brasileira, pois foi a primeira vez que uma unidade geológica em território nacional foi datada com base no conteúdo paleontológico (CARVALHO e SANTOS, 2005).

A criação do Serviço Geológico e Mineralógico do Brasil, em 1907 contribuiu para uma nova fase de coleta de material paleontológico na região. A estrutura geológica básica da Bacia do Araripe foi definida pela primeira vez pelo geólogo Horace L. Small, em 1913. Em sua proposta, Small (1913) dividiu a estratigrafia da bacia em quatro unidades: Conglomerado basal; Arenito Inferior; Calcário Santana e Arenito Superior. Nesta subdivisão, as camadas carbonáticas e margosas de origem lacustre constituíam o chamado "Calcário Santana". A partir de 1960, o professor da Universidade Federal de Pernambuco (UFPE), Karl Beurlen, realizou uma série de mapeamentos geológicos na região. Beurlen (1962) cunhou o termo Formação Santana e a definiu como uma série de calcários, folhelhos, siltitos, gipsitas, concreções carbonáticas e margas divididas em três membros informais: Membro inferior, composto de calcários laminados intercalados por folhelhos; Membro intermediário, representado por depósitos de gipsita; e Membro superior, delimitado por rochas margosas com concreções carbonáticas. Beurlen (1962) renomeou o "Conglomerado basal" de Small (1913) como Formação Cariri, e também introduziu o termo Formação Missão Velha para se referir ao pacote siliciclástico abaixo da Formação Santana e acima da Formação Cariri. Em outros trabalhos, Beurlen também descreveu moluscos e equinóides no topo da Formação Santana. Com base nesses achados, ele foi um dos primeiros a propor uma influência marinha para este intervalo (BEURLEN, 1964; 1966). Braun (1966) utilizou ostracodes fósseis para correlacionar a Bacia do Araripe com outras bacias da margem costeira do Nordeste do Brasil, principalmente a Bacia de Sergipe-Alagoas. Embora as primeiras menções de lenhos petrificados na Formação Missão Velha datem de 1859 (ALEMÃO e ALEMÃO, 1862), Braun (1966) usou esses fósseis para correlacionar esta unidade com a Formação Sergi da Bacia do

Recôncavo-Tucano-Jatobá.

A grande diversidade paleontológica preservada nos depósitos da Bacia do Araripe começou a ficar evidente durante a década de 1970, quando várias espécies de diferentes grupos biológicos foram descritos na então chamada Formação Santana. Infelizmente, foi também nesta década que o comércio ilegal de fósseis da bacia se intensificou (CARVALHO e SANTOS, 2005). Em resposta a essa situação, foram discutidas as primeiras medidas para proteger os jazigos fossilíferos da Bacia do Araripe. Em 1979, Oliveira e colaboradores apresentaram um projeto que visava estudar, cadastrar e proteger áreas de interesse paleontológico. Em 1971, Buerlen reconsidera sua proposta original e subdivide a Formação Santana em três membros formais, sendo esses em ordem ascendente: Membro Crato (calcários laminados); Ipubi (evaporitos) e Romualdo (concreções carbonáticas).

Na década de 1980, o Membro Crato da Formação Santana começa a se destacar pela abundância e beleza dos fósseis. Nesta unidade, os fósseis de paleoinvertebrados, principalmente insetos, se destacam pela diversidade. A. Costa Lima, I. D. Pinto, I. Purper, M. A. Vulcano e R. G. Martins Neto são pesquisadores que contribuíram para esse primeiro avanço do conhecimento paleoentomólogico na Bacia do Araripe. No final da década de 80, com a finalidade de manter os fósseis na região de origem, foi criado o Museu de Paleontologia de Santana do Cariri, Ceará.

A década de 1990 foi também extremamente produtiva em termos de acúmulo de conhecimento paleontológico para Bacia do Araripe. Novos gêneros e espécies de peixes, terópodes e, principalmente, pterossauros foram descritas a partir das concreções calcárias do Membro Romualdo (MAISEY, 1991; FREY e MARTILL, 1994; KELLNER, 1996; MARTILL *et al*., 1996; CAMPOS e KELLNER, 1997). Nos calcários laminados do Membro Crato, novos fósseis de vegetais foram descobertos, assim como várias espécies de artrópodes (MARTINS NETO, 1990; DUARTE, 1993; RASNITSYN e MARTÍNEZ-DELCLÓS, 1999). Com relação aos insetos, especificamente, Grimaldi (1990) lançou um livro sobre os insetos encontrados no Membro do Crato. Nesse período, outras unidades da bacia também mostraram relevância do ponto de vista paleontológico, foi o caso dos siltitos e folhelhos esverdeados da Formação Brejo Santo, onde foram encontrados restos de vertebrados, inclusive peixes dipnóicos (GALLO DA SILVA e AZEVEDO, 1996).

Ponte e Appi (1990) subdividiram os arenitos abaixo da Formação Santana em três unidades: Formação Missão Velha, a porção inferior; Formação Abaiara, a parte intermediária; Formação Rio da Batateira, a porção superior. Em 1996, Ponte e Ponte Filho

apresentaram a desenvolvimento da Bacia do Araripe pelo modelo da tectônica de placas, correlacionando sua evolução tectônica com a Margem Continental Brasileira. Em 1999, Neumann e Cabrera elevaram a Formação Santana ao status de Grupo, o qual era composto pelas, agora, formações Rio da Batateira, Crato, Ipubi e Romualdo.

Na primeira década dos anos 2000 houve muito avanço na pesquisa paleontológica no Brasil, em especial na Bacia do Araripe. Muitas novas espécies de insetos, aracnídeos, moluscos, peixes, pterossauros, crocodilimorfos e tartarugas (DUNLOP e MARTILL, 2002; KELLNER e CAMPOS, 2002; SALISBURY *et al.,* 2003; LEAL e BRITO, 2004; FIELDING *et al.,* 2005). Neste intervalo, também houve avanço na descoberta de angiospermas primitivas nos depósitos do Araripe (MOHR e RYDIN, 2002; MOHR e EKLUND, 2003). Também houve evolução no entendimento geológico e estratigráfico da bacia, Assine (2007) dividiu a Bacia do Araripe, da base para o topo, em Formação Cariri, Grupo Vale do Cariri e Grupo Araripe, onde o Grupo Araripe é composto pelas formações Barbalha, Santana, Araripina e Exu. Na segunda década dos anos 2000, Assine *et al.* (2014) reconheceram o status de Grupo da Formação, a partir de então Grupo Santana, composto pelas formações Barbalha, Crato, Ipubi e Romualdo, enquanto que o Grupo Araripe seria constituído pelas formações Araripina e Exu.

Ainda neste período, intensificaram-se estudos empregando técnicas de alta resolução aplicadas em fósseis da Bacia do Araripe (PINHEIRO *et al.,* 2012; DELGADO *et al.,* 2014; MALDANIS *et al.,* 2016). Os trabalhos revelando a preservação de microestruturas, estruturas reprodutivas e tecidos moles trouxeram muito progresso para o conhecimento tafonômico, geoquímico e paleontológico da bacia. Esses estudos ajudaram a reconhecer o título de *Konservat-Lagerstätte* concedido a Formação Crato.

1.2.1 Estudos tafonômicos prévios sobre o modo de preservação das paleoentomofaunas das formações Crato e Fonseca

Particularmente com relação aos insetos da Formação Fonseca, poucos trabalhos abordam o estilo de preservação dos fósseis nesta unidade. Alguns autores reportaram que os macrofósseis desta formação geológica são encontrados na forma de compressões/impressões incarbonificadas (DUARTE e MELLO-FILHA, 1980; MAIZATTO, 2001; FANTON, 2013). Assim, esta tese representa o primeiro trabalho cujo foco é investigar mais detalhadamente os aspectos fossildiagenéticos da Fm. Fonseca. Em contrapartida, vários estudos têm verificado os fatores tafonômicos e diagenéticos que controlaram a preservação excepcional dos insetos

fósseis encontrados na Formação Crato. Grimaldi e Maisey (1990) foram os primeiros a propor uma hipótese geoquímica a respeito da preservação dos insetos. Os autores identificaram o mineral goethita como o principal componente dos fósseis, logo, eles interpretaram que esse mineral seria o responsável por substituir a matéria orgânica presente na cutícula e em outros órgãos dos insetos durante a diagênese. Grimaldi e Maisey (1990) sugeriram que um paleoambiente com água doce e altamente oxigenada seria necessário para possibilitar tal modo de preservação.

Menon e Martill (2007) forneceram uma discussão mais aprimorada sobre a preservação dos insetos do Crato *Lagerstätte*, eles observaram que essa paleoentomofauna apresenta uma leve tendência em preservar indivíduos grandes. No entanto, Menon e Martill (2007) atestaram que não há distinção na fidelidade preservacional, uma vez que táxons maiores e menores estão preservados com alta fidelidade de detalhes. Os autores foram os primeiros a observar pelo menos dois tipos de preservação nos insetos da Formação Crato: um tipo com indivíduos marrons alaranjados constituídos de hidróxidos de ferro e outro com insetos de coloração escura formados por compostos fosfatados e sulfatados. A partir disso, Menon e Martill (2007) concluíram que a fase de hidróxidos de ferro representa um produto de intemperismo lento e *in situ* das versões escuras sulfatadas. Desse modo, os insetos marrons alaranjados seriam replicas produzidos, por um evento tardio, a partir dos insetos escuros (originais). Os autores inferiram que um paleoambiente anóxico, rico em enxofre e hipersalino seria o ideal para possibilitar essa preservação. Portanto, eles sugeriram que tapetes microbianos com bactérias redutoras de sulfato desempenharam papel fundamental na alta fidelidade morfológica destes insetos.

Delgado *et al.* (2014) também observaram a presença de goethita em um ortóptero da Formação Crato. No entanto, esses autores aplicaram técnicas de microscopia mais sofisticadas e identificaram framboides de pirita pseudomorfizada substituindo a cutícula e os tecidos internos do fóssil. Os framboides de pirita se diferenciavam em tamanho, sendo os cristais ocorrentes em tecidos internos consideravelmente menores do que os encontrados na cutícula (DELGADO *et al.,* 2014). Eles foram os primeiros a reportar a presença de substâncias poliméricas extracelulares associadas a insetos da Formação Crato. Essas substâncias são resultado da atividade metabólica de bactérias e, certamente, foram essenciais para preservação excepcional destes fósseis. Barling *et al.* (2015) forneceram mais exemplos de framboides de pirita e pseudoframboides de tamanhos e formas diferentes compondo os insetos da Formação Crato. Em 2016, Osés e colaboradores utilizaram diferentes ferramentas analíticas de alta resolução para fornecer uma abrangente análise tafonômica da

paleoentomofauna do Crato *Lagerstätte*. Dentre as técnicas aplicadas estavam microscopia eletrônica de varredura, fluorescência de raios-X, espectroscopia de raios-X, emissão de raios-X induzida por partículas e espectroscopia Raman (OSÉS *et al.,* 2016). Em seu modelo, os autores concluíram que a atividade metabólica de bactérias redutoras de sulfato combinado com a decomposição das carcaças de insetos resultou no esgotamento do sulfeto de hidrogênio e, consequentemente, na precipitação dos framboides de pirita. O tamanho dos cristais de pirita foi limitado pela velocidade de deterioração dos tecidos lábeis e disponibilidade de íons, assim, os framboides possuem granulação mais fina dentro das carcaças e granulação mais grossa na cutícula (OSÉS *et al.,* 2016).

Dias e Carvalho (2020) analisaram vários ensíferos da Formação Crato, e reportaram uma série de características anatômicas bem preservadas em micro-escala associadas ao trato digestivo, sistema reprodutivo e tecidos musculares. Também em 2020, Barling e colaboradores propuseram um modelo tafonômico baseado em todos os modelos propostos até aquela data para os insetos da Formação Crato. Neste estudo, Barling *et al.* (2020) classificou três principais *fabrics* minerais presentes nos insetos: 1) composto por pirita framboidal e pseudoframboides; 2) formado por nanocristais de greigita; e 3) incrustações e impregnações de fosfato de cálcio. Neste modelo, o *fabric* 3 preserva tecidos originais lábeis, enquanto que os *fabrics* 1 e 2 foram pseudomorfizados durante eventos posteriores de intemperismo (BARLING *et al*., 2020). Bezerra *et al.* (2020b) sugerem dois tipos principais de preservação para a paleoentomofauna da Formação Crato. Os insetos de coloração marrom alaranjado foram mineralizados via piritização durante a eodiagênese; os espécimes de coloração escura estariam preservados como compressões carbonosas, representando matéria orgânica original ainda preservada. Desta forma, os principais fatores controladores de ambos os tipos de preservação seriam o regime sedimentar e a disponibilidade de íons na interface sedimento-água, onde os insetos piritizados teriam sido depositados na zona de redução de sulfato, enquanto que os indivíduos preservados como compressões carbonosas foram depositados na zona metanogênica (BEZERRA *et al.,* 2020b).

Em 2021, Barling e colaboradores analisaram o grau de preservação e articulação de diferentes grupos de insetos da paleoentomofauna da Formação Crato. Eles identificaram que os Odonata aparecem mais desarticulados, ou seja, menos completos com relação aos demais grupos de insetos desta biota. Iniesto *et al.* (2021) realizaram um experimento tafonômico para verificar a taxa de mineralização comparada à decomposição de larvas de insetos atuais. Observando secções histológicas, os autores documentaram que após 11 dias da morte da larva em um recipiente com água, músculos e tecido adiposo se deterioram

completamente. Após 30 dias ocorre a degradação do trato digestivo e ocorrência de bactérias endógenas. Entre 60 e 120 dias ocorre a deterioração da cutícula. No entanto, as larvas, colocadas no recipiente com esteiras microbianas, permaneceram praticamente intactas tanto com relação a não degradação da cutícula quanto de tecidos internos (INIESTO *et al.,* 2021). Dias e Carvalho (2022) buscaram analisar os efeitos diretos e indiretos das esteiras microbianas na preservação excepcional dos insetos desta unidade. Dias e Carvalho (2022) acabaram complementando os achados de Iniesto *et al.* (2021), eles propuseram um modelo tafonômico onde as esteiras microbianas são responsáveis pela captura, proteção e criação das condições geoquímicas ideais para ocorrer a mineralização dos insetos com alta fidelidade.

1.3 Objetivo

O objetivo geral da presente tese é investigar o contexto preservacional das paleoentomofaunas das formações Crato e Fonseca, no que diz respeito às condições tafonômicas, diagenéticas e paleoambientais de cada unidade.

Objetivos específicos:

- Verificar a composição química e mineralógica dos insetos fósseis e suas possíveis implicações fossildiagenéticas, paleobiológicas e deposicionais;
- Averiguar os aspectos bioestratinômicos e os efeitos da fossildiagênese na paleoentomofauna da Formação Fonseca;
- Comparar qualitativamente e quantitativamente o grau de preservação dos insetos piritizados e querogenizados da Formação Crato;
- Documentar os efeitos da telodiagênese na preservação excepcional dos insetos piritizados da Formação Crato;
- Correlacionar a composição faunística da paleoentomofauna com os aspectos sedimentares observados na Formação Crato e comparar a paleoentomofauna Crato com outras paleoentomofaunas do Cretáceo Inferior.

1.4 Estrutura da Tese

Este documento reúne uma coleção de artigos científicos que visam expandir

nossa compreensão sobre os processos bioestratinômicos, fossildiagenéticos, paleoambientais e paleoecológicos envolvidos na preservação excepcional das paleoentomofaunas das formações Crato e Fonseca. Portanto, os demais capítulos desta tese representam publicações submetidas/aceitas em periódicos científicos, com revisão por pares, dedicados a discutir cada um dos objetivos específicos propostos. O conteúdo de cada capítulo é brevemente apresentado a seguir:

- Capítulo 1: Uma análise tafonômica abordando conceitos bioestratinômicos e fossildiagenéticos da paleoentomofauna preservada nos estratos da Formação Fonseca, Eoceno-Oligoceno de Minas Gerais, é apresentada. Este trabalho foi publicado (BEZERRA *et al*., 2021a) e representa a primeira abordagem paleométrica realizada em invertebrados fósseis desta unidade;

- Capítulo 2: Uma comparação qualitativa e quantitativa do grau de preservação dos insetos piritizados e querogenizados da Formação Crato, Bacia do Araripe, foi fornecida. Esses resultados foram publicados (BEZERRA *et al*., 2021b) e documentam o primeiro estudo propondo que, em condições extremamente excepcionais, fósseis piritizados podem reter mais caracteres morfológicos preservados do que fósseis preservados via querogenização;

- Capítulo 3: Um estudo mais detalhado dedicado a documentar os efeitos da telodiagênese na preservação excepcional dos insetos mineralizados da Formação Crato, Bacia do Araripe, é apresentado. Este estudo foi publicado (BEZERRA *et al*., 2023) e apontou-se três tipos principais de alterações telodiagenéticas observadas nos insetos mineralizados: espécimes apresentando sobreposições por óxido de ferro; espécimes associados a formação de dendritos; e espécimes preservados apenas como uma impressão no calcário;

- Capítulo 4: Um trabalho integrando dados tafonômicos e paleoecológicos da paleoentomofauna da Formação Crato, Bacia do Araripe, é proposto. O manuscrito foi recentemente submetido (BEZERRA *et al*., submetido) e aborda que dados tafonômicos obtidos a partir dos insetos fósseis corroboram com dados sedimentológicos e deposicionais inferidos para unidade. A organização trófica e importância da paleoentomofauna dentro do paleobioma Crato também são discutidas. Realizou-se uma comparação, em nível de espécies publicadas, entre a paleoentomofauna Crato e outras paleoentomofaunas do Cretáceo Inferior ao redor do mundo.

2 FUNDAMENTAÇÃO TEÓRICA

2.1 Contexto geológico da Formação Fonseca

2.1.1 Evolução estratigráfica da Formação de Fonseca

Gorceix (1884) foi o primeiro a confeccionar um perfil litológico dos depósitos que formam a Bacia de Fonseca (Figura 11), relacionando-os com sistemas deposicionais lacustres alimentados por águas pluviais.

Figura 11 – Perfil litológico apresentado por Gorceix (1884) para a Bacia de Fonseca

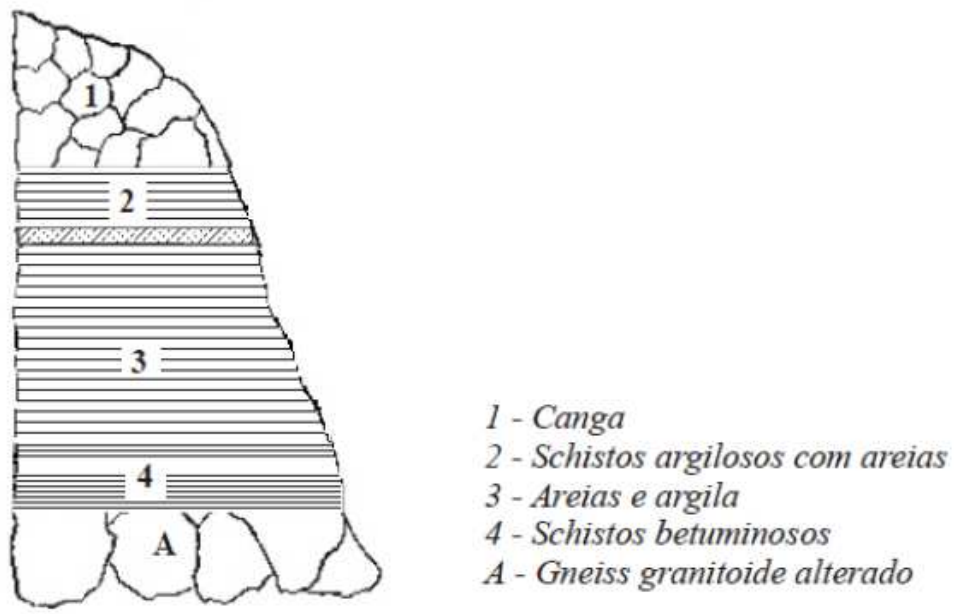

Fonte: Maizatto (2001).

Maxwell (1972) propõe a criação da unidade litoestratigráfica denominada Formação Fonseca sendo representada pelos depósitos sedimentares terciários localizados no Quadrilátero Ferríferro. Neste trabalho, Maxwell descreve essa unidade como sendo constituída predominantemente por arenitos, siltitos arenosos, conglomerados e linhitos associados a um sistema deposicional flúvio-lacustre. Em 1994, Sant´Anna descreveu uma unidade sedimentar constituída por conglomerados contendo seixos de itabirito envolvidos em uma matriz ferruginosa. Sant´Anna (1994), então, propôs a criação de uma nova unidade litoestratigráfica denominada Formação Chapada de Canga. De acordo com a autora, o sistema deposicional destas unidades estaria vinculado a um sistema fluvial meandrante com a instalação de planícies de inundação.

Em 1997, Castro e Ferreira definiram uma nova unidade designada Formação

Cata Preta, sendo constituída por arenitos maciços de coloração avermelhada e diamictitos apresentando seixos subangulosos a subarredondados de filitos, quartzitos ferruginosos, quartzo e magnetita envolvidos por uma matriz argilosa. De acordo com estes autores, a Formação Cata Preta foi descrita próximo a cava da antiga mina de ouro Cata Preta, e encontra-se sobreposta pelos conglomerados laterizados da Formação Chapada de Canga. No mesmo ano, Sant´Anna e Schorscher (1997) dissociaram a Fm. Fonseca da Fm. Chapada de Canga, e restringiram o preenchimento da bacia a esta formação.

Maizatto (2001) reconheceu cinco fácies associadas a um sistema deposicional constituído pelas fácies arenito fino, arenito grosso e conglomerado relacionado a um registro fluvial meandrante; e as fácies argilito e linhito, relacionado a depósitos de meandro abandonado. O autor destacou que a fácies linhito é caracteristicamente fossilífera.

2.1.2 Idade

Gorceix (1884) foi o primeiro a propor uma idade para as rochas da Bacia de Fonseca. Neste trabalho, o autor considerou uma idade neomiocênica-pliocênica para esta unidade baseada nas formas vegetais fossilizadas. Posteriormente, Sommer e Lima (1967) e Duarte (1974) mantiveram a idade neomiocênica-pliocênica da bacia, baseada na ocorrência das seguintes famílias vegetais: Begoniaceae, Leguminosae, Combretaceae, Menispermaceae e Podocarpaceae. Lima e Salard-Cheboldaeff (1981) realizaram uma análise palinológica mais completa na qual foram identificadas a presença de *Cicatricosisporites dorogensis*, *Spinizonocolpites*, *Perisyncolporites* e ausência de *Verrucatosporites usmensis*, *Jandufouria seamrogiformis*, *Magnastriatites*, sendo atribuída uma idade eocênica para estes depósitos. Os dados palinológicos apresentados por Maizatto (2001) também sugerem uma idade neoeocênica.

Com base nos trabalhos pioneiros de zoneamento palinológico de Regali *et al*. (1974a,b), duas biozonas palinológicas foram determinadas na Bacia de Fonseca: a biozona *Retibrevitricolpites triangulatus*, na base, seguida pela biozona *Dacrydiumites florinii*, no topo, ambas pertencentes à superzona palinológica *Cicatricosisporites dorogensis* (MAIZATTO, 2001). A biozona *Retibrevitricolpites triangulatus* foi identificada na base da Fm. Fonseca, tendo seu limite marcado pela extinção de *Margocolporites vanwijhei*, correspondendo ao Eoceno Superior (Figura 12). A biozona *Dacrydiumites florinii* ocorre no topo da Fm. Fonseca, onde se observa um aumento no número de espécimens de grãos de pólen vesiculados, correspondente ao Eoligoceno (MAIZATTO, 2001; MAIZATTO *et al.*,

2008).

Figura 12 – Unidades bioestratigráficas e cronoestratigráficas identificadas na bacia de Fonseca

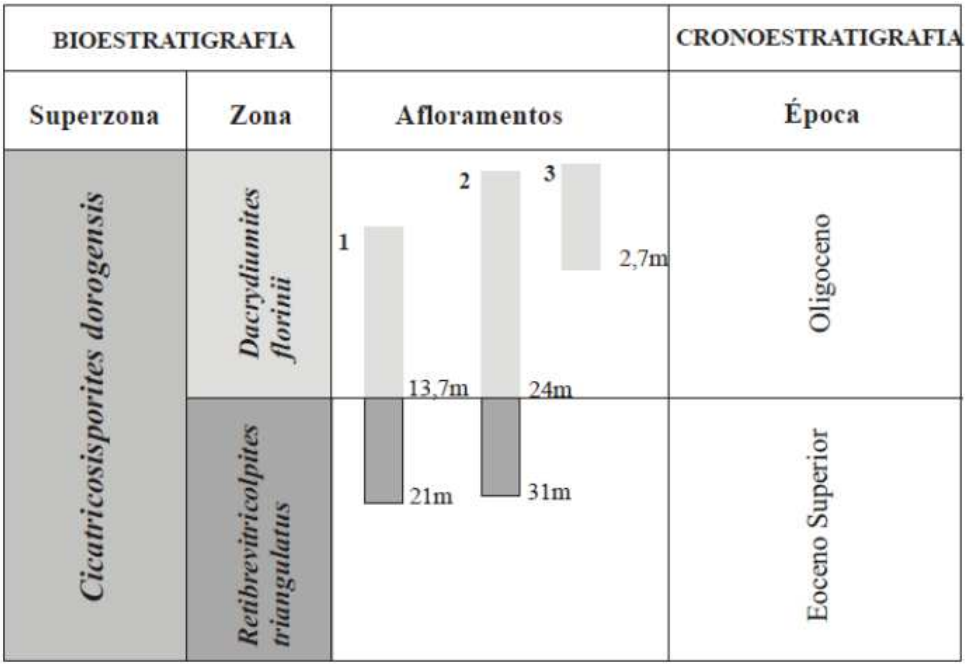

Fonte: Maizatto (2001).

Alguns dados paleotermocronológicos obtidos nos arredores da Bacia de Fonseca colocam em dúvida a idade de soterramento máximo desta bacia. Segundo estes dados, a deposição da Fm. Fonseca deve ter ocorrido entre os episódios de reativação tectônica ocorridos do Eoceno até o Mioceno, no final do Paleógeno, ou mesmo durante boa parte do Neógeno (JAPSEN *et al*., 2012). Entretanto, a hipótese de idade neoeocena–eoligocena para Bacia de Fonseca é considerada razoável por outros pesquisadores (FANTON, 2013; FANTON *et al.,* 2014; BITTENCOURT *et al.,* 2015).

2.1.3 Litologia e paleoambiente

Na seção colunar formalizada por Sant´Anna e Schorscher (1997), a Formação Fonseca é caracterizada por conglomerados, arenitos médios a grossos, arenitos finos, argilitos e siltitos com níveis fossilíferos e papiráceos. A análise faciológica apresentada por Maizatto (2001) reconheceu cinco fácies sedimentares na Fm. Fonseca descritas a seguir:

Fácies Conglomerado

A espessura desta fácies varia entre 15 e 70 cm e é constituída por conglomerados

oligomíticos, suportados por clastos de argila subarredondados à subangulosos (1-15 cm de diâmetro) associados a uma matriz arenosa com granulometria areia média a grossa.

Fácies Arenito Grosso

Fácies apresentando espessura variando entre 2 e 70 cm, composta de arenitos maturos formados por grãos de quartzo subarredondados com granulometria variando entre areia média à grossa com estratificações cruzadas e, provavelmente, estratificações acanaladas mal preservadas.

Fácies Arenito Fino

Esta fácies chega atingir até 6 m de espessura, e é constituída por arenito com grãos de quartzo subarredondados com granulometria areia fina a média, sendo observada a presença de estratificações plano-paralelas.

Fácies Argilito

Esta fácies apresentou uma espessura entre 2 cm e 1,2 m. O argilito apresenta coloração variando entre o vermelho e o branco, laminações planoparalelas e estruturas de boudinagem sedimentar.

Fácies Linhito

Apresentando até 1,1 m de espessura, esta fácies é representada por laminações bem desenvolvidas de linhito com intercalações milimétricas de siltito, onde foram observadas diversas impressões de folhas e outros restos vegetais carbonizadas bem preservadas.

O caráter granodecrescente ascendente e a predominância de sedimentos finos na sucessão de fácies da Fm. Fonseca permitiram a interpretação de um ambiente com canais fluviais meandrantes associados a planícies de inundação (SANT´ANNA e SCHORSCHER, 1997; MAIZATTO, 2001). Esse sistema de rios meandrantes se desenvolveu em um período de pouca movimentação tectônica e sob um clima quente e úmido, com intemperismo avançado das rochas de idades pré-cambrianas na área-fonte (SANT´ANNA e SCHORSCHER, 1997).

Em seu trabalho, Maizatto (2001) reconheceu diferentes associações verticais de fácies na Formação Fonseca: A sucessão das fácies conglomerado, arenito grosso, arenito fino e argilito foi interpretada como depósitos de canais ativos/ barra em pontal; a sucessão das fácies conglomerado, arenito fino, argilito, linhito e argilito foi interpretada como depósitos

de meandro abandonado; e a sucessão das fácies arenito médio a grosso, argilito e linhito foi interpretada como depósitos de planície de inundação. Maizatto (2001) também observou a preseça abundante de *Botryococcus braunii*, uma microalga verde, na fácies Linhito da Fm. Fonseca. A granulometria fina dos sedimentos e a abundância de algas verdes nos linhitos permitiram que Maizatto (2001) interpretasse esse paleoambiente como dulciaquícola raso, com baixa turbulência e baixa turbidez, tais como brejos, pântanos e lagoas. Após o rompimento do canal, os depósitos de planície de inundação caracterizam-se pela deposição de carga suspensa durante eventos episódicos de inundação, enquanto que areias finas e médias também se acumularam nos locais onde as correntes de inundação foram suficientemente fortes para transportá-las. As intercalaões de linhitos (turfas) e sedimentos finos são extremamente sugestivos de subambientes pantanosos relacionados com depósitos de planície de inundação.

2.1.4 Paleogeografia

O registro megafóssilífero da Formação Fonseca exibe uma diversidade alta, composto particularmente por angiospermas, sendo as eudicotiledôneas o grupo mais diverso (FANTON *et al*., 2012). Diferentes estudos demonstraram ainda a presença de Fabaceae (Caesalpinioideae e Mimosoideae), Bignoniaceae, Combretaceae, Euphorbiaceae, Lauraceae, Myrtaceae, Malpighiaceae, Meliaceae, Myrsinaceae, Sapindaceae, Sapotaceae, Siparunaceae Menispermaceae, Malvaceae, Melastomataceae e Annonaceae (FANTON *et al*., 2012; FANTON, 2013). Lima e Salard-Cheboldaeff (1981) e Maizatto (2001) também reportaram uma grande abundância de esporos de fungos e pteridófitas e uma alta diversidade de grãos de pólen de angiospermas. Essa macroflora é altamente representativa de acumulações modernas de folíolos em ambientes fluviais de florestas tropicais (RICARDI-BRANCO *et al*., 2009). Fanton *et al*. (2014) aplicaram diferentes modelos de Análise de Margem Foliar (LMA) e obtiveram um valor médio de paleotemperaturas em torno de 26,9ºC para a Fm Fonseca.

Maizatto (2001) observou que o universo polínico da Bacia de Fonseca durante o Neoeoceno apresentou uma contribuição mais expressiva de palinomorfos oriundos de plantas arbóreas, seguidos por palinomorfos associados a plantas arbustivas e herbáceas. Tal constatação corrobora um contexto de clima tropical quente e úmido, até o inicio do Eoceno. No entanto, Maizatto (2001) encontrou uma contribuição equivalente entre os palinomorfos produzidos por plantas arbóreas e arbustivas e, secundariamente, por plantas herbáceas durante o Oligoceno. Assim, as condições paleoclimáticas tropicais e subtropicais foram

inferidas nos depósitos da Fm. Fonseca, a abundância de esporos de fungos e pteridófitas atestam clima quente e úmido no Neoeoceno e uma oscilação para condições mais campestres durante o inicio do Oligoceno (contexto subtropical).

O registro palinológico e a distribuição dos depósitos de carvão durante o Paleoceno até o final do Eoceno indicam que as florestas paleógenas teriam evoluído em nível global em três cinturões latitudinais: equatorial, tropical norte e tropical sul (ZIEGLER *et al*., 2003). No cinturão tropical norte, há registros de florestas tropicais úmidas para o norte dos Estados Unidos durante o Eoceno (GREENWOOD e WING, 1995), enquanto que no cinturão tropical sul, há registros no sul da Argentina e Chile (WILF *et al*., 2003). As florestas tropicais úmidas no leste do Brasil devem ter experimentado invernos sem ou com pouco resfriamento, uma vez que naquele momento não havia frentes frias polares expressivas por causa da ausência de gelo nos pólos (ZIEGLER *et al*., 2003).

De acordo com Ziegler *et al*. (2003), do Paleoceno ao fim do Eoceno, existia um cinturão equatorial de florestas úmidas acompanhado por cinturões equivalentes em latitudes médias em ambos os hemisférios, embora a composição taxonômica de cada cinturão fosse distinta. Dessa forma, uma faixa de temperaturas tropicais cobriu cerca de dois terços do continente sul-americano durante o Eoceno. A Bacia de Fonseca foi depositada mais ou menos na paleolatitude 25°S (FANTON, 2013) e relativamente próximas à costa atlântica (leste do Brasil) e dentro do Cinturão tropical sul. Durante o final do Paleoceno, a porção mais meridional do Cinturão tropical sul ficou conhecida como província Neotropical (um conjunto fitogeográfico sul-americano baseado no registro microflorístico, proposto por Romero em 1993). A Bacia de Fonseca estava inserida na provìncia Neotropical onde Fabaceae, Malpighiaceae, Annonaceae, Malvaceae e Bignoniaceae eram constituintes importantes (ROMERO, 1993).

A separação entre América do Sul e Antártica, e a consequente abertura da passagem de Drake, afetou profundamente a circulação de massas oceânicas e atmosféricas, que culminou na grande glaciação Antártica do Cenozoico. Este evento ocorreu aproximadamente no limite Eoceno/Oligoceno (Priaboniano/Rupeliano, 34 Ma)(SCHER e MARTIN, 2006). Em decorrência, as florestas úmidas progressivamente se retraíram até atingirem os limites atuais e o Oligoceno é considerado como uma época de transição entre períodos de aquecimento e de resfriamento global, no final do Cenozoico (ZACHOS *et al*., 2008). Na Bacia de Fonseca, o registro de folhas fósseis parece indicar apenas condições tropicais quentes e úmidas, enquanto que o registro de palinomorfos apresenta uma importante oscilação climática na transição do Eoceno para o Oligoceno. Assim, as evidências

paleobotânicas da bacia apresentam um cenário fitogeográfico concordante para o Paleoceno e Eoceno da América do Sul, e com as reconstruções climáticas para a transição do Eoceno/Oligoceno.

2.1.5 Contexto Estrutural

A Bacia de Fonseca está inserida entre dois grandes conjuntos de estruturas tectônicas no contexto geológico do Quadrilátero Ferrífero: o primeiro é composto por dobras recumbentes regionais que formam os principais sinclinais responsáveis pelos itabirítos ricos em ferro do Supergrupo Minas (DORR, 1969; SCHORSCHER, 1992); O segundo conjunto de estruturas é representado por diferentes sistemas de falhas e lineamentos visíveis nas partes leste e sudeste da região (SANT´ANNA *et al*., 1997). O segundo conjunto afeta, particularmente, a Bacia de Fonseca na forma de falhas reversas variando de N-S/30-50”E a NW/40-50”NE (DORR, 1969), que causaram a imbricação do Supergrupo Espinhaço documentada nos quartzitos da Serra do Caraça, a oeste da Bacia do Fonseca (SCHORSCHER, 1980), e os lineamentos transcorrentes (NE e NW) de expressão regional (falhas de Fundão e rio Piracicaba) (Figura 6).

De acordo com SANT´ANNA *et al*. (1997), o Embasamento Pré-cambriano subjacente à Bacia do Fonseca exibe fraturas proeminentes em duas direções principais perpendiculares, uma geralmente N-S, variando ligeiramente de NNE-SSW a NNW-SSE, e a outra E-W (Figura 13). As falhas de orientação N-S e NW-SE são, por vezes, de expressão regional (SANT´ANNA *et al*., 1997). As rochas de Fonseca foram afetadas por falhas pós-sedimentares, principalmente normais, geralmente de NNE a NE. Algumas falhas normais mostram direções NE e NW. No limite norte da bacia, tais falhas normais podem compreender o contato basal da Formação Fonseca com rochas do embasamento.

Figura 13 – Mapa da região da Bacia do Fonseca: 1 - Embasamento Pré-cambriano; 2 - Formação Fonseca; 3 - Formação Chapada de Canga; 4 - Falhas principais. Diagramas estruturais: 5 - Juntas E-W e N-S nas rochas do Embasamento Pré-cambriano; 6(A) - Falhas com componente normal predominante cortando a Formação Fonseca e 6(B) diagrama com a posição de σ1 (vertical) e σ3 (NW-SE); 7(A) - Falhas com componente normal predominante cortando a Formação Fonseca e 7(B) diagrama com a posição dos eixos de tensão σ1 (vertical) e σ3 (NE-SW); 8 – Pólos representando o acamamento sedimentar da Bacia de Fonseca. 9(A) - Juntas no Embasamento Pré-cambriano e 9(B) na Formação Chapada de Canga, ambas com orientação preferencial N-S e E-W

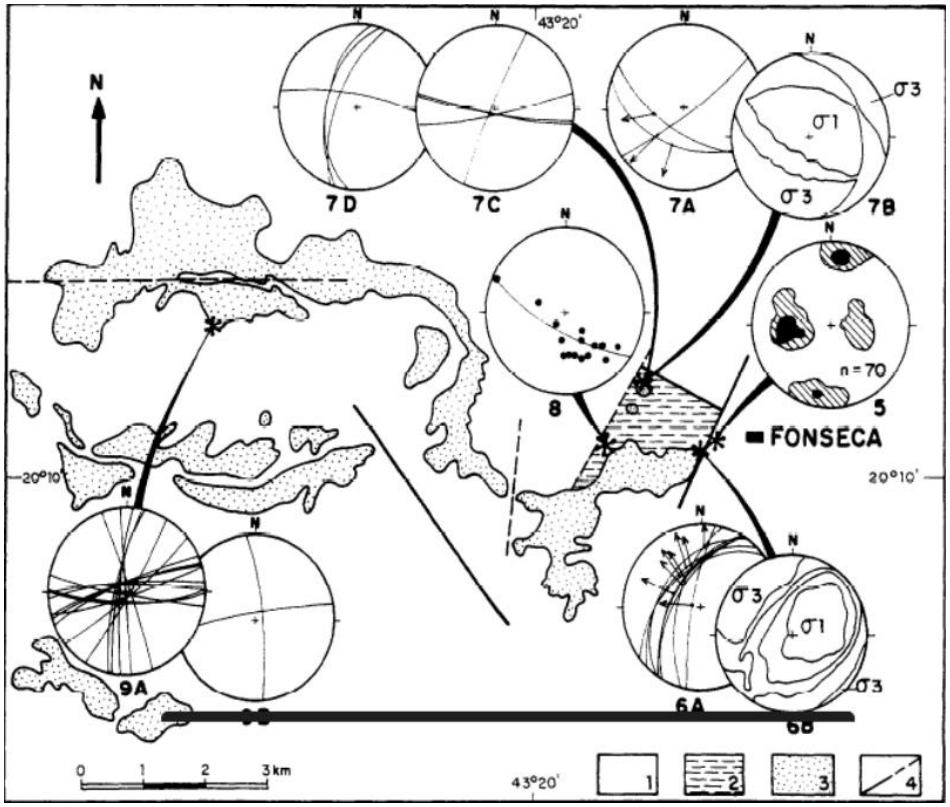

Fonte: Sant´Anna et al. (1997).

Na parte oeste da Bacia de Fonseca ocorrem microfalhamentos e estruturas que variam desde ondulações até microdobramentos nos estratos laminados. As dobras possuem plano axial orientado em torno de N30E e eixos mergulhando em ângulos baixos para NE. Sant´anna *et al*. (1997) atestaram que as dobras representam um movimento de arrasto relacionado a movimentos de falhas nas zonas limítrofes da bacia. Sant´anna *et al*. (1997) não encontraram evidências de tectônica sin-sedimentar na bacia. Por outro lado, os autores descobriram brechas nas rochas do Embasamento Pré-cambriano, que foram interpretadas como indícios de tectônica pré-sedimentar. Sant´anna *et al*. (1997) também buscaram correlacionar a evolução da Bacia de Fonseca com outras bacias do SE do Brasil, especialmente, aquelas do Rift Continental do Sudeste do Brasil (RICCOMINI, 1989). Entre essas unidades, os autores encontraram uma série de similaridades entre Fonseca e as formações São Paulo e Pindamonhangaba, que também foram depositadas em sistemas fluviais sinuosos durante períodos tectônicos calmos (RICCOMINI, 1989).

2.2 Contexto geológico da Formação Crato

2.2.1 Evolução estratigráfica da Formação Crato

O primeiro a nomear esta unidade como uma formação geológica distinta foi Beurlen (1963), porém, em trabalhos posteriores o autor voltou a se referir a esta unidade como membro (BEURLEN, 1971). Estas inconsistências perduraram até os anos 90, quando os primeiros trabalhos visando definir a estratigrafia da Formação Crato aparecem. Martill e Wilby (1993) destacaram uma série de localidades como potenciais seções tipo da Fm. Crato, na região entre os municípios de Nova Olinda, Santana do Cariri e Jamacaru. Em 1994, Berthou e colaboradores cunharam o termo *Crato lithological*, referente à natureza litográfica (granulação fina e homogenia) dos calcários.

A proposta de Martill e Wilby (1993) para subdividir a Fm. Crato, consistia em reconhecer o nível basal composto de calcários laminados como um membro a parte, eles nomearam esse nível de Membro Nova Olinda. Martill e Wilby (1993) também reconheceram outros dois membros distintos de calcários, o Membro Barbalha e, sobreposto a esse, o Membro Jamacaru. Berthou *et al.* (1994) dividiram a Fm. Crato em duas sub-unidades: *Crato Cascata Term* (inferior) que correspondia ao Membro Nova Olinda de Martill e Wilby (1993); e *Crato Bebida Term* (superior) que correspondia, mais ou menos, aos membros Barbalha e Jamacaru de Martill e Wilby (1993). Mais tarde, depois de uma série de campanhas de campo e a descoberta de novos afloramentos, Martill e Heimhofer (2007) apresentaram uma proposta mais elaborada de divisão da Fm. Crato (Figura 14). Essa proposta foi publicada no famoso livro *Crato Fossil Beds of Brazil*, lançado em 2007. Segundo os autores, a Fm. Crato pode ser dividida em quatro diferentes membros, da base para o topo: Membro Nova Olinda; Caldas; Jamacaru; e Casa de Pedra, sendo essa a divisão adotada neste trabalho (Figura 15).

Figura 14 – Diferentes perfis estratigráficos da Formação Crato ao redor da Bacia do Araripe

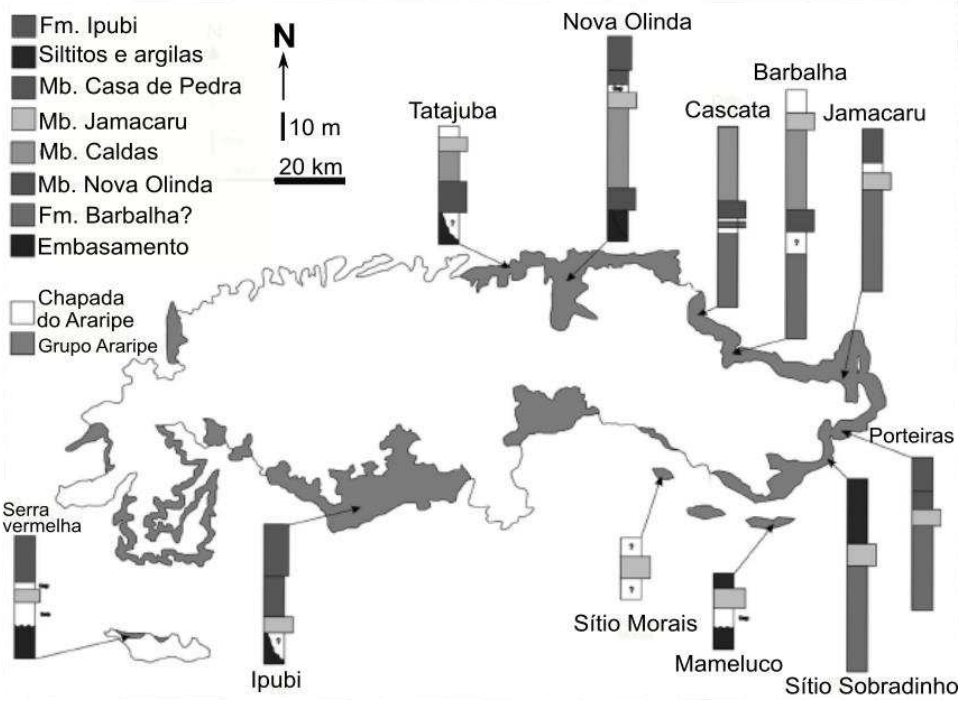

Fonte: Martill e Heimhofer (2007).

Figura 15 – Esquema mostrando os diferentes membros da Formação Crato, conforme a proposta de Martill e Heimhofer (2007)

GRUPO	FORMAÇÃO	MEMBRO	LITOLOGIA
ARARIPE	CRATO	**CASA DE PEDRA**	Folhelhos negros e arenitos finos
		JAMACARU	Calcário Laminado
		CALDAS	Siltitos, argilitos folhelhos negros e arenitos
		NOVA OLINDA	Calcário Laminado
		camadas de transição	
	BARBALHA		

Fonte: Martill e Heimhofer (2007).

O Membro Nova Olinda de Martill e Heimhofer (2007) corresponde ao substancial primeiro pacote de calcários milimetricamente laminados de tons bege e azulado, este membro tem entre 6 e 8 m de espessura em Nova Olinda (parte norte da bacia), mas pode atingir uma espessura máxima de 13-14 m em Tatajuba (parte noroeste da bacia). Estes calcários afloram fartamente em pedreiras nos arredores de Nova Olinda e Santana do Cariri, sendo também observados mais a leste próximo a Barbalha. O Mb. Nova Olinda hospeda o chamado Crato *Fossil Lagerstätte*, mundialmente famoso por ser uma associação fossilífera extremamente bem preservada e diversa (MARTILL *et al.,* 2007a). O Membro Caldas compreende folhelhos negros, siltitos, argilas, arenitos, calcários micríticos e horizontes ricos em ostracodes e conchostráceos. Esse membro tem sua seção tipo foi estabelecida na Mina Caldas e pode atingir 10 m de espessura (MARTILL e HEIMHOFER, 2007). O Membro Jamacaru retém o primeiro pacote de calcários laminados acima do Mb. Nova Olinda. O topo desta unidade é marcado pela presença de calcários silicificados, muitas vezes com pseudomorfos de halita substituídos por sílica. Apesar da semelhança litológica com o Mb. Nova Olinda, o Mb. Jamacaru não possui conteúdo fossilífero significativo. Em geral, esta unidade atinge quatro metros de espessura e pode ser observado no flanco oeste da bacia (Serra vermelha) até porções mais orientais como Sítio Sobradinho (MARTILL e HEIMHOFER, 2007). O Membro Casa de Pedra foi estabelecido na Mina Casa de Pedra, entre Trindade e Ipubi, no oeste de Pernambuco. Este Membro é composto por folhelhos negros ricos em pirita associados com arenitos finos, próximo do contato com os evaporitos da Formação Ipubi (MARTILL e HEIMHOFER, 2007). O Mb. Casa de Pedra é rico em ostracodes e fósseis de pequenos vertebrados (*Dastilbe* sp) também podem ser encontrados. A espessura desta unidade é dúbia, mas pode chegar aos 10 m ou mais (da SILVA, 1986, 1988).

2.2.2 Idade

A idade das unidades litoestratigráficas da Bacia do Araripe têm sido objeto de debate há décadas. Ponte e Appi (1990) foram uns dos primeiros a fazerem extenso uso de dados bioestratigráficos para a construção do primeiro arcabouço cronoestratigráfico da bacia. No entanto, os trabalhos de Arai *et al.* (2001) e Coimbra *et al.* (2002) foram os primeiros a propor um arcabouço bioestratigráfico detalhado para a Bacia do Araripe. Estes autores revelaram a presença de um grande hiato na sequência brasileira do Cretáceo Inferior, entre os andares Rio da Serra e Alagoas. Na Sequência Pós-Rifte I da Bacia do Araripe, Arai *et al.* (2001) e Coimbra *et al.* (2002) identificaram a biozona baseada em ostracodes do

aptiano/albiano superior *Cytheridea* spp. 201/218 e as palinozonas *Sergipea variverrucata* e *Cicatricosisporites avnimelechi* (Aptiano Superior). A Formação Crato corresponde à porção superior da palinozona *S. variverrucata*, enquanto que a palinozona *C. avnimelechi* ocorre na Formação Romualdo. A maioria das amostras provenientes da Formação Ipubi se mostrou estéril, sendo possível identificar apenas a ocorrência da biozona *Cytheridea* spp. 201/218, os palinomorfos observados não foram diagnósticos de nenhuma biozona (COIMBRA e FREIRE, 2021). No entanto, a Fm. Ipubi foi correlacionável à palinozona *C. avnimelechi* (COIMBRA *et al.,* 2002). Embora tenha se mostrado escasso em ostracodes, a abundância de palinomorfos permitiu posicionar a Formação Barbalha na palinozona *S. variverrucata* (COIMBRA *et al.,* 2002) (Figura 16). Outros autores também estudaram amostras provinientes da Formação Crato, e revelaram uma fauna autoctone de ostracodes do gênero *Harbinia*, que ocorrem associados com outros membros das famílias Darwinulidae e Limnocytheridae (SOUZA *et al*., 2017). Todos esses ostracodes são mencionados na literatura como espécies aptianas, ocorrendo no andar Alagoas (ANTONIETTO *et al.,* 2012; DO CARMO *et al.,* 2008; COIMBRA *et al.,* 2002), algumas espécies de *Harbinia* também podem ser registradas no Albiano (SOUZA *et al*., 2017).

Figura 16 – Distribuição das biozonas baseadas em ostracodes e palinozonas da Bacia do Araripe. Retângulo em vermelho destaca a palinozona *Sergipea variverrucata* e o retângulo azul destaca a palinozona *Cicatricosisporites avnimelechi*

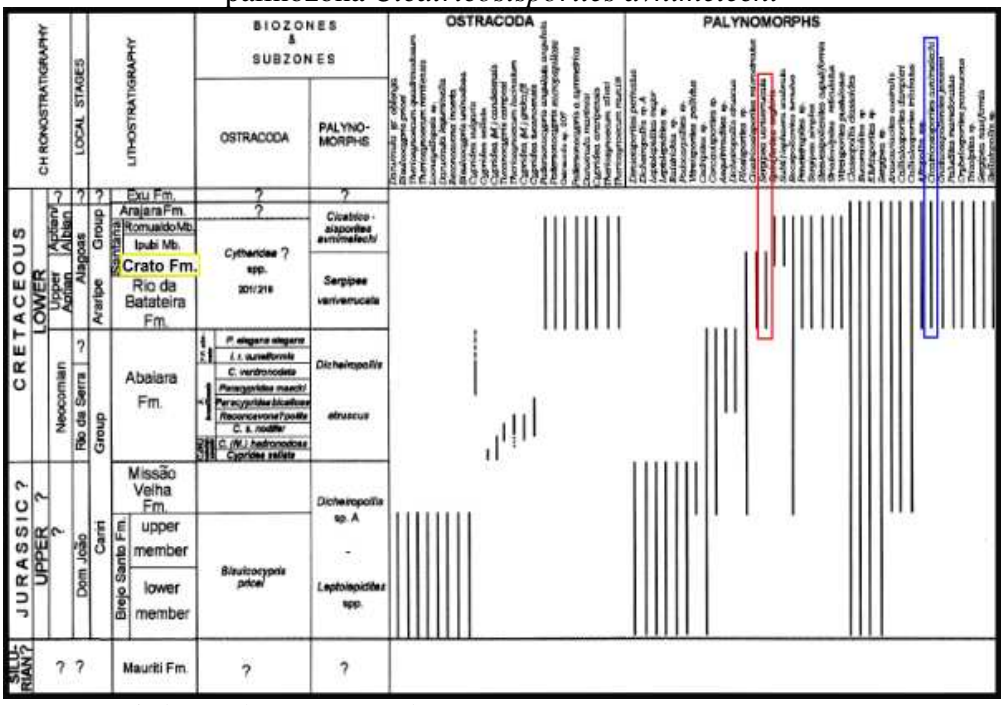

Fonte: Coimbra et al. (2002, com adaptações).

Recentemente, Arai e Assine (2020) realizaram um cuidadoso estudo palinológico em cerca de 40 amostras oriundas de uma seção conhecida como Sítio Sobradinho, uma seção bem completa, com cerca de 100 m de espessura, da Formação Romualdo. Neste trabalho, os autores destacam a completa ausência de palinomorfos exclusivamente albianos nesta seção. Melo *et al*. (2020) também analisaram o conteúdo de foraminíferos da mesma seção estudada por Arai e Assine (2020), os autores não identificaram nenhum táxon típico do Albiano. Desta forma, Melo *et al*. (2020) postularam que essa seção se restringe ao Aptiano, posicionada na palinozona *S. variverrucata* (Figura 17). Consequentemente, baseado nas pesquisas micropaleontológicas recentes, a Sequência Pós-rifte I inteira da Bacia do Araripe corresponde à palinozona *S. variverrucata*, a qual determina a parte superior do Aptiano nas bacias brasileiras.

Figura 17 – Esquema correlacionando os bioeventos estudados na Bacia do Araripe com outras zonas cronoestratigráficas em escala global e local. O retângulo laranja marca a seção estudada. Palinozona: 1. Bacia Sergipe-Alagoas; 2. quadro integrado; 3. Bacia do Araripe; Zona Ostracoda: 4. Bacia Sergipe-Alagoas; 5. Bacia Potiguar; 6. quadro integrado; 7. Bacia do Araripe; Foraminíferos Planctônicos: 8. Bacia de Sergipe; 9. DSDP (Projeto de Perfuração em alto Mar, furo 364 = Bacia de Angola); 10. Bacia Umbria-Mache; 11. ODP (Programa de Perfuração Oceânica, furo 1049C = Atlântico Norte e furo 511 = Planalto das Malvinas); 12. Bacia de Vocontii

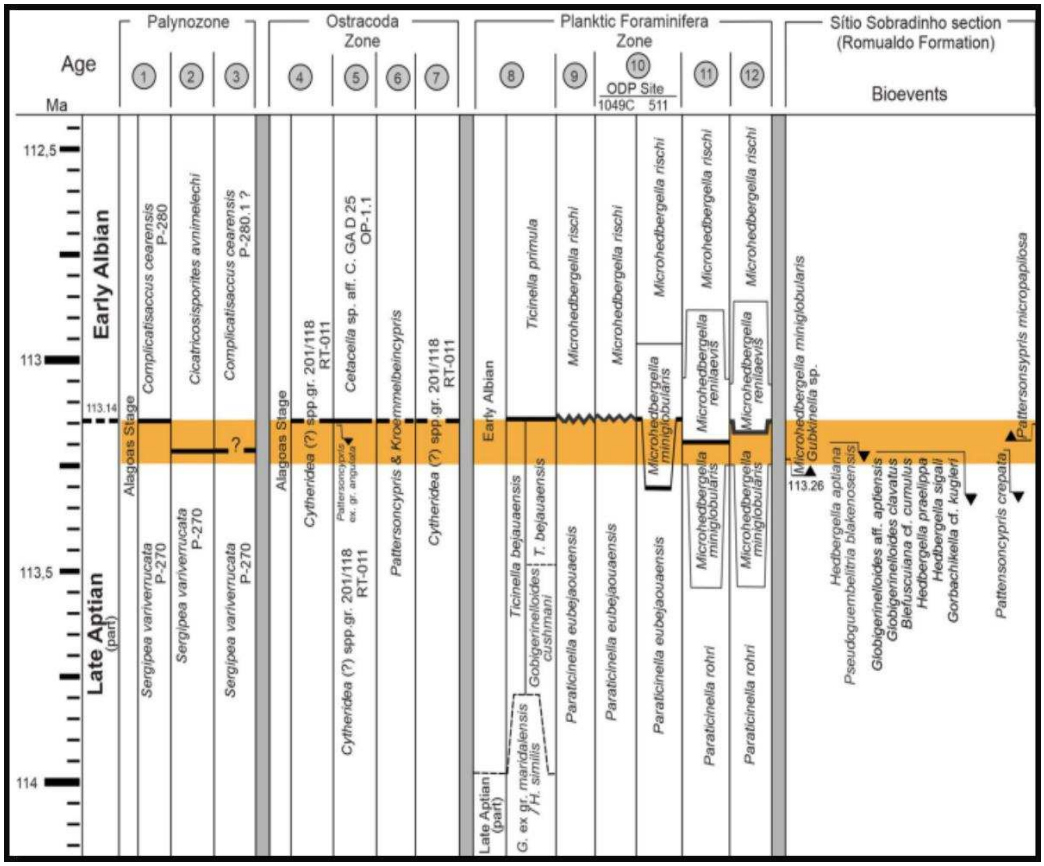

Fonte: Melo et al. (2020).

O debate sobre a idade da Sequência Pós-rifte I, consequentemente, da Formação Crato também foi centrado em análises radiométricas. Lúcio e colaboradores (2020) analisaram o conteúdo isotópico de Rênio e Ósmio (Re-Os) em nove amostras de folhelho negros da Formação Ipubi. Os autores registraram uma idade absoluta 123±3,5 Ma, posicionando os folhelhos negros entre o Barremiano Superior/Aptiano Inferior. Segundo Lúcio *et al.* (2020) os depósitos das formações Crato e Barbalha são de idade Barremiano Superior, enquanto que as formações Ipubi e Romualdo correspondem ao intervalo Aptiano/Albiano. Coimbra e Freire (2021) contestaram frontalmente a proposta publicada por Lúcio *et al*. (2020). De acordo com Coimbra e Freire (2021), a interpretação de Lúcio e colabodores (2020) apresenta várias inconsistências, e reiteram que o arcabouço bioestratigráfico das bacias do Nordeste brasileiro é bastante robusto, tanto no contexto da análise de bacias, quanto no contexto da estratigrafia de sequências.

2.2.3 Litologia e paleoambiente

A Formação Crato representa um registro de um sistema deposicional carbonático, predominantemente lacustre, constituído por seis níveis de calcários laminados, informalmente denominados C1 a C6 (Figura 18). De acordo com Neumann e Cabrera (1999), os níveis de calcários laminados são separados, tanto lateralmente como verticalmente, por níveis de arenitos, siltitos e folhelhos calcíferos:

- ✓ O nível C1 possui aproximadamente 1 m de espessura e só foi detectado no poço PS11 (região da borda norte da bacia). Este nível tem extensão total desconhecida e ocorre intercalado a camadas de folhelhos lacustres.
- ✓ O nível C2 subdivide-se em três sub-níveis: C2a, C2b e C2c. Este nível foi detectado no poço na borda norte da bacia (poço PS11), em testemunhos na região da Mina Caldas e na região do perfil do Rio da Batateira.
- ✓ O nível C3 foi registrado na Mina Caldas, no perfil do Rio da Batateira e nos testemunhos do poço PS-12 (borda sul da bacia). Este nível apresenta uma espessura de 5 a 10m, e extensão quilométrica.
- ✓ O nível C4 apresenta dois subconjuntos denominados C4a e C4b, onde o C4a é observado no poço PS-12 e o C4b é detectado no poço PS-11 e no perfil do Rio da Batateira.
- ✓ O nível C5 também ocorre dividido em dois sub-níveis, C5a e C5b. A parte basal

(C5a) foi detectada no poço PS-12, a parte intermediária foi observada na região da Mina Caldas, enquanto que o sub-nível superior (C5b) foi registrado no poço PS-11, no perfil do Rio da Batateira e na região de Nova Olinda.

- ✓ O nível C6 foi detectado em todos os perfis e poços executados para a estratigrafia da bacia na região da chapada e representa a sequência carbonática mais extensa da Formação Crato. Este nível corresponde essencialmente aos afloramentos de calcário laminado localizados na região de Nova Olinda.

Figura 18 – Esquema ilustrando a localização dos níveis carbonáticos da Formação Crato, conforme Neumann (1999)

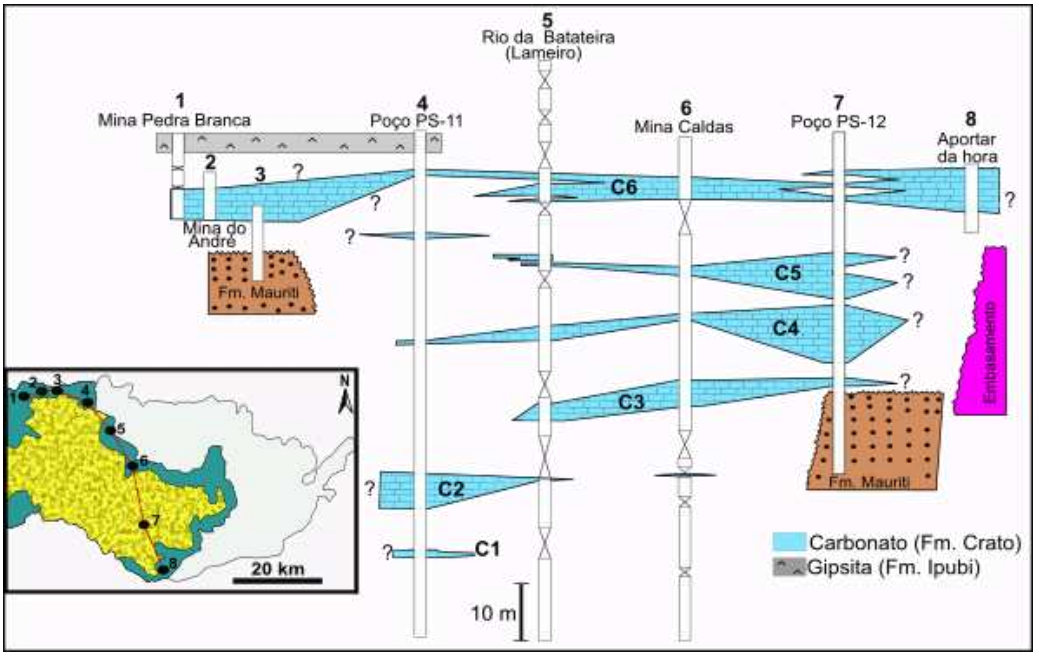

Fonte: Neumann (1999, com adaptações).

O nível C6 é caracterizado pela presença de calcários milimetricamente laminados, constituídos por carbonatos micríticos com baixo teor de magnésio (CATTO *et al.,* 2016). Heimhofer *et al.* (2010), propuseram que a origem destes calcários laminados se deu a partir da precipitação de calcita autigênica, presente na coluna d'água do paleolago Crato. Estes autores sugeriram que o processo de deposição dos carbonáticos foi induzido por organismos planctônicos na parte superior da coluna d'água, sem qualquer evidência de contribuição importante de comunidades microbiais bentônicas.

No entanto, nos últimos anos, alguns autores têm defendido que, de fato, os calcários laminados teriam sido produzidos pela mediação microbiana. Catto *et al.* (2016) apresentaram uma série de estruturas microscópicas que denotam produção de carbonato associado a filmes algálicos. A influência de microbialitos é evidenciada por estruturas

filamentosas e romboédricas de dimensões micro a nanométricas, relacionadas à ação de bactérias que desenvolveram o tecido polimérico característico de filmes algálicos (EPS) (CATTO *et al.,* 2016) (Figura 19). Posteriormente, Warren *et al.* (2017) publicaram o registro vários exemplos de estromatólitos (montículos, cúpulas e pseudocolunas) em níveis estratigráficos distintos na parte intermediária da Formação Crato (Figura 20). Os microbialitos possuem dimensões macro, meso e microscópicas, confirmando a existência de atividade metabólica de origem microbiana durante a formação dos calcários laminados. Recentemente, muitos autores têm defendido que a atividade microbiana desempenhou um papel importante na excelente preservação dos fósseis desta unidade (OSÉS *et al*., 2017; DIAS e CARVALHO, 2020).

Figura 19 – Micrografias obtidas a partir de amostras de calcário laminado da Formação Crato: A) Textura alveolar preservada na matriz carbonática relacionada à preservação do EPS (*Extracellular Polymeric Substance*), produzido em esteiras microbianas; B) Esferas calcíticas associadas à EPS (apontado pela seta); C) Filamentos calcificados; D) Aglomerados de cristais de pirita framboidal em meio ao biofilme

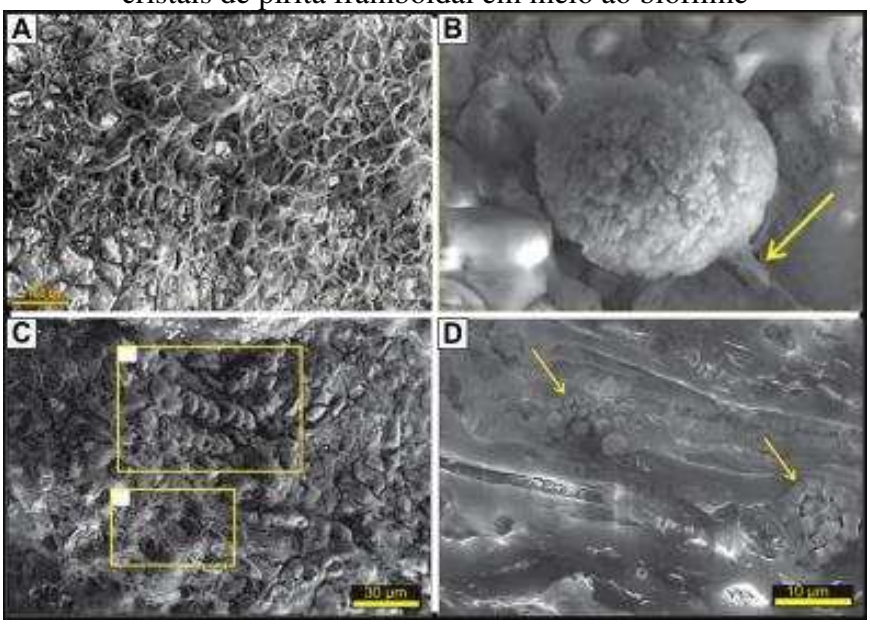

Fonte: Catto et al. (2016).

Figura 20 – Estromatolitos da Formação Crato: B) Seção estratigráfica composta de laminitos da Formação Crato com níveis de microbialitos; C) Seção estratigráfica composta de laminitos nas pedreiras de Nova Olinda, mostrando as posições dos níveis de estromatólitos. As bandas em cinza claro se correlacionam com os níveis de microbialitos nas duas localidades. M = mudstone ; W = wackestone; G = grainstone; B = boundstone

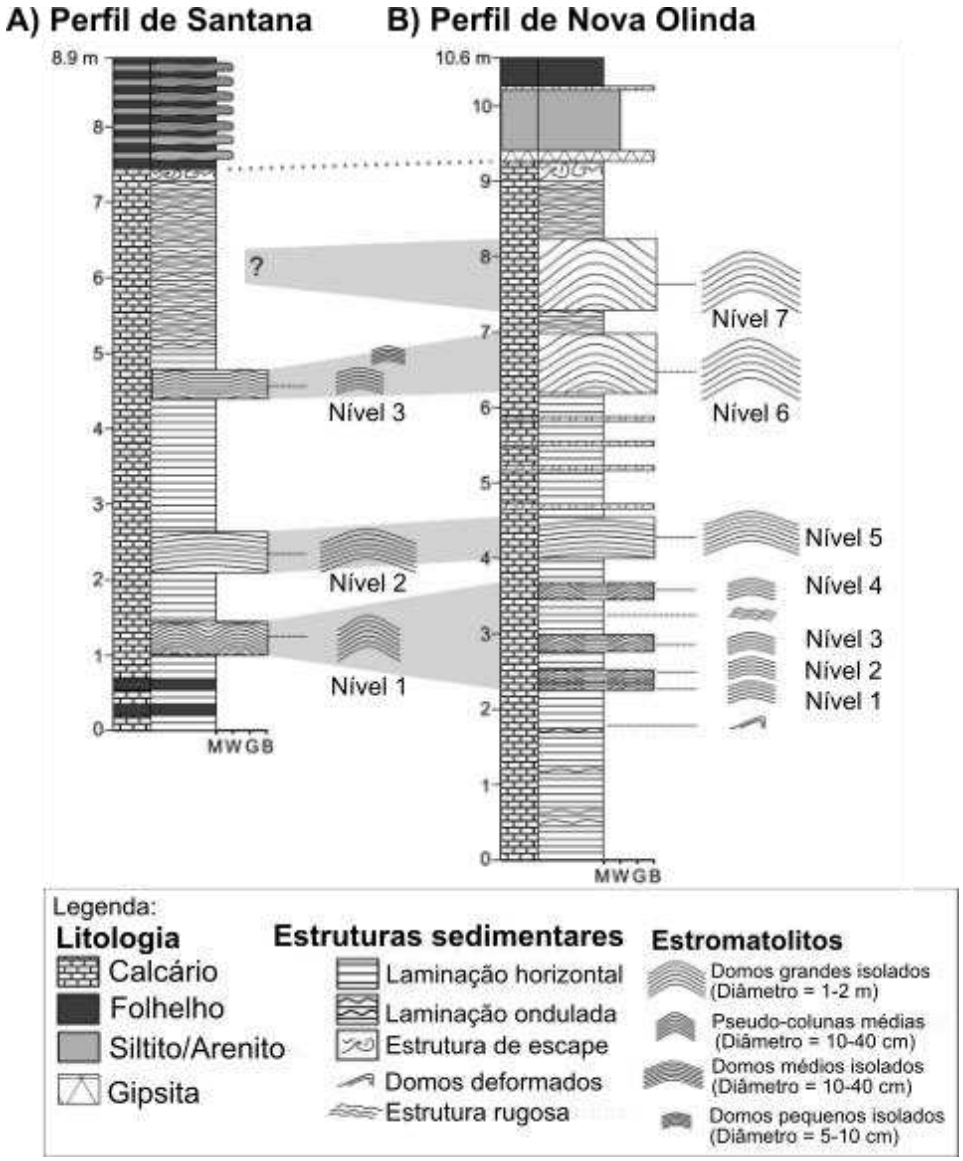

Fonte: Warren et al. (2017).

Heimhofer *et al.* (2010) também avaliaram a composição química dos calcários laminados através de Fluorescência de Raios-X, e identificaram um padrão de teores mais positivos de Fe e S nas lâminas escuras em relação às lâminas mais claras, de composição calcítica mais pura. De acordo com os autores, essa variação é atribuída a variações no nível da coluna d'água do paleolago Crato. Segundo o modelo de Neumann *et al.* (2003), a deposição dos calcários da Formação Crato foi controlada por diferentes episódios de subida e descida do nível d'água em um ambiente basinal restrito, onde as laminações escuras correspondem a momentos de início e término da fase de lago alto, enquanto que as laminações mais claras representam deposição na parte mais distal do sistema lacustre, durante a fase de lago alto. Heimhofer *et al.* (2010) também avaliaram a composição isotópica dos calcários e registraram assinaturas de $\delta^{18}O$ sugerindo uma fonte meteórica pobre em $\delta^{18}O$

(Figura 21). Os dados isotópicos apontam para um sistema não marinho para os calcários da Formação Crato, os valores de $\delta^{18}O$ obtidos são atribuíveis a reservatórios continentais de água doce (HEIMHOFER *et al.,* 2010). Na camada Caldas, um pouco acima estratigraficamente do principal nível de calcário laminado, Varejão *et al.* (2021a) encontraram valores de $\delta^{18}O$ aproximados aos de Heimhofer *et al.* (2010). A composição isotópica associada à composição paleontológica da camada Caldas, também indica sistema lacustre (VAREJÃO *et al.,* 2021a). No entanto, vale ressaltar que os valores isotópicos registrados nestes depósitos podem ser derivados de fluídos meteóricos de origem telodiagenética (SILVEIRA *et al*., 2023; VAREJÃO *et al*., 2021b).

Figura 21 – Valores de isótopos estáveis de C e O obtidos a partir de três amostras de calcário laminado oriundas de uma pedreira em Tatajuba-CE

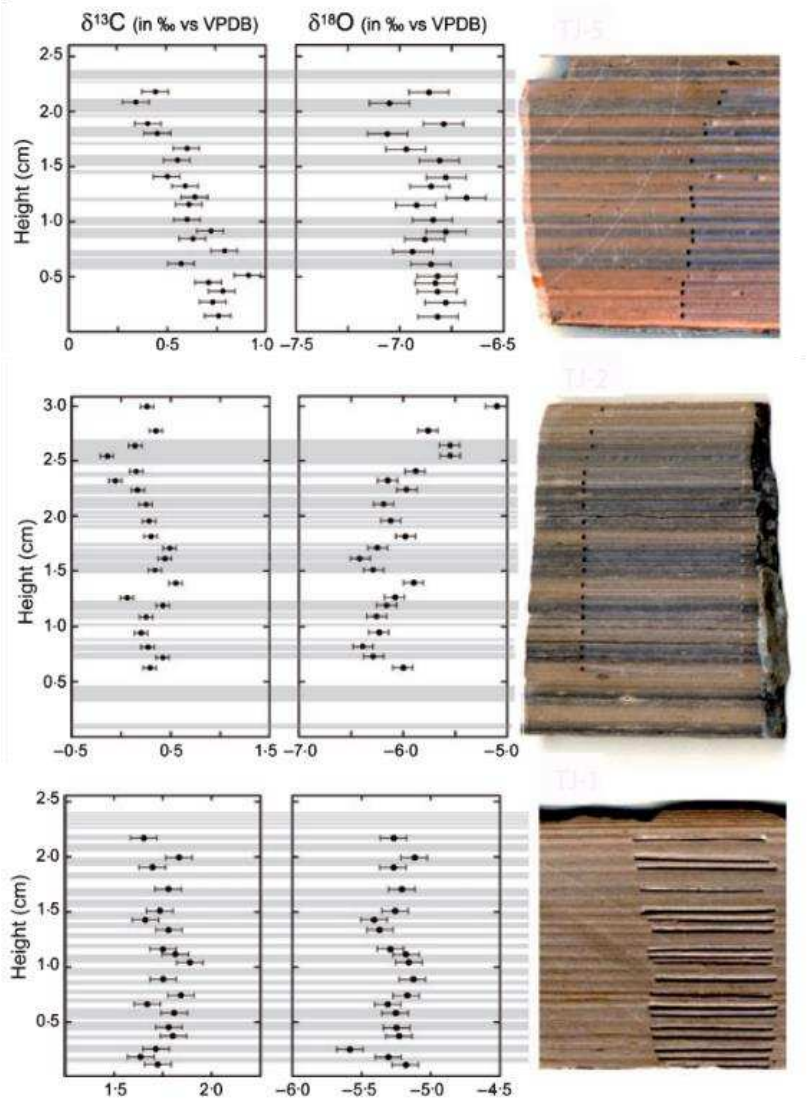

Fonte: Heimhofer et al. (2010).

Muitos autores defendem que a deposição dos laminitos da Formação Crato

ocorreu sob condições protegidas de baixa energia devido à ausência de estruturas de correntes e predomínio de laminações horizontais (NEUMANN, 1999; NEUMANN *et al.,* 2003; HEIMHOFER *et al.,* 2010). O não registro de níveis bioturbados nos calcários tem sido justificado pela ocorrência de condições anóxicas na interface água – sedimento no fundo do paleolago Crato (NEUMANN *et al.,* 2003; MARTILL *et al.,* 2007a). Segundo Neumann *et al.* (2003), a deposição da sequência lacustre da Fm. Crato foi afetada por ciclos de aridez e maior umidade, e a presença de pseudomorfos de halita (NaCl) nos calcários registram momentos de hipersalinidade e diminuição da entrada de água doce no lago (NEUMANN, 1999). Martill *et al*. (2007b) observaram variados tipos de cristais de halita, indicando condição de aridez extrema nesta unidade (Figura 22). A dinâmica ambiental desse sistema também pode ser verificada pela presença de ostracodes das famílias Cyprididae, Limnocytheridae e Darwinulidae, que evidenciam condições variáveis de salinidade (SOUZA *et al*., 2017). Cyprididae e Darwinulidae se proliferam em ambientes mais salinos, portanto, são consideradas tolerantes a variações de salinidade (DO CARMO *et al.,* 1999), já Limnocytheridae tendem a apresentar melhor desenvolvimento em ambientes com condições hipohalinas (DO CARMO *et al.,* 1998). Recentemente, Varejão *et al.* (2021b) posicionaram o principal nível de calcário laminado dentro do conjunto de fácies *FA-4* (lago hipersalino), essa seção é interpretada pelos autores como um sistema lacustre hipersalino de águas rasas que favoreceram o crescimento de esteiras microbianas. Este sistema salino foi continuamente se expandindo até ser sucedido pela associação de fácies *FA-5*, interpretado como um sistema lacustre de água doce caracterizado pela abundância de uma biota não marinha (VAREJÃO *et al.,* 2021b).

Figura 22 – Diferentes tipos de pseudomorfos de halita encontrados nos calcários laminados da Formação Crato: A) Estrela com estruturas concêntricas de colapso (tipo 1); B) Cristal formado pela substituição de marcassita, parcialmente colapsado (tipo 2); C) *Hopper* (molde) de halita vazia (tipo 3); D) Pseudomorfo zonado com núcleo de quartzo bordejado por calcita esferoidal (tipo 4); e E) Cristal formado pela substituição de sílica apresentando crescimento sintaxial (tipo 5)

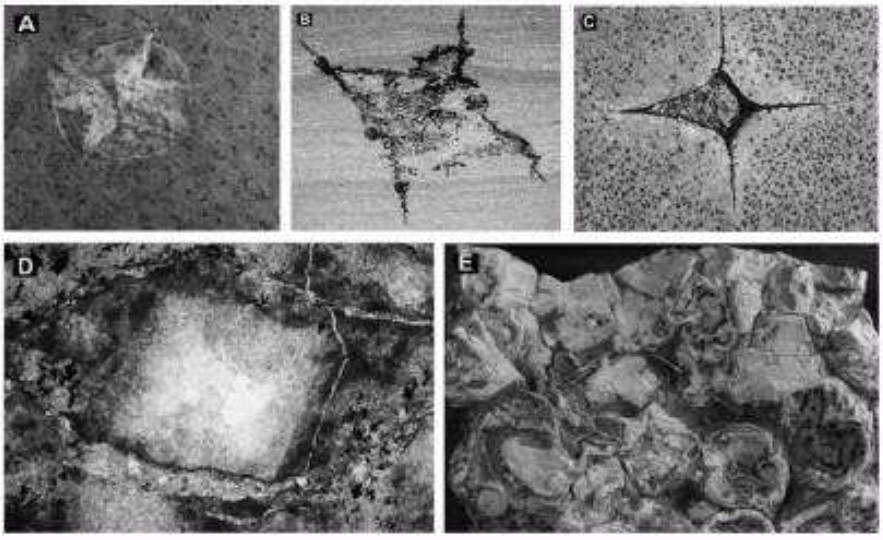

Fonte: Martill et al. (2007b, com adaptações).

2.2.4 paleogeografia

A reconstrução paleogeográfica do intervalo Aptiano-Albiano do nordeste do Brasil sempre foi controversa, sendo a Formação Crato de papel fundamental neste debate. É consenso que este intervalo representa um ciclo trangressivo-regressivo influenciado por eventos de ingressões marinhas, cuja sedimentação é controlada pela separação da América do Sul e a África. No entanto, são aventados pelo menos três sentidos diferentes para ingressão marinha na Bacia do Araripe durante o intervalo Aptiano-Albiano: a partir da Bacia Potiguar, a nordeste; a partir da Bacia do Parnaíba, a noroeste e a partir da Bacia Sergipe-Alagoas, a sudeste.

Arai (2007) usou principalmente dinoflagelados para reconstruir a paleogeografia da Sequência Aptiana-Albiana. Os dinoflagelados são preferencialmente plataformais e vivem em baixas e médias latitudes, sendo mais diversificados em águas tropicais do que em temperadas (WALL *et al.,* 1977). Baseado nestas características ecológicas, Arai (2007) propôs zonas climáticas oceânicas, paleocorrentes marítimas e barreiras fisiográficas para explicar a distribuição das espécies durante o Cretáceo Inferior do Nordeste brasileiro. Arai e Coimbra (1990) registraram ostracodes, pólens do tipo *Classopolis*, dinoflagelados do gênero *Subtilisphaera* e *Spiniferites*, foraminíferos bentônicos e microforaminíferos em testemunhos oriundos da parte mais basal da Formação Romualdo. Estes autores observaram uma abundância de dinoflagelados em estratos abaixo da Formação Romualdo, o que indicaria a ocorrência de ingressão marinha antes da deposição da Formação Romualdo. Neste mesmo estudo, os autores identificaram alta densidade de carapaças fechadas de ostracodes em

diferentes estágios ontogenéticos, o que sugere morte súbita, provavelmente, causada pelo aumento de salinidade devido à entrada do mar transgressivo e, consequentemente, aumento populacional de dinoflagelados.

Arai (2009) pondera que o processo tectônico notoriamente evoluiu do sul para o norte, porém a entrada do mar nas bacias do Nordeste ocorreu de norte para sul (Figura 23). O autor sustenta sua hipótese, principalmente na Ecozona de *Subtilisphaera*, que globalmente é diacrona, mas no Brasil é exclusivamente do Aptiano. A distribuição geográfica desta Ecozona é restrita basicamente as paleolatitudes 20º nos hemisférios Norte e Sul, além disso, essa Ecozona é mais proeminente nas bacias de São Luís, Parnaíba e Araripe e menos acentuada nas bacias Potiguar e Sergipe-Alagoas, indicando ingressão marinha via norte. Arai (2009) postula que a principal diferenciação paleobiogeográfica no Aptiano ocorreu por consequência de barreiras físicas como a Dorsal São Paulo (DSP), que atuou separando o Atlântico Sul em dois compartimentos: o Setentrional e o Meridional. As barreiras devem ter sido eficientes em separar os compartimentos até, pelo menos, o final do Aptiano e início do Albiano (ARAI, 2009).

Figura 23 – Mapa paleogeográfico do Aptiano Superior mostrando a separação do Nordeste brasileiro e a África. As áreas em cor violeta representam as principais bacias evaporíticas; a linha vermelha representa um alto estrutural (barreira); os círculos vermelhos (A – J) são ocorrências da Ecozona *Subtilisphaera* que sugerem influência tetiana; os círculos amarelos (L – M) são ocorrências de palinofloras marinhas tipicamente austrais; e o círculo azul (K) corresponde à ocorrência de radiolários da Formação Areado. A) Morocco; (B) Senegal; (C) Bacia Maracaibo, Venezuela; (D) Bacia de São Luís; (E) Bacia do Ceará; (F) Bacia Potiguar; (G) Bacia do Parnaíba; (H) Bacia do Araripe; (I) Bacia de Almada; (J) Bacia de Sergipe; (M) Bacia de Pelotas; (L) Río Fosiles, Argentina. NSA = Atlântico Sul Setentrional; SSA = Atlântico Sul Meridional

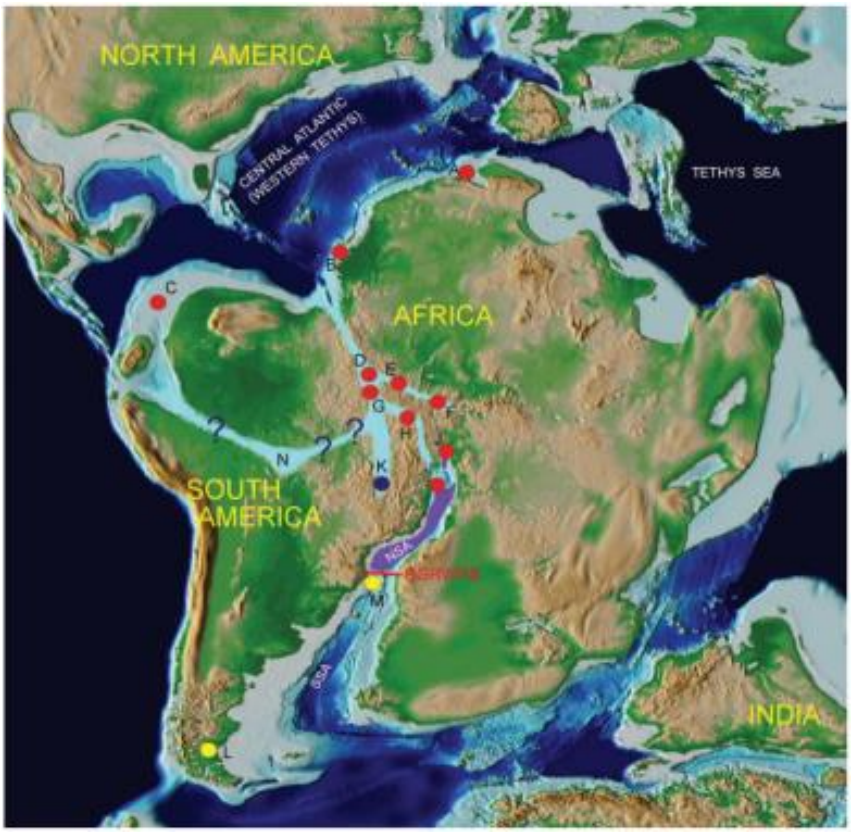

Fonte: Arai (2014, com adaptações).

Em sistemas deposicionais continentais, a topografia do terreno controla a direção do fluxo das águas em superfície, assim, do ponto de vista geológico, as medidas de paleocorrentes indicam o mergulho das camadas e, consequentemente, a paleodrenagem continental à época da sedimentação. Utilizando medidas de paleocorrentes obtidos em diferentes afloramentos da Bacia do Araripe, Assine (1994) observou que as paleocorrentes fluviais da Formação Barbalha e Marizal (bacias do Araripe e Tucano norte, respectivamente), indicam paleodrenagem para sul e sudeste. Assim, baseado nestes dados, a ingressão marinha teria ocorrido de sul-sudeste para norte-noroeste, uma vez que, a ingressão ocorre exatamente no sentido oposto ao da paleodrenagem continental. Dessa forma, tem-se aqui um novo paradigma. Assine (1994) sugere que o mar teria alcançado a Bacia do Araripe a partir da Bacia Sergipe – Alagoas, constituindo um *onlap* de leste para oeste. A ausência de estratos pertencentes às formações Barbalha e Crato (base do Grupo Santana) do lado oeste dão suporte para as alegações de Assine (1994). Tal constatação também sugere a presença de um alto estrutural na região de Araripina, também chamado plataforma Araripina (PONTE FILHO e PONTE, 1992)(Figura 24). A plataforma Araripina teria sido eficaz até quando a ingressão aptiana-albiana alcançou seu máximo e os sedimentos do Grupo Santana passam para o lado oeste da bacia, materializando extensas jazidas de gipsita e concreções

carbonáticas fossilíferas. Subsequentemente, durante o Albiano, a Bacia do Araripe retorna as condições continentais, o que é devidamente registrado nos arenitos fluviais da Formação Exu, cuja paleodrenagem indica fluxo para oeste-sudoeste rumo a Bacia do Parnaíba (ASSINE, 1992, 1994). Portanto, considerando os dados de paleocorrentes do intervalo Aptiano-Albiano, a paleodrenagem da Bacia do Araripe fluía para sul. Souza *et al*. (2022), baseado em dados de proveniência obtidos a partir de minerais de zircão, sugerem uma conexão entre a Bacia do Araripe e o Atlântico Equatorial através da Bacia Potiguar a nordeste, durante o Aptiano Superior. Independentemente de qualquer hipótese apresentada, é inquestionável que a primeira ingressão marinha na Bacia do Araripe ocorreu no tempo correspondente à Palinozona *Sergipea variverrucata* durante o final do Aptiano, pois essa palinozona ocorre em, praticamente, todas as bacias do Norte e Nordeste do Brasil.

Figura 24 – Mapa paleogeográfico do Nordeste do Brasil durante o intervalo Aptiano-Albiano, baseado em paleocorrentes de depósitos fluviais, bem como as drenagens resultantes das três bacias hidrográficas e o provável caminho das ingressões marinhas

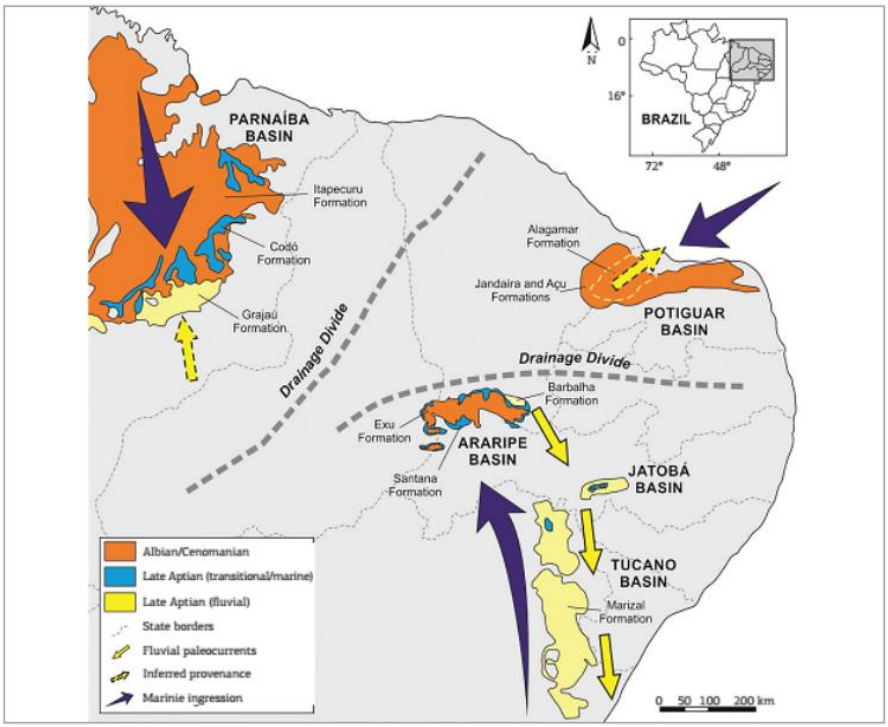

Fonte: Assine et al. (2016).

2.2.5 Contexto estrutural

A Formação Crato é constituída principalmente pelas litofácies de ritmito argila-carbonato (submicrofácies Sm1) e calcário laminado (NEUMANN e CABRERA, 1999).

Estas litofácies registram estruturas de microfalhas e microdeformações associadas as seguintes submicrofácies: Sm2, lâminas onduladas do tipo *loop bedding*; Sm3, lâminas com pelóides; Sm4, lâminas onduladas do tipo *microslumps* e *microripples*; Sm5, lâminas plano paralelas; e Sm6, horizontes ricos em ostracodes. Todo esse pacote sedimentar foi submetido a processos deformacionais em escala regional e local.

Um dos primeiros pesquisadores a estudar as características estruturais da Formação Crato foi Silva (2003). Em seu trabalho, Silva descreveu três padrões principais de estruturas deformacionais que ocorrem nos calcários laminados: microfalhas rúpteis-dúcteis distencionais, microfalhas dúcteis-rúpteis compressionais e falhas normais. Silva (2003) nomeou estes eventos deformacionais como D1, D2 e D3. O estágio D1 foi responsável pela formação dos *loop beddings*, *microslumps* e microfalhas normais que ocorrem em alguns níveis das unidades carbonáticas. Esse evento de pequeno porte, possivelmente foi causado por pequenos sismos. Os níveis ainda inconsolidados apresentaram deformação rúptil-dúctil em resposta a pulsos sísmicos esporádicos, seguidos por intervalos de calmaria tectônica. O evento D2 é marcado por movimentos compressionais que afetaram todo o pacote sedimentar da Formação Crato. Por fim, o evento D3 é caracterizado pela presença de falhas normais, o que indica o retorno das condições distensivas da bacia, desta vez, os movimentos extensivos foram mais intensos do que os registrados durante o evento D1.

Em 2008, Martill e colaboradores descreveram estruturas verticais e sub-verticais semelhantes a “pipes” (*pipe-like*) compostos por dolomita nos arredores de Nova Olinda. No entanto, a gênese destes *pipes* não foi satisfatoriamente esclarecida pelos autores. Um trabalho muito mais completo sobre o contexto estrutural da Formação Crato foi apresentado por Miranda *et al.* (2018), no estudo, os autores apontam que as fraturas cisalhantes e extensionais são as principais estruturas identificadas nos calcários laminados (Figura 25). Os autores também foram capazes de documentar que essas fraturas ocorrem em dois conjuntos principais: o conjunto 1, de direção preferencial NNW-SSE; e o conjunto 2, de direção preferencial NE-SW. A maioria das fraturas extensionais ocorre como veios verticais preenchidos por calcita ou gipsita.

Figura 25 – Padrão de fraturamento em laminitos da Formação Crato. A) Quadro mostrando a densidade de fraturamento por metro em pedreira de calcário laminado. B) Diagrama apresentando modelo conceitual de feições estruturais dos laminitos da Formação Crato. Fc - fratura cisalhante; St - estilolito; Vv - veio vertical; J - junta; Vh - veio horizontal; Fv - fratura não preenchida

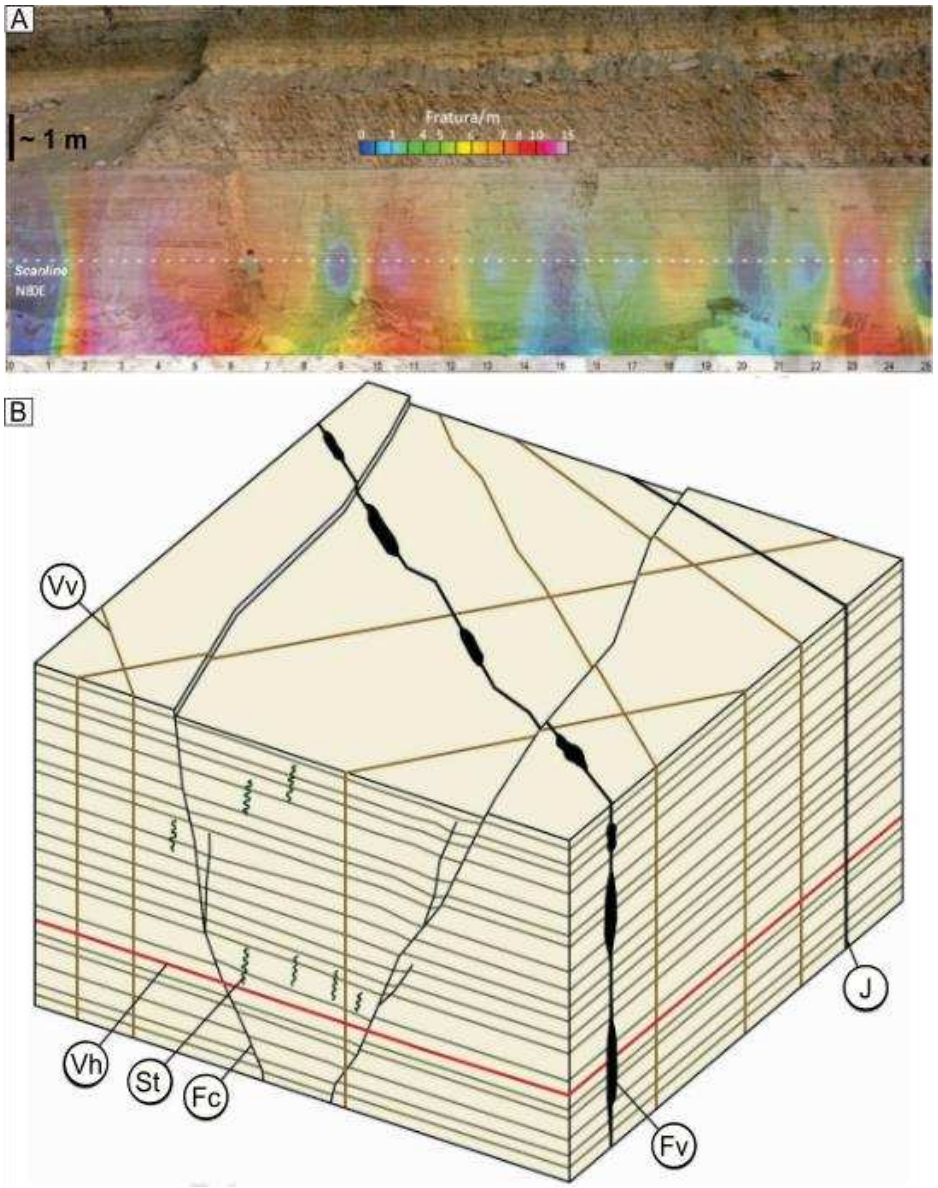

Fonte: Miranda et al. (2012, com modificações).

2.3 Tafonomia e paleoecologia

A primeira definição de tafonomia foi concebida por Efremov (1940) como “a ciência das leis do soterramento”. Contudo, o conceito original de tafonomia de Efremov incluía muito mais do que o mero soterramento de restos orgânicos; ele claramente pretendia que a ciência incluísse outros processos ambientais que interagem com os restos orgânicos ao longo de toda a sua história *postmortem*. Nesse contexto, a tafonomia contribui com um aspecto muito importante dentro da paleontologia (Figura 26), pois os atributos individuais dos fósseis como sua ecologia, paleobiogeografia e evolução só podem ser compreendidos com o conhecimento da história pós-morte dos organismos. Segundo Lawrence (1979),

tafonomia é a disciplina que permite aos paleontólogos fornecer “vida após a morte” aos organismos antigos.

Figura 26 – Eventos importantes na história de um organismo e a relação com os conceitos de tafonomia

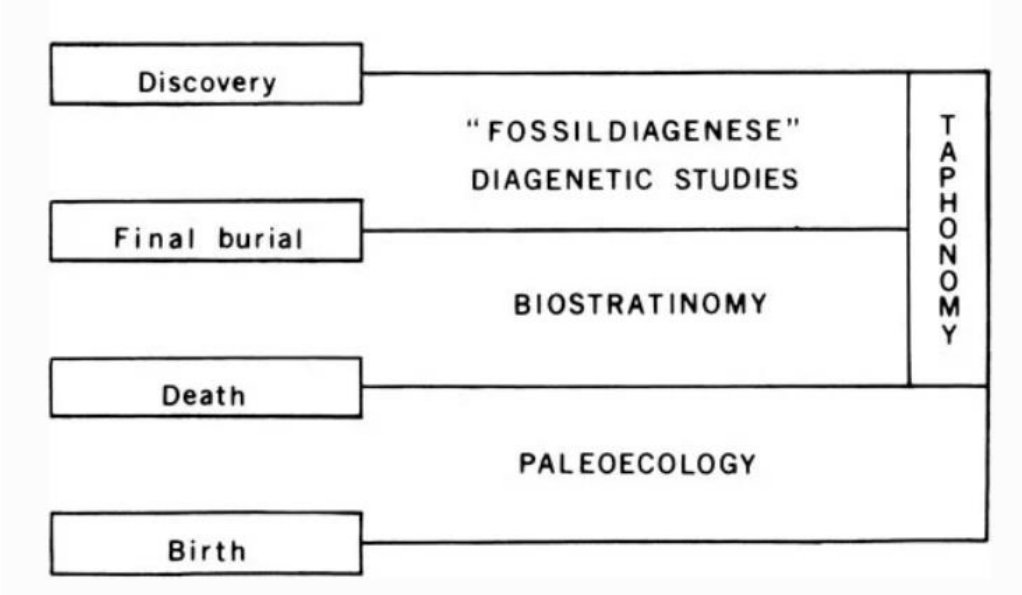

Fonte: Lawrence (1968).

Nas primeiras décadas do século XX, os cientistas europeus reconheceram quatro eventos importantes na história de um determinado fóssil: nascimento, morte, soterramento final e ser encontrado por um cientista. A importância da morte, soterramento final e escavação é refletida em termos mais amplamente usados para conjuntos fósseis: *tanatocenose*, para organismos que morreram juntos, *tafocoenose*, para restos que foram enterrados juntos, e *orictocoenose*, para restos que foram encontrados juntos em afloramento (HECKER, 1965; SARTENAER, 1959). A disciplina expandiu-se rapidamente na segunda metade do século XX em resposta a novas questões sobre ambientes deposicionais. Johannes Weigelt é reconhecido pela influência na tafonomia dos vertebrados e por lançar as bases da compreensão atual de "biostratonomia", o estudo dos processos que operam em restos orgânicos desde o momento da morte até sua integração no registro geológico. A ampla aplicabilidade da obra de Weigelt decorre de sua preocupação com os processos de decomposição e soterramento, que ele observou em ambientes contemporâneos como um meio para entender a formação de registros fósseis. Por sua vez, A. H. Müller estudou os efeitos da diagênese após o soterramento dos restos orgânicos, ou seja, as transformações geoquímicas, incluindo substituição mineral que ocorre durante a fossilização, esses trabalhos

fundamentaram o conceito de fossildiagênese (STINER, 2008).

Os estudos envolvendo tafonomia tendem a focar em conjuntos de espécimes, e não na história de espécimes isolados, já que o primeiro é uma fonte mais rica de informações sobre o passado. A maioria das observações também detalha o contexto sedimentar no qual se encontra aquela associação fossilífera. Os dados são então examinados em conjunto para elaboração de um diagnóstico de danos, distribuições espaciais e outras indicações. Como a história de cada objeto em um conjunto pode diferir um do outro, as avaliações gerais da formação do conjunto tendem a ser complexas e são construídas a partir de argumentos de probabilidade. Assim, os levantamentos tafonômicos buscam não apenas identificar os agentes dominantes e secundários de uma determinada associação fóssil, mas também a sequência de eventos que resultaram naquela acumulação fossilífera. Portanto, quanto maior o tempo de formação de uma associação fossilífera, maior a probabilidade de que múltiplos fatores tenham contribuído para moldar o caráter geral desse agrupamento. Em suma, os tópicos comuns abordados na pesquisa tafonômica são; composição das populações fósseis, tamanho e forma das carcaças, influência de correntes de água ou gravidade na orientação dos fósseis, alterações químicas provocadas por sedimentos ou água ao redor das carcaças, danos superficiais resultantes da mastigação ou digestão por outros animais, por raízes de plantas ou exposição atmosférica ('intemperismo')(STINER, 2008).

Outro fator importante a ser considerado na tafonomia é a limitação do registro fossilífero. Mesmo as camadas sedimentares mais ricas em conteúdo fossilífero não refletem em 100% a diversidade de fauna e flora que outrora habitara ali. Uma análise excelente da limitação do registro fóssil foi fornecida por Clark e Kietzke (1967) em seu estudo sobre as coleções de mamíferos do Oligoceno da Dakota do Sul. Eles assinalaram sete grupos de fatores que determinaram se um determinado mamífero se tornaria ou não um espécime identificado em suas coleções. Esses fatores foram associados com: (1) atributos de vida dos organismos, (2) sua morte, (3) a decomposição dos cadáveres, (4) soterramento, (5) exposição subsequente, (6) técnicas de coleta e (7) métodos de preparação e curadoria (Figura 27). Logo, Clark e Kietzke identificaram diferentes fontes de vieses e erros que nos limitam conceber, em sua totalidade, a diversidade da vida durante períodos geológicos passados.

Figura 27 – Relação entre coleções de fósseis, faunas e floras antigas, mostrando que apenas uma parte da diversidade outrora viva pode ser observada

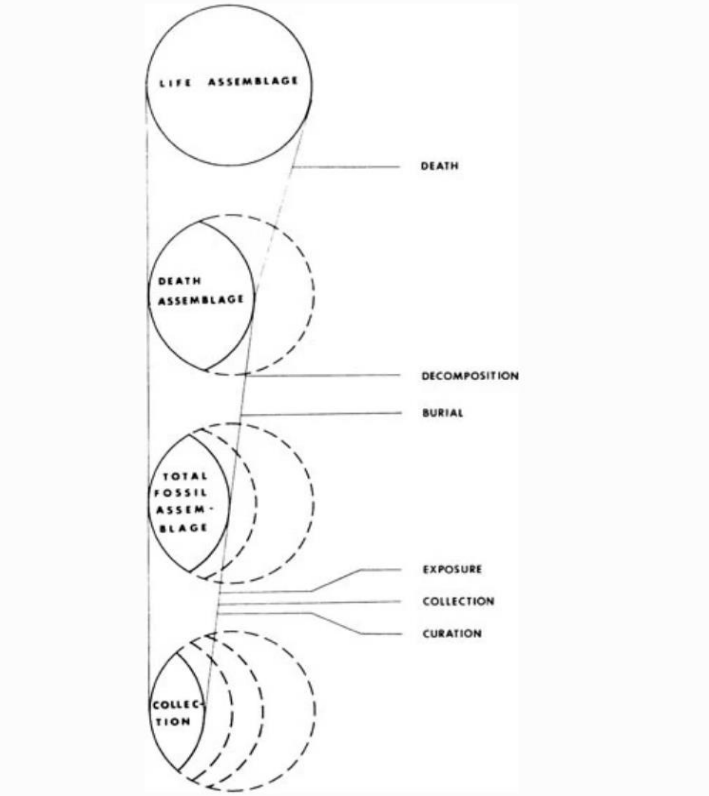

Fonte: Clark e Kietzke (1967).

Nos últimos anos, o desenvolvimento e disponibilidade de técnicas analíticas de alta resolução como microscopia eletrônica de varredura, fluorescência, espectroscopia, microtomografias etc, expandiram muito os estudos sobre fossildiagênese. Esta área de pesquisa tafonômica tem desenvolvido cada vez mais trabalhos relatando alterações *postmortem* em materiais fósseis, incluindo alterações na composição química, cristalinidade mineral, porosidade, dissolução e precipitação de novas fases minerais. A paleometria é uma disciplina que ganhou muito espaço dentro do universo da tafonomia. Em resumo, a paleometria se dedica em classificar os processos geoquímicos, geomicrobiológicos e sedimentológicos envolvidos na preservação de associações fossilíferas (DELGADO *et al*., 2014).

Paleoecologia é o estudo das relações entre os organismos e seu ambiente no passado. Esta ciência se destaca por seu caráter histórico descritivo, envolvendo raciocínio indutivo, aspecto experimental e técnicas oriundas das Ciências da Terra e Biológicas. Como a linguagem da paleoecologia é derivada de ambas as ciências, os fósseis desempenham papel central em suas contribuições. Portanto, nos estudos paleoecológicos é fundamental que se busque, em paralelo, um processo de identificação cuidadoso, taxonomia sólida e nomenclatura inequívoca.

Embora os gregos antigos já reconhecessem que os fósseis forneciam pistas para ambientes passados, o título de fundador da paleoecologia é creditado ao naturalista britânico Edward Forbes (1815-1854)((HEDGPETH, 1957; CLOUD, 1959). Em seu trabalho no Mar Egeu, Forbes relacionou as mudanças de faunas com as diferentes zonas batimétricas, reconhecendo a conexão entre os processos modernos e o que é preservado no registro geológico (FORBES, 1843). Com seu trabalho, Forbes lançou as bases para a paleoecologia aplicando o método que ele próprio denominou na época de "Zoogeologia", onde explicava como zonas de diferentes profundidades no ambiente marinho podem ser reconhecidas em camadas rochosas soerguidas na ilha de Neo Kaimeni, na Grécia. No entanto, o uso mais antigo do termo paleoecologia é creditado aos paleobotânicos Berry e Clements no início do século XX (BERRY, 1911, 1914; CLEMENTS, 1916, 1918). Apesar da publicação anterior de Berry, Böger (1970) credita Clements (1916) como o “criador” do termo paleoecologia, pois o autor faz uma clara diferenciação entre ecologia e paleoecologia e reconhece a comparação do registro paleoecológico com o registro geológico como um meio de verificação cruzada dos resultados.

Os trabalhos de paleoecologia são frequentemente quantitativos e consistem de muitas variáveis e amostras. Os métodos numéricos, como a análise de componentes principais, são ferramentas valiosas para resumir os principais padrões de variação em dados paleoecológicos complexos e multivariados. Técnicas estatísticas (e.g., regressão) são importantes para testar hipóteses sobre possíveis causas para mudanças observadas no registro paleoecológico. Como indivíduos e ambientes do passado não podem ser observados diretamente, a maioria das pesquisas paleoecológicas busca determinar ocorrências, distribuições e abundâncias passadas de organismos e reconstruir populações, comunidades, paisagens, ambientes e ecossistemas usando evidências geológicas e biológicas. Dessa forma, em muitos casos, várias hipóteses são possíveis para explicar mudanças bióticas ou abióticas em um dado paleoecossistema. Assim, um método de hipóteses múltiplas é essencial na paleoecologia. O princípio da simplicidade (navalha de Occam) também é essencial, pois propõe que, dado um conjunto de explicações concorrentes, todas as quais oferecem uma explicação adequada para um determinado conjunto de dados, a explicação mais simples é preferível. Outro princípio filosófico fundamental na paleoecologia é o uniformitarismo, ou seja, “o presente é a chave para o passado” de James Hutton (século XVIII). Esse pressuposto chave nas ciências da Terra postula que os processos geológicos atuais (e.g., erosão fluvial e deposição de carbonatos no fundo de lagos alcalinos) ocorriam a taxas constantes no passado. Charles Lyell (século XIX), e, mais tarde, Stephen Jay Gould refinaram esse pressuposto e

cunharam o uniformitarismo metodológico ou atualismo, onde a natureza dos processos e suas leis subjacentes são consideradas as mesmas ao longo do tempo, mas as taxas podem variar em momentos diferentes. Catástrofes como erupções vulcânicas ocorrem e ocorreram no passado, porém as taxas de ocorrência destes eventos podem variar muito de um período para o outro. No entanto, toda erupção vulcânica segue as leis básicas da natureza porque as propriedades da matéria e da energia são invariáveis com o tempo. Esse princípio filosófico é a base para supormos que as paleocomunidades se estruturavam, mais ou menos, segundo a organização trófica observada nos ecossistemas atuais. Assim, o uniformitarismo metodológico representa a abordagem, não testável, mais simples da paleoecologia e, portanto, resume bem a aplicação dos princípios de simplicidade e indução.

A paleoecologia pode ser estudada em qualquer período da história da Terra em que a vida esteve presente. Os paleoecólogos estão interessados em escalas de tempo de centenas, milhares ou milhões de anos. A principal divisão dentro da paleoecologia é entre a paleoecologia do tempo profundo (*deep-time paleoecology*) e a paleoecologia do Período Quaternário (*Quaternary-time paleoecology*)(BIRKS, 2008). Em contraste, os ecologistas estão interessados principalmente em escalas de tempo de horas, dias, semanas, meses, anos ou décadas (o chamado tempo real, ou seja, dentro da observação humana direta). Portanto, existem várias abordagens possíveis para a pesquisa paleoecológica, como pesquisas baseadas na paleoecologia de indivíduos (adaptação, evolução) população, comunidade, paisagem, ecossistema, e/ou paleoecologia global (BIRKS, 2008). Pesquisadores interessados na paleoecologia de tempo profundo usam os fósseis para estudar a distribuição, evolução e dinâmica da biota passada com ênfase na adaptação, evolução, extinção e biogeografia em escalas de tempo de milhares a milhões de anos. Já os paleoecólogos do Período Quaternário buscam reconstruir a biota e os ambientes do passado durante os últimos dois milhões de anos da história da Terra, onde os estudos são focados nas mudanças climáticas recentes e nos impactos da presença humana no meio físico. Na presente tese, aplicaram-se conceitos relacionados à paleoecologia do tempo profundo, a fim de verificar a dinâmica e a interação da entomofauna e o sistema deposicional preservado nos estratos da Formação Crato.

2.4 Microscopia Eletrônica de Varredura

A história da microscopia eletrônica de varredura teve seu início com o trabalho de Max Knoll em 1935. Em 1938, von Ardenne construiu o primeiro microscópio eletrônico rudimentar adaptando bobinas de varredura ao microscópio eletrônico de varredura,

conseguindo aumento máximo de 8.000x e resolução aproximada de 50 nm. O Microscópio Eletrônico de Varredura (MEV) moderno possui uma alta resolução, na ordem de 2 a 5 nm (20 - 50 A^{o}), atualmente é possível encontrar instrumentos com até 1 nm (10 A^{o}). O MEV é um instrumento muito usado na análise de materiais, pois sua elevada profundidade de foco (imagem com aparência tridimensional) e a possibilidade de combinar a análise microestrutural com a microanálise química são fatores que contribuem para o amplo uso desta técnica (MANNHEIMER, 2002).

O MEV consiste basicamente da coluna óptico-eletrônica (canhão de elétrons e sistema de demagnificação), da unidade de varredura, da câmara de amostra, do sistema de detectores e do sistema de visualização da imagem (Figura 28). Na coluna ótico-eletrônica fica localizado o canhão de elétrons, que gera os elétrons primários, as lentes condensadoras, que colimam o feixe de elétrons primários e, as bobinas, que promovem a deflexão do feixe de elétrons primários. O canhão de elétrons é formado por um filamento de tungstênio, que serve como cátodo, o cilindro de Wehnelt e o ânodo. O filamento de tungstênio tem seu funcionamento quando é fornecido calor suficiente e os elétrons podem ultrapassar a barreira de energia para escapar do material. Dessa forma, o canhão de elétrons é responsável pela produção dos elétrons e a sua aceleração para o interior da coluna. Esse feixe eletrônico é então demagnificado por várias lentes eletromagnéticas, cuja finalidade é produzir um feixe de elétrons focado com um pequeno diâmetro. Se o diâmetro do feixe de elétrons for muito grosseiro ou instável não irá produzir uma boa imagem em grandes aumentos. A maioria dos MEV produz um feixe eletrônico da ordem de 10 nm (100 A^{o}) de diâmetro e ainda com corrente suficiente para formar uma imagem com boa resolução.

Figura 28 – Representação esquemática dos componentes do Microscópio Eletrônico de Varredura

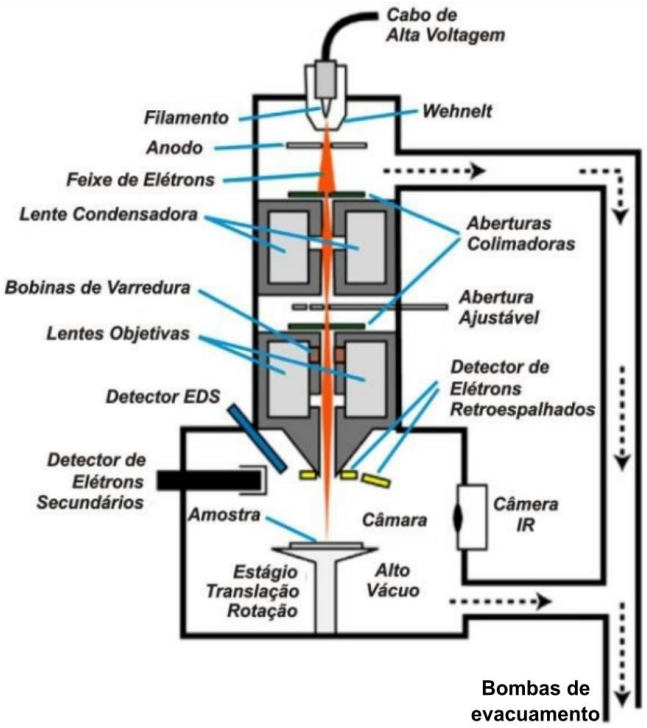

Fonte: Xavier (2018).

O feixe eletrônico ao atingir a superfície da amostra irá interagir com os átomos ali presentes, como consequência, este elétron sofrerá modificação na sua velocidade inicial. Esta variação da velocidade pode ser somente na direção ou pode ocorrer tanto na direção quanto no módulo (magnitude). As interações nas quais ocorre a mudança na trajetória do elétron, sem que ocorra variação na sua energia cinética são ditas interações elásticas. Aquelas em que há transferência de energia do elétron primário para os átomos da amostra são chamadas de interações inelásticas. O elétron do feixe ao penetrar no átomo irá interagir também com os elétrons ao redor do átomo resultando principalmente em espalhamento inelástico. Como resultado destas interações, elétrons das várias camadas do átomo poderão ser liberados e excitados. A profundidade de penetração dos elétrons depende da composição da amostra. Em particular o espalhamento inelástico é mais intenso para materiais com número atômico (Z) elevado do que para materiais com baixo Z. Isso significa que a profundidade de penetração é menor para materiais com elevado Z. O comportamento dos espalhamentos elásticos e inelásticos pode ser verificado pela simulação de Monte-Carlo, que oferece uma boa aproximação do volume de interações entre feixe eletrônico e superfície da amostra (Figura 29).

Figura 29 – Simulação de Monte-Carlo para o volume de interação de amostra de Carbono, Alumínio, Cobre e Ouro com o feixe de elétrons primários de 20 KeV

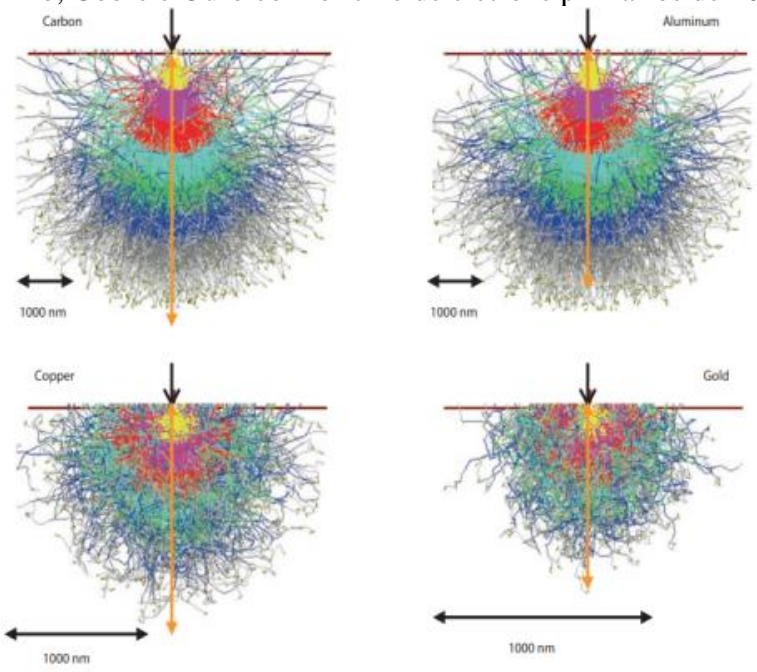

Fonte: Goldstein et al. (2018).

As interações elásticas e inelásticas podem produzir elétrons com energia máxima igual a energia do elétron primário, ou seja, um elétron retroespalhado (ERE). Também pode ocorrer a produção de elétrons ionizados, esses elétrons são chamados de elétrons secundários (ES) e são ejetados do material com uma energia média de 2 a 5 eV. Caracteristicamente, os elétrons ERE são oriundos de regiões mais profundas da amostra, enquanto que os elétrons ES são provenientes de porções mais rasas. Os elétrons auger são aqueles que preenchem o vazio deixado pelos elétrons ES ejetados, devido à interação com o feixe de elétrons primários (GOLDSTEIN e NEWBURY, 1992).

O sinal de elétrons secundários é o mais usado para análise de amostras no MEV. O detector mais usado é o do tipo Everhart-Thornley (ET). Este detector é isolado do resto do microscópio e possui na sua frente uma grade com potencial de +300 eV. Os elétrons secundários são atraídos por esta grade carregada positivamente. Todos os elétrons que penetram no detector são acelerados em direção ao cintilador, e são conduzidos a uma fotomultiplicadora onde são transformados num sinal elétrico (Figura 30). A intensidade de ES que atingem o detector varia com a inclinação da amostra em relação ao feixe de elétrons primários, ou seja, o número de ES aumenta à medida que a amostra é inclinada, aumentando também o contraste da imagem gerada. Assim, pequenas rugosidades e detalhes na superfície das amostras podem se tornar visíveis. É basicamente por esta razão que as imagens de ES

são "mais" fáceis de interpretar.

Figura 30 – Esquema da captação de ES e ERE pelo detetor Evehart-Thornley

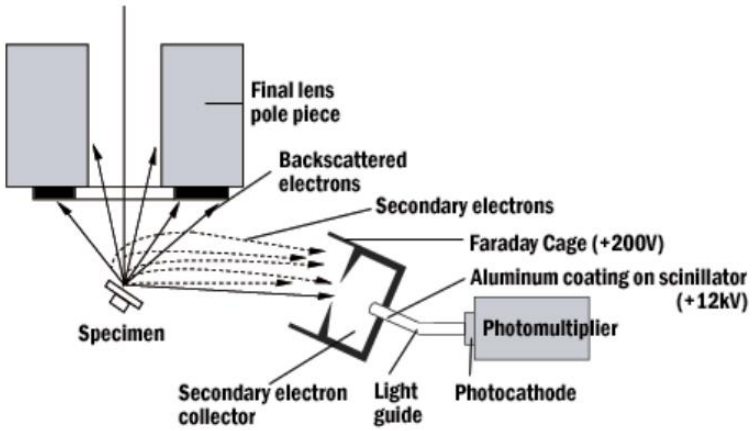

Fonte: https://cmrf.research.uiowa.edu/scanning-electron-microscopy.

2.5 Espectroscopia por Energia Dispersiva

A espectroscopia por energia dispersiva (EDS), ou microanálise, é um dos mais importantes instrumentos para a análise química de materiais. Através da microanálise é possível determinar a composição de regiões com até 1 μm de diâmetro, além de ser uma técnica não destrutiva. A microanálise também oferece a possibilidade de se obter mapas composicionais da região em observação, permitindo que se correlacione as feições morfológicas detalhadas com informações microcomposicionais (GOLDSTEIN e NEWBURY, 1992).

A origem da microanálise é relacionada ao da técnica de análise espectroquímica, na qual os elementos presentes numa amostra podem ser identificados através do espectro de raios-X emitido pela amostra. No entanto, ao invés de analisar uma área muito grande (>1 mm^2), a microanálise usa um feixe de elétrons para excitar uma área muito menor. O feixe eletrônico interage com os elétrons de camadas mais internas dos átomos causando a ejeção destes elétrons e deixando uma vacância nesta camada. O átomo fica então num estado excitado e cuja tendência é voltar ao estado fundamental, onde é permitido que os elétrons de camadas mais externas se desloquem para preencher o vazio das camadas internas. A diferença de energia na transição de camadas mais externas para camadas mais internas é característica de cada átomo e a quantidade de energia de cada camada varia de maneira discreta com o número atômico. Em cada camada, os elétrons de um átomo ocupam níveis de energia específicos e estes níveis de energia são designados por K, L, M, N, etc (MALISKA,

2011). A desexcitação do átomo após a retirada do elétron é realizada através da transição dos elétrons de uma camada para outra. A partir da ionização da camada K, a transição para preencher esta vacância pode ocorrer tanto da camada M quanto da camada L. Como os elétrons destas camadas externas possuem diferentes energias, os raios-X criados a partir destas duas camadas também têm energias diferentes e são designados diferentemente. As letras gregas minúsculas α, β, γ, designam a camada a partir da qual saiu o elétron para preencher o vazio deixado pela ionização (Figura 31).

Figura 31 – Diagrama dos níveis de energia de um átomo mostrando a excitação das camadas K, L, M e N e a formação de raios-X Kα, Kβ, Lα e Mα

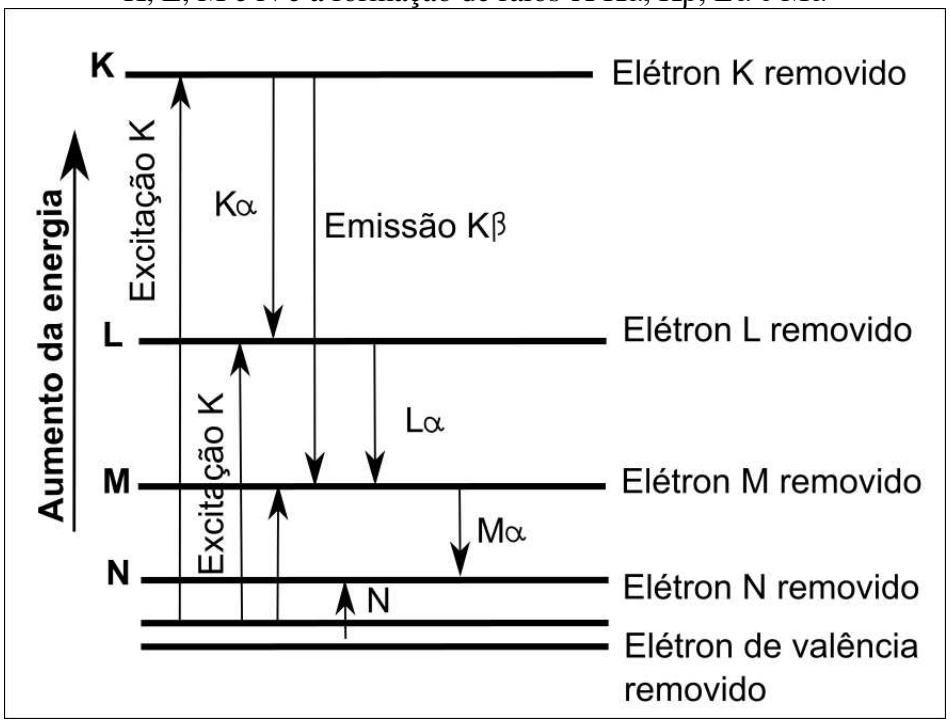

Fonte: o autor.

A microanálise química por energia dispersiva se caracteriza pela análise qualitativa dos elementos presentes na amostra. Os elementos em maior quantidade são identificados com precisão, mas quando os elementos estão presentes em pequenas quantidades podem conceber erros de interpretação em consequência de artefatos produzidos durante a análise. É aceitável que acima de 10% em peso um elemento esteja presente em grande quantidade, entre 1 e 10% em pequena quantidade e menor que 1% apenas traços. Um espectro de EDS consiste de picos característicos e do background (em suma, é um sinal que não fornece nenhum dado sobre os elementos presentes na amostra). Os elementos são identificados ao se comparar os diversos picos com a as energias dos elementos previamente

tabelados (MALISKA, 2011).

2.6 Espectroscopia

2.6.1 Infravermelho

Em geral, a espectroscopia estuda a interação da radiação eletromagnética com a matéria. Os métodos espectroscópicos são aplicados para medir a quantidade de radiação emitida ou absorvida pelas moléculas ou átomos. Esses métodos são categorizados nas diferentes regiões do espectro eletromagnético (ex. raios-X, ultra-violeta, visível, infravermelho etc) e fornecem diferentes informações sobre a matéria em estudo (LONG, 1977).

A espectroscopia de infravermelho se baseia na absorção de energia na região do infravermelho do espectro eletromagnético (número de onda 4000-400 cm^{-1}, ou comprimento de onda 2,5-25 μm)(Figura 32). Assim como nas demais técnicas espectroscópicas, as moléculas se agitam, quando absorvem radiação, até atingirem um estado maior de energia. A absorção da radiação no infravermelho corresponde à faixa (8 a 40 kj/mol) que engloba vibrações de estiramento e dobramento das ligações na maioria das moléculas covalentes (PAIVA *et al.,* 2015). As frequências de radiação absorvidas equivalem às frequências vibracionais da molécula, resultando no aumento da amplitude vibracional das ligações desta molécula. Desta forma, se a molécula receber radiação eletromagnética com 'aproximadamente' a mesma energia de uma dessas vibrações, então a luz será absorvida. Contudo, uma molécula é composta por diferentes tipos de ligações, ou seja, nem todas as ligações são capazes de absorver radiação no infravermelho, mesmo tendo uma frequência de radiação exatamente igual ao movimento vibracional. Apenas as ligações que possuem momento de dipolo se alterando em função do tempo são capazes de absorver radiação no infravermelho. Assim, para que uma vibração apareça no espectro infravermelho, a molécula precisa sofrer uma variação no seu momento dipolar durante essa vibração. O dipolo elétrico de uma ligação precisa mudar na mesma frequência da radiação incidente para que ocorra a transferência de energia (PAIVA *et al.,* 2015). Portanto, ligações simétricas que tenham grupos idênticos em cada ponto não absorverão radiação infravermelha.

Figura 32 – Esquema mostrando a relação do espectro infravermelho vibracional com outros tipos de radiação

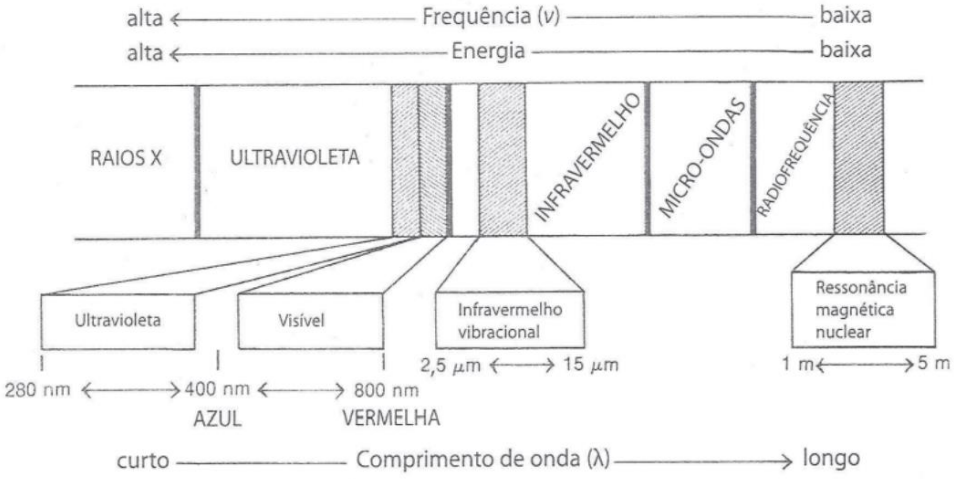

Fonte: Paiva et al. (2015).

Cada tipo de ligação tem sua frequência vibracional individual, logo, os padrões de absorção no infravermelho nunca serão exatamente idênticos em duas moléculas diferentes, mesmo se tratando do mesmo tipo de ligação (PAIVA *et al.,* 2015). Apesar de a radiação absorvida ser igual, jamais os espectros infravermelhos de duas moléculas diferentes serão idênticos. Portanto, o espectro de infravermelho de cada ligação possui um padrão único, dessa forma, podemos utilizar os espectros de infravermelho de uma substância para identificar e quantificar os diferentes elementos químicos nela presentes, como se fosse uma impressão digital. Tendo isso em mente, em geral, é possível predizer os níveis de absorção de alguns tipos de ligações em certas regiões do espectro do infravermelho vibracional (Figura 33).

Figura 33 – Ilustração mostrando esquematicamente a distribuição de tipos comuns de ligações no espectro infravermelho vibracional

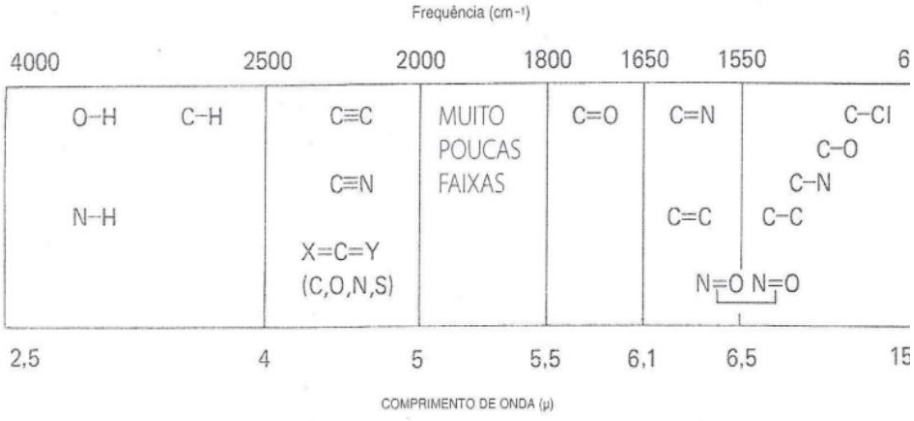

Fonte: Paiva et al. (2015).

2.6.2 Efeito Raman

Em 1922, Leon Brillouin tratou o espalhamento de luz como o aparecimento de duas bandas de em torno da frequência de um feixe de luz incidente em um cristal. Em 1923, A. Smekal previu teoricamente o que viria ser o efeito Raman que descreve o fenômeno de espalhamento inelástico da luz através da matéria. No entanto, a interpretação correta foi feita pela primeira vez pelos indianos Chandrasekhara Venkata Raman e Kariamanikkam Srinivasa Krishnan em 1928. Simultaneamente e independente, Grigory Landsberg e Leonid Mandelstam deram contribuições semelhantes sobre o espalhamento da luz na Rússia. Quando um feixe de luz monocromática incide em um material ocorre uma interação entre os fótons da luz e as vibrações dos átomos que compõem o material, isso que dá origem ao espalhamento da luz (Figura 34). A maior parte da luz passa diretamente pela amostra, porém, um pouco dessa luz (cerca de 10^{-3}) interage com o material. Assim, os fótons são elasticamente dispersos em todas as direções, ou seja, apresentam o mesmo comprimento de onda da luz incidente e este espalhamento é conhecido como espalhamento Rayleigh. No entanto, uma pequena fração da luz espalhada pode ser dispersa inelasticamente, ou seja, não tem a mesma frequência que a luz incidente (BENTO *et al*., 2003). Quando a frequência da luz espalhada é menor que a frequência da luz incidente, a radiação Raman espalhada é chamada radiação Stokes. Contudo, se a luz espalhada apresentar frequência maior que a luz incidente, significa que houve transferência da molécula para o fóton, esse fenômeno é chamado de efeito anti-Stokes (Figura 35). Tipicamente, os picos de alterações (deslocamentos) associados com o espalhamento Stokes são utilizados nas análises.

Figura 34 – Esquema simplificado ilustrando o espalhamento de luz

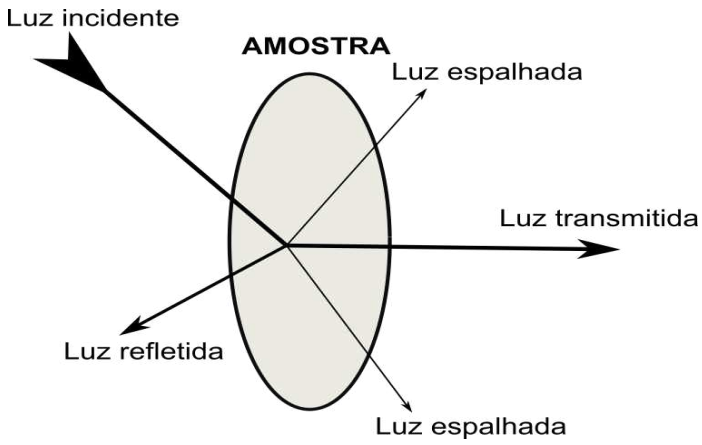

Fonte: o autor.

Figura 35 – Diagrama mostrando o mecanismo básico para o espalhamento Raman

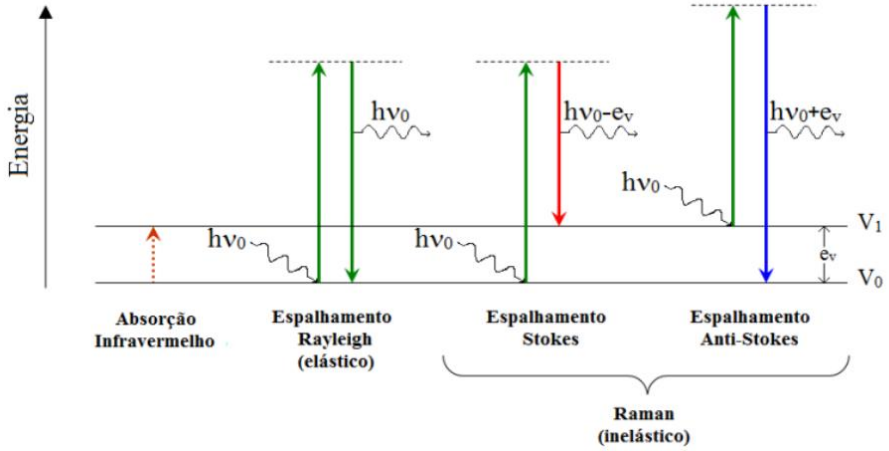

Fonte: Franzen e Windbergs (2015).

Na época, C. V. Raman e seu aluno K. S. Krishnan dispunham de um equipamento bem rudimentar, ainda assim, eles constataram que a frequência da luz espalhada difere daquela do feixe incidente e que a alteração depende da estrutura química das moléculas do meio responsável pelo espalhamento. Esse achado rendeu o prêmio Nobel de Física para C. V. Raman em 1930.

Até os anos 50, a técnica consistia de arcos de mercúrio, como fonte de excitação, que produziam radiação com comprimento de onda 435,8 nm, o que limitava a utilização dessa técnica para estudar substâncias coloridas (absorvem intensamente esse comprimento de onda) ou que fossem fotossensíveis. Nos anos 60, grande esforço foi aplicado no teste de novas fontes de excitação e nesse cenário, os estudos realizados no Laboratório de Espectroscopia Molecular da Universidade de São Paulo tiveram protagonismo (SALA *et al*., 1984). Se aproveitando de uma fonte de descarga de Hélio, as radiações produzidas com comprimentos de ondas com 587,6, 667,8 e 706,5 nm, permitiram o estudo de substâncias coloridas e fotossensíveis. Em 1962, o físico brasileiro Sérgio P. S. Porto foi um pioneiro no uso da radiação laser (pulsado de rubi) na espectroscopia Raman.

Os equipamentos modernos com transformada de Fourier possibilitam até a obtenção simultânea de espectros de Raman e no infravermelho. Apesar de ambos serem vertentes da espectroscopia vibracional, a espectroscopia infravermelha analisa a absorção de frequências de vibrações específicas que provocam mudanças de momento de dipolo. Já a espectroscopia Raman observa a mudança de polarizabilidade de uma molécula provocada por alterações nas frequências de radiação espalhada. Assim, a espectroscopia Raman é mais sensível a ligações homonucleares como C-C, C=C e C≡C.

Portanto, podemos afirmar que as principais vantagens das espectroscopias Raman e de infravermelho em relação a outras práticas que visam à caracterização de materiais é que ambas apresentam caráter não destrutivo, rápida aquisição e a possibilidade de análise micrométrica.

3 CAPÍTULO 1

Taphonomic analysis of the paleoentomofauna assemblage from the Cenozoic of the Fonseca Basin, southeastern Brazil

Este capítulo foi publicado no jornal científico "PALAIOS"; O material suplementar vinculado ao artigo citado abaixo pode ser encontrado online em https://www.sepm.org/supplemental-materials.

Referência:

Francisco Irineudo Bezerra, Enzo Victorino Hernández Agressot, Mónica M. Solórzano-Kraemer, Paulo Tarso C. Freire, Alexandre Rocha Paschoal, João Hermínio da Silva, Márcio Mendes (2021) Taphonomic Analysis of the paleoentomofauna assemblage from the Cenozoic of the Fonseca Basin, Southeastern Brazil. PALAIOS; 36(5): 182–192. doi: https://doi.org/10.2110/palo.2020.067

TAPHONOMIC ANALYSIS OF THE PALEOENTOMOFAUNA ASSEMBLAGE FROM THE CENOZOIC OF THE FONSECA BASIN, SOUTHEASTERN BRAZIL

FRANCISCO IRINEUDO BEZERRA[1], ENZO VICTORINO HERNÁNDEZ AGRESSOT[2], MÓNICA M. SOLÓRZANO-KRAEMER[3], PAULO TARSO C. FREIRE[2], ALEXANDRE ROCHA PASCHOAL[2], JOÃO HERMÍNIO DA SILVA[4], AND MÁRCIO MENDES[1]

[1]Departamento de Geologia, Universidade Federal do Ceará, 64049-550, Fortaleza, Ceará, Brasil

[2]Departamento de Física, Universidade Federal do Ceará, 60455-970, Fortaleza, Ceará, Brasil

[3]Department of Palaeontology and Historical Geology, Senckenberg Research Institute, Senckenberganlage 25, 60325 Frankfurt am Main, Germany

[4]Campus de Juazeiro do Norte, Universidade Federal do Cariri, 63000-000, Juazeiro do Norte, Ceará, Brasil

ABSTRACT

The Fonseca Formation (Eocene–Oligocene boundary, Minas Gerais, Brazil) is well known for its paleoflora, especially of flowering plants. The richness of this insect-bearing fossil locality is significantly less well understood, but we can shed light on the insect paleocommunity. One hundred and eight fossil insect specimens were examined and separated into four grades based on their preservational quality. We conducted analyses of taphonomic features, including body orientation, size, articulation, and chemical composition. Our results reveal differences in the body articulation of the insects. The fully articulated specimens apparently did not experience extensive flotation time at the water-air interface, whereas for partially articulated and disarticulated specimens the opposite is true. These taphonomic features would be acquired during the biostratinomy stage, and not early diagenesis. We also employed high resolution techniques (SEM-EDS and Raman spectroscopy) to understand their fossilization potential. Our chemical data suggest that the Fonseca insects are preserved as organic remains in carbonaceous compressions. Thus, chitin biomolecules most likely were transformed into more resistant biopolymers during diagenesis. This interpretation may also imply that the carbonaceous material originated from the insect itself. In this study, we document new discoveries and also provide future prospects for study of the Fonseca Formation.

INTRODUCTION

Fossil insects date to Lower Devonian, approaching 410 million years in age. However, the early fossil record of insects is problematic and controversial (Engel and Grimaldi 2004; Nel et al. 2013; Haug et al. 2016; Haug and Haug 2017; Schachat et al. 2018). Compared with other arthropod groups, the preservation of insects is essentially restricted to *Lagerstätte* deposits (Schachat and Labandeira 2020). Insects have an exoskeleton made of chitin that does not preserve well in most oxygenated and high energy environments. Despite being soft-bodied organisms, fossil insects can be preserved in large numbers in several continental environments such as fossilized resin, fluvial and lacustrine deposits, and even shallow marine strata (Sepkoski et al. 1981; Henwood 1993; Smith 2001, 2012; Rasnitsyn and Quicke 2002; Mart´ınez-Delcl`os et al. 2004; Grimaldi and Engel 2005; Smith and Moe-Hoffman 2007; Solórzano-Kraemer 2007; Rust et al. 2010; Solórzano-Kraemer et al. 2018).

Several studies report that insect assemblages may exhibit different taphonomic patterns depending on a suite of characters related to their biology and their taphonomic

history (Martínez-Delclòs and Martinell 1993; Peñalver 2002; Duncan et al. 2003; Martínez-Delclòs et al. 2004; Wang et al. 2013; Anderson and Smith 2017; Tian et al. 2020). Relevant factors include taxonomic bias, behavior, diversity, and ecology as well as paleoenvironment, sedimentation, and geochemical conditions. More detailed investigations of taphonomic patterns are important to understand, insofar which of these biases are important in insect accumulation processes in the geological record, therefore, allowing us to use fossil insects more effectively in paleoecological reconstructions, paleodiversity and paleoenvironmental analyses.

The Fonseca Basin is located in the southeastern Brazil. The strata occupy an area of about 2.2 km^2 and comprises a sedimentary succession dominated by finer deposits, with subordinate medium to fine-grained sandstones and conglomerates (Sant'Anna et al. 1997). At the base of the succession are clast- supported conglomerates with subangular clasts. The middle portion is composed of medium-grained sandstones with planar cross-stratification fining up towards medium- to fine grained sandstones with horizontal stratification. The upper part of the succession consists of claystones with horizontal lamination with sedimentary boudinage structures. The Fonseca sediments were affected by normal faults that caused a general westward tilt of the strata. The sandy-clayey continental deposits of the Fonseca basin are interpreted as having been deposited within a fluvial system of meandering streams that overly Precambrian basement rocks (Sant'Anna et al. 1997). Precambrian basement rocks underlying the Fonseca Basin are commonly composed of granite and gneiss terrains that are also covered by the Rio das Velhas Supergroup, Minas Supergroup and Espinha¸co Supergroup (Fig. 1).

The fossiliferous layers of the Fonseca Formation correspond to the lignite facies characterized by laminated pelites of Maizatto (2001). Sommer and Lima (1967), considered this formation to be Miocene in age based on paleobotanical studies. However, the presence of the palynological biozones of *Retibrevitricolpites triangulatus* (late Eocene) and *Dacrydiumites florinii* (early Oligocene) adjusted the age to Eocene–Oligocene (Maizatto 2001; Maizatto et al. 2008).

This study aims to investigate how the fossil insects are preserved in the Fonseca Formation with emphasis on its significancefor paleoenvironmental interpretations. Specifically, our work utilizes data collected with scanning electron microscopy (SEM), energy-dispersive X-ray spectroscopy (EDS) and Raman spectroscopy to describe the composition and ultrastructure of the fossils. Using these results, we provide an overall picture of preservation quality of specimens and highlight the potential for future discoveries

in this basin.

MATERIALS AND METHODS

Fossil Material

One hundred and eight insect fossils (Fig. 2) were excavated four kilometers from the Fonseca village, Alvinópolis city, state of Minas Gerais, in southeastern Brazil. The specimens were collected from an outcrop alongside the Fonseca Creek on private property owned by CENIBRA (Celulose Nipo-Brasileira). The fossils are deposited in the Scientific Palaeontological Collection of the Laboratório de Paleontologia (LP) at the Universidade Federal do Ceará (UFC), in northeastern Brazil. All fossil insects were preserved as carbonaceous compressions inside paper shale, so we added hardener compound on the sides in order to prevent the fossils from fragmenting (Wilson 1965). The fossils received minimal or no additional preparation to avoid biasing the dataset. The insects were identified at the ordinal level. However, the suborder Isoptera was designated separately from its more inclusive order (Blattodea) because we consider that the morphological differences between these taxonomic groups are significant for the purposes of the current study. Unidentified specimens were present as either a faint body impression or as isolated parts of a body.

Taphonomic Classification

Taphonomic classification is useful to express the preservational quality of fossil assemblages (Smith and Moe-Hoffman 2007; Wang et al. 2013). In this study, the taphonomic grade was determined by the degrees of completeness and articulation of the fossils. Preservation-quality indicators (morphological features and number of characters) were designated to establish the taphonomic grade. Thus, the features used in the classification of the insects were the presence/absence of the head, antennae, legs, thorax, abdomen, and wings. All specimens were divided into four groups based on the degree of disarticulation. The taphonomic grades ranged from 1 through 4, with being level 1 the highest degree of preservation and level 4 the poorest (Table 1). Grade 1 includes complete specimens with head, antenna, legs, thorax, abdomen, and wings. All partially disarticulated specimens were divided into two taphonomic grades: grade 2, individuals showing at least one morphological character absent (e.g., specimens missing the head or abdomen); and grade 3, individuals

displaying the absence of at least two morphological characters (e.g., specimens missing the head and abdomen or thorax and abdomen). Finally, grade 4 encompasses strongly disarticulated insects (isolated body parts) (Table 1). A chi-square analysis was conducted to determine whether the number of specimens in each taxonomic group was dependent on their taphonomic grade.

The orientation of the fossil insects on the bedding plane, either a dorsoventral or lateral position, was also recorded. Chi-square analysis was used also to ascertain whether there were differences between the orientation patterns of specimens and the taphonomic grade. The area of each specimen was calculated by multiplying the length and width of the sample. Length was measured from the anteriormost aspect of the mouth parts to the posteriormost tip of the abdomen, excluding any protruding appendages. The width was measured across the middle of the thorax. Only fully articulated and dorsoventral specimens were used in body-size measurements. A list of all specimens and their associated data can be found in the Online Supplemental File. The differences in the frequency distributions were tested with an α of 0.05. The statistical analyses were performed using PAST version 3.09.

Scanning Electronic Microscopy (SEM) Analysis and Large-Field Energy Dispersive Spectroscopy (EDS)

The SEM–EDS analyses were performed in the Central Anal´ıtica at the Universidade Federal do Ceará (UFC). The large-field scan was carried out in a Quanta-450 electron microscope (FEI) with a field-emission gun (FEG) equipped with a gaseous analytical detector (GAD), 10 mm working distance and a X-ray detector (model 150, Oxford) for energy dispersive Xray spectroscopy (EDS). Images were acquired at a beam acceleration voltage of 20 kV, using a resolution of 1024x884 pixels per image. The fossil insects were inserted into the microscope chamber without previous preparation. The analyses were performed in a low vacuum to avoid sample charging. The images were processed and exported on AZtec software (version 3. 0/Oxford).

Raman Spectroscopy

We employed Raman spectroscopy system housed in the Laboratório de Espectroscopia Vibracional e Microscopia (LEVM), Departmento de Física, at the Universidade Federal do Ceará. Raman analyses were obtained using an objective lens of

100x/NA=0. 90. An optical microscope was connected to the WiTeC alpha 300 Raman spectrometer. The experiments were carried out using an Argon laser (Ar), green laser with a λ=532 nm wavelength, and a Gaussian field profile with maximum output power adjustable in mW as the excitation source. Raman spectra were analyzed using Origin software (version 9. 2).

RESULTS

Taxonomic Composition and Taphonomic Distributions

One hundred and eight insects from the Fonseca Formation, southeastern Brazil, were analyzed in this study. Counting all specimens, 19.4% of insects were considered undetermined because they were poorly preserved and could not be assigned to any taxonomic group. Eighty-seven identifiable insects were included in the following groups: Coleoptera (36.1%); Hymenoptera (12.9%); Hemiptera (12.9%); Isoptera (10.2%); and Blattodea (8.3%) (Fig. 3).

Of the specimens, 40.7% were whole bodies with wings (grade 1); 29.6% of bodies were incomplete (grades 2–3) as they had lost characters such as their antennae, head, abdomen, wings, or discernible legs (Fig. 4). Considering all insects, 13.8% were placed in grade 2, while 15.7% belonged to grade 3.29.6% of the sample corresponded to grade 4 (these disarticulated insects consisted only of isolated components, mainly isolated wings and isolated abdomens). The proportion of insects (Table 2) that received different taphonomic grades was significant ($x^2 = 19.32$; $p < 10^{-4}$; $df = 3$).

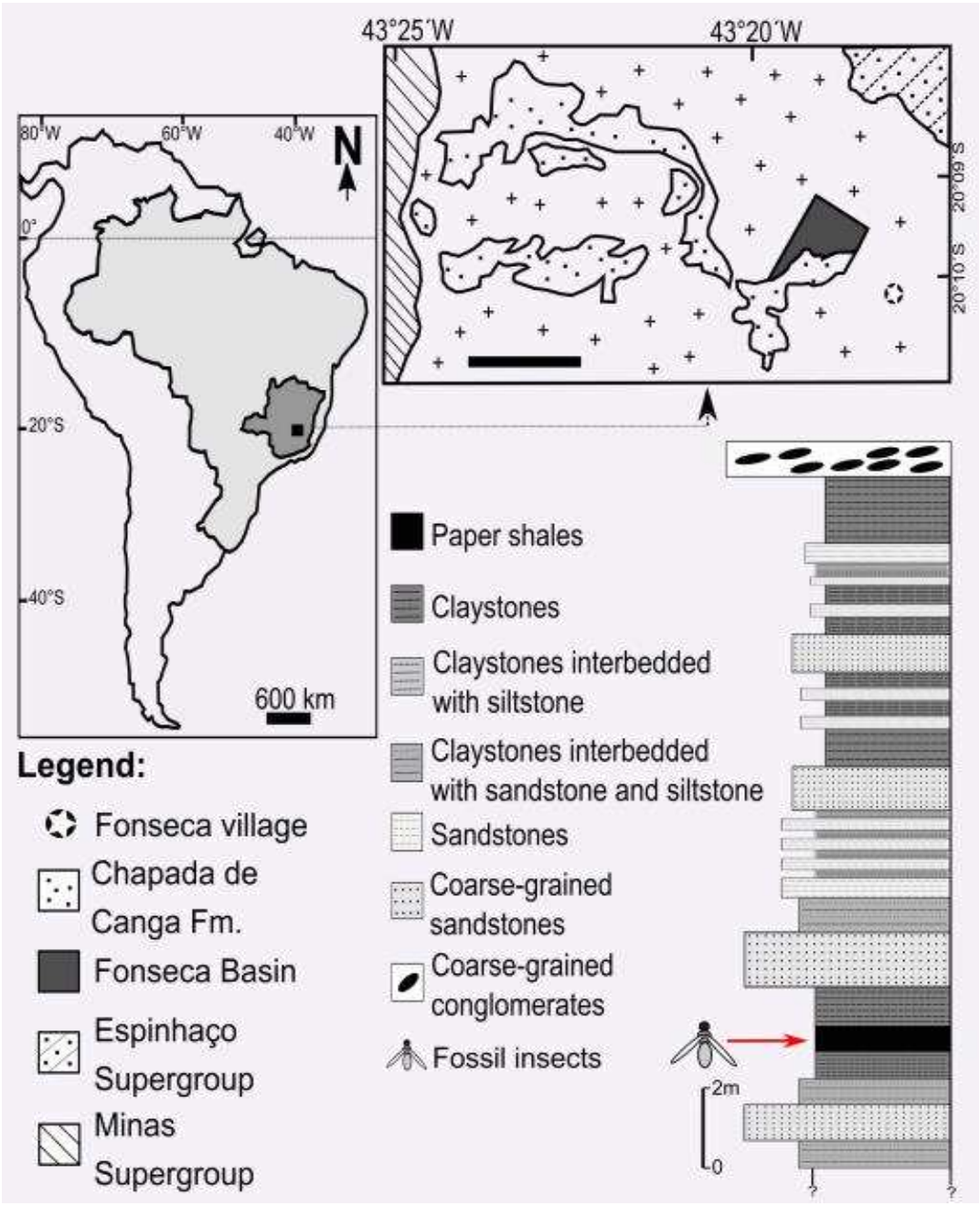

FIG. 1.—Geological map and a general stratigraphic column of the Fonseca Basin. The map in the upper left corner shows the relative position of the Fonseca Basin within South America.

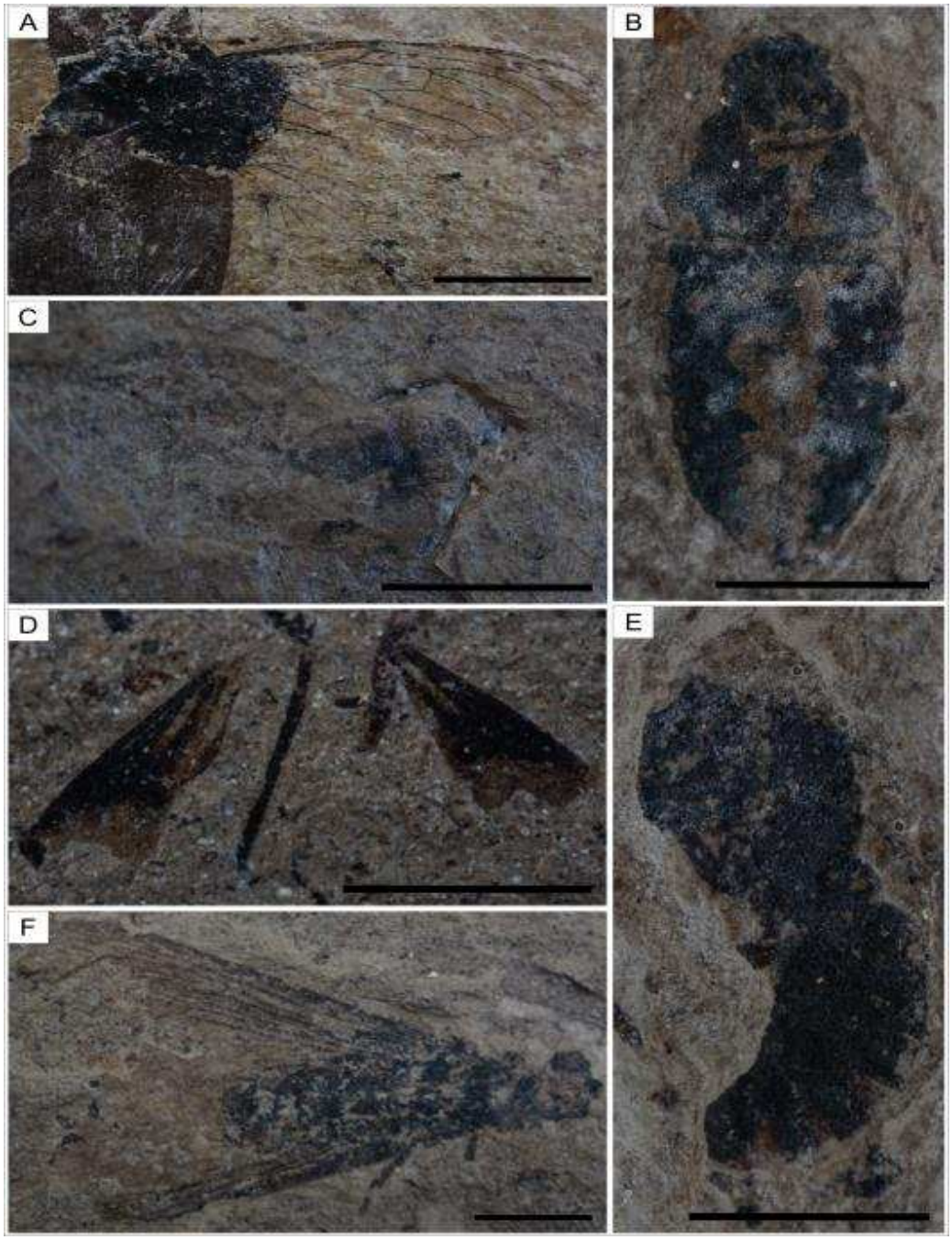

FIG. 2.—Examples of Fonseca insects of various taphonomic grades. A) Hemiptera missing head, assigned taphonomic grade 2 (LP CRT/UFC* 416). B) Fully articulated Coleoptera, taphonomic grade 1 (LP CRT/UFC 435). C) Undetermined insect of taphonomic grade 4 (LP CRT/UFC 412). D) Isolated wings of taphonomic grade 4 (LP CRT/UFC 414). E) A potential Hymenoptera preserved by its thorax and abdomen of taphonomic grade 3 (LP CRT/UFC 364). F) Fully articulated Isoptera of taphonomic grade 1 (LP CRT/UFC 429). Scale bars = 5 mm. Abbreviations: *LP = Laboratório de Paleontologia; CRT = Coleção Reserva Técnica; UFC/Universidade Federal do Ceará.

Taphonomic grade	Characters used for designation of specimens to the taphonomic grade
1	Insects displaying an entirely articulated body: presence of head; antennas; legs; thorax; abdomen and wings
2	Partially articulated insects. Individuals showing at least one morphological character absent. Example, specimens missing the head; specimens missing the abdomen; specimens without legs or thorax; or even winged specimens missing the wings
3	Partially articulated insects. Individuals displaying at least two morphological characters absent. Example, specimens missing head+abdomen; specimens missing the thorax+abdomen; specimens without the abdomen+wings
4	Disarticulated insects. Isolated wings; isolated abdomens; isolated legs; isolated thorax; or isolated head

TABLE 1.—Detailed characters for designation of insects to the different taphonomic grades.

The orientation, dorsoventral or lateral positioning, was recorded for 82% of the specimens. When considering all insects, 55.5% were preserved in a dorsal position, while 19.4% and 7.4% of the insects were preserved in ventral and lateral positions, respectively. The number of individuals in each category is shown in Table 3.

Interestingly, there was a significant difference between the orientation of an individual and its taphonomic grade ($x^2 = 10.26$; $p = 0.016$; $df = 3$).

Enumerating the specimens in grade 1, the mean body area of insects from the Fonseca Formation is 51.9 mm^2 (Fig. 5). Considering the taxonomic groups individually, the mean size for Coleoptera was 37.0 mm^2. Blattodea had a mean body size of 32 mm^2. Both Hemiptera and Hymenoptera have 76.2 and 47.9 mm^2 as an average body size, respectively. Isoptera are visibly larger, however, only one specimen was fully articulated (217 mm^2). Therefore, we could not calculate the mean size of the Isoptera separately.

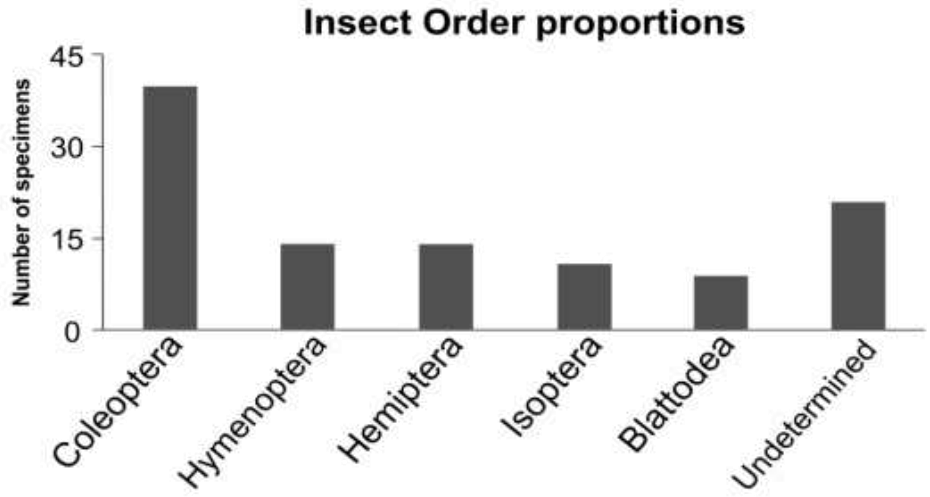

FIG. 3.—The proportional distribution of insects identified to order level from the Fonseca Formation.

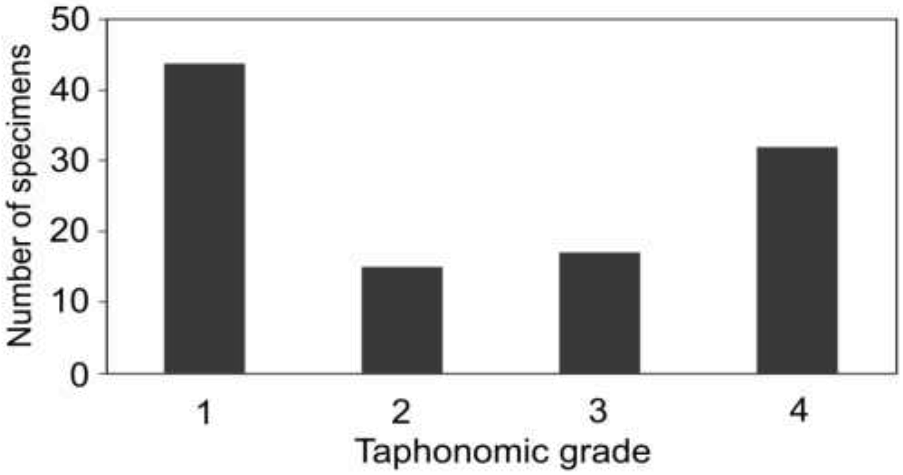

FIG. 4.—The distribution of the insects in each taphonomic grade.

Microscopy and Spectroscopy Analysis

The Fonseca insects are preserved as flattened dark-hued fossils. These fossils consist of thin black material without a consistent pattern of mineralization. The bulk of these organic remains lack a mineral phase, which decreases their resistance to compaction. SEM analyses of Coleoptera and Hymenoptera specimens revealed a structural distinction between the fossil and matrix. The insects exhibited no obvious variation in surface microtopography, suggesting that the fossils experienced the same degree of compaction as carbonaceous compressions (Martı Mus 2014; Muscente and Xiao 2015; Muscente et al. 2017). The elemental EDS mapping showed the localization of carbon within specimen bodies and

relative abundances of other elements. Carbon abundances on the fossils range from 1.51 to 2.50 wt. % (Online Supplemental File). Overall, SEM–EDS analysis shows preservation of carbonaceous material or organic remains (Fig. 6). The amount of organic matter forming the fossil film suggests that the source of the organic matter was the carcass, instead of a putative external source.

The absence of a microfabric, and the homogeneous, isotropic and carbonaceous composition of the specimens, indicate amorphization of non-mineralized organic material during diagenesis. The identification of Al, K, and Si indicates the siliciclastic origin of the host rock, which consists of fine-grained sandstone and/or micaceous shale. S and Fe are present but they cannot be associated with the pyrite. The concentrations of S and Fe are disproportional and their elemental maps are different. The S can be derived from organic waxes or was incorporated into organic compounds during early diagenesis (McNamara et al. 2006). Most likely Fe comes from terriginous sediments deposited in the lake.

The Raman spectra of the fossils indicate that different representatives of the paleoentomofauna from the Fonseca Formation exhibited peaks in the same spectral region. Raman data revealed a range of signals associated with organic compounds. Figure 7 displays a spectral region with bands related to stretching vibrations of carbon. The Raman spectra of the Fonseca insects report two characteristic first-order peaks in the region identified as D and G bands, observed respectively at 1350 and 1580 cm^{-1}. D-mode is caused by structural disorder in *sp2*-hybridized carbon systems, while G-band arises from the stretching of the C-C bond common to all *sp2* carbon systems.

Insect orders	**Numbers of specimens in each taphonomic grade**				**Total**
	1	**2**	**3**	**4**	
Coleoptera	23	1	4	11	39
Hemiptera	8	2	0	3	13
Hymenoptera	8	2	1	3	14
Blattodea	2	0	1	6	9
Isoptera	1	4	3	3	11
Undetermined	2	6	8	5	21
Total	44	15	17	32	108

TABLE 2.—The proportional distribution of insects identified to order and number of specimens in each taphonomic grade.

Orientation pattern	Taphonomic grade				Total
	1	2	3	4	
Dorsal	31	9	10	10	60
Ventral	9	6	6	0	21
Lateral	4	0	0	4	8
Total	44	15	16	14	89

TABLE 3.—Orientation distribution of insect bodies in each taphonomic grade.

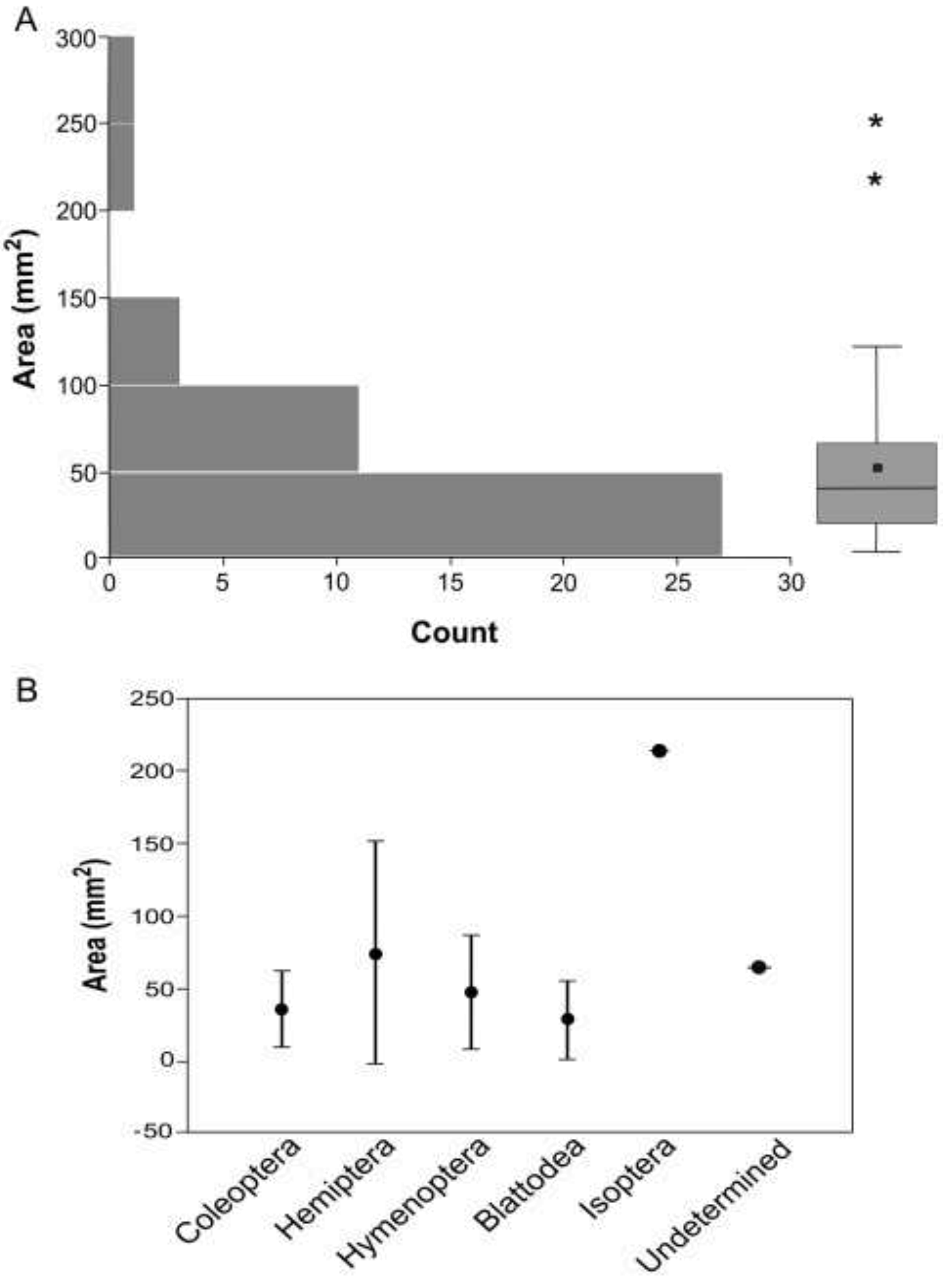

FIG. 5.—Body areas of all dorsoventral Fonseca insects. A) Distribution of untransformed measurements of areas reported in square millimeters. B) Size of specimens found in each identified insect order.

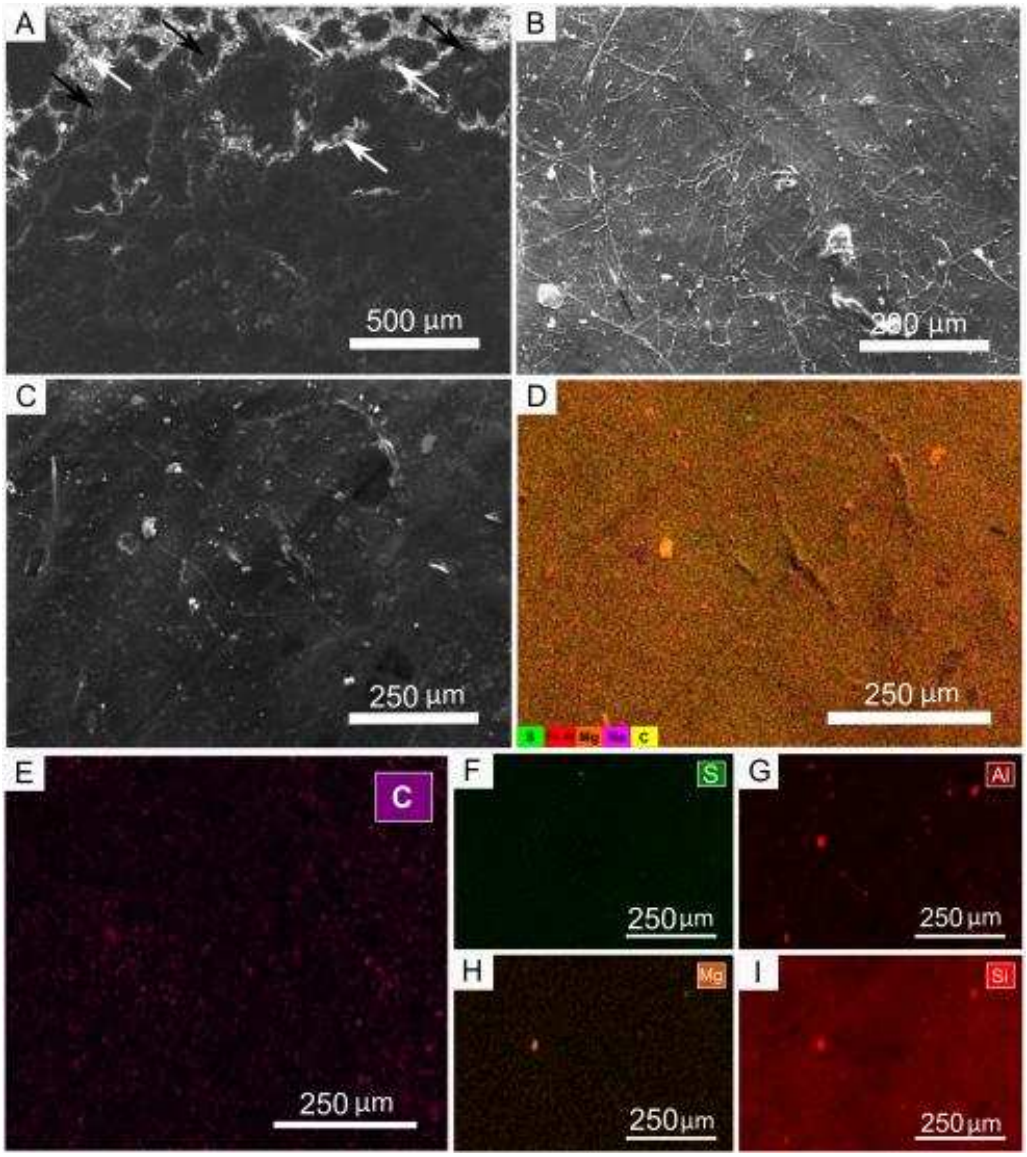

FIG. 6.—Scanning electron microscopy secondary electron micrograph and energy dispersive X-ray spectroscopy for characterization of insects. A) Secondary electron micrograph of the Coleoptera elytron showing boundaries between the fossil (black arrows) and the matrix (white arrows). B) SE image revealing the lack of distinctive segmentation of its abdomen. C) SEM micrograph of the thorax of Coleoptera. D) EDS element map of the image in C. E–I) EDS individual element maps of the image in C.

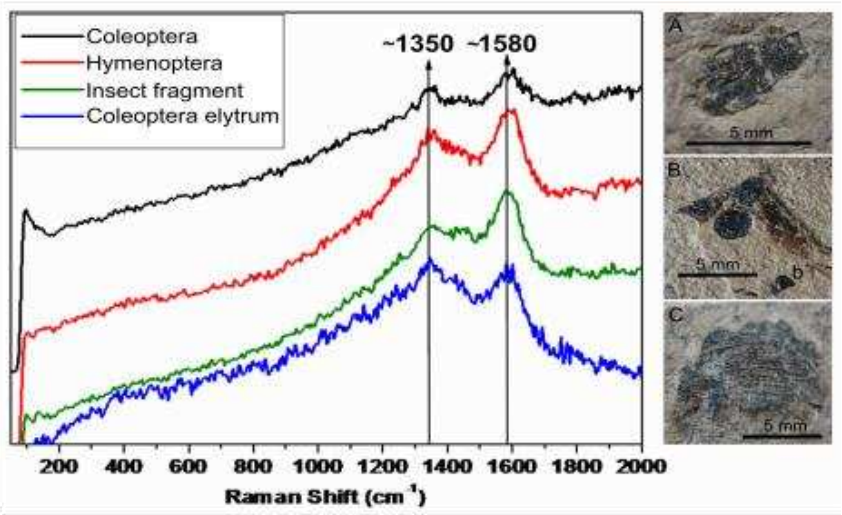

FIG. 7.—Raman spectra of fossil insects from the Fonseca Formation. A) Fully articulated Coleoptera. B) Hymenoptera, b' insect fragment around Hymenoptera body. C) Isolated elytrum of Coleoptera.

DISCUSSION

The set of insects from the Fonseca Formation studied here were derived from a terrestrial ecosystem. The cause and time of death of the Fonseca insects cannot be accurately determined. However, an overview of taphonomic patterns suggests that the final burial site for Fonseca's insects was most likely a low-energy, permanent body of freshwater. Most of the fully articulated and partially articulated insects lie with their largest surface area parallel to the bedding planes, suggesting that they settled vertically through the water column and came to rest on the sediment-water interface under low-energy conditions. Duncan et al. (2003) revealed that the pattern of fracturing of cockroach forewings occurs across veins in dry terrestrial environment. The absence of this pattern in the winged insects of the Fonseca Fm. indicates that most of the biostratinomic events were the result of decay in water, and not due to damage on the forest floor or predation. Most of the Fonseca insects may have fallen into the body of water or been immersed by rising water levels or even were washed into the lake shortly after death on land. The minimal damage of specimens included in grade 1 suggest that these insects likely dropped into water while flying over the lake, or alternatively underwent a very short period of decay on land before entering the water. Of the specimens studied, 40.6% are fully articulated, suggesting that these specimens have not experienced extensive flotation times at the water-air interface, shortening the opportunity for decomposition under aerobic conditions. Assemblages of insects are usually biased towards

smaller sizes in the fossil record (Wilson 1988; Martínez-Delclòs et al. 2004; Wang et al. 2013). Other studies have suggested that lacustrine environments preserve death assemblages with a greater proportion of smaller size and more robust groups (Smith 2000; Smith et al 2006). The results presented here show that smaller-winged insects tend to be fully articulated. Our study is, therefore, consistent with previous quantitative studies based on lacustrine assemblages (Smith 2000; Smith et al 2006). Most of the fully/partially disarticulated insects from the Fonseca Fm. are preserved in a dorsoventral position. Large insects are capable of floating on the water surface without ever sinking (Martínez-Delclòs and Martinell 1993). Thus, the preservation of fully articulated specimens decreases with floating time because decomposition is more extensive as the buoyancy time increases. Among the partially disarticulated insects (grades 2 and 3), six specimens lack the abdomen. The abdomen begins to deteriorate immediately after death; swelling due to gas fermentation facilitating buoyancy and causing rupture of the abdomen (Martínez-Delclòs et al. 2004; Ilger 2011). Twelve individuals lost their heads suggesting that they floated on the water surface for approximately two weeks (Peñalver 2002; Wang et al. 2013). Twenty-nine point six percent (29.6%) of insects are strongly disarticulated (grade 4), 16 and 14 of which are isolated abdomens and wings, respectively. Disarticulated body parts support a longer flotation time and/or an increase in distance from the source (Smith 2000). This is not surprising, as the Fonseca Basin records a complex meandering river system comprising small lakes formed when a meander was cut off. Thus, the taphonomic bias toward lower overall preservation quality of insects placed in grades 3 and 4 reflects a greater duration of time or exposure to higher levels of energy earlier in their biostratinomic history, before final burial of the insects in the lake. The increased time of transport under higher-energy conditions could lead to disarticulation.

Upon reaching the bottom of the lake, the insects experienced the initial phase of the fossil diagenetic process (Fig. 8). Specimens of the Fonseca assemblage show a color contrast with the surrounding rock matrix. Fossil soft tissues preserved as carbonaceous materials are composed of a variety of compounds, including N- heterocyclic polymers, carbonyl and carboxyl groups. Most of these organic compounds represent the fossilization products of proteins, polysaccharides (e.g., chitin), and lipids (Wiemann et al. 2018; McCoy et al. 2020). The structural tissues of many types of insect chitin are composed almost entirely of polysaccharides. The preservation of morphological characteristics can be designated as ‘exceptional’ preservation of soft tissues compared to carbonaceous compressions in non-marine shales. The flattening process of most megascopic carbonaceous insects in the Fonseca

Formation leads to retention of their morphological features and lack distortion. This indicates collapse of the cuticle under its own weight as it decays *in situ* on the lake floor, ruling out hypotheses that involve initiation of any type of mineralization of these fossils. The precipitation of diagenetic minerals was somehow not favored in the free-standing body of water (in an abandoned meander loop within the meandering river system of Fonseca). It is probable that a high postburial sedimentation rate could have supressed any mineral replacement process. The laminated bedding reflects the lack of strong currents in the Fonseca paleolake supporting a low-energy preservational environment. Thus, the most plausible hypothesis for the absence of mineralization is the unavailability or low concentration of reactive elements and ions (e.g., Fe^{2+}, Ca^{2+}, SO_4^{2-}, PO_4^{3-}).

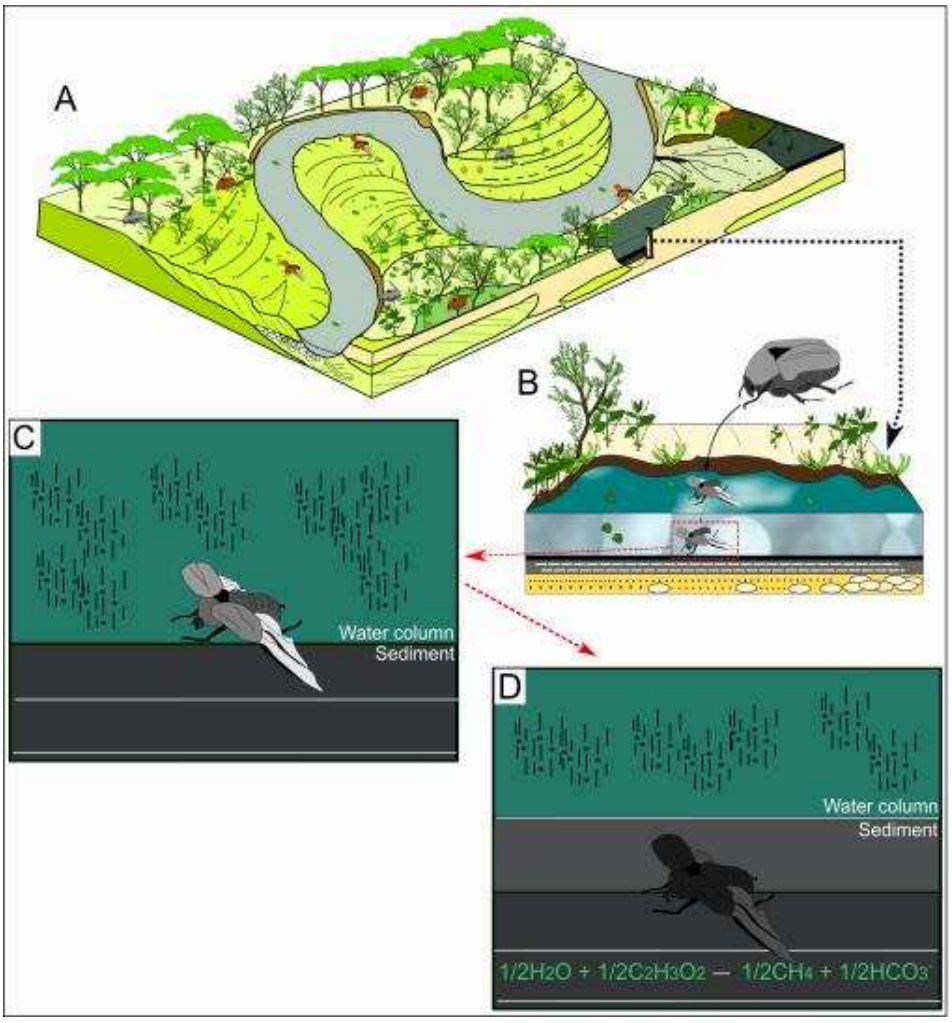

FIG. 8.—Taphonomic model for the insect preservation in the Fonseca Formation. A) Paleoenvironmental reconstruction of the meandering fluvial system based on previous studies (Sant'Anna and Schorscher 1997; Sant'Anna et al. 1997; Maizatto 2001). B) A meandering river system with a meander loop. Due to the river's eroding bank the meander becomes entrained, eventually the neck of the meander becomes narrower and the river

breaches through the neck during a flood forming an oxbow lake. This small lake collected and preserved insects that capsized or were transported into the lake. C) Upon reaching the lake, the fully articulated insects did not experience longer flotation times on the water surface, were transported to the bottom of the lake and, from there, were buried by sediments. D) Diagram shows entombed insect, post-burial sedimentation and onset of insect's cuticle preservation under anoxic conditions.

The Raman data revealed signals associated with D and G bands related to sp^2 carbon systems. The carbonaceous sp^2-bonded materials can be formed from carbonaceous compounds of biological origin. Thermal alteration processes in sedimentary rocks can transform products of biological origin into sp^2-bonded carbonaceous materials. Consequently, the presence of these bands represents organic constituents that are products of the original cuticle such as proteins, polysaccharides and lipids. However, carbonaceous sp^2-bonded materials can also be formed by hydrothermal fluids (Brasier et al. 2002), serpentinization (Pasteris 1988), or even high-temperature heating of inorganic compounds (Pasteris and Wopenka 2003). To overcome possible misinterpretations, we used Raman data in conjunction with SEM-EDS technique.

The preservation of fossil soft-tissues in siliciclastic facies can be driven by several diagenetic processes (Cai et al. 2012; Schiffbauer et al. 2014). Our taphonomic data show that the Fonseca insects underwent polymerization of organic compounds under anoxic conditions. The chitin may have been transformed into more stable biopolymers and labile lipids that could be incorporated into a more resistant aliphatic macromolecules via *in situ* polymerization during diagenesis (Stankiewicz et al. 1997; Gupta 2007). In other deposits, different types of fossilization have been observed for insects from the same bed or adjacent strata (Peñalver 2002; Wang et al. 2009; Anderson and Smith 2017; Dias and Carvalho 2020). Fossil insects from the Fonseca Formation, however, share the same preservation mode.

An increasingly warm climate during the lower to middle Paleogene influenced the widespread distribution of insects (Wappler et al. 2012). The entomofauna of the Fonseca Formation probably inhabited mainly a humid and warm tropical forest with leaf litter. Leaf litter would have been the main source of food for Coleoptera and Blattodea. The foliar physiognomy and floristic composition of the Fonseca paleoflora indicate that the mean annual temperature (MAT) was < 26ºC (Fanton et al. 2014). The arboreal families Annonaceae (custard apples), Meliaceae (mahoganies), Sapindaceae (soapberries), Malvaceae (mallows), Myrsinaceae (myrsines) and Bignoniaceae (bignonias) are typical

representatives of Atlantic forests of Southeast Brazil. These families also occur in the Fonseca strata, preserved as leaves, fruits or pollens (Fanton et al. 2012). These occurrences indicate that the Fonseca paleoflora being a possible precursor of the current Atlantic Forest. The above characteristics point to a rich and dynamic ecosystem that allows the potential of this paleoentomofauna to yield future discoveries. The relevance of Fonseca Fm. is herewith highlighted, not just as a *Lagerstätte* but as strata representing one of the last records of a warmer interval during the Cenozoic of Brazil.

CONCLUSIONS

This study evaluated the preservational quality of insects from the Fonseca Basin (Eocene–Oligocene boundary, Brazil) in order to recognize which factors might control taphonomic patterns in this new fossil assemblage. Our results reveal significant differences in the preservational quality of the Fonseca insects. The majority of the specimens are fully articulated, suggesting that these specimens experienced limited flotation times on the water-air interface. Partially articulated and disarticulated specimens also occur. These different preservational patterns may reflect different taphonomic biases controlled by factors such as transport distance, ecological traits, and floating time. Therefore, these differences in articulation measures probably occurred during the biostratinomy phase of their taphonomic history. The dark-colored materials in the fossil insects at the Fonseca site represent organic matter. Our SEM-EDS and Raman analyses reveal the preservation of collapsed carbonaceous material preserved via diagenetic polymerization of biomacromolecules into long chain aliphatic components. Thus, the fossils likely contain organic remains of the organisms. The possibility that the carbonaceous material was introduced into the fossil insects via migration of organic components in the arenaceous/micaceous host rock is minimal. In this case, the carbonaceous material may represent remains from the insect's original chitin. To date, some types of organic compounds have been discovered from fossil remains, and future work should aim to determine the exact properties of this carbonaceous material. Here, we did not attempt to classify the Fonseca Formation as a *Lagerstätte* with respect to criteria such as type of sedimentary basin, geological age, and palaeontological, stratigraphic, or environmental features. However, recognition as a *Lagerstätte* is not necessary to initiate and encourage further studies. The Eocene–Oligocene boundary interval was a mostly ice-free warmhouse period that preceded global cooling. From the middle Oligocene, the world acquired a more seasonal climate (Westerhold et al. 2020). This interval is insufficiently studied in South America, especially in Brazil. In addition to the poorly understood paleoentomofauna, the

lack of stratigraphic control does not currently allow accurate paleoenvironmental interpretation of the entire basin, providing potential for future studies.

ACKNOWLEDGMENTS

We thank Mr. José Alves Patrício, a local resident, for his assistance with fieldwork. We are grateful to the Dr. Patrick Orr, Palaios science Editor, and the reviewers Dr. Bo Wang, Dr. Enrique Peñalver and an anonymous, whose comments have improved our original manuscript. FIB is grateful for his doctorate scholarship (Coordenação de Aperfeiçoamento de Pessoal de Nível Superior, Brasil - CAPES, process 88882. 454892/2019-01). JHS acknowledges CNPq for the support granted through project (no. 302372/2018-0).

SUPPLEMENTAL MATERIAL

Data are available from the PALAIOS Data Archive:

https://www.sepm.org/supplemental-materials

REFERENCES

ANDERSON, E. AND SMITH, D.M., 2017, The same picture through different lenses: quantifying the effects of two preservation pathways on Green River Formation insects: Paleobiology, v. 43, p. 224–247, doi: 10.1017/pab.2016.29.

BEZERRA, F.I., MENDES, M., AND DE SOUZA, O., 2020, A new record of Mastotermitidae from Fonseca Basin, Eocene–Oligocene boundary of southeastern Brazil: Biologia, doi: 10.2478/s11756-020-00441-x.

BRASIER, M.D., GREEN, O.R., JEPHCOAT, A.P., KLEPPE, A.T., VAN KRANENDONK, M.J., LINDSAY, J.F., STEELE, A., AND GRASSINEAU, N.V., 2002, Questioning the evidence for Earth's oldest fossils: Nature, v. 416, p. 76–81, doi: 10.1038/416076a.

BURNHAM, R.J. AND JOHNSON, K.R., 2004, South American palaeobotany and the origins of neotropical rainforests: Philosophical Transactions of the Royal Society B, Biological Sciences, v. 359, p. 1595–1610, doi: 10.1098/rstb.2004.1531.

CAI, Y., SCHIFFBAUER, J.D., HUA, H., AND XIAO, S., 2012, Preservational modes in the Ediacaran Gaojiashan *Lagerstätte*: pyritization, aluminosilicification, and carbonaceous compression: Palaeogeography, Palaeoclimatology, Palaeoecology, v. 326-328, p. 109–117, doi: 10.1016/j.palaeo.2012.02.009.

DIAS, J.J. AND CARVALHO, I.S., 2020, Remarkable fossil crickets preservation from Crato Formation (Aptian, Araripe Basin), a *Lagerstätten* from Brazil: Journal of South American Earth Sciences, v. 98, p. 102443, doi: 10.1016/j.jsames.2019.102443.

DUNCAN I.J., TITCHENER, F., AND BRIGGS, D.E.G., 2003, Decay and disarticulation of the cockroach: implications for preservation of the blattoids of Writhlington (upper Carboniferous), UK: PALAIOS, v. 18, p. 256–265, doi: 10.1669/08831351(2003)018,0256: DADOTC.2.0.CO;2.

ENGEL, M.S. AND GRIMALDI, D., 2004, New light shed on the oldest insect: Nature, v. 427, p. 627–630.

FANTON, J.C., RICARDI-BRANCO, F., AND MENDES, M., 2014, As paleofloras de Fonseca e Gandarela revisadas e insetos associados: Paleógeno do Sudeste brasileiro, in I.S. Carvalho, M.J. Gárcia, C.C. Lana, and O. Strohschoen (eds.), Paleotologia: Cenários de vida–Paleoclima: Interciência, Rio de Janeiro, p. 241–253.

FANTON, J.C.M., RICARDI-BRANCO, F., AND SILVA, A.M., 2012, *Terminalia Palaeopubescens* sp. nov. (Combretaceae) da Formação Fonseca (Eoceno/Oligoceno) de Minas Gerais, Brasil: morfologia foliar, fungos epifilicos associados e paleoclima: Ameghiniana, v. 49, p. 273–288, doi: 10.5710/AMGH.v49i3(344).

GRIMALDI, D. AND ENGEL, M.S., 2005, Evolution of the Insects: Cambridge University Press, New York, 755 p.

GUPTA, N.S., 2007, Evidence for the in situ polymerisation of labile aliphatic organic compounds during the preservation of fossil leaves: implications for organic matter preservation: Organic Geochemistry, v. 38, p. 499–522, doi: 10.1016/j.orggeochem.2006.06.011.

HAUG, C. AND HAUG, J.T., 2017, The presumed oldest flying insect: more likely a myriapod?: PeerJ, v. 5, e3402, doi: 10.7717/peerj.3402.

HAUG, J.T., HAUG, C., AND GARWOOD, R.J., 2016, Evolution of insect wings and development—new details from Palaeozoic nymphs: Biological Reviews, v. 91, 53–69, doi:

10.1111/brv.12159.

HENWOOD, A., 1993, Ecology and taphonomy of Dominican Republic amber and its inclusions: Lethaia, v. 26, p. 237–245, doi: 10.1111/j.1502-3931.1993.tb01525.x.

ILGER, J.M., 2011, Young bivalves on insect wings: a new taphonomic model of the *Konservat-Lagerstaette* Hagen-Vorhalle (early late Carboniferous; Germany): Palaeogeography, Palaeoclimatology, Palaeoecology, v. 310, p. 315–323, doi: 10.1016/j.palaeo.2011.07.023.

MAIZATTO, J.R., 2001, Analise bioestratigrafica, paleoecologica e sedimentologica das bacias terciárias de Gandarela e Fonseca, Quadrilátero Ferrífero, Minas Gerais, com base nos aspectos palinologicos e sedimentares: Unpublished Ph.D. dissertation, Universidade Federal de Ouro Preto, Ouro Preto, 333 p.

MAIZATTO, J.R., REGALI, M.S.P., AND CASTRO, P.T.A., 2008, Analise biocronoestratigrafica e paleoclimática das bacias paleogenas e neogenas do Gandarela e Fonseca, Quadrilátero Ferrífero-Minas Gerais, Brasil: 128 Simpósio Brasileiro de Paleobotânica e Palinologia, Florianópolis, Boletim de Resumos, p. 1–133.

MARTÍMUS, M., 2014, Interpreting ‘shelly’ fossils preserved as organic films: the case of hyolithids: Lethaia, v. 47, p. 397–404, doi: 10.1111/let.12066.

MARTÍNEZ-DELCLOÒS, X., BRIGGS, D.E.G., AND PEÑALVER, E., 2004, Taphonomy of insects in carbonates and amber: Palaeogeography, Palaeoclimatology, Palaeoecology, v. 203, p. 19–64, doi: 10.1016/S0031-0182(03)00643-6.

MARTÍNEZ-DELCLÒS, X. AND MARTINELL, J., 1993, Insect taphonomy experiments: their application to the Cretaceous outcrops of lithographic limestones from Spain: Kaupia, v. 2, p. 133–144.

MARTINS-NETO, R.G., 2005, Estágio atual da paleoartropodologia brasileira: hexapodes, miriapodes, crustáceos (Isopoda, Decapoda, Eucrustacea e Copepoda) e quelicerados: Arquivos do Museu Nacional do Rio de Janeiro, v. 63, p. 471–494.

McCOY, V.E., WIEMANN, J., LAMSDELL, J.C., WHALEN, C.D., SCOTT LIDGARD, S., MAYER, P., PETERMANN, H., AND BRIGGS, D.E.G., 2020, Chemical signatures of soft tissues distinguish between vertebrates and invertebrates from the Carboniferous Mazon Creek *Lagerstätte* of Illinois: Geobiology, v. 18(5), p. 1–6, doi: 10.1111/gbi.12397.

McNAMARA, M.E., ORR, P.J., KEARNS, S.L., ALCALA, L., ANADON, P., AND PEN˜

ALVER-MOLLA, E., 2006, High-fidelity organic preservation of bone marrow in ca 10 Ma amphibians: Geology, v. 34, p. 641–644, doi: 10.11310/ G22526.1.

MUSCENTE, A.D., CZAJA, A.D., RIEDMAN, L.A., AND COLLEARY, C., 2017, Organic matter in fossils, in W.M. White (ed.), Encylopedia of Geochemistry, Encyclopedia of Earth Science Series: Springer, Cham, p. 1–5, doi: 10.1007/978-3-319-39193-9.

MUSCENTE, A.D. AND XIAO, S., 2015, Resolving three-dimensional and subsurficial features of carbonaceous compressions and shelly fossils using backscattered electron scanning electron microscopy (BSE-SEM): PALAIOS, v. 30, p. 462–481, doi: 10.2110/palo.2014.094.

NEL, A., ROQUES, P., NEL, P., PROKIN, A.A., BOURGOIN, T., PROKOP, J., SZWEDO, J., AZAR, D., DESUTTER-GRANDCOLAS, L.,WAPPLER, T.,GARROUSTE, R., COTY, D., HUANG, D., ENGEL, M.E., AND KIREJTSHUK, A.G., 2013,The earliest known holometabolous insects: Nature, v. 503, p. 257–261, doi: 10.1038/nature12629.

PASTERIS, J.D., 1988, Secondary graphitization in mantle derived rocks: Geology, v. 16, p. 804–807, doi: 10.1130/0091-7613(1988)0162.3.CO;2.

PASTERIS, J.D. AND WOPENKA, B., 2003, Necessary, but not sufficient: Raman identification of disordered carbon as a signature of ancient life: Astrobiology, v. 3, p. 727–738, doi: 10.1089/ 153110703322736051.

PEÑALVER, E., 2002, Los insectos dípteros del Mioceno del Este de la Península Ibérica; Rubielos de Mora, Ribesalbes y Bicorp Tafonomía y sistemática: Published Ph.D. thesis, Universitat de València, València, 550 p.

RASNITSYN, A.P. AND QUICKE, D.L., 2002, History of Insects: Kluwer Academic Publishers, Dordrecht, 517 p.

RUST, J., SINGH, H., RANA, R.S., MCCANN, T., SINGH, L., ANDERSON, K., SARKAR, N., NASCIMBENE, P.C., STEBNER, F., THOMAS, J.C., SOLÓRZANO KRAEMER, M.M., WILLIAMS, C.J., ENGEL, M.S., SAHNI, A., AND GRIMALDI, D., 2010, Biogeographic and evolutionary implications of a diverse paleobiota in amber from the early Eocene of India: Proceedings of the National Academy of Sciences, v. 107, p. 18360–18365, doi: 10.1073/pnas.1007407107.

SAADT, A., 1991, Ensaio sobre a morfotectônica de Minas Gerais: Unpublished Ph.D. dissertation, Universidade Federal de Minas Gerais, Belo Horizonte, 285 p.

SANT'ANNA, L.C., 1994, Minerologia das argilas e evolução geológica da Bacia de Fonseca, Minas Gerais: Unpublished M.S. thesis, Universidade de Sao Paulo, São Paulo, 151 p.

SANT'ANNA, L.C. AND SCHORSCHER, H.D., 1995, Leques aluviais cenozóicos do flanco leste da Serra da Caraça (MG): a Formação Chapada de Canga: Anais da Academia Brasileira de Ciências, v. 67(4), p. 5–19.

SANT'ANNA, L.G., SCHORSCHER, H.D., AND RICCOMINI, C., 1997, Cenozoic tectonics of the Fonseca Basin region, Eastern Quadrilatero Ferrífero, MG, Brazil: Journal of South American Earth Sciences, v. 10, p. 275–284, doi: 10.1016/S0895-9811(97)00016-3.

SCHACHAT, S.R. AND LABANDEIRA, C.C., 2020, Are insects heading toward their first mass extinction? Distinguishing turnover from crises in their fossil record: Annals of the Entomological Society of America, v. 114, p. 99–118, doi: 10.1093/aesa/saaa042.

SCHACHAT, S.R., LABANDEIRA, C.C., SALTZMAN, M.R., CRAMER, B.D., PAYNE, J.L., AND BOYCE, C.K., 2018, Phanerozoic pCO_2 and the early evolution of terrestrial animals: Proceedings of the Royal Society B, Biological Sciences, v. 285, p. 20172631, doi: 10.1098/rspb.2017.2631.

SCHIFFBAUER, J.D., XIAO, S., CAI, Y., WALLACE, A.F., HUA, H., HUNTER, J., XU, H., PENG, Y., AND KAUFMAN, A.J., 2014, A unifying model for Neoproterozoic–Palaeozoic exceptional fossil preservation through pyritization and carbonaceous compression: Nature Communications, v. 5, p. 112, doi: 10.1038/ncomm6754.

SEPKOSKI, J.J., BAMBACK, R.K., RAUP, D.M., AND VALENTINE, J.W., 1981, Phanerozoic marine diversity and the fossil record: Nature, v. 293, p. 435–437.

SMITH, D.M., 2000, Beetle taphonomy in a recent ephemeral lake in southeastern Arizona: PALAIOS, v. 15, p. 152–160, doi: 10.1669/0883-1351(2000)015,0152: BTIARE.2.0.CO;2.

SMITH, D.M., 2001, Taphonomic bias and insect diversity: a lesson from the beetles and flies: PaleoBios, v. 21, p. 117.

SMITH, D.M., 2012, Exceptional preservation of insects in lacustrine environments: PALAIOS, v. 27, p. 346–353, doi: 10.2110/palo.2011.p11-107r.

SMITH, D.M., COOK, A., AND NUFIO, C.R., 2006, How physical characteristics of beetles affect their fossil preservation: PALAIOS, v. 21, p. 305–310, doi: 10.2110/palo.2004.p04-91.

SMITH, D.M. AND MOE-HOFFMAN, A.P., 2007, Taphonomy of Diptera in lacustrine environments: a case study from Florissant Fossil Beds, Colorado: PALAIOS, v. 22, p. 623–629, doi: 10.2110/palo.2006.p06-119r.

SOLÓRZANO-KRAEMER, M.M., 2007, Systematic, palaeoecology, and palaeobiogeography of the insect fauna from Mexican amber: Palaeontographica Abteilung A, v. 282, p. 1–133, doi: 10.1127/pala/282/2007/1.

SOLÓRZANO KRAEMER, M.M., DELCLÒS, X., CLAPHAM, M.E., ARILLO, A., PERIS, D., JA¨ GER, P., STEBNER, F., AND PEÑALVER, E., 2018, Arthropods in modern resins reveal if amber accurately recorded forest arthropod communities: Proceedings of the National Academy of Sciences, v. 115, p. 6739–6744, doi: 10.1073/pnas.1802138115.

SOMMER, F.W. AND LIMA, C.D., 1967, Contribuição a paleoflora de Fonseca, Minas Gerais: Anais da Academia Brasileira de Ciências, v. 39, p. 537–538.

STANKIEWICZ, B.A., BRIGGS, D.E.G., AND EVERSHED, R.P., 1997, Chemical composition of Paleozoic and Mesozoic fossil invertebrate cuticles as revealed by pyrolysis-gas chromatography/mass spectrometry: Energy Fuel, v. 11, p. 515–521, doi: 10.1021/ef9601778.

TIAN, Q., WANG, S., YANG, Z., MCNAMARA, M.E., BENTON, M.J., AND JIANG, B., 2020, Experimental investigation of insect deposition in lentic environments and implications for formation of *Konservat Lagerstaetten*: Palaeontology, v. 63, p. 565–578, doi: 10.1111/pala.12472.

WANG, B., LI, J.F., FANG, Y., AND ZHANG, H.C., 2009, Preliminary elemental analysis of fossil insects from the Middle Jurassic of Daohugou, Inner Mongolia and its taphonomic implications: Chinese Science Bulletin, v. 54, p. 783–787, doi: 10.1007/S11434-008-0561-5.

WANG, B., ZHANG, H., JARZEMBOWSKI, E.A., FANG, Y., AND ZHENG, D., 2013, Taphonomic variability of fossil insects: a biostratinomic study of Palaeontinidae and Tettigarctidae (Insecta: Hemiptera) from the Jurassic Daohugou *Lagerstätte*: PALAIOS, v. 28, p. 233–242, doi: 10.2110/palo.2012.p12-045r.

WAPPLER, T., LABANDEIRA, C.C., RUST, J., FRANKENHA¨ USER, H., ANDWILDE, V., 2012, Testing for the effects and consequences of mid Paleogene climate change on insect herbivory: PLoSOne, v. 7, e40744, doi: 10.1371/journal.pone.0040744.

WESTERHOLD, T., MARWAN, N., DRURY, A.J., LIEBRAND, D., AGNINI, C.,

ANAGNOSTOU, E., BARNET, J.S., BOHATY, S.M., DE VLEESCHOUWER, D., FLORINDO, F., AND FREDERICHS, T., 2020, An astronomically dated record of Earth's climate and its predictability over the last 66 million years: Science, v. 369(6509), p. 1383–1387, doi: 10.1126/science.aba6853.

WIEMANN, J., FABBRI, M., YANG, T.R., STEIN, K., SANDER, P.M., NORELL, M.A., AND BRIGGS, D.E.G., 2018, Fossilization transforms vertebrate hard tissue proteins into Nheterocyclic polymers: Nature Communications, v. 9, p. 4741, doi: 10.1038/s4146 7-018-07013-3.

WILSON, M.V.H., 1988, Reconstruction of ancient lake environments using both autochthonous and allochthonous fossils: Palaeogeography, Palaeoclimatology, Palaeoecology, v. 62, p. 609–623, doi: 10.1016/0031-0182(88)90074-0.

WILSON, R.L., 1965, techniques and materials used in the preparation of vertebrate fossils: Curator, v. 8(2), p. 135–143, doi: 10.1111/j.2151-6952.1965.tb00857.x.

4 CAPÍTULO 2

Distinct preservational pathways of insects from the Crato Formation, Lower Cretaceous of the Araripe Basin, Brazil

Esse capítulo foi publicado no jornal científico "Cretaceous Research"; o material suplementar associado ao artigo citado abaixo pode ser encontrado online em https://doi.org/10.1016/j.cretres.2020.104631.

Referência:

Francisco Irineudo Bezerra, Mónica M. Solórzano-Kraemer, Márcio Mendes (2021) Distinct preservational pathways of insects from the Crato Formation, Lower Cretaceous of the Araripe Basin, Brazil. Cretaceous Research 118, 104631. doi: 10.1016/j.cretres.2020.104631

Distinct preservational pathways of insects from the Crato Formation, Lower Cretaceous of the Araripe Basin, Brazil

Francisco Irineudo Bezerra[a], Mónica M. Solórzano-Kraemer[b], Márcio Mendes[a]

[a]Departamento de Geologia, Universidade Federal Do Ceará, 64049-550, Fortaleza, Ceará, Brazil

[b]Department of Palaeontology and Historical Geology, Senckenberg Research Institute, Senckenberganlage 25, 60325 Frankfurt Am Main, Germany

Abstract

This study compares two different preservation pathways of fossil insects in the lacustrine deposits of the Crato Formation, Lower Cretaceous (Aptian) of the Araripe Basin, northeastern Brazil. Three hundred seventy-seven specimens were examined and separated into ten taxonomic groups. Of this total, one hundred twenty-three are kerogenized insects, and two hundred fifty-four are pyritized insects. We carried out quantitative analyses of their taphonomic characters, such as body articulation, and morphological preservational quality (e.g. discernible eyes). Of all morphological categories, the thorax presented the highest degree of preservation quality, while the antennae had the lowest. Our statistical results show significant differences in the preservation quality of individual morphological categories among the insect taxa. We expected that mineralized insects would have lower preservational quality than the kerogenized ones, but instead found the opposite pattern to be true. Counter to the findings of other studies, we found that pyritized insects had higher preservation quality than kerogenized insects. The expected lower preservation fidelity of pyritized fossils occurs due to longer time exposed to microbial decay before final burial. Few studies have presented a quantitative comparison of reservational/biostratinomic patterns in different insect taxa, especially within the same geological setting. In this context, the Crato Formation presents an intriguing and unique opportunity to understand the taphonomic bias that results from two different preservation pathways of insects.

Keywords: Taphonomy, Kerogenization, Pyritization, Limestone, Depositional environment

1. Introduction

Since the Carboniferous insects have been a group that has experienced a nearly continuous increase in diversity. Today, they represent the most diverse and widespread animal clade in the history of life on Earth (Labandeira and Sepkoski, 1993; Grimaldi and Engel, 2005). The large insect fossil record extends from different terrestrial to marine environments (Smith et al., 2006; Smith and Moe-Hoffman, 2007; Smith, 2012). Among different geological settings in which fossil insects can occur, those preserved in amber and in lacustrine deposits have been highlighted for their quality of preservation (Henwood, 1992, 1993; Martínez-Declòs and Martinell, 1993; Smith, 2000, 2012; Martínez-Declòs et al., 2004; Smith et al., 2006; Edwards et al., 2007; Thoene Henning et al., 2012; Wang et al., 2013; Barling et al., 2015; McCoy et al., 2018; Bezerra et al., 2020). Insects preserved in amber display higher morphological fidelity, though the sticky resin only captures insects living in and around the resiniferous trees (Solórzano-Kraemer et al., 2015, 2018). Amber inclusions occur rarely in the Triassic (Schmidt et al., 2012). However, amber accumulations increase in importance only after the Early Cretaceous (Smith, 2012). Lacustrine deposits can be found since the Carboniferous, preserving taxa from distinct ontogenetic stages, distinct habits and variable sizes. The insect accumulation in lake sediments is a significant complement to the insect fossil record in terms of diversity. Hence, increasing our understanding about the taphonomic processes involved in these insect assemblages is essential to interpreting both the palaeoecology and palaeoenvironment (Martínez-Delclòs et al., 2004).

In this context, the Crato Formation (Aptian of the Araripe Basin, northeastern Brazil) is one of the world's premiere Fossil-lagerstätten (Seilacher, 1970), yielding an exceptionally well-preserved entomofauna in a series of lake deposits. The Crato Fm. consists of laminated limestones interbedded with a series of claystones, siltstones and sandstones, deposited in at lacustrine system (Heimhofer et al., 2010). Typically, Crato carbonate facies can be dividided into two different sub-facies: clayecarbonate rhythmites (CCR) and laminated limestones (LL) (Neumann et al., 2003). Normally, CCR facies yield dark-grey-colored layers while LL occurs in yellow-colored layers (Fig. 1). The Crato insects commonly appear as an orange to brown friable material or as a seemingly amorphous dark matter. Previous studies have hypothesized this difference in preservation as a result of rock weathering (Delgado et al., 2014; Oses et al., 2016). But Oses et al. (2017) reported two distinct taphonomic modes: carbonaceous compressions in dark limestones and iron oxy-hydroxide after pyrite in yellow-colored limestone. In addition, Bezerra et al. (2018)

identified a cockroach preserved into carbonaceous compressions in dark limestones. Thus, we consider that the insects are preserved in a kerogenization zone (dark limestone) and a pyritization zone (yellow limestone).

Preservation by keroginization represents cyclic hydrocarbons and aliphatic components which have undergone chemical transformation from original organic material into the fossil record (Stankiewicz et al., 1998; Briggs, 1999; McNamara et al., 2013; Schiffbauer et al., 2014). According to Schiffbauer et al. (2014), this preservation style occurs when the carcass is placed most of time into a metanogenesis zone of the sediment column. In the bacterial sulfate reduction zone (BSR), an organism becomes pyritized when ions generated by bacterial activity produce minerals that replaces the body soft-tissue (Raiswell et al., 1993; Schiffbauer et al., 2014). Both keroginization and pyritization are able to preserve recalcitrant components of soft-bodied material. However, pyritized fossils tend to undergo further degradation than kerogenized ones, given the greater amount of time in the BSR which is more metabolically efficient than the Methanogenesis Zone (Anderson and Smith, 2017). Surprisingly, pyritized insects from the Crato Formation are preserved with ultrastructural cuticular details (Barling et al., 2015; Oses et al., 2016). Therefore, the Crato Fm. offers a rare opportunity to compare how two very different preservational pathways differ within the same geological setting. Thus we compared the preservational fidelity between keroginized and pyritized insects from the Crato Formation of the Araripe Basin in northeastern Brazil to understand which preservational style is superior for preserving soft-bodied fossils.

2. Geological setting

The Araripe Basin is one of the largest basins in the interior of the Brazilian northeast (Fig. 2). The Crato Fm. comprises a 70-m thick succession and consists of carbonate layers interbedded with siliciclastic sediments (shales, claystones and sandstones), whose origin is attributed to transgressive-regressive events associated with the expansion and contraction of a lacustrine system (Neumann, 1999). Crato strata (Aptian) represent the second lacustrine phase in the development of the Araripe Basin (Assine et al., 2014).

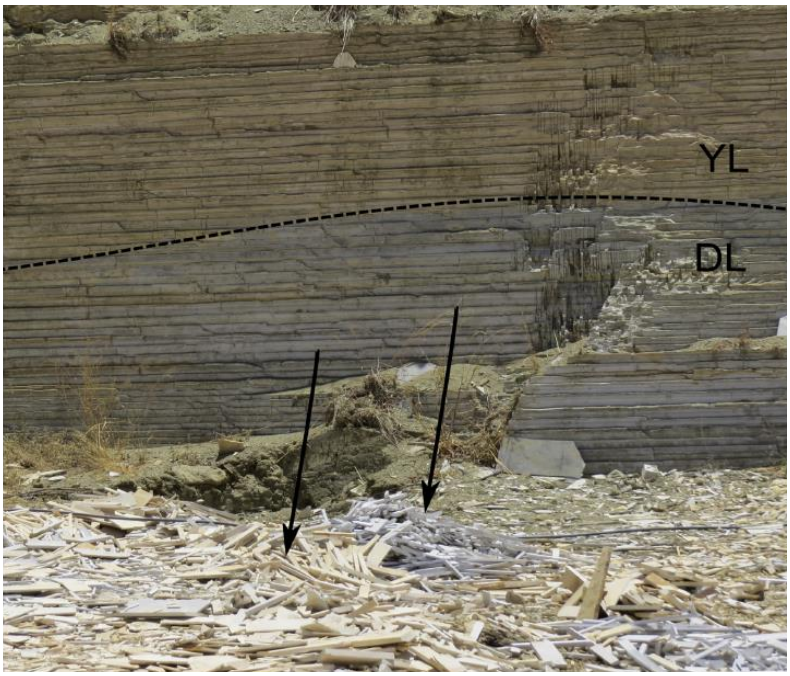

Fig. 1. View of the Crato limestone exposure in one of the quarries located between Nova Olinda and Santana do Cariri, Ceará. Here, the contact between the pyritization zone and kerogenized zone is shown. The arrows showing the two types that are left over after extraction of Pedra Cariri.

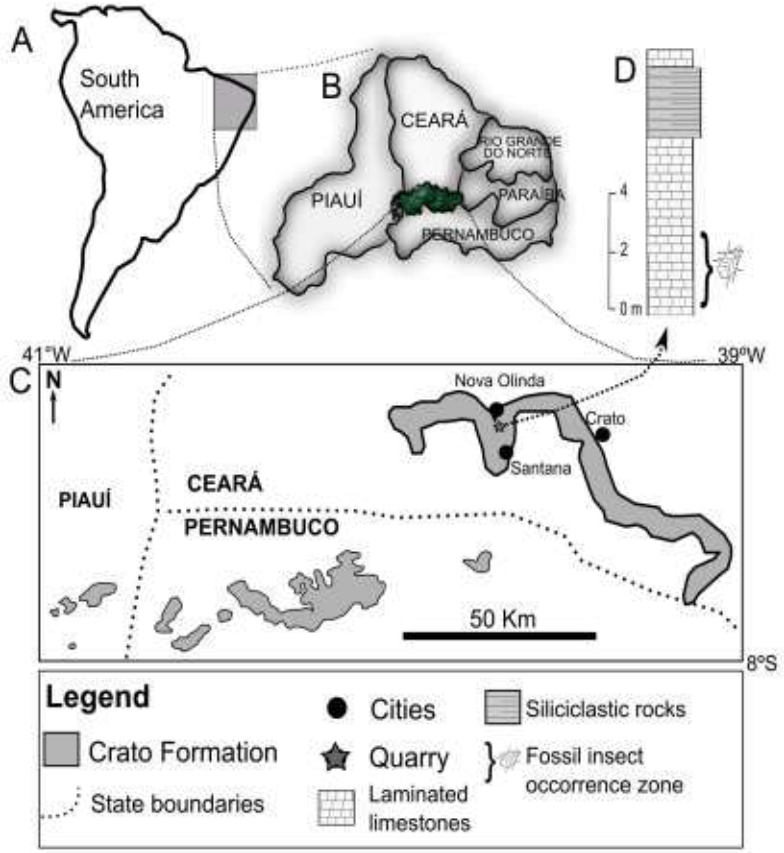

Fig. 2. Simplified map showing the location of the Crato Formation. A. The map of the South

America continent shows the position of some states in northeastern Brazil. B. Black square showing the position of the Araripe Basin. C. Local map showing the main outcrops of the Crato Formation. D. Generalized stratigraphy of the Crato Formation in the Nova Olinda, Ceará.

The Crato carbonate facies have a micritic calcite composition with low magnesium content (Neumann, 1999; Catto et al., 2016). This unit is part of the Aptian post-rift I sequence (Assine, 2007). The origin of the Crato laminated carbonates has been attributed to chemical precipitation associated with fine clastic sediments (Heimhofer et al., 2010). Catto et al. (2016) investigated the evidence of microbial influence on the formation of the Crato limestones. The presence of halite pseudomorphs in some levels suggests deposition under fluctuating salinity conditions (Martill et al., 2007). The excellent preservation of Crato fossils have made it known worldwide as a Cretaceous Fossil *Lagerstaette*. Most of the outcrops of laminated limestones are exposed due to the commercial extraction of pedra cariri (Pedra = stone; Cariri = Southern region of Ceará) in small quarries.

3. Material and methods

All insects analyzed in this study are deposited in the Laboratório de Paleontologia from Universidade Federal do Ceará (UFC). The fossils were collected over several years during different fieldwork campaigns. All fieldwork activities involved geology and biological sciences undergraduate students. The collections focused on the materials left over after the process of separating the lucrative Pedra Cariri. Taxonomic classification was made to order level. The suborders Heteroptera and Auchenorrhyncha (Hemiptera) and the suborders Caelifera and Ensifera (Orthoptera) were separated from their broad orders because we consider that the morphological differences between these suborders are sufficiently considerable for the purpose of this study. In order to avoid possible nomenclature problems we preferred to gather the specimens using a general term, taxon. All insects were analyzed using a standard quantitative method of scoring preservational quality.

The preservation-quality indicators were quantitatively assigned scores for different categories of insect morphology: head; antennae; eyes; legs; thorax; abdomen and wings. The maximum score for a category depended on the morphological variability within each category. The antennae, legs, thorax, abdomen have four potential scores, where 0: not preserved; 1: present without details; 2: present showing major segments; 3: present showing

all segments. The wings have four potential scores, 0: absence; 1: present as an outline; 2: at least one wing with partially erased veins or folded; 3: at least one extended wings with all veins. The head and eyes have three potential scores, 0: not preserved; 1: present; 2: present with details. For comparisons of "presence" or "absence" of each morphological category between the pyritized and kerogenized insects, we assigned the score 0, when the trait is absent, and the score 1, when the trait is present even without anatomical details. For the "articulation" state, we considered articulated insects those which display the head, thorax, abdomen, and at least one articulated wing (if preserved in dorsal view), and head, thorax, abdomen, at least one leg, and at least one wing articulated (if preserved in both lateral and ventral views). Almost complete bodies such as specimens with head, thorax and wings; thorax and abdomen; head and abdomen; or winged specimens missing wings or specimens with no legs were considered "partially articulated". Isolated wings or legs represent the "disarticulated" specimens. The orientation of each fully/partially articulated specimen in the host slab, dorsoventral or lateral position, was also documented. The proportions of the quality scores of the articulation states were determined by comparing the completeness of entire insect bodies between the two preservation types, where 0: disarticulated (Fig. 5H), 1: partially articulated (Fig. 5D); 2: fully articulated (Fig. 5E).

To compare pyritized and kerogenized insects we used the chi square tests (Franke et al., 2012). A chi-square contingency test was used to compare the frequency distributions among all taxa and the number of samples within each insect taxon. The chi-square goodness of fit test was used to compare the observed distribution to the expected distribution of the maximum values (score of 3), zero values (score of 0) and the articulation state. The differences in the frequency distributions were tested with an α of 0.05. A list of these specimens and their associated data can be found in the online supplementary material. All statistical analyses were performed using EXCEL and PAST version 3.09.

The percolation of late diagenetic meteoric fluids leading to loss of fine details is a taphonomical factor that should be considered. Thus, intensely weathered specimens were not included in this study.

4. Results

4.1. Taxonomic and taphonomic distributions

In this study we analyzed 377 insects from the Crato Formation: 123 insects were

described from the kerogenized zone and 254 insects were described from the pyritized zone. Only insects identifiable to orders were considered as a result, ten insect taxa were included in this study: Blattodea (Without Isoptera), Ensifera (Orthoptera), Caelifera (Orthoptera), Odonata, Ephemeroptera, Neuroptera, Coleoptera, Diptera, Auchenorrhyncha (Hemiptera) and Heteroptera (Hemiptera) (Table 1).

Taxon	**Kerogenized insects**	**Pyritized insects**	**Chi-squared tests**	
			$\chi 2$	***P-value***
Blattodea	11	42	3.397	0.065
Neuroptera	36	17	**12.53**	**$< 10^{-4}$**
Auchenorrhyncha	18	27	1.113	0.291
Caelifera	11	33	1.164	0.280
Ensifera	16	33	$< 10^{-4}$	0.996
Odonata	12	27	0.061	0.804
Heteroptera	7	24	1.426	0.232
Ephemeroptera	0	27	_	_
Coleoptera	4	14	0.886	0.346
Diptera	8	10	1.143	0.284
Total	123	254		

Table 1. Number of insects for each taxonomic group from the Crato Formation. Statistically significant values are given in bold.

Of the 123 kerogenized insects, the most abundant taxa are Neuroptera (28.8%), Auchenorrhyncha (14.4%), Ensifera (12.8%) and Blattodea (10.4%). There were no kerogenized Ephemeroptera found. Of 254 pyritized insects, the most abundant are Blattodea (17.2%), Caelifera (13.5%), Odonata (11%) and Ephemeroptera (11%) (Fig. 3).

Of the total of specimens, 59.2% were whole bodies with wings, 37.9% of bodies were not complete; they had lost delicate structures, such as their antennae, head or discernible legs. Only 2.1% of specimens were isolated wings, and only 0.8% were isolated legs. 55.4% of all specimens were preserved in a dorsal position, 14.6% and 27% were preserved in lateral and ventral positions, respectively. The antennae were the most affected feature, only 3.2% of insects exhibited complete antennae with all segments. Only 9.3% of all

insects showed discernible eyes. 26% of insects displayed at least one articulated leg. One-third of the winged insects preserved in a lateral position have wings folded, while 83% of the winged insects preserved in a dorsal position were with forewings partially spread in flight position.

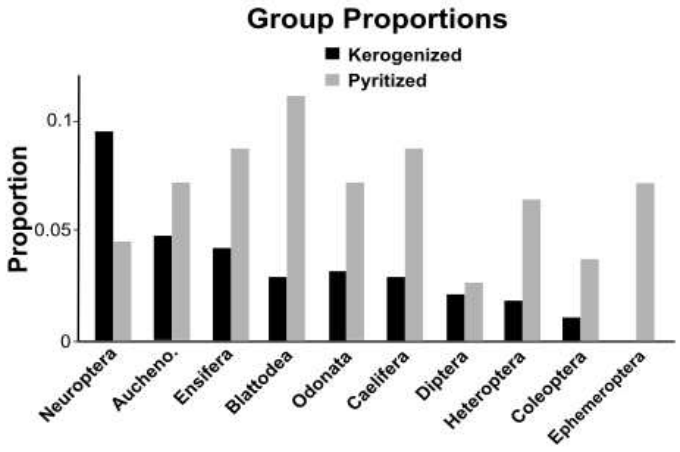

Fig. 3. The proportional distribution of identified kerogenized and pyritized insects from the Crato Formation.

4.2. Comparison of preservational fidelity for individual morphological categories

We compared all kerogenized and all pyritized insects and the distribution of quality scores is significantly different between both types of preservation. The quantitative analyses revealed significant differences in the frequency distributions of scores for the head ($x^2 = 4.134$; $p = 0.042$; $df = 1$), the legs ($x^2 = 8.446$; $p = 0.014$; $df = 2$), the abdomen ($x^2 = 34.321$; $p < 10^{-4}$; $df = 2$) and the eyes ($x^2 = 9.596$; $p = 0.0019$; $df = 1$). There was no significant difference in the frequency of preservational fidelity scores of the antennae ($x^2 = 1.270$; $p = 0.529$; $df = 2$) and thoraces ($x^2 = 3.913$; $p = 0.141$; $df = 2$) between the two preservation types. The wings also showed no significant difference ($x^2 = 2.755$; $p = 0.252$; $df = 2$). For wings, the preservational process was not selective; both membranous and heavily sclerotized forewings (tegmina) are often present. Even membranous wings beneath the elytra of Coleoptera and hemelytra of Heteroptera are usually preserved for both the pyritized and kerogenized insects.

When we compared only individual insect taxa, the distributions of the individual morphological categories were often significantly different between the mineralized and kerogenized insects. In addition to the abdomen, the other morphological categories that had significant differences were wings, head, antennae and legs among the included taxa. For

example, the comparison between the kerogenized Ensifera and pyritized Ensifera revealed differences in the abdomen ($x^2 = 6.975$; $p = 0.030$; $df = 2$); head ($x^2 = 5.216$; $p = 0.022$; $df = 1$) and legs ($x^2 = 6.543$; $p = 0.037$; $df = 2$) categories. Besides Ensifera, Neuroptera, Odonata, Caelifera, Blattodea, Diptera and Auchenorrhyncha also displayed differences in the individual morphological categories. Neuroptera showed significant differences in the antennae ($x2 = 6.371$; $p = 0.041$; $df = 2$) and wings ($x2 = 9.990$; $p = 0.006$; $df = 2$). Auchenorrhyncha also presented significant differences in the head ($x^2 = 4.008$; $p = 0.045$; $df = 1$) and abdomen ($x^2 = 11.954$; $p = 0.002$; $df = 2$) categories. Diptera showed relevant differences in the thorax ($x^2 = 7.348$; $p = 0.025$; $df = 2$) and wings ($x^2 = 8.66$; $p = 0.013$; $df = 2$). Some individual insect taxa showed relevant differences in only one individual morphological category. For Caelifera, quantitative analysis revealed significant differences in the frequency distributions of scores for the wing ($x^2 = 8.249$; $p = 0.016$; $df = 2$) category. For Heteroptera, the distribution of scores for the abdomen preservation fidelity was statistically significant ($x^2 = 21.13$; $p < 10^{-4}$; $df = 2$). Lastly, the quantitative analysis also revealed significant differences in the frequency distributions of the abdomen preservation for pyritized Blattodea versus kerogenized Blattodea ($x^2 = 13.85$; $p < 10^{-4}$; $df = 2$).

When we compared only individual insect taxa, Ensifera presented the highest number of differences among the individual morphological categories between the two preservation types. When analyzing only the individual insect features, the thorax preservation-fidelity score stood out as the best-preserved morphological component, when all insects were considered (Fig. 4). In contrast, the antennae were the worst and the least frequently preserved for both pyritized and kerogenized insects.

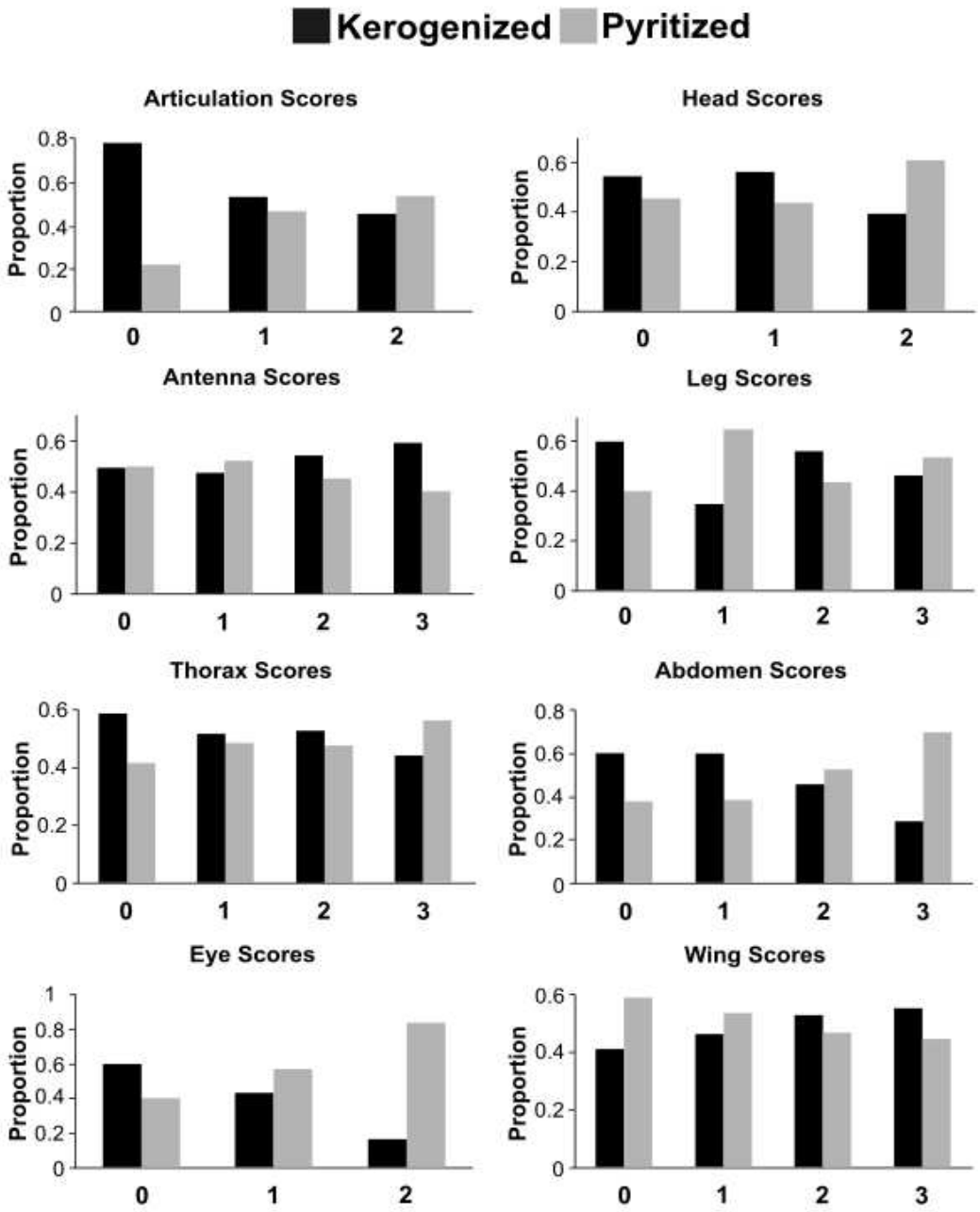

Fig. 4. The distribution of all quality scores for the individual morphological categories of all kerogenized and pyritized insects from the Crato Formation.

4.2.1. The distribution of top scores for the individual morphological categories

The quality of preservation of insect exoskeletal materials in the Crato Formation can be classified as excellent (Fig. 5). This exceptional preservation makes it possible to easily identify specimens to the order level. Most insects have received at least one maximum-score-value (in this case 3) for at least one morphological category for both preservation types. For example, 18.8% of the specimens received a score of 3 for the head

morphological category, considering all insects from the two preservation types (Fig. 6). Among all the insect taxa, 28.9% received a score of 3 for the abdomen. For legs, 25.9% of all specimens scored 3. Auchenorrhyncha have the highest proportion for the maximum score of the thorax and leg morphological categories, 75.5% and 64.4%, respectively. Considering all insects, 25.4% of the specimens received score 3 for wings. 46.1% of all Odonata specimens had this score for wings. Only 9.2% of all insects have discernible eyes, but 33.3% of the Odonata scored 3. Interestingly, considering the Odonata that received score 3 for eyes, 84.6% are pyritized specimens.

The thorax was the individual morphological category that received the highest number of maximum scores, 31% for insects preserved by both pathways. In contrast, the individual morphological category with the lowest number of maximum scores was the antenna. The antennae were lost more than any other feature. Only 3.1% of all insects scored a 3.

Comparing the mineralized and kerogenized insects separately, the proportions of the maximum-score value for the individual morphological categories show that the preservational quality of the mineralized insects was often higher than that of the kerogenized ones. Counting only the pyritized insects 35.4% of the specimens received a score of 3 for the abdomen, 33.5% for the thorax, 27.1% for the legs, 23.6% for the wings, 21.2% for the head, 12.6% for the eyes and 3.1% for the antennae. When we observe only the kerogenized insects, 15.4% of the specimens received a score of 3 for the abdomen, 26% for the thorax, 23.6% for the legs, 29.2% of specimens scored 3 for the wings, 13.8% for the head, 13.8% for the eyes and 3.2% for the antennae. The distribution of the maximum-score-value was significantly different between the mineralized and kerogenized insects for eyes and abdomen (Table 2).

Considering the head morphological category, we noticed that 18.2% of the pyritized Caelifera scored 3, while no kerogenized Caelifera reached that mark. For thoraces, the highest difference among all insect taxa was attributed to Odonata and Diptera. 20.5% and 16.6% of the pyritized Odonata and Diptera scored a 3, respectively, while none of the kerogenized Odonata and Diptera scored a 3. Quantitative analysis revealed that the abdomen and eyes are the mostly completely preserved in the pyritized specimens in comparison to the kerogenized ones. For eyes, the highest difference among all insects was attributed to Odonata. Heteroptera, Blattodea, Caelifera, Ensifera, Diptera, Coleoptera and Neuroptera not reach the maximum value, when we considered the kerogenized insects (Fig. 7).

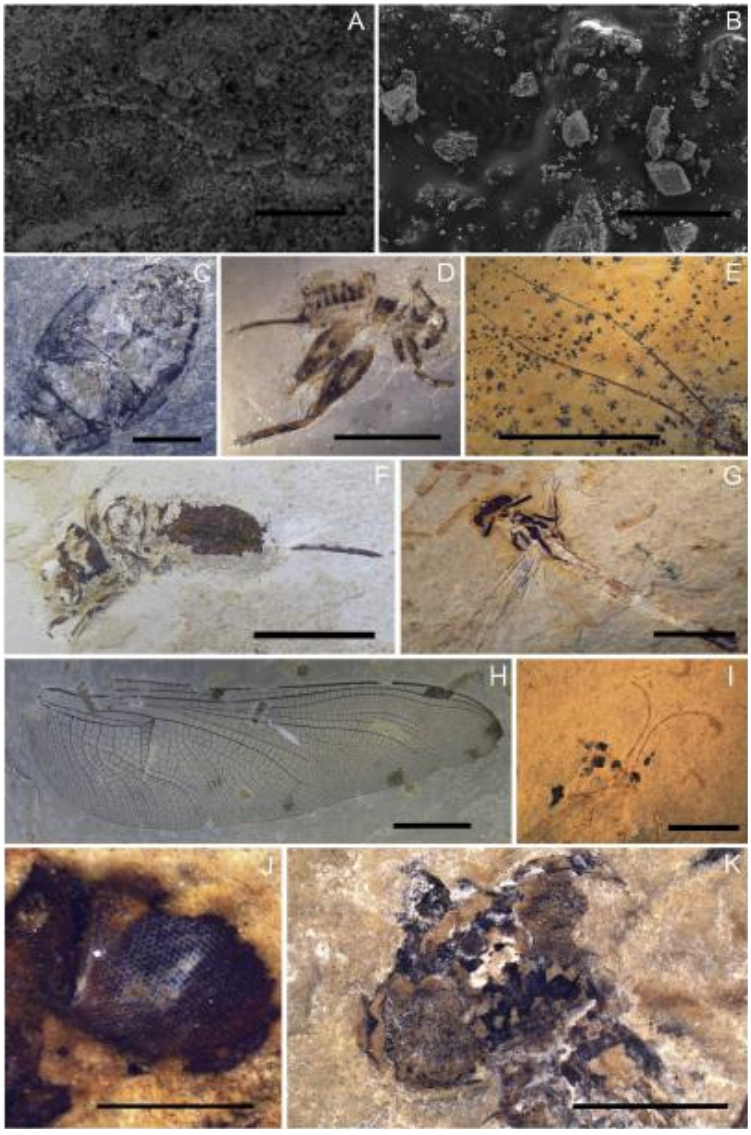

Fig. 5. Examples of Crato insects in varying degrees of preservation and completeness. A. Scanning electron micrograph of the pyritized cuticle of Ensifera (CRT/UFC 2659). B. Secondary electron micrograph of the kerogenized Ensifera showing no discernible microfabrics (CRT/UFC 2400). C. Kerogenized Heteroptera, the head missing (CRT/UFC 703). D. Kerogenized Ensifera, partially articulated (CRT/UFC 2303). E. Pyritized Blattodea showing antennae preserved spectacularly (CRT/UFC 2060). F. Pyritized Ensifera, abdomen and ovipositor preserved (CRT/UFC 2388). G. Pyritized Odonata, almost whole abdomen left as impression (CRT/UFC 1923). H. Kerogenized Odonata, isolated wing (CRT/UFC 1154). I. Kerogenized Neuroptera preserved as a faint impression, the eyes in particular (CRT/UFC 100). J. Pyritized Odonata displaying individual ommatidia (CRT/UFC 95). K. Kerogenized Odonata with preserved eyes and ommatidia (CRT/UFC 1213). Scales bars: A = 30 mm; B = 50 mm; C = 5 mm; D = 5 mm; E = 10 mm; F = 5 mm; G = 5 mm; H = 10 mm; I = 4 mm; J = 2 mm; K = 3 mm.

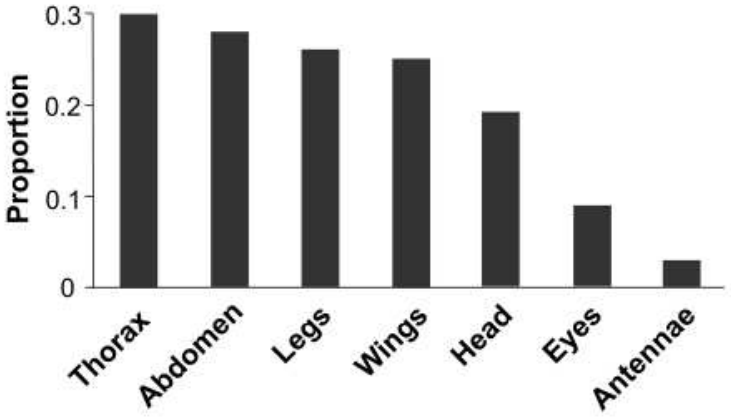

Fig. 6. Histogram showing the maximum-score value proportions for the individual morphological categories of all pyritized and kerogenized insects of the Crato Formation.

Morphological Categories	All insects	Pyritized insects	Kerogenized insects	chi-squared tests	
				$\chi 2$	*P-value*
Head	71	54	17	2.434	0.118
Eye	35	32	3	**9.213**	**0.002**
Antenna	12	8	4	0.002	0.958
Thorax	117	85	32	1.481	0.223
Leg	98	69	29	0.410	0.521
Wing	96	60	36	1.037	0.308
Abdomen	109	90	19	**11.448**	**$< 10^{-4}$**

Table 2. The distribution of the maximum-score values for the individual morphological categories, for pyritized and kerogenized insects of the Crato Formation.

4.3. Articulation states

The majority of kerogenized and pyritized insects from the Crato Formation have complete articulated bodies and partially articulated bodies. The comparison of the distribution of scores for articulation state of the specimens was not significantly different between kerogenized and pyritized insects from the Crato Formation ($x^2 = 4455$; $p = 0.107$; $df = 2$). When we compared only individual insect taxon, the distribution of articulation state was significantly different between the mineralized and kerogenized Ensifera ($x^2 = 10.26$; $p = 0.0059$; $df = 2$) and Neuroptera ($x^2 = 28.66$; $p < 10^{-4}$; $df = 2$).

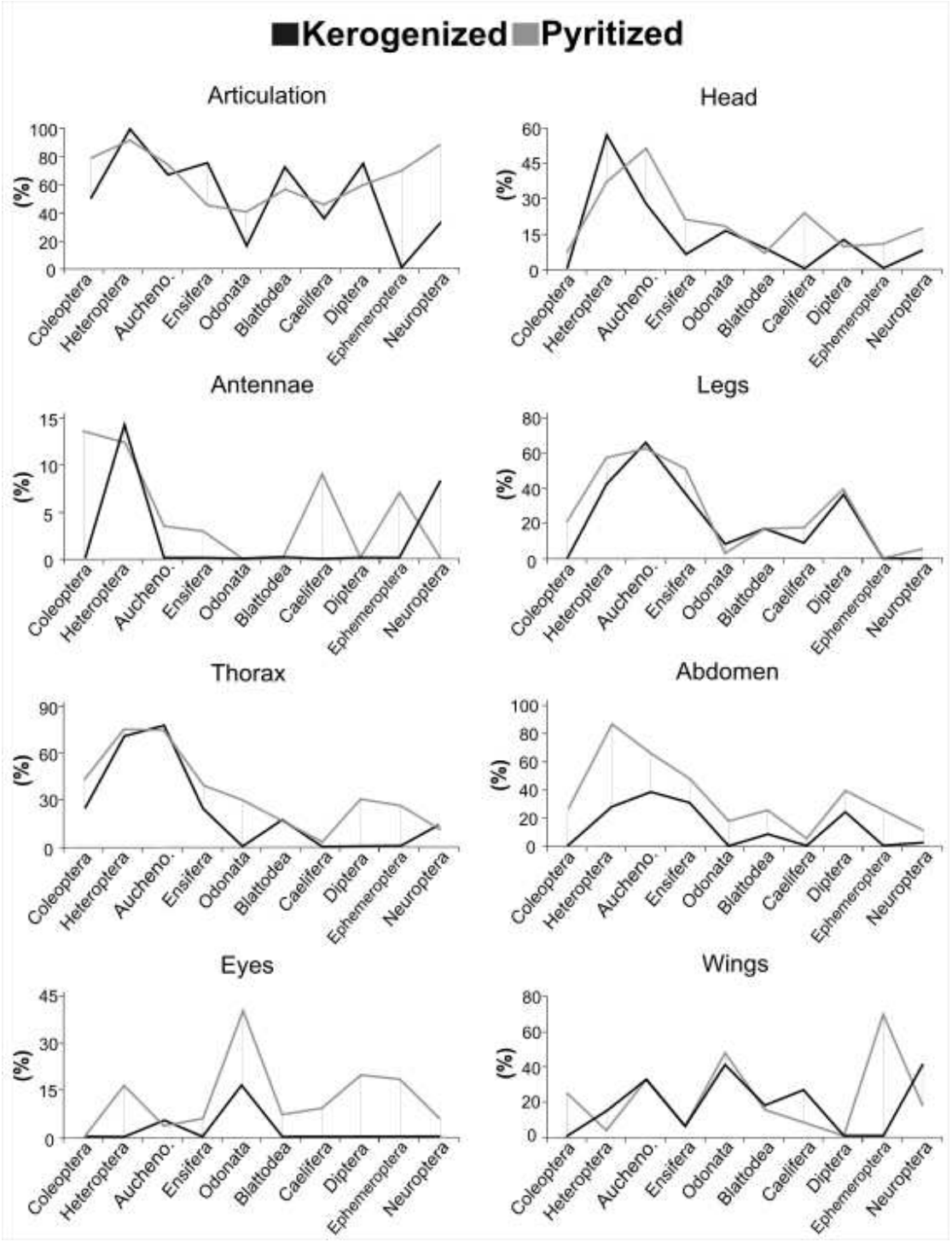

Fig. 7. The comparison of the proportion of the maximum quality scores for the individual morphological categories between all the mineralized and kerogenized specimens for all the considered taxa.

For all insects, fully articulated specimens are the most common (223) (Table 3). Considering all fully articulated insects, 158 are pyritized. The differences between pyritized and kerogenized insects were not significant ($x^2 = 1.227$; $p = 0.267$; $df = 1$) when only the

fully articulated specimens were considered. 143 of all specimens are partially articulated, when we observe only the partially articulated insects, 92 are mineralized. For partially articulated specimens, the difference between pyritized and kerogenized insects was not significant ($x^2 = 0.6$; $p = 0.438$; $df = 1$). However, the comparison ($x^2 = 4.812$; $p = 0.028$; $df = 1$) of the proportion of disarticulated specimens (11) was significantly different between iron-oxide insects and kerogenous insects (Table 3).

Articulation state	**All insects**	**Pyritized insects**	**Kerogenized insects**	**chi-squared tests**	
				χ2	***P-value***
Fully articulated	59.2%	62.2%	52.8%	1.227	0.267
Partially articulated	37.9%	36.2%	41.5%	0.600	0.438
Disarticulated	2.9%	1.6%	5.7%	**4.812**	**0.028**

Table 3. Percentages and results of chi-squared tests for articulation state differences between the kerogenized and pyritized insects from the Crato Formation. Statistically significant values are given in bold.

When considering all specimens, 20.9% of insects were missing the head. When considering only pyritized insects, 19.6% were missing the head. On the other hand, 23.6% of specimens were assigned to this state when considering only kerogenized insects. 76.1% of all specimens received a score 0 for antennae and 49% for eyes. Counting only the pyritized insects, 76.4% of the specimens score 0 for antennae, and 42.1% of the specimens score 0 for eyes. Counting only the kerogenized insects, 75.6% and 63.4% score 0 for antennae and eyes, respectively. 10.6% of kerogenized insects are missing the thorax against 7.5% of pyritized insects. When we considered all specimens, 17.7% of the insects lost their abdomen. The abdomen is absent in 14.9% of the specimens, when considering only pyritized insects, and in 23.5% of specimens, when considering only kerogenized insects. For wings, the results were similar for both types of preservation, 10.6% of the pyritized insects and 7.3% of the kerogenized insects lost their wings. Only 9.5% of all insects score 0 for wings. The distribution of the zero-values was significantly different between the mineralized and kerogenized insects for eyes and legs (Table 4).

Morphological Categories	All insects	Pyritized insects	Kerogenized insects	chi-squared tests	
				$\chi 2$	*P-value*
Head	79	50	29	0.599	0.428
Eye	185	107	78	**7.653**	**0.005**
Antenna	287	194	93	0.006	0.936
Thorax	32	19	13	0.931	0.334
Leg	114	66	48	**4.660**	**0.030**
Wing	36	27	9	0.952	0.329
Abdomen	67	38	29	3.462	0.062

Table 4. The distribution of the individual morphological categories scoring zero for all kerogenized and pyritized insects from the Crato Formation. Statistically significant values are given in bold.

When comparing the proportion of the presence or absence of individual morphological categories, regardless of anatomical details, for all mineralized and kerogenized insects from the Crato Formation, the majority are fully articulated, while less than 3% are disarticulated. Of all the partially articulated specimens, only the pyritized insects have representatives missing the head and thorax, the head and abdomen or the head and wings: 3.9%, 2.9% and 2.9%, respectively. This suggests that pyritized insects have a greater number of disarticulation styles. However, when we investigated the percentages of individual morphological categories missing, the kerogenized insects show higher values. The presence/absence proportions were statistically significant for eyes, legs and abdomen morphological categories (Table 5).

Morphological Categories	$\chi 2$	*P-value*
Head	0.853	0.355
Eye	**21.037**	**$< 10^{-4}$**
Antenna	0.043	0.835
Thorax	1.069	0.301
Leg	**8.096**	**0.004**
Wing	1.099	0.294
Abdomen	**4.7**	**0.030**

Table 5. The results of the statistical analyses comparing the proportions of presence or absence for each morphological category of the insects from the two modes of preservation in the Crato Formation.

5. Discussion

Our results show that the two modes of preservation have a significantly different quality of preservation. Surprisingly, the preservation quality of pyritized insects is consistently higher than that of the kerogenized insects of the Crato Formation. The kerogenized insects only showed higher preservation quality for the wing and antenna morphological categories. Contrary to expectations, keroginized insects do not show preservation quality that is as high as that of the specimens preserved by pyritization.

Kerogenization includes a transformation from original organic material by partial or complete chemical alteration of organic matter into cyclic and aliphatic hydrocarbons (Stankiewicz et al., 1997; Stankiewicz et al., 1998; Gupta et al., 2006). According to Schiffbauer et al. (2014), the fossils preserved as carbonaceous compressions with only rare and diffuse pyrite were likely rapidly buried in the methanogenesis zone of the sediment column. On the other hand, pyritization requires degradation of organic matter, reactive iron and sulphate from environmental sources (Berner, 1984). The precipitation of pyrite occurs when the degradation of organic matter by microbial activity produces ionic constituents necessary for mineralization (Raiswell et al., 1993; Briggs, 2003). Schiffbauer et al. (2014) hypothesized that completely pyritized fossils spent more time in the bacterial sulfate reduction (BSR) zone. Degradation in the BSR zone is more efficient than degradation in the methanogenesis zone because BSR is more metabolically efficient than the degradation pathways available in the methanogenesis zone (Elsayed et al., 2015; Mao et al., 2015). Therefore, it is expected that a specimen preserved in the BSR zone will undergo more degradation than a specimen preserved in the methanogenesis zone (Anderson and Smith, 2017).

Based on the argument above, our results do not match this prediction and diverged from those of Anderson and Smith (2017). In their study, there is a significant difference between iron mineralized and keroginized insects from the Green River Formation, where the preservation quality of mineralized insects was consistently lower than the kerogenized insects.

The distributions of quality scores were significantly different for four morphological categories (head, legs, abdomen and eyes) when comparing all insects between the two preservation types. However, there were no significant differences in the frequency of preservation scores of antennae, thoraces and wings between both the pyritized and

kerogenized insects. For thoraces, this is not surprising as they tend to have thick and sclerotized tissues. The proportions of the maximum-score-value for the individual morphological categories show that the preservational quality of the mineralized insects was often higher than that of the kerogenized insects. The head, wings and abdomen were the morphological categories that most frequently presented substancial differences among the individual insect taxa. Four individual taxa showed significant differences for the abdomen (Auchenorrhyncha, Blattodea, Ensifera and Heteroptera), whereas three are significantly different for the wings (Caelifera, Diptera and Neuroptera). For the head, two individual taxa presented significant differences (Auchenorrhyncha and Ensifera). Only one taxonomic group showed differences for the antenna (Neuroptera), thorax (Diptera) and legs (Ensifera) categories. The abdomen was more affected in insects in the kerogenized zone, as only 15.4% of kerogenized insects scored maximum value.

The articulation state of insects is not significant different between the two modes of preservation. The specific articulation states of fully articulated and partially articulated specimens do not vary significantly either. The lack of a significant difference for articulation state could likely be explained by the fact that the fully articulated individuals were the most common in both pyritization and kerogenization zones. Otherwise, when comparing only disarticulated specimens, the articulation state was significantly different between the two modes of preservation, with kerogenized insects having higher disarticulation values. The high preservational fidelity of insect morphological components suggest that these insects likely dropped intowater while flying over the lake or were immersed by risingwater levels (still alive or after undergoing a short period of decay on land).

The Crato paleolake was most probably a permanent freshwater environment with no evidence of subaerial exposure (Neumann et al., 2003; Assine et al., 2014). Our results strongly corroborate this interpretation. The low number of disarticulated insects supports that the Crato paleolake experienced a low energy deposition. Insect carcasses can require prolonged decay and disturbance to disarticulate before the final burial (Martínez-Delclòs and Martinell, 1993; Smith et al., 2006). Additionally, disarticulation during reworking is an unlikely possibility in the finely laminated limestones of the Crato Formation.

The difference in the taxonomic composition between the two modes of preservation is unlikely to be the source of preservation quality trends in our results, as only the Ephemeroptera is present solely as pyritized specimens (Fig. 3). Ephemeroptera only preserved in the pyritized zone is notable because adult mayflies are known for their extremely short life spans and emergence in large numbers in the summer months. This also

suggests that a mass mortality event likely happened during that time of year.

We hypothesize that the higher preservation quality of pyritized insects is because of the shortened period of microbial decay needed to generate Fe^{2+} and HS^-, thus leading to the mineralization of organic matter (Raiswell et al., 1993; Sagemann et al., 1999; Schiffbauer et al., 2014). The pyritized insects could have been deposited in the most distal part of the lake reflecting maximum highstand of the lacustrine system (Neumann et al., 2003; Heimhofer et al., 2010). Thus, this deposition would have occurred under lower-energy conditions, bottom water anoxia, and a near absence of bioturbation and carbonate precipitation mediated by microbial communities (Catto et al., 2016; Osés et al., 2016; Warren et al., 2017). At this stage, the Crato paleolake sediments were predominantly calcareous and iron-poor. Sedimentary iron may have reached the lake through pulses of freshwater (Catto et al., 2016). Therefore, the pyritization process was probably ironlimited. Nevertheless, the amount of organic matter was also low in the pyritization zone (Neumann et al., 2003). Thus, this scenario would allow the fixation of sulphide by iron at decay sites and thus pyritization in insects instead of yield widespread pyritization.

These suitable conditions promoted the early mineralization of insects. The pyritized Odonata retain much higher values of discernible eyes (ommatidia) than the kerogenized Odonata, which shows how quickly and early the mineralization of the pyritized insects occurred (Fig. 5K). Osés et al. (2016) hypothesized that predation or diseases could have facilitated the pyritization of partially disarticulated and fragmented fossil insects with fine details. In contrast, areas where kerogenizaton dominated would have existed during the early and late phase of lake-level highstand (Neumann et al., 2003; Heimhofer et al., 2010). The dark color of these strata is likely due to a combination of higher organic matter, clay content and terrigenous influence. During this phase, the water body of the lake was influenced by rising water level but throughflow most probably was limited (Heimhofer et al., 2010). Increased residence time of water in a restricted basin would have promoted stagnant conditions and increased contribution of clay minerals accompanied by decreased carbonate content. The slightly highest values of organic matter in the kerogenization zone (Heimhofer et al., 2010; Catto et al., 2016) yielded widespread pyritization at the bottom of the lake. Osés et al. (2017) proposed that clay content and low microspar porosity contributed to a narrow BSR zone, and it is possible that there may have been a decrease in sulphate percolation in these strata. Thus, the low supply of ions allowed the kerogenous insects to experience a minimum of microbial degradation within the BSR. A short BSR would have decreased the period of microbial decay available to generate the ions that can promote mineralization.

Both pyritized and kerogenized insects come from the same pronounced rhythmically bedded deposit, so it is expected that the biostratinomic processes experienced by insects should be similar. However, the greater degree of disarticulation of insects in the kerogenization areas would have to have taken place during the biostratinomy stage. Nevertheless, it is difficult to estimate the exact source of biostratinomic differences between the pyritized and kerogenized insects from the Crato Formation.

There is a possibility that specimens were initially preserved with finer details, but during later diagenesis that preservation fidelity has been lost. Insects affected by intense oxidation process can exhibit iron-oxide overgrowths, or even changes in articulation state (Anderson and Smith, 2017). In the case of the pyritized insects, many specimens initially mineralized have been affected by narrow fractures. These breaks in the host rock facilitate the percolation of oxidizing fluids, which could dissolve away the fossil material leaving behind only the outline of former insect (personal observation of FIB, 2019). Specimens bearing these signals were not including in this study.

6. Conclusion

Here, we compared the preservational quality of insects preserved via pyritization and kerogenization from the Crato Formation. The pyritization process requires partial degradation of the carcass leading to a decrease in preservation of their morphological details. But, surprisingly, our results show that the pyritized insects have higher overall preservation quality than fossil insects that have been preserved by kerogenization.

Of all insects studied, the differences in distribution of scores for individual morphological categories were significant in the abdomen, head, legs and eyes. Thorax, antennae and wings did not present statistically significant differences. For all insects, the differences in measures of articulation state between the two modes of preservation were similar. However, when comparing only the proportions of the disarticulated insects, the differences were statistically significant. Our results suggest that these preservation patterns may be controlled by factors such as morphological characteristics, ecology and also abiotic factors such as depositional environment. Overall, in comparisons in which the difference between pyritized and kerogenized insects are statistically significant, the higher preservation-fidelity scores tended to belong to the pyritized specimens. Clearly, Crato Formationwas not selective as it has several insect groups (pyritized plus kerogenized) displaying preservation of biomineralized tissues on a micron-scale as well as gross morphological features. Thus,

different groups of insects may have different taphonomic processes, but all can be classified as exceptional.

It seems likely that the low degree of disarticulation in pyritized insects suggests a greater concentration of ions (sulfate and ferrous iron) allowing for the rapid mineralization of insects with fine details. In contrast, sediments slightly richer in organic matter in the kerogenization zone yielded widespread pyritization, thus decreasing the contributions of sulphate and iron to fossil mineralization. In summary, the taphonomic bias towards lower quality of kerogenized insects is most likely due to the combination of the processes that occurred during both biostratinomy and early diagenesis stages. Comparing two different preservational pathways is a complex task in and of itself, mainly when two or more different preservational pathways are simultaneously associated with the same fossil deposit. Therefore, it is not always easy to highlight which preservational pathway is the best. We recognize that due to lack of the appropriate storage space to accommodate large collections, paleontologists often focus their search for specimens on the highest quality, while poorly preserved specimens are not often collected. Clearly, taphonomic analysis of biased paleontological collections can lead to biased results. However, statistical analysis and taphonomic studies of assemblages dominated by high-level taxa will allow us to understand the influence of depositional environment on the preservation of insects as a whole as well as the biological factors that may control their taphonomic patterns.

The comparison of very similar representatives preserved by two different pathways showed that mineralized fossils can also be preserved with a high level of fidelity. This study suggests that fossil deposits preserved via pyritization, have as much influence on the overall preservation quality as those preserved by keroginization. Others studies comparing kerogenized and partially or fully mineralized soft-tissues are performed in different periods or even in different depositional environments (Penney and Langan, 2006; Lin and Briggs, 2010). Whereas the Crato Fm. is one of the few lithological units in the world where kerogenized and pyritized insects of the same taxonomic group with similar taphonomic histories may be preserved within the same strata, and even at the same outcrop, and this is where the greatest importance of the present study lies.

Acknowledgments

We thank Dr Wellington Ferreira da Silva Filho from Geology Department-UFC for his assistance with fieldwork. We would also like to thank Dr Daniel Rodrigues

Nascimento Júnior from the Geology Departament-UFC for his helpful discussions on the depositional environment of the Crato Formation. We thank the reviewers Evan Anderson and Dena Smith for critical comments that greatly helped us to improve the quality of this report.We are also grateful to Professor Jose Antônio Beltrão Sabadia, in memoriam, for his stimulating and insightful ideas. FIB is grateful for his doctorate scholarship (Coordenação de Aperfeiçoamento de Pessoal de Nível Superior, Brasil e CAPES, process 88882.454892/2019e01). This study was funded by the Probral Program, CAPES (Project-ID 88881.198776/2018e01) and DAAD (Project-ID 5744688) joint project entitled “Towards an integrated Analysis of the Early Creaceous Crato Fossil Lagerstätte".

References

Anderson, E.P., Smith, D.M., 2017. The same picture through different lenses: quantifying the effects of two preservation pathways on Green River Formation insects. Paleobiology 43 (2), 224–247.

Assine, M.L., 2007. Bacia do Araripe. Boletim de Geociências da Petrobras, vol. 15, pp. 371–389.

Assine, M.L., Perinotto, J.A., Neumann, V.H., Custódio, M.A., Varejão, F.G., Mescolotti, P.C., 2014. Sequências deposicionais do Andar Alagoas (Aptiano superior) da Bacia do Araripe, Nordeste do Brasil. Boletim de Geociencias da Petrobras 22, 3–28.

Barling, N., Martill, D.M., Heads, S.W., Gallien, F., 2015. High fidelity preservation of fossil insects from the Crato Formation (Lower Cretaceous) of Brazil. Cretaceous Research 52 (B), 605–622.

Berner, R.A., 1984. Sedimentary pyrite formation: An update. Geochimica et Cosmochimica Acta 48, 605–615.

Bezerra, F.I., Da Silva, J.H., De Paula, A.J., Olveira, N.C., Paschoal, A.R., Freire, P.T.C., Viana, B.C., Mendes, M., 2018. Throwing light on an uncommon preservation of Blattodea from the Crato Formation (Araripe Basin, Cretaceous), Brazil. Revista Brasileira de Paleontologia 21 (3), 245–254.

Bezerra, F.I., Da Silva, J.H., Miguel, E.C., Paschoal, A.R., Nascimento Jr., D.R., Freire, P.T.C., Viana, B.C., Mendes, M., 2020. Chemical and mineral comparison of fossil insect cuticles from Crato *Konservat Lagerstätte*, Lower Cretaceous of Brazil. Journal of Iberian

Geology 46, 61–76.

Briggs, D.E.G., 1999. Molecular taphonomy of animal and plant cuticles: Selective preservation and diagenesis. Philosophical Transactions of the Royal Society of London, ser. B: Biological Sciences 354, 7–16.

Briggs, D.E.G., 2003. The role of decay and mineralization in the preservation of soft-bodied fossils. Annual Review of Earth and Planetary Sciences 31, 275–301.

Catto, B., Jahnert, R.J., Warren, L.V., Varejão, F.G., Assine, M.L., 2016. The microbial natureof laminated limestones: lessons from the Upper Aptian, vol. 341. Araripe Basin, Brazil, pp. 304–315. Sedimentary Geology.

Delgado, A. de O., Buck, P.V., Osés, G.L., Ghilardi, R.P., Rangel, E.C., Pacheco, M.L.A.F., 2014. Paleometry: a brand new area in Brazilian science. Materials Research 17, 1434–1441.

Edwards, H.G.M., Farwell, D.W., Villar, S.E.J., 2007. Raman microspectroscopic studies of amber resins with insect inclusions. Spectrochimica Acta 68, 1089–1095.

Elsayed, O.F., Maillard, E., Vuilleumier, S., Millet, M., Imfeld, G., 2015. Degradation of chloroacetanilide herbicides and bacterial community composition in lab-scale wetlands. The Science of the Total Environment 520, 222–223.

Franke, T.M., Ho, T., Christe, C.A., 2012. The Chi-Square test: Often used and more often misinterpreted. American Journal of Evaluation 33 (3), 448–458.

Grimaldi, D., Engel, M.S. (Eds.), 2005. Evolution of the insects. Cambridge University Press, p. 755.

Gupta, N.S., Michels, R., Briggs, D.E.G., Evershed, R.P., Pancost, R.D., 2006. The organic preservation of fossil arthropods: an experimental study. Proceedings of the Royal Society B 273, 2777–2783.

Heimhofer, U., Ariztegui, D., Lenniger, M., Hesselbo, S.P., Martill, D.M., Rios-Netto, A.M., 2010. Deciphering the depositional environment of the laminated Crato fossil beds (Early Cretaceous, Araripe Basin, North-eastern Brazil). Sedimentology 57, 677–694.

Henwood, A., 1992. Soft-part preservation of beetles in Tertiary amber from the Dominican Republic. Palaeontology 35, 901–912.

Henwood, A., 1993. Ecology and taphonomy of Dominican Republic amber and its Inclusions. Lethaia 26, 237–245.

Labandeira, C.C., Sepkoski Jr., J.J., 1993. Insect diversity in the fossil record. Science 261, 310–315.

Lin, J.P., Briggs, D.E.G., 2010. Burgess Shale-Type preservation: a comparison of Naraoiids (Arthropoda) from three Cambrian localities. PALAIOS 25 (7), 463–467.

Mao, C., Feng, Y., Wang, X., Ren, G., 2015. Review on research achievements of biogas from anaerobic digestion. Renewable and Sustainable Energy Reviews 45, 540–555.

Martill, D.M., Loveridge, R.F., Heimhofer, U., 2007. Halite pseudomorphs in the Crato Formation (Early Cretaceous, Late Aptian-Early Albian), Araripe Basin, Northeast Brazil: further evidence for hypersalinity. Cretaceous Research 28, 613–620.

Martínez-Delclòs, X., Martinell, J., 1993. Insect taphonomy experiments: Their application to the Cretaceous outcrops of lithographic limestones from Spain. Kaupia 2, 133–144.

Martínez-Delclòs, X., Briggs, D.E.G., Peñalver, E., 2004. Taphonomy of insects in carbonates and amber. Palaeogeography, Palaeoclimatology, Palaeoecology 203, 19–64.

McCoy, V.E., Soriano, C., Gabbott, S.E., 2018. A review of preservational variation of fossil inclusions in amber of different chemical groups. Earth and Environmental Science Transactions of the Royal Society of Edinburgh 107 (2e3), 203–211.

McNamara, M.E., 2013. The taphonomy of colour in fossil insects and feathers. Palaeontology 56 (3), 557–575.

Neumann, V.H., 1999. Estratigrafía, sedimentología, geoquímica y diagenesis de los sistemas lacustres Aptienses-Albienses de la Cuenca de Araripe (Noreste de Brasil) (Unpubl. PhD thesis). Universidad de Barcelona, p. 250.

Neumann, V.H., Borrego, A.G., Cabrera, L., Dino, R., 2003. Organic matter composition and distribution through the Aptian-Albian lacustrine sequences of the Araripe Basin, northeastern Brazil. International Journal of Coal Geology 54, 21–40.

Osés, G.L., Petri, S., Becker-Kerber, B., Romero, G.R., Rizzutto, M.A., Rodrigues, F., Galante, D., Silva, T.F., Curado, J.F., Rangel, E.C., Ribeiro, R.P., Pacheco, M.L., 2016. Deciphering the preservation of fossil insects: a case study from the Crato Member, Early Cretaceous of Brazil. PeerJ 4, 1–28.

Osés, G.L., Petri, S., Voltani, C.G., Prado, G.M., Douglas, G., Rizzutto, M.A., Rudnitzki, I.D., Silva, D., Rodrigues, F., Rangel, E.C., Sucerquia, P.A., Pacheco, M.L., 2017. Deciphering

pyritization-kerogenization gradient for fish soft-tissue preservation. Scientific Reports 7, 1–15.

Penney, D., Langan, A.M., 2006. Comparing amber fossil assemblages across the Cenozoic. Biology Letters 2 (2), 266–270.

Raiswell, R., Whaler, K., Dean, S., Coleman, M.L., Briggs, D.E.G., 1993. A simple threedimensional model of diffusion-with-precipitation applied to localized pyrite formation in framboids, fossils and detrital iron minerals. Marine Geology 113, 89–100.

Sagemann, J., Bale, S.J., Briggs, D.E.G., Parkes, R.J., 1999. Controls on the formation of authigenic minerals in association with decaying organic matter: an experimental approach. Geochimica et Cosmochimica Acta 63, 1083–1095.

Schiffbauer, J.D., Xiao, S., Cai, Y., Wallace, A.F., Hua, H., Hunter, J., Xu, H., Peng, Y., Kaufman, A.J., 2014. A unifying model for Neoproterozoic-Palaeozoic exceptional fossil preservation through pyritization and carbonaceous compression. Nature Communications 5, 1–12.

Schmidt, A.R., Jancke, S., Lindquist, E.E., Ragazzi, E., Roghi, G., Nascimbene, P.C., Schmidt, K., Wappler, T., Grimaldi, D.A., 2012. Arthropods in amber from the Triassic Period. Proceedings of the National Academy of Sciences 109 (37), 14796–14801.

Seilacher, A., 1970. Begriff und Bedeutung der Fossil-Lagerstätten. Neues Jahrbuch für Geologie und Paläontologie, pp. 34–39. Monatshefte.

Smith, D.M., 2000. Beetle taphonomy in a recent ephemeral lake, southeastern Arizona. PALAIOS 15, 152–160.

Smith, D.M., 2012. Exceptional preservation of insects in lacustrine environments. PALAIOS 27, 346–353.

Smith, D.M., Moe-Hoffman, A.P., 2007. Taphonomy of Diptera in lacustrine environments: a case study from Florissant fossil beds, Colorado. PALAIOS 22, 623–629.

Smith, D.M., Cook, A., Nufio, C.R., 2006. How physical characteristics of beetles affect their fossil preservation. PALAIOS 21 (3), 305–310.

Solórzano-Kraemer, M.M., Kraemer, A.S., Stebner, F., Bickel, D.J., Rust, J., 2015. Entrapment bias of arthropods in Miocene amber revealed by trapping experiments in a tropical forest in Chiapas, Mexico. PloS One 10 (3), e0118820.

Solórzano-Kraemer, M.M., Delclòs, X., Clapham, M.E., Arillo, A., Peris, D., J*ä*ger, P., Stebner, F., Peñalver, E., 2018. Arthropods in modern resins reveal if amber accurately recorded forest arthropod communities. Proceedings of the National Academy of Sciences of the United States of America 115 (26), 6739–6744.

Stankiewicz, B.A., Briggs, D.E.G., Evershed, R.P., 1997. Chemical composition of Paleozoic and Mesozoic fossil invertebrate cuticles as revealed by pyrolysis-gas Chromatography/Mass Spectrometry. Energy & Fuels 11, 515–521.

Stankiewicz, B.A., Scott, A.C., Collinson, M.E., Finch, P., Mösle, B., Briggs, D.E.G., Evershed, R.P., 1998. Molecular taphonomy of arthropod and plant cuticles from the Carboniferous of North America: implications for the origin of kerogen. Journal of the Geological Society 155, 453–462.

Thoene-Henning, J., Smith, D.M., Nufio, C.R., Meyer, H.W., 2012. Depositional setting and fossil insect preservation: A study of the late Eocene Florissant Formation, Colorado. PALAIOS 27, 481–488.

Wang, B., Zhuang, H., Jarzembowski, E.A., Fang, Y., Zhen, D., 2013. Taphonomic variability of fossil insects: a biostratinomic study of Palaeontinidae and Tettigarctidae (Insecta: Hemiptera) from the Jurassic Daohugou lagerstatten. PALAIOS 28, 233–242.

Warren, L.V., Varejão, F.G., Quaglio, F., Simões, M.G., Fürsich, F.T., Poiré, D.G., Catto, B., Assine, M.L., 2017. Stromatolites from the Aptian Crato Formation, a hypersaline lake system in the Araripe Basin, northeastern Brazil. Facies 63 (3), 1–19.

5 CAPÍTULO 3

Effects of chemical weathering on the exceptional preservation of mineralized insects from the Crato Formation, Cretaceous of Brazil: implications for late diagenesis of fine-grained Lagerstätten deposits

Esse capítulo foi publicado no jornal científico “Geological Magazine”; o material suplementar vinculado ao artigo abaixo citado pode ser encontrado em https://doi.org/10.1017/S0016756823000043

Referência:

Bezerra FI, da Silva JH, Agressot EVH, Freire PTC, Viana BC, and Mendes M. (2023) Effects of chemical weathering on the exceptional preservation of mineralized insects from the Crato Formation, Cretaceous of Brazil: implications for late diagenesis of fine-grained *Lagerstätten* deposits. Geological Magazine 160(5), p. 911-926. https://doi.org/10.1017/S0016756823000043

Effects of chemical weathering on the exceptional preservation of mineralized insects from the Crato Formation, Cretaceous of Brazil: implications for late diagenesis of fine-grained Lagerstätten deposits

Francisco Irineudo Bezerra[1], João Hermínio da Silva[2], Enzo Victorino Hernández Agressot[3], Paulo Tarso C. Freire[4], Bartolomeu Cruz Viana[5], Márcio Mendes[1]

[1]Programa de Pós-graduação em Geologia, Universidade Federal do Ceará, Fortaleza, Ceará 64049-550, Brasil;

[2]Centro de Ciências e Tecnologia, Universidade Federal do Cariri, Juazeiro do Norte, Ceará 63048-080, Brasil;

[3]Campus Foz do Iguaçu, Instituto Federal do Paraná, Foz do Iguaçu, Paraná 85860-000, Brasil;

[4]Programa de Pós-graduação em Física, Universidade Federal do Ceará, Fortaleza, Ceará 60455-970, Brasil;

[5]Laboratório interdisciplinar de materiais avançados, Universidade Federal do Piauí, Teresina, Piauí 64049-550, Brasil

Abstract

Many studies have improved our understanding of the mode of preservation at the Crato fossil Lagerstätte. The high degree of preservation of the Crato mineralized insects is thought to be a consequence of the diffusion of ions through carcasses and envelopment by bacteria that, in turn, created microenvironmental conditions that led to mineralization, mainly pyritization. Pyritized insects have been oxidized by in situ weathering to more stable oxide/hydroxy minerals during Quaternary time. This transformation is essential to maintain the palaeontological information acquired during microbially induced pyritization in an oxidizing atmosphere. However, intense weathering can diminish or obscure the morphological fidelity, and little attention has been paid to the post-diagenetic processes experienced by these fossils.

Here, we aim to determine the degree of alteration undergone by Crato pyritized insects using the following combination of analytical tools: scanning electron microscopy, energy dispersive X-ray spectroscopy, Fourier transform infrared and Raman spectroscopy. Our results show that well-preserved insects are preferentially replaced by haematite and poorly preserved fossils are replaced by goethite. In addition, we recorded three types of post-diagenetic alteration: insects with iron-oxide overgrowths; insects associated with black coatings, sometimes with the formation of dendrites; and insects preserved as an impression, where only the outline of the body remains. All of these alterations have the potential to distort or tarnish palaeontological information. Here, we measured the effects of such telodiagenetic alterations at macro and micro scales. Therefore, this taphonomic approach has wide applicability wherever fine-grained deposits bearing mineralized insects are found.

Keywords: taphonomy; mineralization; *in situ* weathering; pseudomorphism; oxidation; post-diagenesis; palaeontological information

1. Introduction

Over the past few years, our knowledge of fossil insects has increased exponentially. Studies focusing on behavioural advances, eusociality, plant–insect interactions, extinction–origination rates and biostratinomic issues have helped us to understand why insects have the highest described species-level diversity we find today (Clapham & Karr, 2012; Karr & Clapham, 2015; Nicholson et al. 2015; Clapham et al. 2016; Labandeira et al. 2016; Labandeira, 2019; Barden & Engel, 2021). Although insects have a rich fossil record, they contain large temporal and taxonomic gaps in their evolutionary history (Schachat & Labandeira, 2021). This is due to the overwhelming majority of described insect fossils coming from fossil *Lagerstätte* assemblages. Insect assemblages embedded in *Lagerstätten*-type deposits allow a vast number of specimens to be collected (*Konzentrat Lagerstätten*), and they often exhibit exceptionally well-preserved insects (*Konservat-Lagerstätten*). Fossil insects in the *Lagerstätte* assemblages are generally preserved in lacustrine or amber deposits. For lacustrine deposits, insects are usually preserved as fossil compressions via mineralization. As an example, one of the best-studied *Lagerstätten* bearing insects is the Green River Formation from the Piceance Creek Basin in Colorado. After a thorough study was carried out in this unit, Anderson & Smith (2017) reported that insects are typically preserved by haematite after pyrite and as carbonaceous compressions, both

preservational modes having a high fidelity of anatomical detail for individual body parts. The Jehol biota in northeastern China also hosts a significant palaeoentomofauna in a freshwater deposit with volcanogenic sediments. Wang et al. (2012) observed that many insects in the Jehol biota were preserved by framboids and microcrystalline pyrite.

The excessive attention given to the insects encountered in *Konservat-Lagerstätten* localities has given rise to the interest of many researchers in unravelling the taphonomic causes of this preservation in fine detail. The taphonomy of a fossil can be divided into three stages: biostratinomy, diagenesis and recovery (Donovan, 1991; Henwood, 1993). According to Henwood (1992, 1993), biostratinomy and recovery probably have substantially more taphonomic influence than diagenesis for insects preserved in amber inclusions. For those preserved in lacustrine deposits, diagenesis seems to stand out as the most relevant stage. More and more palaeoentomologists have invested in taphonomic investigations, and most of these studies focus on biostratinomic events and/or early–middle diagenetic processes (Duncan & Briggs, 1996; Zhehikhin, 2002; Martínez-Delclòs et al. 2004; Smith et al. 2006; Smith & Moe-Hoffman, 2007; McNamara et al. 2011, 2012; Smith, 2012; Thoene-Henning et al. 2012; Wang et al. 2012; McNamara, 2013; Pan et al. 2014; Greenwalt et al. 2015; Anderson & Smith, 2017; Tian et al. 2020; Iniesto et al. 2021; Heingård et al. 2022).

The Crato palaeoentomofauna, from the Aptian of northeastern Brazil, is perhaps the most studied palaeoentomofauna preserved in fine carbonate strata in the world. Crato insects are commonly complete and three-dimensionally preserved, revealing characteristics such as abdominal segmentation, wings displaying well-defined venation and head appendages. A consequence of this exceptional preservation is that the majority of studies on the Crato palaeoentomofauna are focused on taxonomic and evolutionary issues. However, an increasing number of investigations have analysed the general insect taphonomy, with a focus on early- diagenetic issues (Delgado et al. 2014; Barling et al. 2015, 2020, 2021; Osés et al. 2016; Bezerra et al. 2018, 2020, 2021; Dias & Carvalho, 2020, 2021; Prado et al. 2021). These authors briefly mentioned the effect of weathering. The high degree of fidelity of the Crato insects was achieved during early-mesodiagenesis under reducing conditions mediated by microbial mats (Osés et al. 2016; Varejão et al. 2019; Dias & Carvalho, 2021). After final burial, ions and sulfate-reducing bacteria favour the formation of framboidal pyrite, which replaces cuticle and labile tissues and prevents the total collapse of the carcass. Then, telodiagenetic processes transform the pyritized replicas into more stable minerals as the specimens approach atmospheric conditions by denudation of the rock package. This process,

under certain circumstances, ensures that the morphological information acquired during early diagenesis survives oxidizing agents and reaches today's palaeoentomologists. However, the weathering of fossils has the potential to lead to taphonomic consequences, including loss of morphological information. This process can make the weathered specimen unsuitable for systematic studies, which may induce palaeoentomologists/researchers to become disinterested in collecting these specimens during field campaigns. Under extreme conditions, intense weathering can leach away the fossil insect without leaving any evidence of its existence. McNamara et al. (2012) recognized that the exceptionally preserved characters of the cuticle layers, as well as the insect staining pattern are directly associated with a low rate of chemical weathering.

In this study, we do not consider telodiagenetic effects a part of the fine-scale preservation process. Rather, we suggest that late diagenesis limits preservation potential. To address the lack of information about telodiagenetic processes we integrate mineralogical, chemical and spectroscopic data to identify the post-diagenetic alterations affecting mineralized insects of the Crato *Lagerstätte*.

2. Geological background

The Araripe Basin is an intracratonic basin located in northeastern Brazil, situated in the central part of Borborema province. The basement of this region consists of Precambrian gneiss and migmatite terrains, which were affected by extensive rifting processes resulting from the split between Africa and South America during the break-up of Pangaea (Matos, 1992). The Araripe Basin is composed of the Cariri Formation, proposed by Beurlen (1962) (Late Ordovician/Early Devonian). There are four further supersequences (Assine et al. 2014): (1) the Pre-rift Supersequence: siliciclastic fluvial-lacustrine sediments from both the Brejo Santo and Missão Velha formations (Late Jurassic); (2) the Rift Supersequence: deltaic, fluvial and lacustrine siliciclastic sediments from the Abaiara Formation (Early Cretaceous); (3) the Post-rift I Supersequence: siliciclastic fluvial-lacustrine sediments from the Barbalha (pelites and sandstones), Crato (pelites and carbonates), Ipubi (evaporites) and Romualdo (carbonate concretions) formations, these units occurring within the Santana Group (Aptian); (4) the Post-rift II Supersequence: Cenomanian siliciclastic fluvial sediments from both the Araripina and Exu formations. The relief is marked in the landscape by the Chapada do Araripe, a plateau smoothly inclined westwards and surrounded by steep cliffs. The Chapada do Araripe is bordered by plain sedimentary deposits distributed mainly on the east

and NE flanks, a region named Vale do Cariri (Fig. 1).

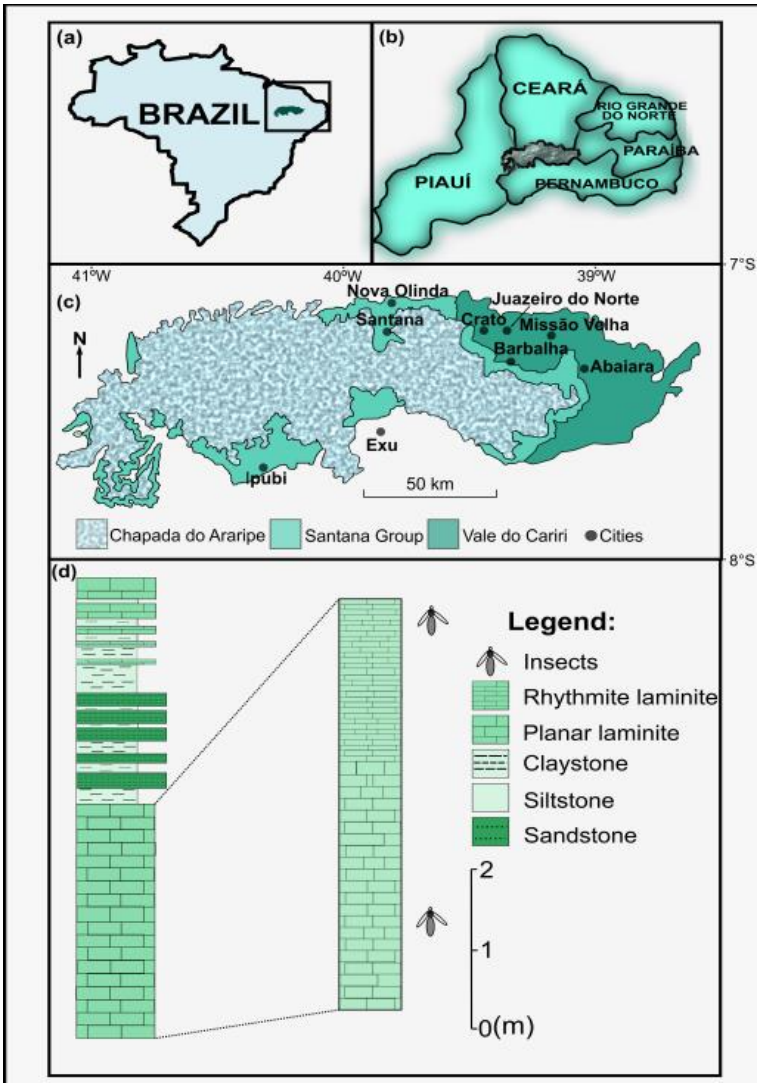

Fig. 1. Location and geological setting of the Crato *Lagerstätte*. (a) Position of the Araripe Basin in the Brazilian territory. (b) Position of the Araripe Basin in NE Brazil. (c) Toponymic and geological map of the Araripe Basin Crato Formation outcrops associated with the Santana Group. (d) Stratigraphic scheme of the Crato Formation highlighting the Nova Olinda Member, recognized as the Crato *Lagerstätte*.

Several lacustrine depositional episodes have been recognized in the Araripe Basin. The second lacustrine episode took place during late Aptian time and led to deposition of fine-grained deltaic sandstone units (Barbalha Formation), which interlink with several carbonate and siliciclastic units in the Crato Formation (Arai & Assine, 2020; Melo et al. 2020; Coimbra & Freire, 2021). These lacustrine carbonate facies are predominantly composed of micritic laminated limestones and have a calcite composition with a low magnesium content (Catto et al. 2016).

The Crato Formation consists of carbonate layers more than 20m thick (Assine, 2007), interbedded with siliciclastic sediments. Their origin is attributed to transgressive–regressive events associated with the expansion and contraction of a lacustrine system (Heimhofer et al. 2010). The depositional environment of the Crato Formation is interpreted as a restricted lacustrine or lagoon system with a stratified water column. The lake/lagoon bottom was hypersaline and anoxic (Heimhofer et al. 2010). Recently, Warren et al. (2017) and Varejão et al. (2019, 2021) suggested a shallow hypersaline coastal lacustrine system dominated by benthic microbial mats. The Crato Formation is divided into four members including, from bottom to top: the Nova Olinda, Caldas, Jamacaru and Casa de Pedra (Martill et al. 2007). The lowest Nova Olinda Member crops out in the northern and eastern flanks of the Araripe Basin, where the fossil insects from this study were found. The palaeoenvironmental conditions and exceptional preservation of fossils have made the Crato Formation well known worldwide as a Cretaceous fossil *Lagerstätte* (Martill et al. 2007).

3. Material and methods

3.a. Fossil material

Specimens used in this research are deposited in the scientific palaeontological collection of the Laboratório de Paleontologia of the Universidade Federal do Ceará (Brazil). In all, 138 mineralized insects recovered from the Nova Olinda Member were studied for this analysis (online Supplementary Material Table S1). The main analysis, at hand scale, was performed on mineralized specimens preserved in pale-yellow limestone slabs. At this stage, we observed the degree of completeness, articulation and compaction of each mineralized insect. The microscopic and spectroscopic results presented here are from the analyses of the following samples: LP/UFC CRT 122, LP/UFC CRT 708, LP/UFC CRT 720, LP/UFC CRT 1156, LP/UFC CRT 1822, LP/UFC CRT 1834, LP/UFC CRT 1896, LP/UFC CRT 2055, LP/UFC CRT 2083, LP/UFC CRT 2204, LP/UFC CRT 2388, LP/UFC CRT 2529 and LP/UFC CRT 2647.

3.b. Scanning electron microscopy and large-field energy dispersive spectroscopy

The scanning electron microscopy and energy dispersive X-ray spectroscopy (SEM–EDS) analyses were performed in the Central Analítica at the Universidade Federal do

Ceará (UFC). Micromorphological measurements of the fossil insects were conducted by SEM in a Quanta-450 electron microscope (FEI) with a field-emission gun (FEG) equipped with a gaseous analytical detector (GAD), coupled to an X-ray detector (model 150, Oxford) for EDS. Specimens were prepared by mounting on aluminium stubs with a black carbon cement. The fossil insects were then inserted into the microscope chamber without other previous preparation. The micrographs were obtained using a working distance of 10 mm. Analyses were performed in a low vacuum to avoid sample charging. Images were acquired at a beam acceleration voltage of 20 kV, using a resolution of 1024 × 884 pixels per image. The images were processed and exported on AZtec software (version 3.0/Oxford).

3.c. Fourier transform infrared and Raman spectroscopy

The spectroscopic analyses were performed in the Laboratório de Espectroscopia Vibracional e Microscopia (LEVM), Departamento de Física, at the UFC. The Raman spectra were obtained with a LabRAM HR (Horiba) spectrometer equipped with a liquid N2-cooled CCD detector behind a 600 g/mm grating. Acceptable spectra were measured using 785 nm laser radiation for excitation (~2mW at the sample surface). The laser power was set to ~1mW on the samples. In this investigation, the Fourier transform infrared (FTIR) spectra were measured directly by using a Vertex 70 (Bruker). FTIR data were collected in the spectral range from 200 to 4000 cm^{-1}. No sample preparation was necessary. The Raman and FTIR spectra were analysed in the software Origin 9.2.

4. Results

4.a. Morphological details at hand-specimen scale

Crato mineralized insects typically appear as orange-brown to dark-brown specimens preserved in pale-yellow to reddish limestone slabs. This type of preservation consists of iron (III) oxide hydroxy replacements of former sulfide minerals that replicated the original cuticle. Crato Formation insects displaying this type of preservation are often uncompacted, articulated and are complete with antennae, head, thorax, abdomen, legs, articulated wings and other appendages (Fig. 2a–c). These specimens also reveal details of the wings or elytra, often displaying a well-defined venation pattern. Abdomens retain structures such as cerci, caudal gills, ovipositors and legs, which are often well articulated with spines, setae and spurs. These sets of structures are significant in taxonomic phylogenetic analyses,

and are employed to estimate the historical relationships among the different insect taxa.

Exceptionally, many disarticulated oxide-hydroxide insects, preserved as fragmentary remains or isolated body segments, still retain remarkable morphological details. This suggests that damage to these insects was probably caused by biostratinomic processes prior to burial. However, many of the Crato mineralized insects appear poorly preserved in hand specimens, and closer examination shows that the damage has been caused by diagenetic alteration rather than the result of biostratinomic processes (*in vivo* or *post-mortem* decay). These diagenetic altered insects can appear complete but reveal little to no morphological detail (e.g. ommatidia, wing veins and spines). This style of alteration makes a high classification uncertain even at the order, suborder or family level. In particular, these poorly preserved specimens can be easily damaged by touching, and are commonly encountered in the weathered pale-yellow limestones. After thorough investigations, we have found three types of alterations in Crato insects. The most common type involves insects with iron-oxide overgrowths that reduce morphological fidelity (Fig. 2d–f). This distinctive feature provides a rust-like hue to insects. The specimen can be fully articulated but possesses a body obscured by iron-oxide overgrowth (e.g. head or thorax). Here, the loss of palaeontological information is usually partial. Secondly, weathered insects appear with light-grey to black coatings. These later coatings can overlap diagnostic features such as wing veins, head appendages or even entire body parts. In particular, this feature gives a ‘dirty’ appearance to fossil insects and is often associated with dendrites. Insects exhibiting this type of alteration also have a rusty appearance (Fig. 2g, i, j). The third type of alteration corresponds to the insects recorded only by their imprint left on the limestone. These fossils are found as two-dimensional imprints of insects or of their parts (Fig. 2h, k, l). Fossil imprints can record information about the external shape of organisms but without complete details or delicate appendages. Owing to the lack of details of the original cuticle, a faithful taxonomic description is hampered. Overall, this type of alteration process results in ‘depleted’ versions of the specimens, where telodiagenetic fluids dissolve away the mineral replacements leaving behind only the external outlines of former insects.

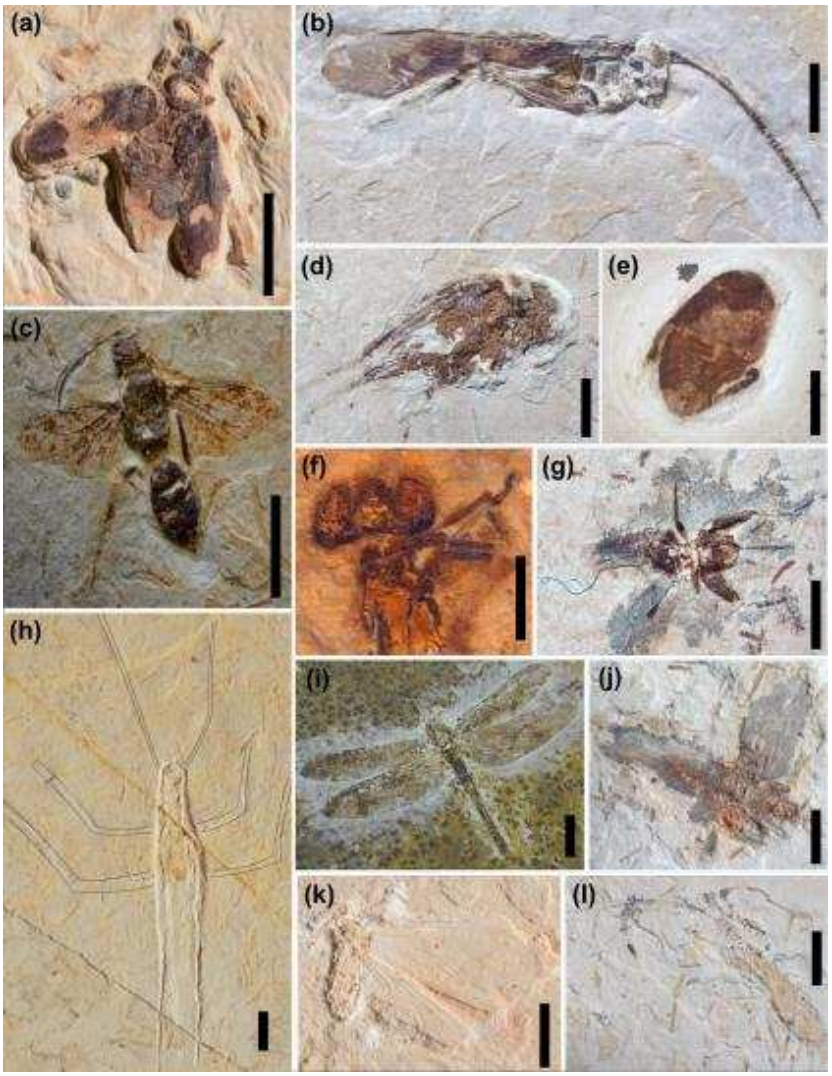

Fig. 2. Examples of mineralized/impression insects from the Crato Formation in different types of preservation. (a–c) Crato insects well preserved at hand scale: Coleoptera (LP/UFC CRT 2529), Caelifera (LP/UFC CRT 2083) and Hymenoptera (LP/UFC CRT 2768), respectively. (d–f) Examples of insects with iron-oxide overgrowths: Ensifera (LP/UFC CRT 1834), Heteroptera (LP/UFC CRT 708) and Odonata (LP/UFC CRT 1152), respectively. (g, i, j) Mineralized insects with black coatings sometimes associated with dendrites: Ensifera (LP/UFC CRT 2388), Odonata (LP/UFC CRT 1156) and Ensifera (LP/UFC CRT (2647), respectively. (h, k, l) Crato insects preserved as imprints: Phasmatodea (LP/UFC CRT 2698), Isoptera (LP/UFC CRT 1896) and Caelifera (LP/UFC CRT 2204), respectively. Scale bars = 10 mm.

4.b. Scanning electron micrograph analysis

The SEM analysis revealed that preservation of the Crato Formation insects

includes individual cuticular surface structures (Fig. 3). Overall, the cuticle surface retains fine morphological details, built by sub-spherical to spherical grains with diameters mainly in the range of 5–15 μm. These structures are commonly arranged as globular aggregates or as close-packing grains. The micrographs also revealed anhedral to euhedral crystals of variable sizes and organization, and many of the grains observed in these fossils were shown to be hollow. This suggests that these crystals may be classified as pseudoframboids (Berner, 1970; Kribek, 1975; Ohfuji & Rickard, 2005) of a mineral precursor. For further clarification of the mineral fabrics of Crato insects, see Barling et al. (2020). These crystal structures have not been observed within extant insect cuticle and do not appear to be of a biological origin; they are often interpreted as mineral fabrics produced during the early diagenesis.

In the best articulated specimens at hand scale, the high magnification revealed that the cuticle can also be replaced by a polygonal lamellar arrangement, with grains of ~1 μm in diameter (Fig. 3a). In these insects, any loss of preservation fidelity is partial or occurs locally on a micron scale (Fig. 3b, c). The cuticle is preserved as a massive film without microtextural differentiation and commonly with sensilla insertion holes in the surface (Fig. 3d). This cuticular arrangement suggests a direct replacement of insect tissue.

The higher magnification investigation of the insects not well preserved at hand scale shows different textural characteristics at the micro scale. Crato Formation insects preserved as two dimensional imprints commonly record details of the original external form. In micrographs, they display clusters of cryptocrystals or isolated pseudomorphs associated with calcite crystals (Fig. 3e). Fossil cuticles are preserved by a thin discontinuous layer. It is sometimes difficult to distinguish the boundaries between the fossil and carbonate matrix.

The presence of microcracks in the insect cuticles of the Crato Formation has been frequently reported (Delgado et al. 2014; Barling et al. 2015, 2020; Osés et al. 2016; Bezerra et al. 2020, 2021; Dias & Carvalho, 2020, 2021; Prado et al. 2021). Crato insects with iron-oxide overgrowths show intricate zones of microcracks associated with compact cuticular surfaces without individualized crystals (Fig. 3f). The microcracks commonly appear in isolation but they can also link up, demonstrating that this type of damage has the potential to be quite extensive. They are connected to each other by straight contacts in a perpendicular way, but curved microcracks have also been observed. These microcracks are commonly empty, and rarely filled with minerals. Crato insects with black coatings show regions of the cuticle replaced by inequidimensional, spherical to sub-spherical microcrystals forming alveolar aggregates with partially corroded surfaces, but sometimes areas without individualized crystals can also occur. Such evidence reveals the intense oxidation of these

mineralized replacements.

Both styles of preservation, associated with black coatings and with iron-oxide overgrowths displaying aggregates of micro-cryptocrystals, replace the external cuticle, with the corroded surfaces and empty cavities previously occupied by crystals (Fig. 3g, h). Specimens with iron-oxide overgrowths also show a locally rugged and pitted surface scratched by sets of grooves (Fig. 3i). The grooves retain a flow aspect and sometimes appear associated with microcracks (Fig. 3j).

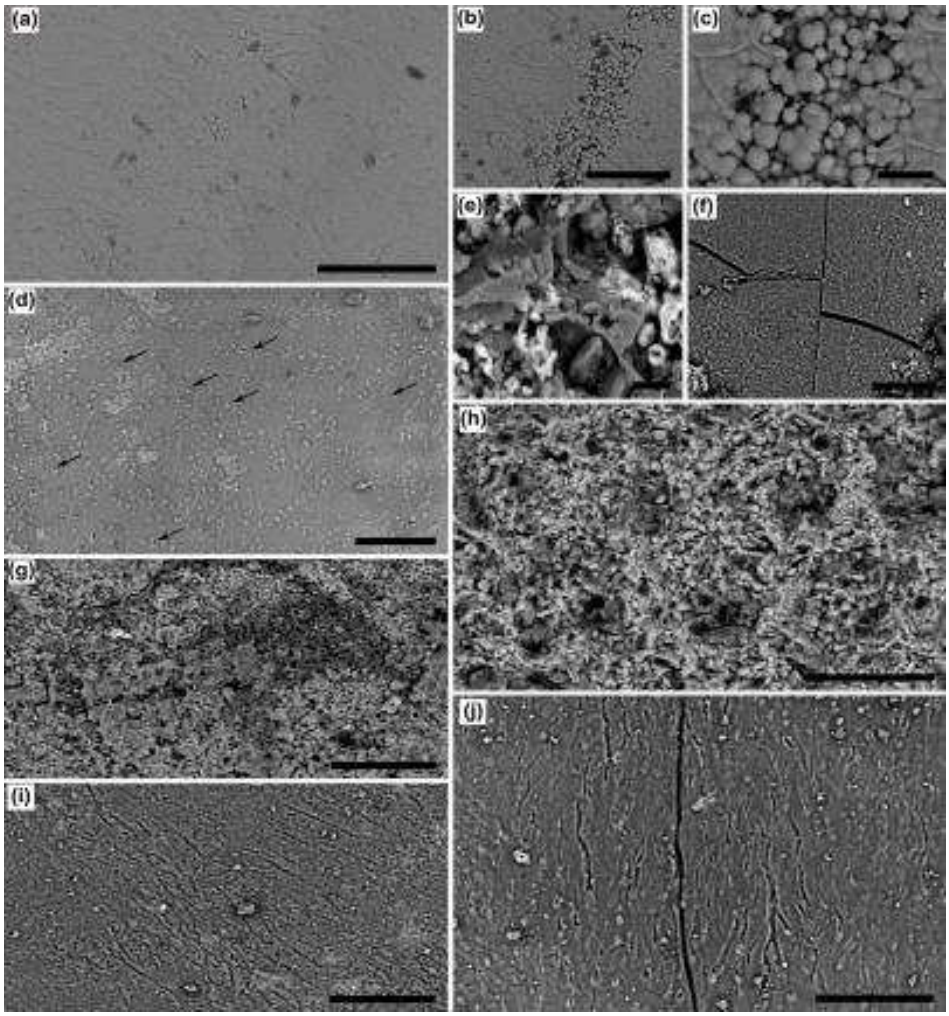

Fig. 3. Scanning electron micrograph analysis for cuticular characterization of Crato Formation insects. (a) Cockroach (LP/UFC CRT 2055) showing cuticular high fidelity; scale bar = 100 μm. (b) Local loss of cuticle fidelity in (a); scale bar = 50 μm. (c) Detail of the microtexture depicted in (b); scale bar = 10 μm. (d) Beetle (LP/UFC CRT 2529) epicuticle with sensilla insertion holes (indicated by arrows) on its surface; scale bar = 50 μm. (e) Caelifera (LP/UFC CRT 2204) preserved as two-dimensional imprints with inequidimensional and spherical to sub-spherical micro-cryptocrystals of iron oxides associated with crystals of calcite; scale bar = 10 μm. (f) Surface microcracking of a cricket epicuticle (LP/UFC CRT

1834) with iron-oxide overgrowths; scale bar = 50 μm. (g) Cricket (LP/UFC CRT 2388) with black coatings showing microfabric formed by sub-spherical loosely packed grains; scale bar = 100 μm. (h) Ommatidia of a Heteroptera (LP/UFC CRT 708) with iron-oxide overgrowths showing pseudoframboids and alveolar aggregates of iron-oxide crystals associated with dissolution cavities; scale bars = 50 μm. (i) Heteroptera (LP/UFC CRT 720) epicuticle with iron-oxide overgrowths scratched by sets of grooves generated by oxidation reactions; scale bar = 50 μm. (j) Detail of the Heteroptera (LP/UFC CRT 720) epicuticle showing grooves associated with microcracks; scale bar = 50 μm.

4.c. Raman and FTIR spectroscopy analyses

Raman spectra of Crato Formation insects are recorded mainly in the spectral range 160–710 cm^{-1} with single peaks between 1280 and 1320 cm^{-1} (online Supplementary Material Table S2). Figure 4a shows the Raman spectra profile obtained from an insect preserved as a two-dimensional imprint with bands at 229, 297, 413, 684 and 1319 cm^{-1}. The bands at 229, 297 and 413 cm^{-1} are attributed to Fe–O symmetry stretching, Fe–OH symmetry bending and Fe–O symmetry bending, respectively (Das & Hendry, 2011; Mohopatra et al. 2011). The intense band at 684 cm^{-1} is attributed to Fe–O symmetric stretching vibration, which is often associated with α-FeOOH (de Faria & Lopes, 2007). The weak peak at 1319 cm^{-1} is characteristic of various iron-oxide and iron-hydroxide minerals (Marshall & Marshall, 2013). Figure 3b shows the Raman spectra obtained from a Crato insect with black coatings bearing two intense bands at 221 cm^{-1} and 281 cm^{-1} attributed to Fe–O symmetry stretching and Fe–O bending, respectively (Legodi & de Waal, 2007). The broad band centred at 1283 cm^{-1} is often assigned to iron oxides (Hassan et al. 2010). The presence of iron oxides is reinforced by the band at 389 cm^{-1}, the vibration of Fe–OH (Li & Hihara, 2015). The band at 592 cm^{-1} attributed toMn–Ostretching mode is taken as characteristic for α-Mn_2O_3 (Julien et al. 2004). This band indicates that iron compounds are found in close association with manganese oxide minerals.

Notably, the Raman spectra obtained from Crato insects with iron-oxide overgrowths display a high background noise (Fig. 4c, d). A possible explanation for this background is the presence of an OH group generating interference. The Raman spectra were also affected by fluorescence artefacts, and the broad bands may reflect the low degree of crystallinity of the fossil material. Regardless, the Raman spectra of the insects with iron-oxide overgrowths show bands associated with the mineral goethite (Zuo et al. 2003). In

Raman spectra of insects that retain fine morphological details, bands attributed to haematite can be observed (Fig. 4e, f). The presence of haematite is marked by bands at 220, 287, 402 and 603 cm^{-1} (Legodi & de Waal, 2007).

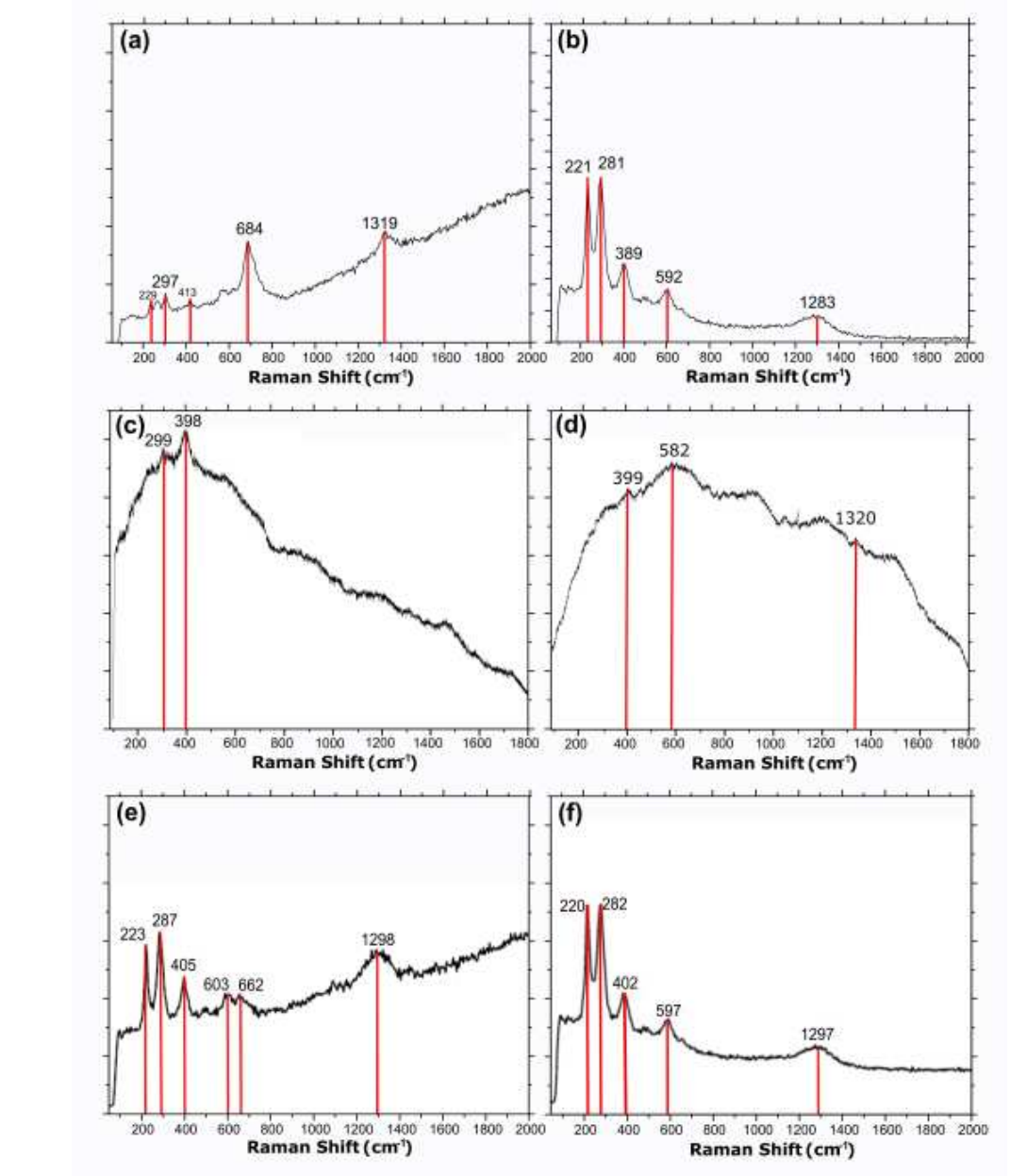

Fig. 4. Raman spectra of insect cuticles of (a) Caelifera (LP/UFC CRT 2204) preserved as two-dimensional imprints, (b) Odonata (LP/UFC CRT 1156) associated with dendrites and (c, d) spectra of crickets with iron-oxide overgrowths, LP/UFC CRT 122 and LP/UFC CRT 1822, respectively. (e, f) Raman spectra of mineralized insects that retain fine details of morphology at hand scale: Blattodea (LP/UFC CRT 2055) and Caelifera (LP/UFC CRT 2083), respectively.

The FTIR spectra of insects show heterogeneity, with different peaks recorded at

various positions. FTIR signals were observed mainly in two spectral regions: 600–1000 cm^{-1} and 3200–3600 cm^{-1} (online Supplementary Material Table S2). The graphics exhibit a spectral region where it is possible to observe bands related to OH-stretching vibrations. The spectrum of a Crato insect preserved as a two-dimensional imprint show bands at 674, 710, 873, 1107, 1414, 1619, 3241, 3404 and 3532 cm^{-1} (Fig. 5a). The band at 674 cm^{-1} is usually attributed to lattice absorption of iron-oxide (Tiwaria et al. 2015). The band at 710 cm^{-1} appears associated with bands at 873 cm^{-1} and 1414 cm^{-1}, which suggests characteristic bands of calcite (Rodriguez-Blanco et al. 2011). The peak at 1107 cm^{-1} can be assigned to the symmetric stretching mode of CaO (Gunasekaran & Anbalagan, 2007). The weak band at 1619 cm^{-1} can be attributed to O–H bending vibration (Raji et al. 2020). Significant bands around 3241, 3404 and 3532 cm^{-1} are assigned to the OH-stretching vibrations of the hydroxyl units ν(OH) (Frost et al. 2011, 2016; Frost & Xi, 2012). These bands show that this sample experienced chemical transformations under extremely wet conditions. The FTIR spectrum (Fig. 5b) of an insect with iron-oxide overgrowths shows awide band centred at 3172 cm^{-1} in the region related to OH-stretching vibrations. This remarkable wavenumber region probably consists of the overlapping of two or more components in the range 3270–3180 cm^{-1}. Bands at 1411 and 1795 cm^{-1} correspond to stretching of CO_3^{2-}. The band at 795 cm^{-1} can be assigned to Fe–O–H bending vibrations commonly associated with α-FeOOH (Musić et al. 2003). Figure 5c shows the FTIR spectrum obtained from a Crato insect with black coatings. The broad band at 3190 cm^{-1} can be attributed to O–H stretching vibration. The bands at 710, 873 and 1400 cm^{-1} are assigned to the antisymmetric stretching modes of calcium carbonate (Frost et al. 2008). The band at 994 cm^{-1} can be tentatively assigned to Fe–O vibrations. This band is often obscured in goethite. The FTIR spectrum (Fig. 5d) of a well preserved insect at hand scale also exhibits the characteristic peaks of calcite. However, the wavenumber region between 3000 and 3600 cm^{-1} appears less prominent here. In addition, the band around 1030 cm^{-1} is caused by the vibration of crystalline Fe–O mode, which is characteristic of haematite (Pal & Sharon, 2000).

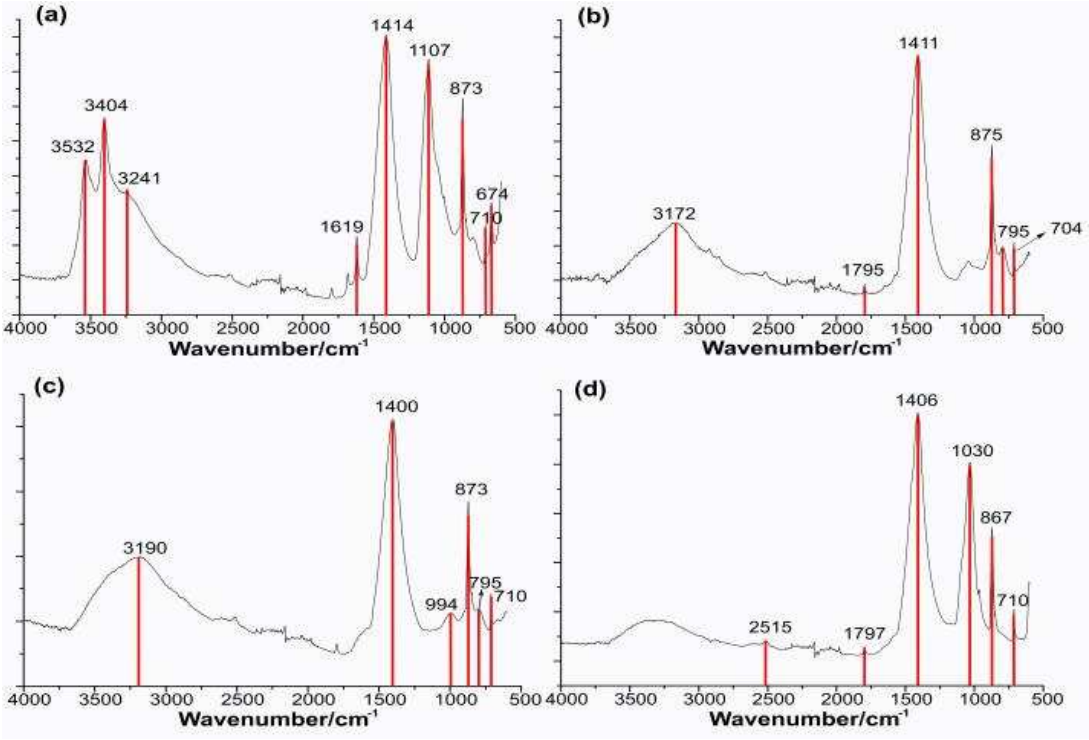

Fig. 5. Infrared spectra of Crato insects. (a) Isoptera (LP/UFC CRT 1896) preserved as two-dimensional imprints, (b) a cricket (LP/UFC CRT 834) with iron-oxide overgrowths, (c) a cricket (LP/UFC CRT 2647) with black coatings and (d) a Heteroptera (LP/UFC CRT 720) well preserved at hand scale.

4.d. Energy dispersive X-ray spectroscopy

Elemental analyses revealed that iron is more concentrated in fossil cuticles than in the carbonate matrix, while calcium is the opposite. The distribution of oxygen is in accordance with the presence of iron compounds replacing the fossils and the carbonate composition of the rock matrix. The insects with iron-oxide overgrowths contain a higher abundance (wt %) of iron than the other specimens (Figs 6a, 7a). In the spectrum of these insects, silicon, carbon, zinc, manganese and phosphorus are also represented. On the other hand, Crato insects with black coatings display a higher abundance (wt %) of manganese (Figs 6b, 7b). The 'depleted' insects preserved as imprints of outer cuticle exhibit a wide range of elements with a predominance of calcium (Figs 6c, 7c). Aluminium, lead, magnesium, potassium, silicon and manganese are also reported (Fig. 6c). Fully articulated insects with fine morphological details display a higher abundance of carbon and a lower abundance of calcium (Fig. 6d), and the conspicuous presence of phosphorus has also been documented (Fig. 7d). Overall, EDS data support that the fossil cuticles have high

concentrations of iron and oxygen, suggesting that original pyrite has been replaced by iron oxides/hydroxides due to post-diagenetic events (Fig. 7).

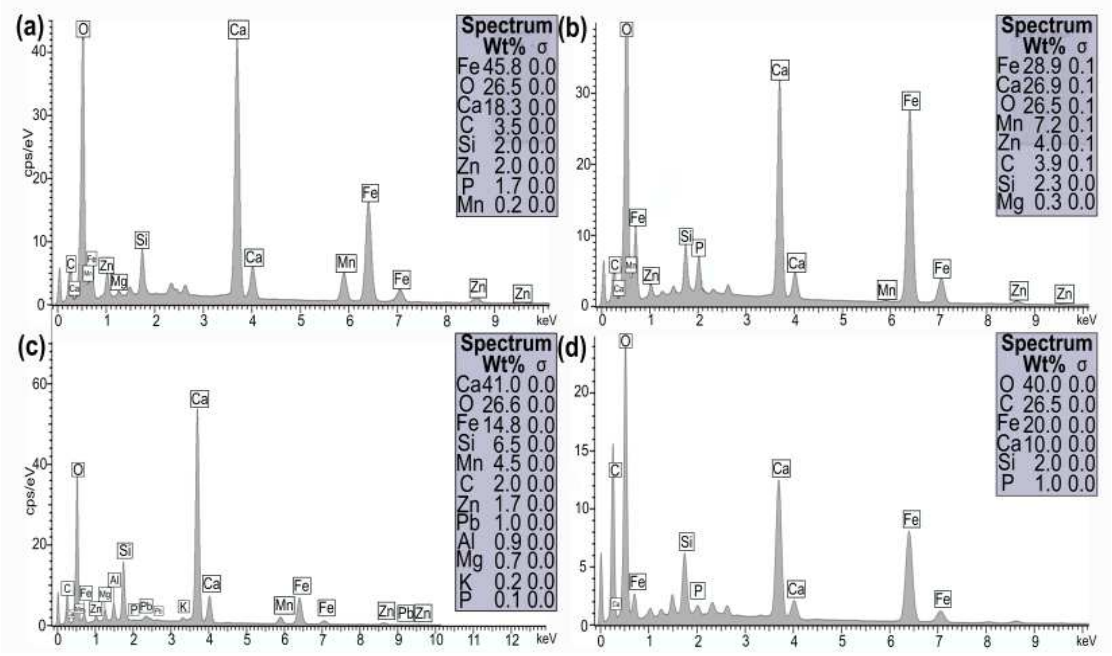

Fig. 6. Energy dispersive X-ray spectroscopy point spectra of (a) rust-like Heteroptera (LP/UFC CRT 708) with iron-oxide overgrowths, (b) a cricket (LP/UFC CRT 2388) with black coatings, (c) Caelifera (LP/UFC CRT 2204) preserved as two-dimensional imprints and (d) a mineralized cockroach (LP/UFC CRT 2055) fully articulated and well preserved.

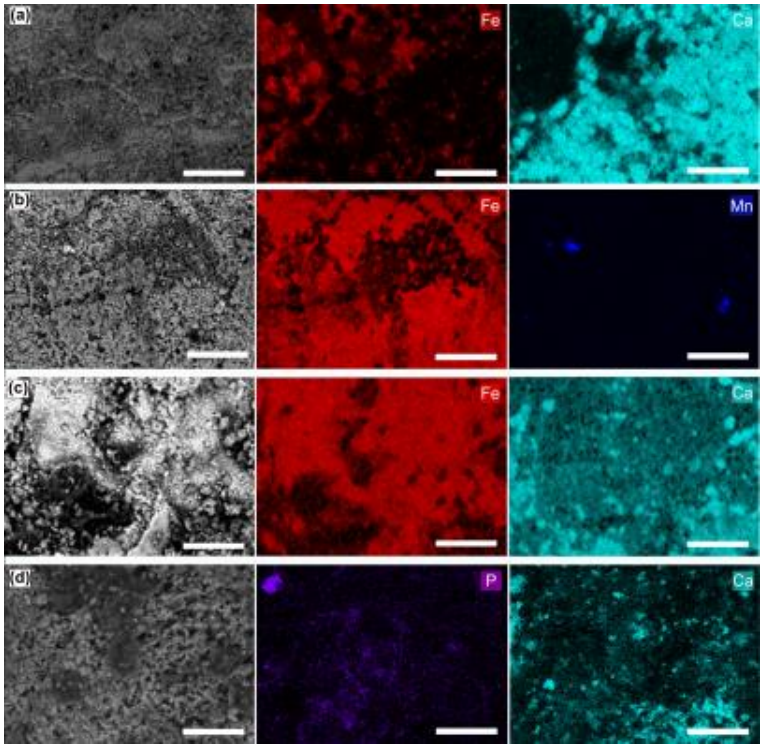

Fig. 7. Energy dispersive X-ray spectroscopy elemental map of Crato insects. (a) Secondary electron micrograph of Heteroptera (LP/UFC CRT 708) with iron-oxide overgrowths and the

elemental maps of iron and calcium; scale bars = 50 μm. (b) Micrograph of a cricket (LP/UFC CRT 2388) with black coatings and the elemental maps of iron and manganese; scale bars = 50 μm. (c) Micrograph of a Caelifera (LP/UFC CRT 2204) preserved as two-dimensional imprints and the elemental maps of iron and calcium; scale bars = 100 μm. (d) Secondary electron micrograph of a well preserved cockroach (LP/UFC CRT 2055) and the elemental maps of phosphorus and calcium; scale bars = 50 μm.

5. Discussion

5.a. Micro-structure preservation of weathered insects from the Crato Formation

The spectroscopic results revealed that the fossil insects studied here are preserved by iron-oxide/oxyhyroxide compounds, mainly haematite and goethite. Overall, SEM analysis showed that insect cuticles are preserved by globular aggregates or close-packing grains. Mineralized specimens exhibiting more morphological details at hand scale (best preserved) show cuticle surfaces with a polygonal lamellar arrangement and grains of ~1 μmin diameter. These insects display microtextural surfaces with little differentiation. The loss of fidelity is only partial and sometimes still maintains sensilla insertion holes. On the other hand, our results also show that Crato mineralized insects poorly preserved at the hand scale level show different textural characteristics at the micro scale. These insects commonly display cuticle details preserved by sub-spherical to spherical crystals in variable organizations with diameters mainly in the range of 5–15 μm. These characteristics are clear evidence of intense weathering experienced by Crato mineralized insects. Macroscopically, we highlighted at least three types of post-diagenetic alterations with the potential to distort morphological information essential for systematic studies. The alterations can be observed in specimens with iron-oxide overgrowths, insects with black coatings sometimes associated with dendrites and those preserved as two-dimensional imprints. Microscopically, Crato insects with iron-oxide overgrowths and black coatings are dominated by one fabric arranged into spherical or cylindrical aggregates sometimes possessing needle-like grains and hollow crystals. They also display microcracks and crystal aggregates associated with an alveolar habit, partially corroded surfaces and empty structures of dissolution cavities. In micrographs of insects with iron-oxide overgrowths, flow structures represented by sets of micro-grooves often appear as a striking feature. These scratches are likely the result of intense surface dissolution. The insects preserved as imprints retain discontinuous clusters of cryptocrystals or isolated

aggregates, evidence of an intense oxidation process. Intrastratal fluids leach away the insect mineral replica, leaving only parts of the body behind. Undoubtedly, Crato insect imprints represent the most intense type of alteration, and individuals showing this condition are rarely recovered for taxonomic purposes.

Our secondary electron analysis shows that Crato mineralized insects are preserved in a variety of mineral styles. They are interpreted as mineral fabrics produced during the early diagenesis that replicated fine details of the cuticle and other soft tissues. The Fe-oxide/hydroxide pseudomorphs are similar to precursor pyrite. The formation of pyrite replacements and their direct involvement in the replication of insect morphology are intrinsically associated with the time the fossils spent in the bacterial sulfate reduction zone of the sediment (Schiffbauer et al. 2014). The taphonomic pathways of pyritized insects during the early diagenesis of the Crato Formation have been well documented in previous studies (Barling et al. 2015, 2020; Osés et al. 2016; Bezerra et al. 2020; Dias & Carvalho, 2020, 2021). Nonetheless, the scattered distribution of the aggregate particles and the variety of their arrangements indicates a complex oxidation process with several probable stages. Dissolution cavities, microcracks, flow structures and hollow crystals with corroded surfaces merged into larger aggregates are microtextural features that evidence chemical weathering under variable water conditions.

5.b. Transformation of Fe-oxide/hydroxide pseudoframboids

Pyrite oxidation is a complicated process that includes several types of oxidation–reduction reactions, hydrolyses and complex ion formation. The transformation of pyrite in an oxygen-containing environment may proceed by different mechanisms under different conditions. Parameters such as temperature, oxygen concentration and flow conditions can all affect the transformation process (Jorgensen & Moyle, 1982). Oxidation is a major process in the dissolution of pyrites, and aqueous oxidation plays a significant role in the production of sulfuric acids as a result of natural weathering of pyritic rocks and shale (Rimstidt & Vaughan, 2003). Overall, ferrihydrite is produced as an intermediate phase between the primary sulfide and the final oxides/hydroxides during the oxidation of pyrite in an aqueous environment (Nordstrom, 1982). Ferrihydrite is metastable under oxic conditions, gradually converting to the more crystalline and stable goethite and haematite (Cudennec & Lecerf, 2006). Ferrihydrite dissolves to neutral pH (7–8) and transforms to haematite. In contrast, goethite formation occurs under either acidic or alkaline conditions (Das et al. 2011). The

preservational textures observed in the cuticle of mineralized insects from the Crato Formation consist primarily of pyrite framboids and pseudoframboids (Barling et al. 2015; Osés et al. 2016; Bezerra et al. 2020). These microtextural characteristics indicate that the mineral fabrics of insects are very similar both after and before post-diagenetic changes. In this case, the hypothesis of transformation of pyrite through the dissolution–crystallization process is unlikely. Therefore, the transformation of pyrite into goethite and haematite most likely occurred in the solid state.

The oxidation of pseudoframboidal pyrite is considered to be fast owing to its high specific surface area (Pugh et al. 1984). However, the formulation of a consistent oxidation reaction of the pyrite surface is not sufficiently characterized, and oxidation of pseudoframboid surfaces may occur upon contact with meteoric water and the Earth's oxygenic atmosphere, where O_2 and Fe^{3+} play a key role. Initially, transformation involves the adsorption of O_2 and water to the pyrite surface. Singer & Stumm (1970) suggested that Fe^{3+} is the major oxidant of pyrite whereas O_2 becomes the predominant oxidant at circumneutral pH. Fe^{3+} is also oxidizing at circumneutral pH, but the reaction cannot be sustained without the presence of dissolved O_2 to perpetuate the oxidation to Fe^{3+} (Evangelou & Zhang, 1994). Schaufuß et al. (1998a) found Fe^{3+} oxyhydroxide to be the main product after sulfate during the oxidation process. Jerz & Rimstidt (2004) reported that the FeS_2 oxidation reaction rate decreases with time, and linked the reduced reaction rate to the development of a thin layer of iron on the pyrite surface. The authors proposed that this layer retards oxygen transport and hence induces a possible change from reaction rate. Eggleston et al. (1996) hypothesized an oxidation mechanism involving surface cycling of Fe^{2+} and Fe^{3+}, where Fe^{3+} hydroxide or oxide products serve as a conduit for electron transfer from the pyrite surface to molecular oxygen. This involves the transfer of electrons from pyrite Fe^{2+} to oxide Fe^{3+}, and this process takes place preferentially from pyrite Fe^{2+} adjacent to the oxide. Schaufuß et al. (1998a,b) also provided a similar explanation for the initial formation of iron oxides on pyrite surfaces. The surface crystal attached to the Fe^{3+} site causes electron transfer from the Fe^{2+} adjacent to the attached O_2. Then, the second Fe^{3+} adjacent to the first induces Fe^{3+} oxide propagation, resulting in the formation of FeOOH, which can be dehydrated to Fe_2O_3 later. Gu et al. (2020) postulated that pyrite oxidation is limited by diffusion of oxygen at the grain scale, which is in turn regulated by fracturing at the clast scale. Thus, the pyrite oxidative transformation progresses inwards from fractures when observed at the clast scale. Oxidized pyrites often have an oxidation shell and an unoxidized core. Du et al. (2021) noted that the degree of pyrite oxidation is relative to the thickness of the oxidation shell. Therefore, the thickness of

the oxidation shell indicates amore oxidizing environment or a longer duration of oxidation. This could be a possible explanation for the numerous hollow crystals observed in the cuticular replicas of Crato insects (Fig. 3e, g, h). Non-oxidized pseudoframboidal crystals would be more vulnerable to erosion. Thus, the hollow crystals observed here could represent a shorter oxidation duration or lower oxygen fugacity.

5.c. Weathering of Crato pyritized insects

Chemical weathering of sedimentary rocks normally produces successions of minerals in different hydration states. Overall, weathered profiles contain several sequences of hydrated–dehydrated–hydrated minerals distributed in zones above and within the ground water table (Chigira & Oyama, 1990). An essential mineralogical change in weathered profiles is the formation of oxides and hydroxides, where goethite and haematite are the main hydrated and dehydrated minerals, respectively (Schwertmann, 1988). Hydrated minerals appear at the bottoms of profiles, close to the ground water table, while dehydrated minerals appear preferentially in the intermediate part between two horizons containing more hydrated minerals. This general distribution is mainly explained by seasonal fluctuations of the intrastratal water within the profiles. The weathering of fossil insects from the Crato Formation seems to have been directly influenced by meteoric fluids. The oxidation of framboidal pyrites of cuticles of Crato insects is limited by diffusion of oxygen through the carbonate matrix. The transport of O_2 depends on the penetration of water, which is in turn limited by the formation of fractures and pores. At the landscape scale, the oxidation process is limited by the movement of meteoric fluids into the carbonate matrix. This idea is supported by observations showing cases where pyrite oxidizes to a depth of metres (e.g. 2 to 10m) in crystalline rocks and pyrite-rich black shales (Wildman et al. 2004; Drake et al. 2009).

Although efforts to delimit the stratigraphic position of the different fossil groups in the Crato Formation are rare in the literature, mineralized insects seem to be restricted to the uppermost part of the interval II proposed by Varejão et al. (2019). This interval consists of yellow to red-coloured laminites with domal stromatolites and halite hoppers (Varejão et al. 2019). According to these authors, these layers are more fossiliferous in the Nova Olinda region, where they crop out on quarry fronts. Recently, Corecco et al. (2022) reported an interval informally named by quarry workers as ‘veio do besouro’, from which most Crato mineralized insects are recovered. This interval corresponds to the uppermost part of the Nova

Olinda Member. The non-homogeneous mineral fabrics observed in Crato insect replicas suggest that the transformation of the pyrite was limited by transport of reactants through the matrix to the grain surface. At this scale, the transport of reactants specifically depends on the porosity and permeability of the matrix. The laminated limestone of the Crato Formation shows average porosity and permeability values of 12 % and 0.04 mD (Miranda et al. 2016). For most relatively unfractured low-porosity carbonate zones within quarry fronts, reactants move by diffusion (Gu et al. 2020). During weathering, iron oxides slowly replace iron sulfide while retaining the external shape. The observation that the oxidation of framboids in Crato insects was accompanied by small changes in volume is consistent with the pseudomorphic nature of the transformation of pyrite to iron oxides (Putnis, 2009).

Although we did not find a characteristic spectroscopic spectrum for each type of post-diagenetic alteration identified here, our data show that insects well preserved at hand scale are preferentially replaced by haematite. However, Osés et al. (2016) and Bezerra et al. (2020) have already reported traces of goethite in well-preserved insects from the Crato Formation. Therefore, pyritized insects that retain privileged morphological information can be slowly oxidized to haematite or goethite by diffusion through the carbonate matrix. In this case, goethized insects faithfully replicated at the micro scale are thought to have been oxidized in wetter conditions than the haematized insects. Nonetheless, our spectroscopic results showed that Crato insects with iron-oxide overgrowths are preferentially preserved by goethite (Fig. 8). This secondary goethite seems to correspond to a rehydration process which is thought to be responsible for the destruction of the morphological fidelity acquired in the pyritization stage during early diagenesis. Specimens with black coatings are often associated with dendrites and other fluid structures related to manganese oxides/hydroxides (Figs 4b, 6b). The genetic mechanism for the formation of manganese dendrites and other low-crystallinity products is the invasion of sedimentary discontinuities by mineralized fluids through cracks. The intensification of this process progressively diminishes the morphological fidelity of the fossil insects affected by it. Both types of alteration with iron-oxide overgrowths and black coatings, the most intuitive sources of Mn^{4+} and Fe^{3+} is the circulation of enriched solutions through the discontinuities of the Crato carbonates. In this scenario, cracking events provoke the injection of these solutions, which travel through the sedimentary body forming different oxidized zones. Under such conditions, manganese ions will precipitate as MnOOH and iron ions as FeOOH (Giovanoli, 1980). These pervasive processes can easily distort or even rub out the morphological information recorded in haematized or goethized insects that maintain the preservation fidelity primarily obtained during pyritization.

Consequently, insects preserved as imprints represent the exacerbation of this process, where mineralized replicas are leached away (Fig. 8). Thus, textural, mineralogical and chemical features of Crato mineralized insects damaged during telodiagenesis are indicative of intense palaeoweathering events limited by erosion. Miranda et al. (2018) identified in the laminated carbonates of the Nova Olinda Member a series of extensional fractures and secondary structures such as horizontal veins, stylolites and vuggy fractures. These structures become conduits for infiltration of meteoric water, favouring an intense dissolution process. In some outcrops of the Nova Olinda Member, fractures are filled with calcite and/or gypsum, indicating an origin related to telodiagenetic processes (Miranda et al. 2012, 2018). Therefore, all types of post-diagenetic deformities observed in Crato insects can be directly linked to these discontinuities in the carbonate matrix. According to Miranda et al. (2018), these structural breaks were formed owing to the uplift of the Crato Formation and evolved along pre-existing planes of weakness, generating karstic features in the laminites. Marques et al. (2014) suggested that the current topography of the region is the result of a major inversion event that occurred in the Araripe Basin during Quaternary time. Thus, porosity can grow through dissolution and fracturing due to the exhumation of the Crato deposits and subsequent erosion. Mineralized insects of the Crato Formation have been slowly oxidized by diffusion of O_2 through a low-porosity matrix. However, this conservative transformation can be obliterated by a late pervasive event.

The slow oxidation of Crato insects must have been essential to maintain the morphological fidelity obtained in the early diagenesis. The transmission of information conceived under anoxic conditions to the modern atmospheric environment greatly favours the recovery of specimens. This clearly demonstrates that the high-quality preservation of Crato mineralized insects is a combination of early diagenetic induced mineralization and slow weathering rates in the low-porosity matrix. Therefore, all types of alterations presented in this research were caused by late events that affected fossils positioned in the vicinity of fractures or other secondary structures.

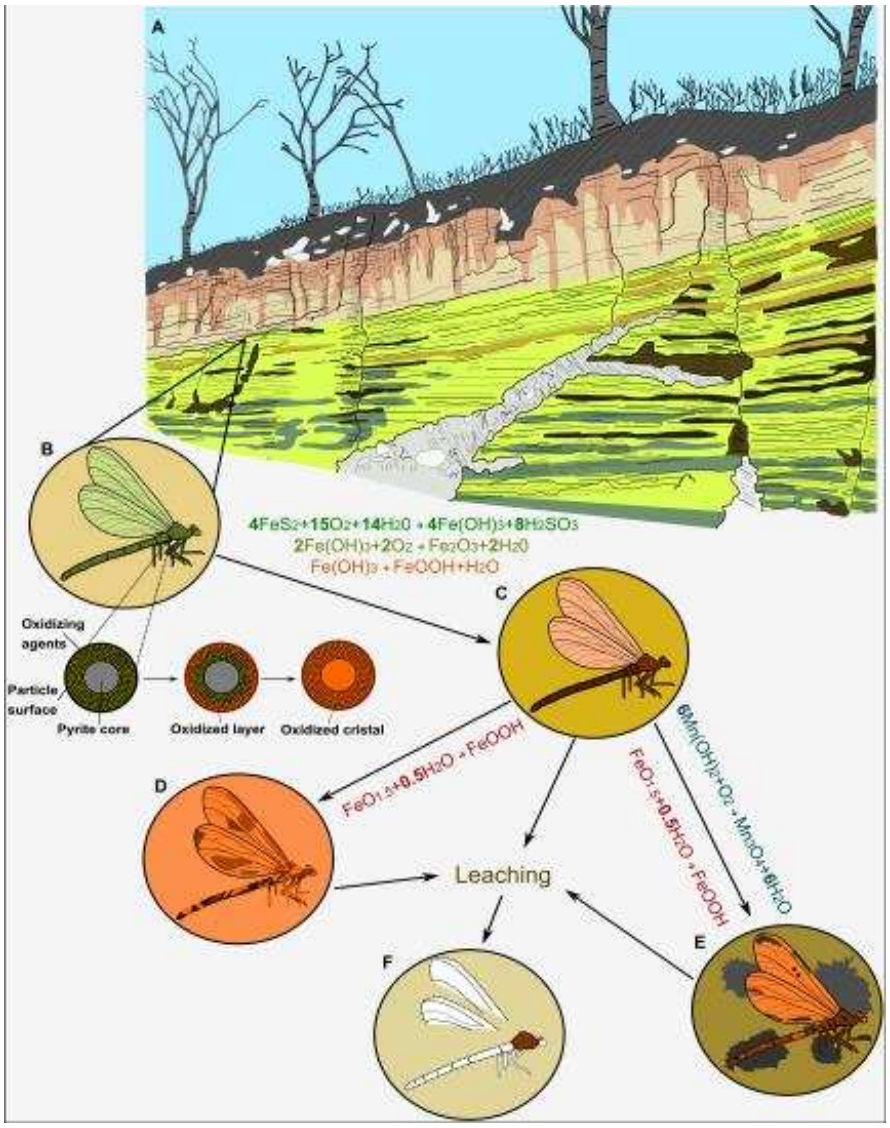

Fig. 8. Hypothetical model for the different weathering pathways of mineralized insects in the Crato Formation after earlier pyritization. (a) Schematic outcrop (quarry front) of laminated limestone from the Nova Olinda Member. (b) Illustration of a pyritized insect where pseudoframboids are transformed into haematite or goethite through the Quaternary by contact with oxidizing agents from the atmosphere. (c) Haematized or goethized insect that retains the fine morphological details acquired during earlier pyritization. (d) Rehydrated insects with iron-oxide overgrowths preserved preferentially by goethite. (e) Rehydrated insects affected by manganese oxides. (f) Maximum degree of weathering of Crato insects where oxidizing agents leach the fossil material away leaving behind only their imprint on the sediment.

6. Conclusions

The exceptional preservation of mineralized insects from the Crato Formation is attributed to geochemical conditions which allowed the pyritization of their cuticles and internal soft tissues during early diagenesis. Our results of imaging and spectroscopy techniques showed that these mineralized insects were pseudomorphed by iron oxides and hydroxides. Mineral pseudomorphism likely materialized during Quaternary time when the last major uplift event in the Araripe Basin took place. This process transformed the original pyrite into haematite and goethite by slow diffusion of O2 through a fine carbonate matrix. In this case, haematized and goethized insects faithfully replicated, even at the micro scale, the morphological information obtained during the earlier pyritization. On the other hand, our results also showed at least three types of post-diagenetic alterations with the potential to distort, or even destroy, morphological information from Crato insects. Overall, altered insects are not well preserved at the hand scale and also show different textural characteristics at the micro scale. The alterations can be observed in specimens with iron-oxide overgrowths, insects preserved as two-dimensional imprints and those with black coatings sometimes associated with dendrites. Crato insects with iron-oxide overgrowths are preferentially pseudomorphed by goethite and exhibit characteristic grooves and scratches on the surface of their cuticle at the micro scale. This type of alteration seems to correspond to a rehydration process, which is thought to be responsible for the destruction of the morphological fidelity acquired during the pyritization stage. Individuals with black coatings are often associated with dendrites and other low-crystallinity products related to manganese oxides/hydroxides that overlap primary preservation at the macro and micro scales. Lastly, insects preserved as imprints retain only parts of the cuticle with discontinuous clusters of cryptocrystals or isolated aggregates. This last type represents the most intense weathering experienced by Crato insects, which is when mineralized replicas are leached away.

In summary, we list three major geochemical steps involved in the taphonomic history of mineralized insects from the Crato fossil Lagerstätte, excluding biostratinomic processes. Firstly, early diagenetic pyritization of cuticle and labile tissues under hypersaline lacustrine system conditions associated with microbial activity (Catto et al. 2016; Varejão et al. 2019). This step yielded threedimensional replicas of insects. Secondly, the transition of palaeontological information obtained under anoxic conditions to an oxic and stable environment. This transformation was provided by slow oxidation in situ, keeping morphological details of delicate features, which can shed light on taxonomy and systematics. Thirdly, the pervasive weathering experienced by oxidized insects near fractures or other secondary structures, where reprecipitation and chemical dissolution is intense. This step

obscures the palaeontological information partially or entirely; therefore, Crato insects involved in this step are less likely to be recovered for taxonomic studies.

Acknowledgements. FIB is grateful for his doctorate scholarship (Coordenação de Aperfeiçoamento de Pessoal de Nível Superior, Brasil – CAPES, process 88882.454892/2019-01). JHS is grateful for the financial support of CNPq no 4/2021 – Research Productivity Grants – PQ, process no. 308064/2021-6. JHS is also grateful for the approved project (FUNCAP) 'Aid to support research group projects' Public Notice 07/2021. We acknowledge Dr Charlotte Williams for language revision. The reviews of Jaime Dias and an anonymous are greatly appreciated and improved the quality of the manuscript. Dr Wellington Ferreira da Silva Filho (UFC) has always encouraged our work on the Crato Formation. The authors would like to thank the Central Analítica-UFC/CT-INFRA/MCTI-SISANO/Pr´o-equipamentos CAPES for the support. We also thank the Federal Police of Brazil for proactive initiatives which have diminished the illegal international trade of fossils from the Crato Formation.

References

Anderson EP and Smith DM (2017) The same picture through different lenses: quantifying the effects of two preservation pathways on Green River Formation insects. *Paleobiology* **43**, 224–47.

Arai M and Assine ML (2020) Chronostratigraphic constraints and paleoenvironmental interpretation of the Romualdo Formation (Santana Group, Araripe Basin, Northeastern Brazil) based on palynology. *Cretaceous Research* **116**, 104610. doi: 10.1016/j.cretres.2020.104610.

Assine ML (2007) Araripe basin. *Boletim de Geociências da Petrobras* **15**, 371–89.

Assine ML, Perinotto JA, Neumann VH, Custódio MA, Varejão FG and Mescolotti PC (2014) Sequências deposicionais do Andar Alagoas (Aptiano superior) da Bacia do Araripe, Nordeste do Brasil. *Boletim de Geociências da Petrobras* **22**, 3–28.

Barden P and Engel MS (2021) Fossil social insects. In Encyclopedia of Social Insects (ed. CK Starr), pp. 1–21. Cham: Springer International Publishing.

Barling NT, Heads SW and Martill DM (2021) Behavioural impacts on the taphonomy of

dragonflies and damselflies (Odonata) from the Lower Cretaceous Crato Formation, Brazil. *Palaeoentomology* **4**, 141–55.

Barling N, Martill DM and Heads SW (2020) A geochemical model for the preservation of insects in the Crato Formation (Lower Cretaceous) of Brazil. *Cretaceous Research* **116**, 104608. doi: 10.1016/j.cretres.2020.104608.

Barling N, Martill DM, Heads SW and Gallien F (2015) High fidelity preservation of fossil insects from the Crato Formation (Lower Cretaceous) of Brazil. *Cretaceous Research* **52**, 605–22.

Berner RA (1970) Sedimentary pyrite formation. *American Journal of Science* **268**, 1–23.

Beurlen KA (1962) Geologia da Chapada do Araripe. *Anais da Academia Brasileira de Ciencias* **34**, 365–70.

Bezerra FI, da Silva JH, de Paula AJ, Oliveira NC, Paschoal AR, Freire PTC, Viana BC and Mendes M (2018) Throwing light on an uncommon preservation of Blattodea from the Crato Formation (Araripe Basin, Cretaceous), Brazil. *Revista Brasileira de Paleontologia* **21**, 245–54.

Bezerra FI, da Silva JH, Miguel EC, Paschoal AR, Nascimento Jr DR, Freire PTC, Viana BC and Mendes M (2020) Chemical and mineral comparison of fossil insect cuticles from Crato *Konservat Lagerstätte*, Lower Cretaceous of Brazil. *Journal of Iberian Geology* **46**, 61–76.

Bezerra FI, Solórzano-Kraemer MM and Mendes M (2021) Distinct preservational pathways of insects from the Crato Formation, Lower Cretaceous of the Araripe Basin, Brazil. *Cretaceous Research* **118**, 104631. doi: 10.1016/j.cretres.2020.104631.

Catto B, Jahnert RJ, Warren LV, Varejão FG and Assine ML (2016) The microbial nature of laminated limestones: lessons from the Upper Aptian, Araripe Basin, Brazil. *Sedimentary Geology* **341**, 304–15.

Chigira M and Oyama T (1990) Mechanism and effect of chemical weathering of sedimentary rocks. *Engineering Geology* **55**, 3–14.

Clapham ME and Karr JA (2012) Environmental and biotic controls on the evolutionary history of insect body size. *Proceedings of the National Academy of Sciences* **109**, 10927–30.

Clapham ME, Karr JA, Nicholson DB, Ross AJ and Mayhew PJ (2016) Ancient origin of

high taxonomic richness among insects. *Proceedings of the Royal Society B: Biological Sciences* **283**, 20152476. doi: 10.1098/rspb.2015.2476.

Coimbra JC and Freire TM (2021) Age of the post-rift Sequence I from the Araripe Basin, Lower Cretaceous, NE Brazil: implications for spatio-temporal correlation. *Revista Brasileira de Paleontologia* **24**, 37–46.

Corecco L, Bezerra FI, Silva Filho WF, Nascimento Júnior DR, da Silva JH and Felix JL (2022) Petrological meaning of ethnostratigraphic units: laminated limestone of the Crato Formation, Araripe Basin, NE Brazil. *Pesquisas em Geociências* **49**, e121139. doi: 10.22456/1807-9806.121139.

Cudennec Y and Lecerf A (2006) The transformation of ferrihydrite into goethite or hematite, revisited. *Journal of Solid State Chemistry* **179**, 716–22.

Das S and Hendry MJ (2011) Application of Raman spectroscopy to identify iron minerals commonly found in mine wastes. *Chemical Geology* **290**, 101–8.

Das S, Hendry MJ and Essilfie-Dughan J (2011) Transformation of two-line ferrihydrite to goethite and hematite as a function of pH and temperature. *Environmental Science & Technology* **45**, 268–75.

de Faria DLA and Lopes FN (2007) Heated goethite and natural hematite: can Raman spectroscopy be used to differentiate them? *Vibrational Spectroscopy* **45**, 117–21.

Delgado AO, Buck PV, Osés GL, Ghilardi RP, Rangel EC and Pacheco MLAF (2014) Paleometry: a brand new area in Brazilian science. *Materials Research* **17**, 1434–41.

Dias JJ and Carvalho IS (2020) Remarkable fossil crickets preservation from Crato Formation (Aptian, Araripe Basin), a Lagerstätten from Brazil. *Journal of South American Earth Sciences* **98**, 102443. doi: 10.1016/j.jsames.2019.102443.

Dias JJ and Carvalho IS (2021) The role of microbial mats in the exquisite preservation of Aptian insect fossils from the Crato *Lagerstätte*, Brazil. *Cretaceous Research* **130**, 105068. doi: 10.1016/j.cretres.2021.105068.

Donovan SK (1991) The Processes of Fossilization. London: Belhaven Press.

Drake H, Tullborg EL and MacKenzie AB (2009) Detecting the nearsurface redox front in crystalline bedrock using fracture mineral distribution, geochemistry and U-series disequilibrium. *Journal of Applied Geochemistry* **24**, 1023–39.

Du R, Xian H, Wu X, Zhu JH, Wei J, Xing J, Tan W and He H (2021) Morphology dominated rapid oxidation of framboidal pyrite. *Geochemical Perspectives Letters* **16**, 53–8.

Duncan IJ and Briggs DEG (1996) Three-dimensionally preserved insects. *Nature* **381**, 30–1.

Eggleston CM, Ehrhardt JJ and Stumm W (1996) Surface structural controls on pyrite oxidation kinetics: an XPS-UPS, STM, and modeling study. *American Mineralogist* **81**, 1036–56.

Evangelou VP and Zhang YL (1994) A review: pyrite oxidation mechanisms and acid mine drainage prevention. *Critical Reviews in Environmental Science and Technology* **25**, 141–99.

Frost RL, Bahfenne S and Graham J (2008) Infrared and infrared emission spectroscopic study of selected magnesium carbonate minerals containing ferric iron – implications for the geosequestration of greenhouse gases. *Spectrochimica Acta Part A: Molecular and Biomolecular Spectroscopy* **71**, 1610–16.

Frost RL, Palmer SJ, Spratt HJ and Martens WN (2011) The molecular structure of the mineral beudantite PbFe3(AsO4,SO4)2(OH)6 – implications for arsenic accumulation and removal. *Journal of Molecular Structure* **988**, 52–8.

Frost RL, Scholz R and López A (2016) A Raman and infrared spectroscopic study of the phosphate mineral laueite. *Vibrational Spectroscopy* **82**, 31–6.

Frost RL and Xi Y (2012) A vibrational spectroscopic study of the phosphate mineral wardite $NaAl_3(PO_4)_2(OH)_4{\cdot}2(H_2O)$. *Spectrochimica Acta Part A: Molecular and Biomolecular Spectroscopy* **93**, 155–63.

Giovanoli R (1980) On natural and synthetic manganese nodules. In Geology and Geochemistry of Manganese (eds IM Varentsov and GY Grasselly), pp. 191–9. Stuttgart: Schweizerbart.

Greenwalt DE, Rose TR, Siljeström SM, Goreva YS, Constenius KN and Wingerath JG (2015) Taphonomy of the fossil insects of the middle Eocene Kishenehn Formation. *Acta Palaeontologica Polonica* **60**, 931–47.

Gu X, Heaney PJ, Reis FDA and Brantley SL (2020) Deep abiotic weathering of pyrite. *Science* **370**, eabb8092. doi: 10.1126/science.abb8092.

Gunasekaran S and Anbalagan G (2007) Spectroscopic study of phase transitions in dolomite mineral. *Journal of Raman Spectroscopy* **38**, 846–52.

Hassan MF, Rahman MM, Guo ZP, Chen ZX and Liu HK (2010) Solventassisted molten salt process: a new route to synthesise α-Fe_2O_3/C nanocomposite and its electrochemical performance in lithium-ion batteries. *Electrochimica Acta* **55**, 5006–13.

Heimhofer U, Ariztegui D, Lenniger M, Hesselbo SP, Martill DM and Rios-Netto AM (2010) Deciphering the depositional environment of the laminated Crato fossil beds (Early Cretaceous, Araripe Basin, North-eastern Brazil). *Sedimentology* **57**, 677–94.

Heingård M, Sjövall P, Schultz BP, Sylvestersen RL and Lindgren J (2022) Preservation and taphonomy of fossil insects from the earliest Eocene of Denmark. *Biology* **11**, 395. doi: 10.3390/biology11030395.

Henwood AA (1992) Exceptional preservation of dipteran flight muscle and the taphonomy of insects in amber. *Palaios* **7**, 203–12.

Henwood AA (1993) Ecology and taphonomy of Dominican Republic amber and its inclusions. *Lethaia* **26**, 237–45.

Iniesto M, Gutiérrez-Silva P, Dias JJ, Carvalho IS, Buscalioni AD and López-Archilla AI (2021) Soft tissue histology of insect larvae decayed in laboratory experiments using microbial mats: taphonomic comparison with Cretaceous fossil insects from the exceptionally preserved biota of Araripe, Brazil. *Palaeogeography, Palaeoclimatology, Palaeoecology* **564**, 110156. doi:10.1016/j.palaeo.2020.110156.

Jerz JK and Rimstidt JD (2004) Pyrite oxidation in moist air. *Geochimica et Cosmochimica Acta* **68**, 701–14.

Jorgensen FRA and Moyle FJ (1982) Phases formed during the thermal analysis of pyrite in air. *Journal of Thermal Analysis and Calorimetry* **25**, 473–85.

Julien C, Massot M and Poinsignon C (2004) Lattice vibrations of manganese oxides. *Spectrochimica Acta Part A: Molecular and Biomolecular Spectroscopy* **60**, 689–700.

Karr JA and Clapham ME (2015) Taphonomic biases in the insect fossil record: shifts in articulation over geologic time. *Paleobiology* **41**, 16–32.

Kribek B (1975) The origin of framboidal pyrite as a surface effect of sulphur grains. *Mineralium Deposita* **10**, 389–96.

Labandeira CC (2019) The fossil record of insect mouthparts: innovation, functional convergence, and associations with other organisms, In Insect Mouthparts: Form, Function, Development and Performance (ed. HW Krenn), pp. 567–671. Cham: Springer.

Labandeira CC, Kustatscher E and Wappler T (2016) Floral assemblages and patterns of insect herbivory during the Permian to Triassic of northeastern Italy. *PLoS One* **11**, e0165205. doi: 10.1371/journal.pone.0165205.

Legodi MA and de Waal D (2007) The preparation of magnetite, goethite, hematite and maghemite of pigment quality from mill scale iron waste. *Dyes and Pigments* **74**, 161–8.

Li S and Hihara LH (2015) A micro-Raman spectroscopic study of marine atmospheric corrosion of carbon steel: the effect of akaganeite. *Journal of the Electrochemical Society* **162**, 495–502.

Marques FO, Nogueira FCC, Bezerra FHR and de Castro DL (2014) The Araripe Basin in NE Brazil: an intracontinental graben inverted to a highstanding horst. *Tectonophysics* **630**, 251–64.

Marshall CP and Marshall AO (2013) Raman hyperspectral imaging of microfossils: potential pitfalls. *Astrobiology* **13**, 920–31.

Martill DM, Bechly G and Loveridge RF (2007) The Crato Fossil Beds of Brazil – Window Into an Ancient World. Cambridge: Cambridge University Press.

Martínez-Delclòs X, Briggs DEG and Peñalver E (2004) Taphonomy of insects in carbonates and amber. *Palaeogeography, Palaeoclimatology, Palaeoecology* **203**, 19–64.

Matos RMD (1992) The northeast Brazilian rift system. *Tectonics* **114**, 766–91.

McNamara ME (2013) The taphonomy of colour in fossil insects and feathers. *Palaeontology* **56**, 557–75.

McNamara ME, Briggs DEG and Orr PJ (2012) The controls of the preservation of structural color in fossil insects. *Palaios* **27**, 443–54.

McNamara ME, Briggs DEG, Orr PJ, Wedmann S, Noh H and Cao H (2011) Fossilized biophotonic nanostructures reveal the original colors of 47-million-year-old moths. *PLoS Biology* **9**, e1001200. doi: 10.1371/journal.pbio.1001200.

Melo RM, Guzmán J, Almeida-Lima D, Piovesan EK, Neumann VHML and Sousa AJ (2020) New marine data and age accuracy of the Romualdo Formation, Araripe Basin, Brazil.

Scientific Reports **10**, 15779.doi: 10.1038/s41598-020-72789-8.

Miranda TS, Barbosa JA, Gomes IF, Santos RF, Neumann VH, Matos GC, Guimarães L, Queiroz RM and Alencar M (2012) Appling scanline techniques to geological/geomechanical modeling of fracturing systems in carbonate and evaporite deposits from Araripe Basin, NE Brazil. *Boletim de Geociências da Petrobras* **20**, 305–26.

Miranda T, Barbosa JA, Gomes IF, Soares A, Santos RFVC, Matos GC, McKinnon EA, Neumann VH and Marrett RA (2016) Petrophysics and petrography of Aptian tight carbonate reservoir, Araripe Basin, NE Brazil. In 78th European Association of Geoscientists and Engineers Conference and Exhibition. Vienna: European Association of Geoscientists and Engineers.

Miranda TS, Santos RF, Barbosa JA, Gomes IF, Alencar ML, Correia OJ, Falcão TC, Gale J and Neumann VH (2018) Quantifying aperture, spacing and fracture intensity in a carbonate reservoir analogue: Crato Formation, NE Brazil. *Marine and Petroleum Geology* **97**, 556–67.

Mohapatra M, Behera D, Layek S, Anand S, Verma HC and Mishra BK (2011) Influence of Ca ions on surfactant directed nucleation and growth of nano structured iron oxides and their magnetic properties. *Crystal Growth & Design* **12**, 18–28.

Musić S, Krehula S, Popović S and Skoko Ž (2003) Some factors influencing forced hydrolysis of FeCl3 solutions. *Materials Letters* **57**, 1096–102.

Nicholson DB, Mayhew PJ and Ross AJ (2015) Changes to the fossil record of insects through fifteen years of discovery. *PLoS One* **10**, e0128554.doi: 10.1371/journal.pone.0128554.

Nordstrom DK (1982) Aqueous pyrite oxidation and the consequent formation of secondary iron minerals. In Acid Sulfate Weathering (eds JA Kittrick, DS Fanning and LR Hossner), pp. 37–56. SSSA Special Publication 10. Madison: Soil Science Society of America.

Ohfuji H and Rickard D (2005) Experimental syntheses of framboids – a review. *Earth-Science Reviews* **71**, 147–70.

Osés GL, Petri S, Becker-Kerber B, Romero GR, Rizzutto MA, Rodrigues F, Galante D, da Silva TF, Curado JF, Rangel EC, Ribeiro RP and Pacheco MLAF (2016) Deciphering the preservation of fossil insects: a case study from the Crato Member, Early Cretaceous of Brazil. *PeerJ* **4**, e2756.doi: 10.7717/peerj.2756.

Pal B and Sharon M (2000) Preparation of iron oxide thin film by metal organic deposition from Fe (III)-acety-lacetonate: a study of photocatalytic properties. *Thin Solid Films* **379**, 83–8.

Pan Y, Sha J and Fürsich FT (2014) A model for organic fossilization of the early Cretaceous Jehol lagerstätte based on the taphonomy of Ephemeropsis trisetalis. *Palaios* **29**, 363–77.

Prado G, Arthuzzi JCL, Osés GL, Callefo F, Maldanis L, Sucerquia P,bBecker-Kerber B, Romero GR, Quiroz-Valle FR and Galante D (2021) Synchrotron radiation in palaeontological investigations: examples from Brazilian fossils and its potential to South American palaeontology. *Journal of South American Earth Sciences* **108**, 102973. doi: 10.1016/j.jsames.2020.102973.

Pugh CE, Hossner LR and Dixon JB (1984) Oxidation rate of iron sulfides as affected by surface area, morphology, oxygen concentration and autotrophic bacteria. *Soil Science* **137**, 309–14.

Putnis A (2009) Mineral replacement reactions. Reviews *in Mineralogy and Geochemistry* **70**, 87–124.

Raji M, Qaiss AK and Bouhfid R (2020) Effects of bleaching and functionalization of kaolinite on the mechanical and thermal properties of polyamide 6 nanocomposites. *RSC Advances* **10**, 4916–26.

Rimstidt JD and Vaughan DJ (2003) Pyrite oxidation: a state-of-the-art assessment of the reaction mechanism. *Geochimica et Cosmochimica Acta* **67**, 873–80.

Rodriguez-Blanco JD, Shaw S and Benning LG (2011) The kinetics and mechanisms of amorphous calcium carbonate (ACC) crystallization to calcite, via vaterite. *Nanoscale* **3**, 265–71.

Schachat SR and Labandeira CC (2021) Are insects heading toward their first mass extinction? Distinguishing turnover from crises in their fossil record. *Annals of the Entomological Society of America* **114**, 99–118.

Schaufuß AG, Nesbitt HW, Kartio I, Laajalehto K, Bancroft GM and Szargan R (1998a) Reactivity of surface chemical states on fractured pyrite. *Surface Science* **411**, 321–8.

Schaufuß AG, Nesbitt HW, Kartio I, Laajalehto K, Bancroft GM and Szargan R (1998b) Incipient oxidation of fractured pyrite surfaces in air. *Journal of Electron Spectroscopy and*

Related Phenomena **96**, 69–82.

Schiffbauer JD, Xiao S, Cai Y, Wallace AF, Hua H, Hunter J, Xu H, Peng Y and Kaufman AJ (2014) A unifying model for Neoproterozoic–Palaeozoic exceptional fossil preservation through pyritization and carbonaceous compression. *Nature Communications* **5**, 5754. doi: 10.1038/ncomms6754.

Schwertmann U (1988) Goethite and hematite formation in the presence of clay minerals and gibbsite at 25 °C. *Soil Science Society of America Journal* **52**, 288–91.

Singer PC and Stumm W (1970) Acid mine drainage-rate determining step. *Science* **167**, 1121–3.

Smith DM (2012) Exceptional preservation of insects in lacustrine environments. *Palaios* **27**, 346–53.

Smith DM, Cook A and Nufio CR (2006) How physical characteristics of beetles affect their fossil preservation. *Palaios* **21**, 305–10.

Smith DM and Moe-Hoffman AP (2007) Taphonomy of Diptera in lacustrine environments: a case study from Florissant Fossil Beds, Colorado. *Palaios* **22**, 623–9.

Thoene-Henning J, Smith DM, Nufio CR and Meyer HW (2012) Depositional setting and fossil insect preservation: a study of the late Eocene Florissant Formation, Colorado. *Palaios* **27**, 481–8.

Tian Q, Wang S, Yang Z, McNamara ME, Benton MJ and Jiang B (2020) Experimental investigation of insect deposition in lentic environments and implications for formation of *Konservat Lagerstätten*. *Palaeontology* **63**, 565–78.

Tiwari I, Singh M, Pandey CM and Sumana G (2015) Electrochemical genosensor based on graphene oxide modified iron oxide–chitosan hybrid nanocomposite for pathogen detection. *Sensors & Actuators, B: Chemical* **206**, 276–83.

Varejão FG, Warren LV, Simões MG, Buatois LA, Mángano MG, Bahniuk AMR and Assine ML (2021) Mixed siliciclastic-carbonate sedimentation in an evolving epicontinental sea: Aptian record of marginal marine settings in the interior basins of north-eastern Brazil. *Sedimentology* **68**, 2125–64.

Varejão FG, Warren LV, Simões MG, Fürsich FT, Matos SA and Assine ML (2019) Exceptional preservation of soft tissues by microbial entombment: insights into the

taphonomy of the Crato *Konservat-Lagerstätte*. *Palaios* **34**, 331–48.

Wang B, Zhao F, Zhang H, Fang Y and Zheng D (2012) Widespread pyritization of insects in the Early Cretaceous Jehol biota. *Palaios* **27**, 707–11.

Warren LV, Varejão FG, Quaglio F, Simões MG, Fürsich FT, Poiré DG, Catto B and Assine ML (2017) Stromatolites from the Aptian Crato Formation, a hypersaline lake system in the Araripe Basin, northeastern Brazil. *Facies* **63**, 3. doi: 10.1007/s10347-016-0484-6.

Wildman RA, Berner RA, Petsch ST, Bolton EW, Eckert JO, Mok U and Evans JB (2004) The weathering of sedimentary organic matter as a control on atmospheric O2: I. Analysis of a black shale. *American Journal of Science* **304**, 234–49.

Zhehikhin VV (2002) Pattern of insect burial and conservation. In History of Insects (eds AP Rasnitsyn and DLJ Quicke), pp. 17–63. Dordrecht: Springer.

Zuo J, Zhao X, Wu R, Du G, Xu C and Wang C (2003) Analysis of the pigments on painted pottery figurines from the Han Dynasty's Yangling Tombs by Raman microscopy. *Journal of Raman Spectroscopy* **34**, 121–5.

6 CAPÍTULO 4

Carrying out an integrated taphonomic and paleoecological analysis of the paleoentomofauna from the Crato Formation, Cretaceous of Brazil: A glimpse into a Central Gondwana ecosystem

Esse capítulo foi recentemente submetido ao jornal científico "Palaeogeography, Palaeoclimatology, Palaeoecology".

Referência:

Bezerra, Francisco I., and Mendes Márcio (2023). Carrying out an integrated taphonomic and paleoecological analysis of the paleoentomofauna from the Crato Formation, Cretaceous of Brazil: A glimpse into a Central Gondwana ecosystem. Palaeogeography, Palaeoclimatology, Palaeoecology (Submetted)

Carrying out an integrated taphonomic and paleoecological analysis of the paleoentomofauna from the Crato Formation, Cretaceous of Brazil: A glimpse into a Central Gondwana ecosystem

Francisco Irineudo Bezerra[1*], Márcio Mendes[1]

[1]Pós-Graduação em Geologia, Universidade Federal do Ceará , 64049-550, Fortaleza, Ceará , Brasil. irineudoufc@gmail.com, paleonto@ufc.br

[*]**Corresponding author:** Francisco Irineudo Bezerra.

Abstract

The Aptian Crato Formation, Araripe Basin, northeastern Brazil, stands out worldwide owing to its basal unit, the Nova Olinda Member, a world-class Fossil *Lagerstätte*. The Crato Formation was deposited close to the heart of the supercontinent Gondwana, when Gondwana was still reasonably intact. In this study, we analyzed 1135 fossil insects, included in 55 families, from both macrofacies (pale yellow and dark gray limestones) of the Nova Olinda Member to collect taphonomical data and measure their ecological relevance, such as their distribution and interaction with their paleoenvironment. Crato paleoentomofauna is composed to a greater extent of fully terrestrial insects despite the paleoenvironment configuring a typical aquatic deposit. The distribution of insect families is similar throughout the Nova Olinda Member, which excludes possible overlapping of one entomofauna over another. The pale yellow limestones near the top of the section are richer in fossil insect content and show a higher incidence of aquatic and semiaquatic insects preserved in dorsoventral view compared to the dark gray limestones. This suggests that specimens used short transport distances or prolonged decay or both. In contrast, insects preserved in the dark gray limestones appear proportionally with higher degrees of disarticulation than those preserved in the pale yellow limestones, indicating that these insects underwent a higher

degree of rework in the biostratinomic stage. Compared to descriptions of other Early Cretaceous assemblages, the taxonomic literature of Crato Paleoentomofauna shows distinct differences. The Yixian and Zaza formations are described as being dominated by beetles and wasps. The Crato Formation, however, records relatively fewer species from these groups and is relatively richer in Paleoptera species. Both the sedimentary facies studied and the paleoentomological content reveal a complex ecosystem inserted in a depositional setting, similar to modern long-standing wetlands, and where periodically flooded zones were surrounded by dry lands with xeromorphic vegetation.

Keywords: paleoentomofauna; paleoecology; taphonomy; *Lagerstätte*; Crato Formation

1.Introduction

Throughout history, geoscientists have sought to understand how ancient ecosystems worked. For this purpose, they have developed different methodologies to circumvent the relentlessness of time and achieve information as filtered from bias as possible (Solórzano-Kraemer et al., 2015, 2018). Paleoecology, broadly speaking, aims to reconstruct a past biota or ecosystem from available geological and biological evidence (Dodd and Stanton, 1990). Nevertheless, a paleoecological study based on elements from a wide range of timescales faces numerous limitations. The central problem of a deep-time paleoecological approach is the incompleteness of the fossil record. On the other hand, taphonomy is concerned with the study of how organisms pass from the biosphere to the lithosphere, and this includes all kinds of physical, chemical, and biological processes that cause changes in organic remains from the time of their death (Behrensmeyer, 2021). This field is strongly interdisciplinary and provides many opportunities to uncover biases caused by the types of organisms and habitats that are and are not represented in a specific paleoenvironment (Behrensmeyer and Hill, 1980). Taphonomy is essential to understanding what the limited samples of past life mean, as only a tiny fraction of the organisms that have inhabited the earth are preserved in the fossil record.

With regard to the incompleteness of the fossil record, the Crato Formation is distinguished by bearing a highly diverse biota compared to similar sites. The Crato Formation itself consists of carbonate layers several meters thick interbedded with siliciclastic sediments, whose origin is attributed to a lacustrine system. Overall, this particular depositional environment associated with microbial mats (Warren et al., 2017) yielded

exceptionally preserved fossils which made it known worldwide as a Cretaceous Fossil *Lagerstätte*. The focus of the present study is the laminated limestones of the Nova Olinda Member (Martill et al., 2007), which consists of the basal and thickest carbonate horizon and hosts the famous Crato *Lagerstätte*. This particular carbonate package contains an exceptionally rich paleoentomofauna associated with microbial entombment (Varejão et al., 2019). These limestones are visually distinguished by their color. In the Nova Olinda quarries laminates carbonates ranging from dark gray to pale yellow can be observed. Osés et al. (2017) named pale-yellow laminites as beige layers (BL) and those dark-gray as gray layers (GL), in their model, Osés and colleagues proposed that the fossils embedded in BL were mineralized via pyritization, whereas the fossils found in GL experienced preservation via kerogenization. Recently, Bezerra et al. (2021a) preferred to refer to BL and GL as pyritization and kerogenization zones, respectively, as the layers are difficult to distinguish by their boundaries. Thus, the terms are restricted to the preservation mode.

In recent years, many efforts have been made to offer a more accurate interpretation of the paleoenvironmental conditions involved in the high-quality preservation of fossil insects from the Crato Formation. However, most studies focus on geochemical models, fossil diagenesis, or different paleoecological implications apart from one another (e.g., Osés et al., 2016; Barling et al., 2015, 2020; Bezerra et al., 2020; Iniesto et al., 2021; Santos et al., 2021; Dias and Carvalho, 2020, 2022). In this sense, it is worth highlighting the attempts to provide an overview of the Crato biome presented by Ribeiro et al. (2021a) and Mendes et al. (2020).

In this study, we sought to verify how Crato insects thrived within a shallow lake depositional system. Therefore, we interlinked taphonomic and paleoecological information to understand how the limited conditions provided by the depositional environment of the Crato Formation, Nova Olinda Member, shaped our current view of the Crato paleoentomofauna.

2.Geological setting

The Araripe Basin is located in the Northeast region of Brazil, between the states of Ceará, Pernambuco, Piauí and Paraíba. This basin has an area of about 9000 km^2 (Ponte and Ponte Filho, 1996), of which more than 50% are over the Ceará territory. The Araripe Basin is nestled over Precambrian terrains of the Transversal Fold Zone of Borborema Province, southwards of the Patos lineament and northwards of the Pernambuco lineament (Brito Neves et al., 2000). These lineaments correspond to dextral shear zones, which would

have conditioned both the installation of the basin and its fragmentation during Cretaceous taphrogenesis (Fossen et al., 2022)(Fig. 1 a). The Araripe Basin is similar to other basins in the interior of Northeast Brazil. These basins are associated with the Neocomian rift event that resulted in the separation of the South American and African continents; specifically in the opening of the Brazilian continental margin (Assine, 2007). This system included a range of onshore aborted rift basins extending from the Recôncavo-Tucano-Jatobá grabens system to the Potiguar graben, all of which were controlled by the main NW extension. In the case of the Araripe Basin, the tectonic rift produced half-grabens controlled by normal faults in the NE direction that are commonly tilted to the SE and associated with strike-slip faults (Matos, 1992, 1999; Cardoso, 2010). The relief is a remarkable feature in the landscape of the Araripe Basin region; the so-called *Chapada do Araripe* is a tableland feature E-W long, smoothly inclined westwards, and bordered by steep cliffs (Assine, 2007) (Fig. 1 b). In the surrounding plains, the sedimentary deposits of the basin are distributed mainly in the east and northeast flanks of the *chapada*.

The Araripe Basin is subdivided into sequences bound by regional unconformities that reflect distinct tectonic stages: (1) the Palaeozoic Sequence is represented by the alluvial sedimentation of the Mauriti Formation and interpreted as the residual deposits of a large intracratonic basin; (2) the Pre-Rift Supersequence (Neojurassic), corresponding to the Brejo Santo and Missão Velha formations; (3) the Rift Supersequence (Neocomian), equivalent to the Abaiara Formation; and (4) the Post-Rift Supersequence which can be subdivided into two higher-frequency sequences: (a) Post-Rift Sequence I (Aptian-Albian), corresponding to the Santana Group; and (b) Post-Rift Sequence II, equivalent to the Araripina and Exu formations (Assine et al., 2014). The present study focuses on the Post-rift I Tectonosedimentary Sequence interval. This group records an almost complete stratigraphic depositional sequence, which represents the apex of the thermal subsidence of the basin during the Cretaceous. Evidence of this comes from sites in the basin where deposits of the Santana Group lie directly on the basement (Marques et al., 2014). The interval of the Post-rift I Sequence started by the deposition of two major fluvial packages, both with fining upward cycles corresponding to the Barbalha Formation (Sherer et al. 2014). The uppmost contact between the Barbalha Fm. deposits with the marly-to-calcareous lacustrine deposits mark the beginning of the Crato Formation, whose basal contact with the Barbalha Fm. is not well-established yet. Deposits of gypsitic evaporites with variable thickness interbedded with green and black shales lie over the Crato Fm. as a discontinuous layer, representing the Ipubi Formation (Nascimento Jr et al., 2016). The contact between the green and black shales of

Ipubi Fm. and the marly shales of the Romualdo Formation is marked by a diastem recognized as a thin conglomerate level.

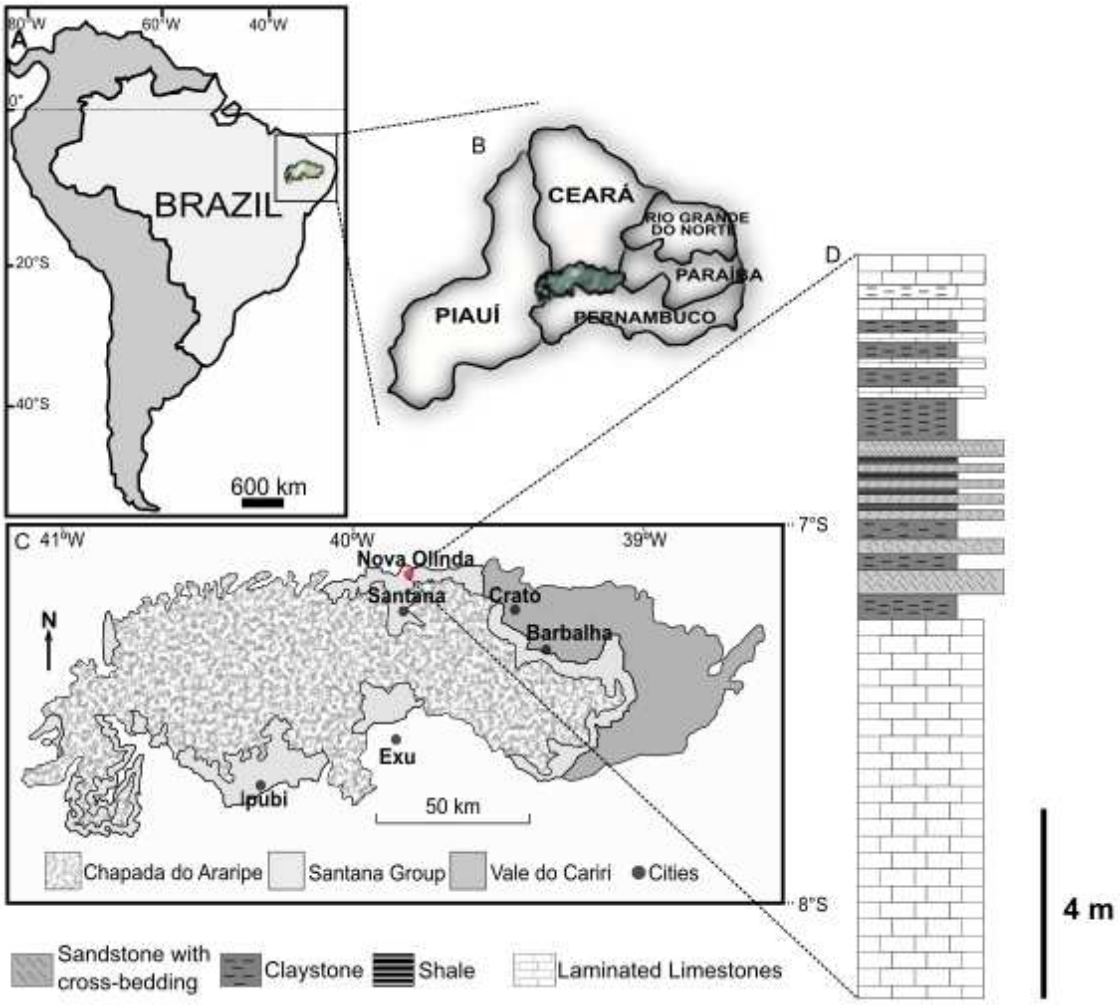

Fig.1 – Scheme showing the location of the study area. A. Map of South America showing the location of the Araripe Basin. B. position of the Araripe Basin in Northeast Brazil. C. simplified geological map of the Araripe Basin with location of the city of Nova Olinda, Ceará. D. stratigraphic column of the Crato Formation in the Nova Olinda.

The Crato Formation consists of several carbonate layers interbedded with a series of shales, claystones, siltstones, and sandstones (Heimhofer et al., 2010; Santos et al., 2017; Catto et al., 2016). The origin of the Crato facies is attributed to transgressive–regressive events associated with the expansion and contraction of a lacustrine system (Neumann, 1999). The lacustrine carbonate facies are predominantly composed of micritic laminated limestones. The Crato Formation can be divided into four different members, from bottom to top: the Nova Olinda, Caldas, Jamacaru and Casa de Pedra Members. Nova Olinda Member represents the lowest and thickest limestone horizon and hosts the world-renowned Crato

Fossil *Lagerstätte* (Martill et al., 2007; Nascimento Jr et al., 2023), which made it the focus of the present study. Nova Olinda limestones are characterized by conspicuous lamination and regular rhythmical bedding (Fig. 1 c). The age of this unit is still not well established because of the absence of diagnostic microfossils, marine macrofossils, or volcanic rocks. Lúcio et al. (2020) proposed a late Barremian age for the Crato Formation based on Re-Os isotopic analysis. However, this work is highly contested in terms of its methodology. A series of studies based on ostracod assemblages and terrestrial palynomorphs (Coimbra et al., 2002; Heimhofer and Hochuli, 2010; Arai, 2014; Coimbra and Freire, 2021) converge in attributing the late Aptian/early Albian age for the entire Crato Formation. Based on microfossil data, Arai and Assine (2020) and Melo et al. (2020) converged to place the entire Post-Rift Sequence I in the Late Aptian.

3. Materials and Methods

3.1 Fossil insect data

All insects analyzed in this study belong to the paleontological collection of the Laboratório de Paleontologia from Universidade Federal do Ceará (UFC). The laboratory receives fossil insects donated by quarry workers, but most of the specimens are collected by undergraduate students, from the tailings of mined areas, during field campaigns over the years. In total, our sample has 1135 specimens collected in quarries in the surroundings of Nova Olinda, Ceará. Seven hundred and forty-nine insects originated from pale yellow laminated limestones, while three hundred and eighty-six insects were collected from dark gray limestones of the Nova Olinda Member, Crato Formation.

In this study, we constructed a taxonomic literature dataset to most accurately compare the Crato paleoentomofauna with the other major assemblages bearing insects of the Early Cretaceous. Global occurrences of insect species from Early Cretaceous were downloaded from the PBDB (https://paleobiodb.org) and EDNA fossil insect database (https://fossilinsectdatabase.co.uk). The occurrence dataset was revised to remove taxonomically indeterminate fossil insects. Indeterminate fossils represent uncertainties or non-consensus among taxonomists. In most cases, indeterminate fossil insects could be associated with a family or a genus, but in other cases, such an association was not possible. Therefore, fossil insects that could not be assigned to a valid genus or species were removed from the dataset.

3.2 Insect taxonomy and the relative abundance of fossil insects

All fossil insects from the Crato Formation were assigned to the lowest taxonomic rank, here, family level. Thus, family-level designations were considered for the purposes of the current study. The proportions of the relative abundance of insects between the two macrofacies were compared using chi-squared tests, for this comparison we adopted the order-level designation. If an insect, included within an order, could not be placed in a family with a certain level of confidence, it was named "indeterminate". If an insect could not be assigned to a family or order with any degree of confidence, it was simply labeled "Insecta". Taxonomic classification was made based on Evans (1956), Kukalová-Peck (1985), Darling and Sharkey (1990), Hamilton (1990), McCafferty (1990), Schuh and Slater (1995), Bechly (1997), Andersen (2001), Béthoux and Nel (2002), Colgan et al. (2003), Martins-Neto (2003), Menon (2005), Menon et al. (2005), Martill et al. (2007), Grimaldi et al. (2008) and Lee (2016).

3.3 Fossil insect articulation and orientation states

In this study, the completeness of insects from the Crato Formation was designated according to Anderson and Smith (2017). Therefore, the different articulation states were measured by comparing the completeness of entire insect bodies between the two macrofacies. Here, "fully articulated" insects represent complete specimens with head, thorax, abdomen, and wings (regardless of whether or not they had their legs, antennae, or other appendages, as they directly depend on the fossil's orientation to be observable). “Partially articulated” fossil insects showing at least one morphological character absent (e.g., specimens missing the head or abdomen). “Disarticulated” insects consisted only of isolated body parts or bodily components that were entirely separate from another (Fig. 2). The orientation of each specimen, dorsoventral or lateral positioning, was also documented for biostratinomic purposes. Both articulation and orientation states of the insects were compared using chi-squared tests.

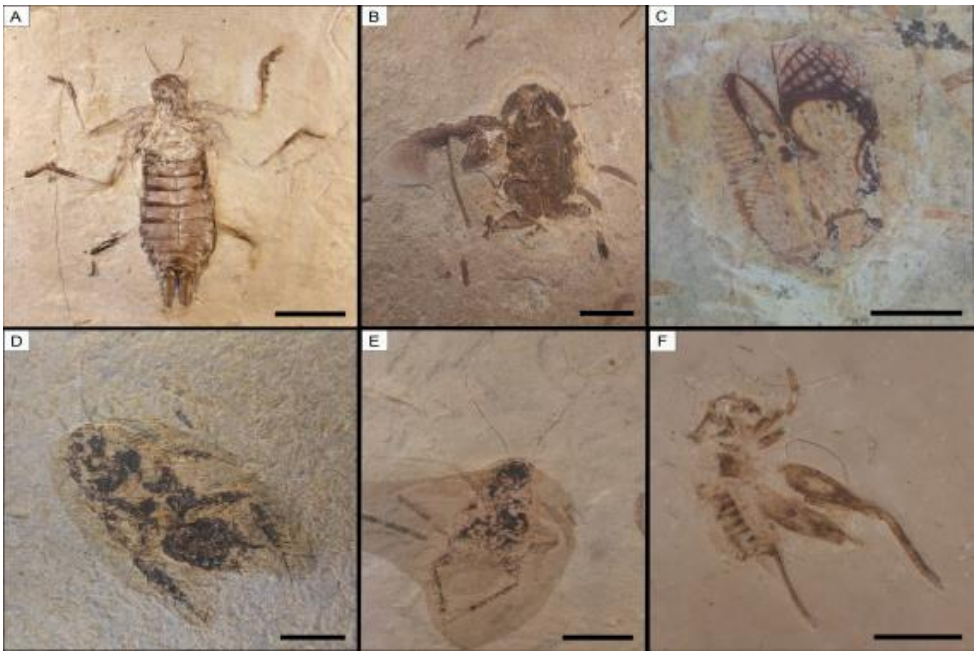

Fig. 2 – Examples of different Crato insects from both pale yellow and dark gray limestones. A. larva of fully articulated *Nothomacromiidae* (LP/UFC CRT 1190) from pale yellow limestones. B. partially articulated *Mesoblattinidae* (LP/UFC CRT 694) preserved in pale yellow limestones. C. Gryllidae tégmina (LP/UFC CRT 2491) isolated from pale yellow limestones. D. fully articulated Blattodea (LP/UFC CRT 665) found in dark gray limestones. E. partially articulated Blattullidae (Mesoblatiniidae) (LP/UFC CRT 572) preserved in dark gray limestones. F. disarticulated Caelifera (LP/UFC CRT 2183) preserved in dark gray limestones. All scale bars = 1 cm.

3.4 Insect body area measurements

The body area of each fossil insect was calculated by multiplying specimen length and width. Length was measured as a straight line from the distal tip of the mouthparts to the distal end of the abdomen, excluding any protruding appendages such as antennae or ovipositors. The width was measured as a straight line across the middle of the thorax, excluding wings or elytra. The lengths and widths of insects were measured based on stereomicroscopic analysis. Only fully articulated fossil insects were included in this calculation, if the specimen lacked a head, thorax or abdomen, it was not used in body-area analyses. Here, laterally preserved insects could not be accurately measured for perpendicular width. Thus, only fossil insects preserved in the dorsoventral position had their dimensions measured in order to keep the variable width consistent. The body-area measurements of individual insects were log transformed for greater normalcy of distribution. The distribution

normalcy was checked with Shapiro-Wilk test.

3.5 Statistical analyses

A chi-square contingency test was used to determine whether there were differences in the orientation patterns of specimens between the two macrofacies from Crato Formation limestones. To determine whether disarticulated specimens were more likely to occur on one of the two macrofacies from Crato limestones, a chi-square contingency analysis was conducted. The chi-square contingency test was also used to determine whether there were differences in the number of specimens within the same insect order between the two macrofacies from Crato limestones.

The principal component analysis (PCA) uses orthogonal transformation to convert multiple variables into a set of uncorrelated axes, principal components (PCs), which account for the variance in multivariate data sets, reducing it to a few variables (Marramà and Kriwet, 2017; Legendre and Legendre, 1998). This approach was employed using a variance-covariance matrix in order to determine the fossil insect assemblage similarities, based on a level-family dataset of Crato Formation. Here, we also use PCA to conduct a descritive analysis between Crato and other insect assemblages across Early Cretaceous with respect to their common relationship (in this case which insect orders), including habitat and feeding habits of insects, based on published literature.

4. Results

A total of 1135 fossil specimens were counted. The insects could be identified in the orders Blattodea, Coleoptera, Dermaptera, Ephemeroptera, Hemiptera, Hymenoptera, Neuroptera, Odonata, Orthoptera and Raphidioptera (Fig. 3)(Suppl. mat. 1). Of the 1135 insects analyzed, 386 insects were described from the dark gray limestones and 749 were described from pale yellow limestones (Fig. 4).

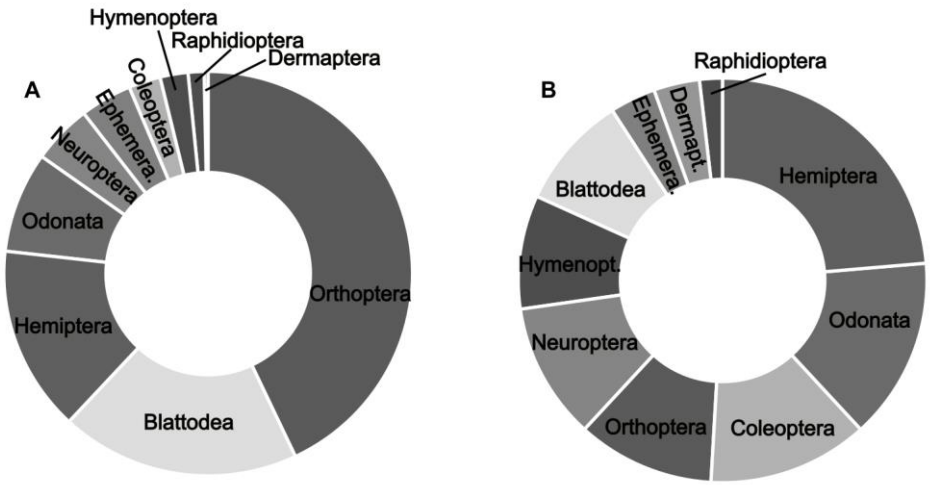

Fig. 3 – Taxonomic composition of the sample studied here (n=). A. proportion of identifiable individuals at family level within each order. B. proportion of families identified within each order.

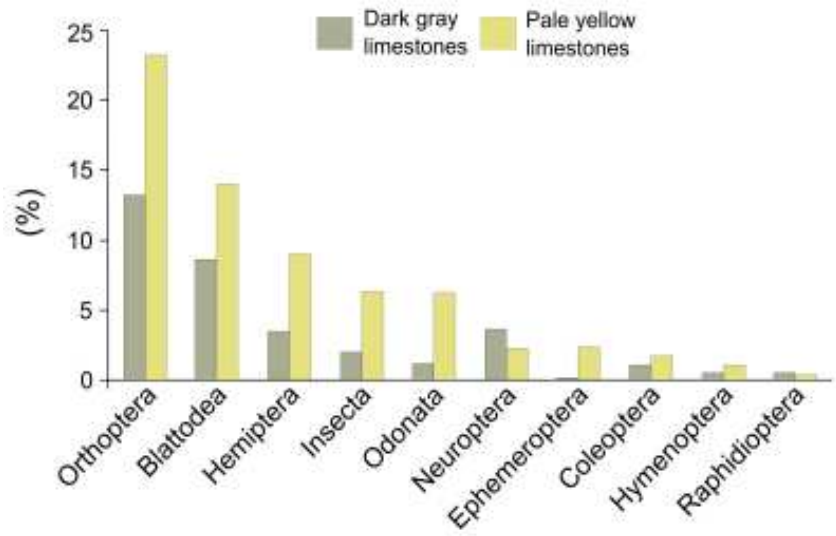

Fig. 4 – The proportional distribution of insects identified to order from the Crato Formation.

In both macrofacies, Orthoptera dominate the sample (36.3%), of which Ensifera contributes with 85%. Blattodea corresponds to 22.5% of all insects analyzed, while Hemiptera accounts for 12.4%. Insects that could not be placed in an Order within Insecta were just named “Insecta”, these make up 8% of the sample. The relative abundance of individuals is only significantly different in the orders Ephemeroptera, Neuroptera and Odonata (Table 1).

Taxon	Number of specimens		chi-squared test	
	Dark Gray limestones	Pale yellow limestones	X^2	*P*-values
Blattodea	97	158	1,8456	0,1742
Coleoptera	11	19	0,0944	0,7586
Dermaptera	2	1	1,4256	0,2324
Ephemeroptera	1	26	**11,048**	**0,0008**
Hemiptera	39	102	2,5327	0,1115
Hymenoptera	5	11	0,0542	0,8158
Insecta	22	71	**4,4414**	**0,0350**
Neuroptera	41	25	**23,241**	**$<10^{-4}$**
Odonata	13	70	**12,447**	**0,0004**
Orthoptera	150	263	0,9826	0,3215
Raphidioptera	5	3	2,8935	0,0889
Total	386	749		

Table 1 – Taxonomic tallies of insects from the Crato Formation. Statistically significant values are given in bold.

4.1 Taxonomic sampling composition

In this study, identifiable insects from the Crato Formation were included in 55 families. Of this total, four families belong to Blattodea and members of the *Meiatermes*-Grade. Ephemeroptera and Dermaptera appear with two families each. Seven families can be assigned to Coleoptera. Neuroptera and Orthoptera contribute six families each. Thirteen families can be included within Hemiptera, while eight belong to Odonata. Hymenoptera is represented by five families, while Raphidioptera appears with only one.

The first and second principal components given for the identifiable insects indicated the relative position of the identified families within the sample. The first and second principal components correspond to 40.3% of the variance, which are also the only factors with variances greater than one. The first principal component accounts for 25%, while the second component accounts for 16% variance. The loadings for the first factor generated by principal component analysis indicate that the relative abundance of Hemiptera families makes the most significant contribution to the first principal component. In comparison, the relative abundance of Odonata families is the most important contribution to the second principal component (Table 2). For this analysis, the loadings generated for each insect family can be seen in Suppl. mat. 2.

Taxa	Factor loadings	
	First princ. comp.	**Second princ. comp.**
Blattodea	-0.028504	-0.033179
Coleoptera	-0.039392	-0.12515
Dermaptera	-0.02015	-0.015782
Ephemeroptera	-0.02015	-0.015782
Hemiptera	0.26989	0.017107
Hymenoptera	-0.028504	-0.033179
Neuroptera	-0.033075	-0.052452
Odonata	-0.048691	0.3243
Orthoptera	-0.033075	-0.052452
Raphidioptera	-0.018356	-0.013434

Table 2 – The factor loadings for the first and second prinicipal component analysis obtained from principal component analysis of identifiable insects from the Crato Formation. Complete dataset given in Supp. mat. 2.

4.2 Taphonomic data

In our sample, fully articulated specimens were the most common, then partially articulated specimens, while there were relatively few disarticulated insects (Table 3). The specific disarticulation state of partially articulated specimens varied widely, being particularly notable the absence of head and abdomen (Suppl. mat. 1). When statistically comparing all insects preserved in pale yellow limestones to all insects preserved in dark gray limestones, the distribution of articulation states was significantly different (χ^2= 19.126; p< 10^{-4}; df= 2). Proportionally, there were greater degrees of disarticulation among insects preserved in dark gray limestones.

Carbonate matrix	disarticuled	Fully articulation	Partially articulation	Total
Dark gray	79	202	105	386
Pale yellow	110	492	147	749
Total	189	694	252	1135

Table 3 – Distribution of articulation state differences between insects preserved in pale yellow limestones and insects preserved in dark gray limestones from the Crato Formation.

Insect orientation also showed a significant difference when comparing all insects preserved in pale yellow limestones to all insects preserved in dark gray limestones (χ^2= 12,398; p=0.002; df=2). The number of specimens preserved in dorsal and ventral views is highest among insects preserved in pale yellow limestones. Interestingly, when we consider

dorsal and ventral position separately, the number of specimens preserved in lateral view is higher among insects preserved in dark gray limestones (Table 4).

Carbonate matrix	Dorsal	Lateral	Ventral	Total
Dark gray	108	112	91	311
Pale yellow	302	191	153	646
Total	410	303	244	957

Table 4 – Distribution of orientation states between insects preserved in pale yellow limestones and insects preserved in dark gray limestones from the Crato Formation.

4.3 Measured body area of Insects

The analyses comparing the body sizes of the fossil insects from Nova Olinda Member show no significant differences between insects preserved in the pale yellow limestones and those preserved in the dark gray limestones. Considering all insects, the mean body area is 83.4 mm^2. The mean of the log-transformed body areas for insects preserved in dark gray limestones is only slightly larger than that of insects in pale yellow limestones (Fig. 5). The raw distributions of areas of each insect group can be seen in suppl. mat. 3.

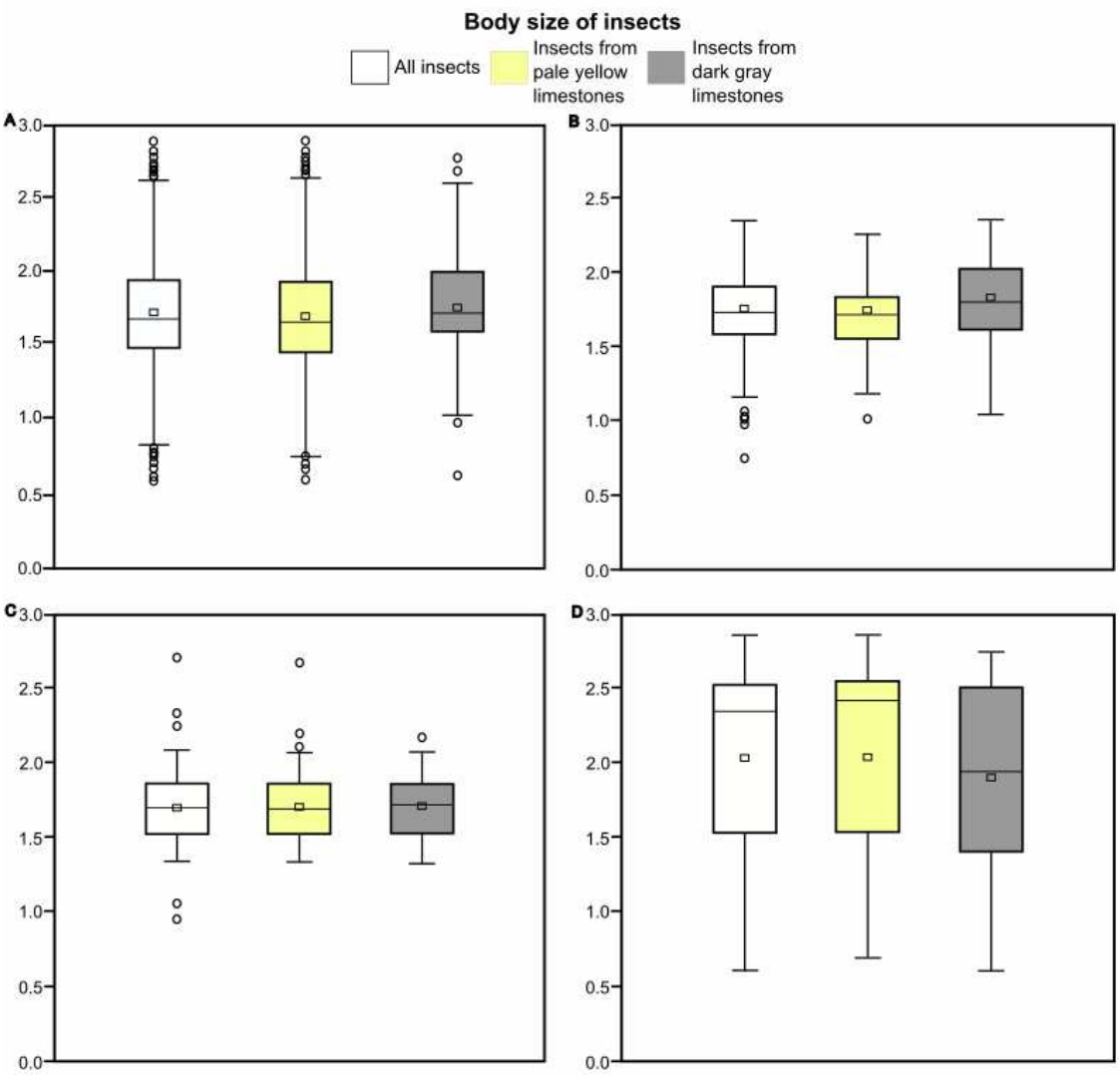

Fig. 5 – The distribution of log-transformed measurements of areas from the fully articulated insects preserved in dorsoventral position. A. Areas of all insects from both macrofacies of the Crato Formation. B. Areas of all Blattodea. C. Areas of all Orthoptera. D. Areas of all Hemiptera.

5. Discussion

5.1 The stratigraphic position of the Crato insects and depositional history of the Nova Olinda Member

The Crato Formation represents transgressive–regressive cycles, where the Nova Olinda Member is interpreted as a period of intense retraction of the lacustrine system. The Nova Olinda succession corresponds to inner lacustrine-laminated limestone facies made up

by finely micritic limestones forming centimeter-to-meter-thick beds (Neumann et al., 2003). The main sources of carbonates in lacustrine environments are clastic input derived from allochthonous carbonates, calcareous skeletons and biogenic hardparts, and biologically mediated precipitation of autochthonous carbonate minerals (Gierlowski-Kordesch, 2010). The carbonate record of the Nova Olinda Member provides little or no evidence of carbonate debris accumulation. An exception is documented by Heimhofer and Martill (2007), who identified a single debris flow layer in the vicinity of Tatajuba. However, in general terms, the absence of detrital dolomite particles, mass-wasting deposits and the well-preserved angular shape of the calcite crystals contradict substantial erosion, rework, transport or re-deposition. According to Heimhofer et al. (2010), the thin-section analyses of the Nova Olinda limestones do not show any small-scale grading or erosive contacts supporting an autochthonous origin. Furthermore, the input of bioclastic carbonate particles and calcareous carapaces are virtually absent. Sedimentary features like conspicuous lamination, regular rhythmical bedding, and vertical stacking pattern have been interpreted to reflect *in situ* precipitation of carbonate particles. Crystal homogeneity, euhedral crystal shape and grain-size distribution of individual calcite crystals rather supports biologically induced precipitation of $CaCO_3$ from the water column (Finkelstein et al., 1999; Folk and Chafetz, 2000; Heimhofer and Martill, 2007). The micro-and ultrastructural analysis of the laminites yielded structures such as coccoid, filamentous cells and extracellular polymeric substances suggest a deposition, at some levels, strongly influenced by microbial activity (Catto et al., 2016). Warren et al. (2017) recorded various examples of stromatolite domes and mounds at distinct stratigraphic levels in the middle part of the Crato Formation, representing relatively deeper water facies.

Overall, petrographic observations point to the absence of substantial cementation of fractures and recrystallization of calcite, which excludes deep burial diagenetic features of these deposits (Heimhofer et al., 2010). Furthermore, the record of intact angiosperm pollen provides additional evidence for thermally immature conditions of the Crato Formation (Baudin and Berthou, 1996). Therefore, the crystal framework of the Nova Olinda laminites suggests preservation of the original texture and mineralogy in a closed diagenetic system. Arribas et al. (2004) interpreted that the retention of primary depositional texture in lacustrine systems is controlled mainly by reduced compaction, stable mineralogy of the original carbonate mud and detention of Mg-enriched fluids in the pore system. According to Heimhofer et al. (2010), the overlying (Caldas Member) and underlying (Barbalha Formation) fine-grained siliciclastics may have reduced fluid flows in the Nova Olinda carbonates, preventing recrystallization and extensive cementation.

Another outstanding feature of Nova Olinda's laminated limestones is their different colors. These laminites can be found with colors ranging from light yellow (with reddish tones) to gray (with dark tones). Martill et al. (2007) attributed such variations to intense weathering. However, the Nova Olinda limestones also show chemical and structural differences. A thorough inspection promoted by Heimhofer et al. (2010) observed that the dark gray limestones are composed almost exclusively of well-developed calcite rhombohedra, where the individual crystals are loosely packed with high interparticle porosity. In contrast, the pale yellow limestones exhibit a higher degree of cementation, hence, reduced interparticle porosity between individual calcite crystals. The contrast mainly involving the interparticle porosity between pale yellow and dark gray carbonates may represent the preservation of their primary texture. A high-resolution μ-XRF analysis also demonstrated geochemical variations on the sub-millimeter scale for the Nova Olinda laminites (Heimhofer et al., 2010). The intensity of certain elements displays a clear correlation with observed color changes. Ca content shows a decreasing trend associated with dark gray laminites. In contrast, the intensity of S is well expressed in the dark gray laminae, whereas Fe fluctuations are most pronounced in the pale yellow limestones (Heimhofer et al., 2010). Thus, color changes in Nova Olinda limestones are unlikely to result from weathering alone.

The stratigraphic position of the different taxa found in Crato *Lagerstätte* has been a challenge for many researchers. The first reason for this is that the overwhelming majority of researchers focus on taxonomic or sedimentological studies apart from one another. The second reason is probably associated with the fact that paleontologists mostly study Crato specimens stored in museums without witnessing their recovery *in situ*. However, few authors have made efforts to precisely constrain the Crato *Lagerstätte* (see Martill and Heimhofer, 2007, Varejão et al., 2019, Ribeiro et al., 2021a, Corecco et al., 2022). The report by Neumann and Cabrera (1999) suggested vertical and lateral variations in the fossiliferous occurrences in Crato limestones. Martill and Heimhofer (2007) assigned the Crato *Lagerstätte* in the Nova Olinda Member. Varejão et al. (2019) showed that Nova Olinda region is more fossiliferous than other regions of the unit. Ribeiro et al. (2021a) provided a detailed framework of the fossil-rich intervals inserted in the columnar section of the Nova Olinda Member. Specifically, fossil insects are constrained at the top of interval II and at the middle part of interval III according to the scheme designed by Varejão et al. (2019) and Ribeiro et al. (2021a)(Fig. 6 a). More recently, Corecco et al., (2022) applied ethnographic surveys with quarry workers from the Nova Olinda quarries in order to understand the stratigraphic position of each taxon.

Based on traditional knowledge, the authors created ethnographic terms compared to the formal succession of Nova Olinda Member. According to these authors, fossil insects can be recovered in the uppermost laminated limestone facies, called the Besouro ethnostratum (Fig. 6 b).

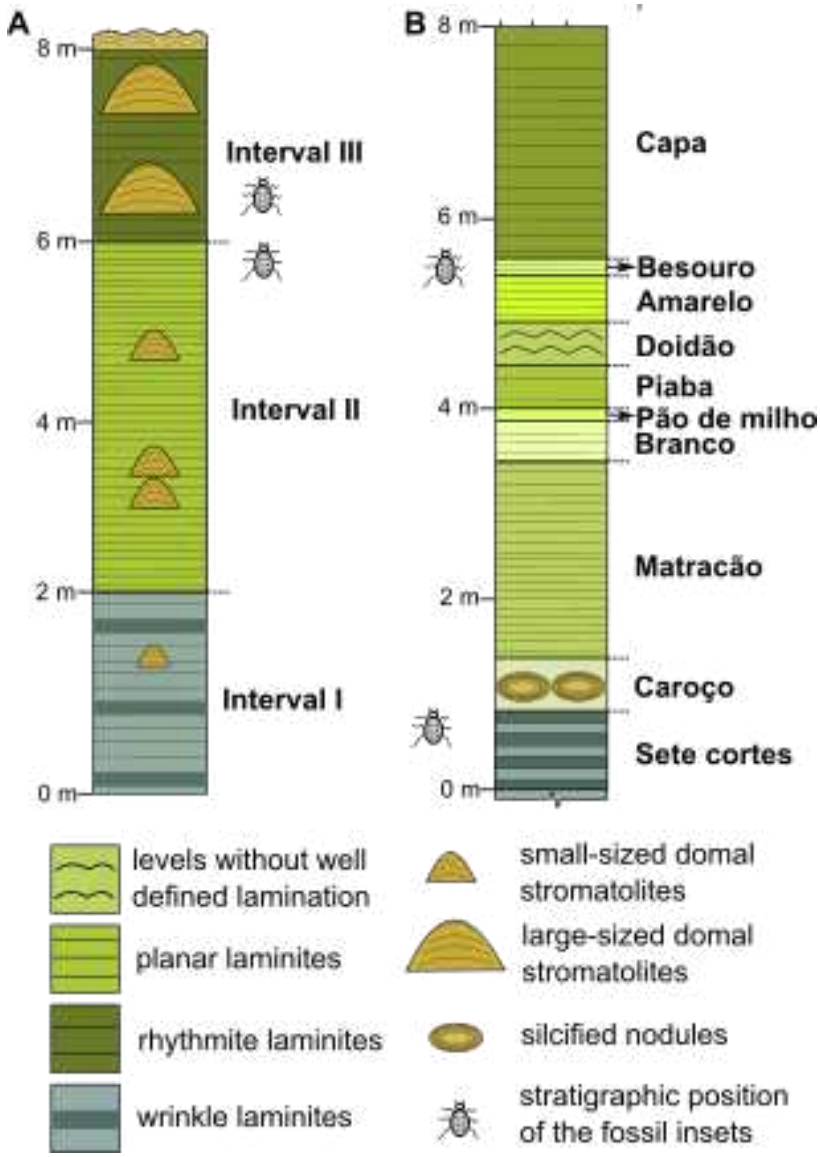

Fig. 6 – The stratigraphic position of the paleoentomofauna Crato in Três Irmãos quarry, Nova Olinda Member, State of Ceará, northeastern Brazil. (A) Simplified columnar section of the Crato *Konservat-Lagerstätte* showing the positions of the fossil insects, modified from Ribeiro *et al.* (2021) and Varejão *et al.* (2019). (B) Detailed ethnostratigraphic succession of Nova Olinda Member, indicating the stratigraphic position of the Crato insects, modified from Corecco *et al.* (2022).

The interval I delimited by Varejão et al. (2019) and Ribeiro et al. (2021a) corresponds to GL facies of Osés et al. (2017) and the Sete cortes ethnostratum by Corecco et

al. (2022). On the other hand, the interval II proposed by Varejão et al. (2019) and Ribeiro et al. (2021a) is highly associated with BL facies by Osés et al. (2017), where specimens appear mineralized via pyritization, also named pyritization zone by Bezerra et al. (2021a). Mineralized insects are the majority among those recovered from the Nova Olinda Member (Bezerra et al., 2021a; Corecco et al., 2022). According to Corecco et al. (2022), the main source of insects from the Crato Formation is the Besouro ethnostratum located in the uppermost interval II. Our data show that most insect families found in dark gray limestones (interval I) are also recorded in pale yellow lamestones (interval II). This indicates that the faunal composition of the Crato paleoentomofauna was similar throughout the entire deposition period of the Nova Olinda Member. The homogeneity of the faunal structure differentiates the Crato entomofauna from other Mesozoic entomofauna assemblages, such as the changes in diversity recorded in the paleoentomofauna of the Yixian Formation, where the number of families greatly declines in the transition from the lower-middle to the upper part of this unit (Zhang et al., 2010). Crato insects are collected from limestone quarries where the dark gray limestones are secondary due to their hardness, consequently, exploitation is more difficult. Thus, quarry workers focus on extracting the overlying pale yellow limestones which are easily mined. This bias probably explains the fact that mineralized insects are more frequent than non-mineralized ones.

5.2 Taphonomic and paleoenvironmental implications

The entire Araripe Basin is part of the South Atlantic rift system, which comprises many basins in the interior of Northeast Brazil. The widespread occurrence of evaporites, absence of coal deposits and dominance of drought-resistant, xerophytic plants are characteristics used to place this region within the Tropical Equatorial Hot arid belt (Scotese, 2014). Heimhofer and Hochuli (2010) placed palynoflora of the Araripe Basin within the Northern Gondwana Province of Brenner (1976) due to predominance of drought-adapted vegetation and/or mangrove communities of Cheirolepidaceae, perhaps with shrub-type plant associations. The authors identified dominance of *Classopollis* and *Ephedripites* pollen produced by drought-resistant plants such as Cheirolepidiaceae in concert with low numbers of fern spores, which are typical features of late Early Cretaceous low-latitude assemblages (Brenner, 1976). In addition to this general framework, a large number of hypotheses have been proposed regarding the specific paleonvironment of the Crato laminated limestones: Martill and Wilby (1993) attested to a lagoon with anoxic bottom waters with episodic

development of hypersaline conditions; Neumann et al. (2003) idealized a stratified anoxic and hypersaline lake affected by alternating humid-arid cycles resulting in significant lake-level fluctuations; Heimhofer et al. (2010) proposed that the Nova Olinda limestones took place under very quiet and protected conditions in a closed to semi-closed lake with hypersaline bottom waters; Warren et al. (2017) and Varejão et al. (2019; 2021) suggested a shallow hypersaline coastal lacustrine system with microbial-dominated bottoms. Regardless, the different hypotheses cited here have converged to catch a glimpse of a hypersaline lake system, indicating semi-arid to arid climatic conditions.

According to Heimhofer et al. (2010), the high-resolution micro-XRF analysis Nova Olinda laminated limestones indicated a low contribution of catchment-derived siliciclastic material. However, significant fluctuations in the Ca/Fe ratio were identified suggesting possible oscillations in the input of allochthonous and autochthonous materials. The high S content within dark laminae is accompanied by increased organic matter (Neumann et al., 2003; Heimhofer et al., 2010), while Fe correlates well with pale yellow laminae deficient in organic matter (Heimhofer et al., 2010). This marked contrast implies seasonality-driven deposition. The implications of seasonality also appear in wood growth rings found in the carbonate facies of the Crato Formation. According to wood ring data, the deposition of fine laminites occurred under a tropical environment with irregular humid periods (Guerra-Sommer et al., 2021). Furthermore, investigations of plant-fungus interactions in wood samples collected in the Nova Olinda Member imply that plant growth was controlled by cyclic alternations in water availability, probably related to variable precipitation (Scaramuzza dos Santos et al., 2020). In addition, despite the distribution of palynomorphs being dominated by drought-adapted forms, this dominance is interrupted, in at least two moments, by fern spores that require moist conditions to reproduce (Heimhofer and Hochuli, 2010). The neighboring units correlated with the Crato Formation in the Parnaíba (northwest) and Tucano (east) basins are also associated with the prevalence of arid climate with humid intervals (Souza-Lima and Silva, 2018; Salgado-Campos et al., 2022).

Neumann et al. (2003) reported two types of organic matter associated with dark gray limestones: (i) structureless planktonic material; and (ii) hand-sample plant remains. The authors attributed the latter to disarticulated branchlets of conifers (tentatively assigned to Cheirolepidiaceae), which would be responsible for the accumulation of type III kerogen documented in the darker laminae. Following the interpretation of Neumann et al. (2003), the deposition of laminated carbonate facies took place during episodes of lake-level highstand. In the episodes, dark gray limestones correspond to the early and late phase of lake-level

highstand, and pale yellow limestones represent deposition during maximum highstand weakly influenced by marginal faces. Ribeiro et al. (2021a) suggested that the Crato Formation depositional system was analogous to the present-day wetland ecosystem observed in alkaline lake Chad in sub-Saharan Africa.

The idea of cyclicity can also be drawn from our data by treating insects as sedimentary grains. Considering all Crato insects, the proportion of disarticulated insects is considerably higher among those preserved in dark gray limestones. While the proportion of fully articulated insects is higher among individuals preserved in pale yellow limestones (Fig. 7). The minimal damage of pale yellow limestone specimens indicates that they did not experience extensive flotation times at the water-air interface, shortening the opportunity for decomposition under aerobic conditions. Overall, disarticulated insects or body parts suggest a longer flotation time and/or an increase in distance from the catchment area (Smith, 2000; Bezerra et al., 2021b). Insects preserved in dark gray limestones also exhibit a higher proportion of partially disarticulated individuals. Common injuries among the partially disarticulated insects are absence or breakages in the abdomen and/or head. The abdomen begins to deteriorate immediately after the insect's death, causing disarticulation (Martínez-Delclòs et al., 2004; Ilger, 2011). After reaching the water surface, the insects lose their head after approximately two weeks (Peñalver, 2002; Wang et al., 2013). Here, it is worth noting that breakages can also be caused by post diagenetic processes, for example, overgrowth of authigenic crystals (Bezerra et al. 2023). However, the taphonomic bias toward lower overall preservation quality of insect bodies reflects a greater duration of time or exposure to higher levels of energy earlier in their biostratinomic history, before burial in the final deposition site.

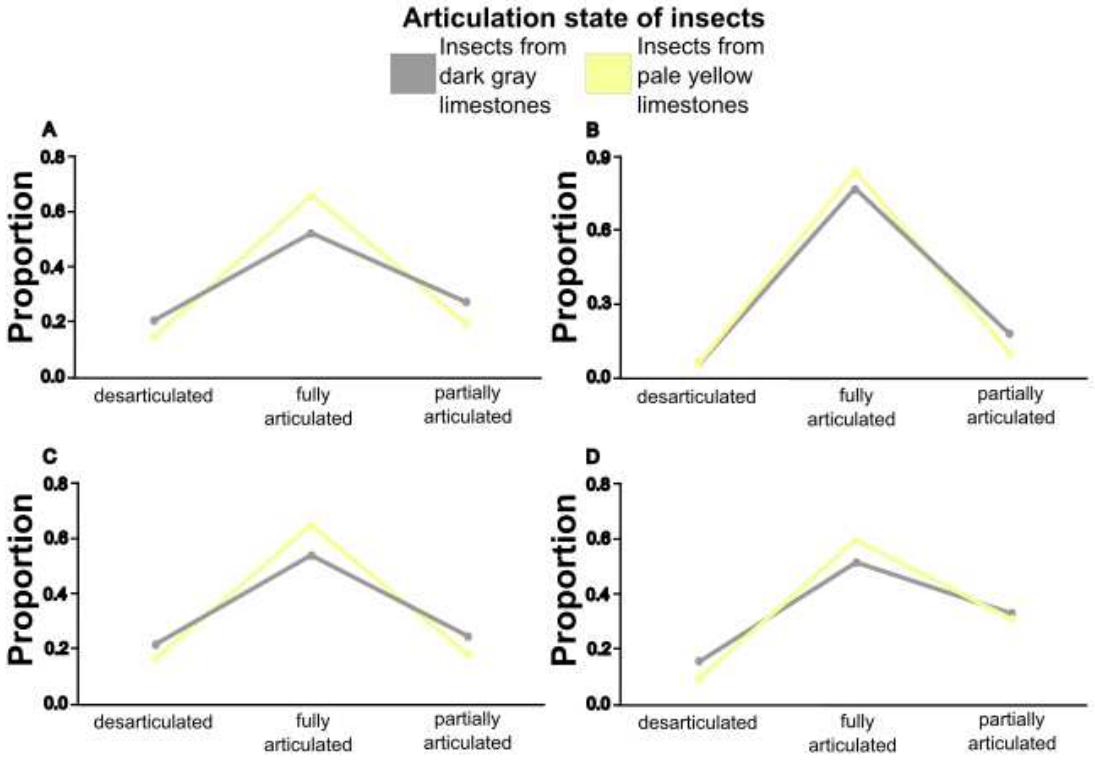

Fig. 7 – Distribution of articulation states for insects from the Crato Formation. A. Distribution of articulation states assessing the completeness of all insects from both macrofacies. B. Distribution of articulation states of all Hemiptera. C. Distribution of articulation states of all Orthoptera. D. Distribution of articulation states of all Blattodea.

Most of the fully articulated and partially articulated insects studied here lie with their largest surface area parallel to the bedding planes, suggesting that they settled vertically through the water column and came to rest on the sediment-water interface under low-energy conditions (Smith, 2000; Wang et al., 2013; Bezerra et al. 2021b). Overall, this pattern indicates that these insects likely dropped into the body of water or were immersed by rising water levels or were even washed into the lake shortly after death on land, except for those who live an aquatic lifestyle. Crato insects from the pale yellow limestones are preferentially preserved in the dorsoventral position, while the proportion of insects preserved in the lateral view is higher in the dark gray limestones (Fig. 8). These observations strongly support an expansion of the margins of the lake system into the hinterlands. For many insect groups, such as Blattodea and some Auchenorrhyncha, the lateral position is not the most stable to settle down in the sediment. Thus, the high number of large insects in lateral view observed in grey limestones is probably due to higher levels of traction during the biostratinomic phase. Together, the higher disarticulation and the individuals preserved in lateral view implies that

land insects recovered from the dark gray limestones experienced higher-energy conditions during transport, before final burial.

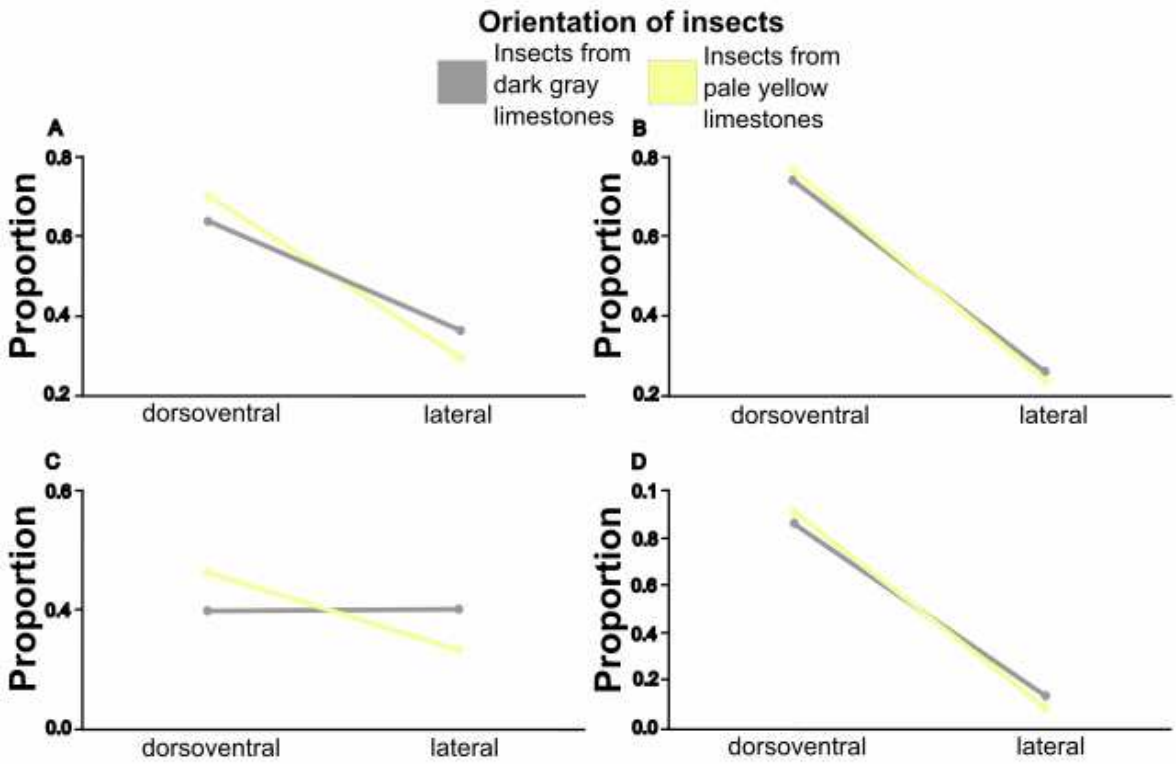

Fig. 8 - Orientation state of insects from the Crato Formation. A. Orientation state considering all Crato insects from both macrofacies. B. Orientation state of all Neuroptera. C. Orientation status of all Orthoptera. D. Orientation state of all Blattodea.

Here, we also identified that the mean body size of insects preserved in dark gray limestones is slightly higher than the insects from the pale yellow limestones (Fig. 5). Many authors have noted that the environment can have a profound effect on body size. For example, adult insects are generally smaller when larvae are reared at higher temperatures, or on lower quality diets (Atkinson, 1994; Azevedo et al., 2002; Nijhout, 2003; Klok and Harrison, 2013). Body size variation in insects could be attributed to environmental stress. However, we were unable to correlate paleoenvironmental changes with our body size measurements. Our dataset identified no significant difference between the insects preserved in the different macrofacies of the Nova Olinda Member.

Although the sedimentological, petrographic, geochemical and palynological data discussed above attest changes in environmental conditions during the deposition of the Crato *Lagerstätte*, these fluctuations did not result in significant changes in the faunal composition.

However, these climatic oscillations were able to produce ephemeral environmental conditions that resulted in the taphonomic differences observed here, e.g. the higher state of articulation exhibited by insects preserved in yellow limestones.

5.3 Paleoecological structure of the Crato paleoentomofauna

Overall, the macrofossil record from Crato *Lagerstätte* shows a highly heterogeneous fossil assemblage, a suitable site for putting together a diverse array of organisms. The Crato paleoentomofauna displays this feature, it accumulates different sorts of terrestrial, aquatic, and semiaquatic insects which highly suggests an active zone represented by the taphonomic assemblage. Ribeiro et al. (2021a) attested that the Crato paleoentomofauna is constituted mainly of generalist herbivore species distributed in different habitats. Our dataset consists of 85.3% of specimens recognized as terrestrial, 9% are fully aquatics, and 5.7% are attributed to semiaquatic habit (Suppl. mat. 4).

A large proportion of the Crato insects are typical representatives of forested habitats (Ribeiro et al., 2021a; Mendes et al., 2020), indicating the existence of this type of habitat providing food resources and shelter from predators. The presence of large logs of wood and charcoal in dark gray limestones is evidence of well-dreined soils supporting arboreal vegetation. The association between large plants and dark gray limestones is probably due to the higher drainage capacity of carrying heavy wood from the hinterlands to the lake. Several insect families recorded here are representatives of such paleoenvironment: Achilidae; Baissopteridae; Cercopidae; Cicadellidae; Palaeontinidae; Sepulcidae; Tettigarctidae; and termites from the *Meiatermes*-grade (Fig. 9). As prominent inhabitants of the hinterlands, our PCA analysis identified the Hemiptera as the most diverse representatives. Considering only the insects preserved in the dark gray limestones, their proportion is higher among individuals that inhabited the hinterlands (Fig. 10 a).

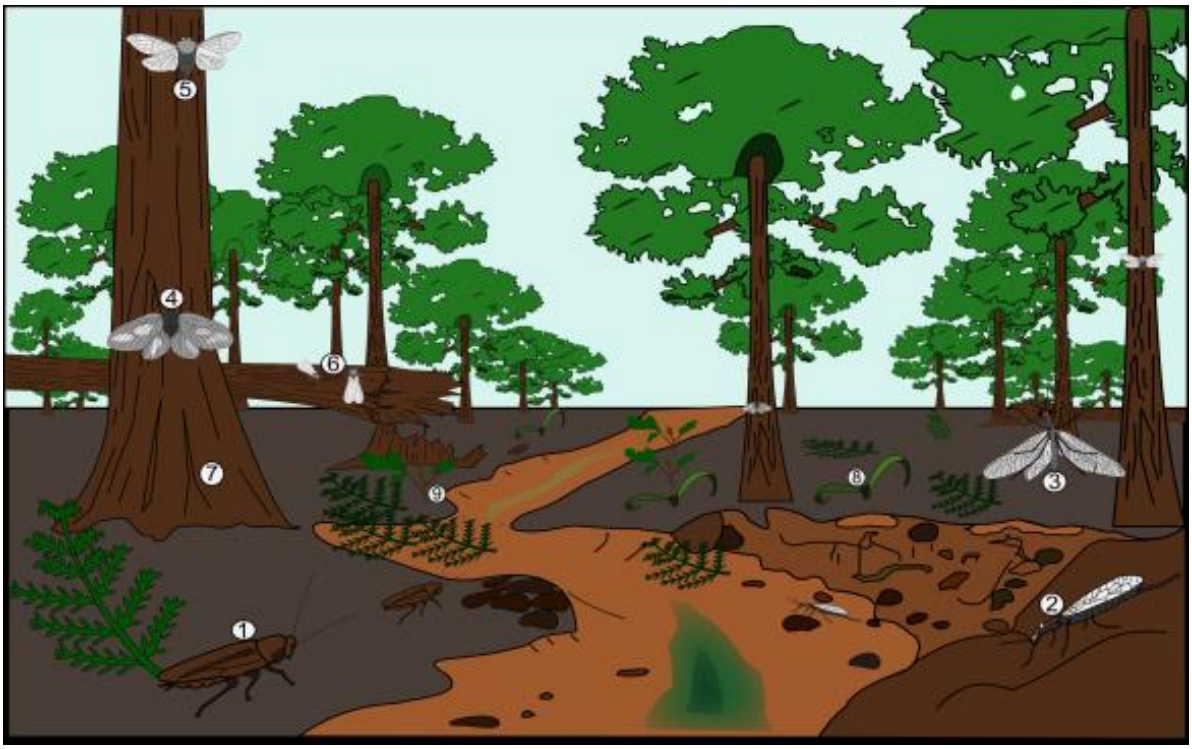

Fig. 9 – Illustration of the paleoenvironmental scenario of the hinterland habitat, Crato Formation: 1 - Umenocoleidae; 2 - Baissopteridae; 3 - Mesochrysopidae; 4 – Palaeontinidae; 5 – Tettigarctidae; 6 – Meiatermes-grade; 7 – Cheirolepidiaceae; 8 – Welwitschiaceae; 9 – Magnoliophyta.

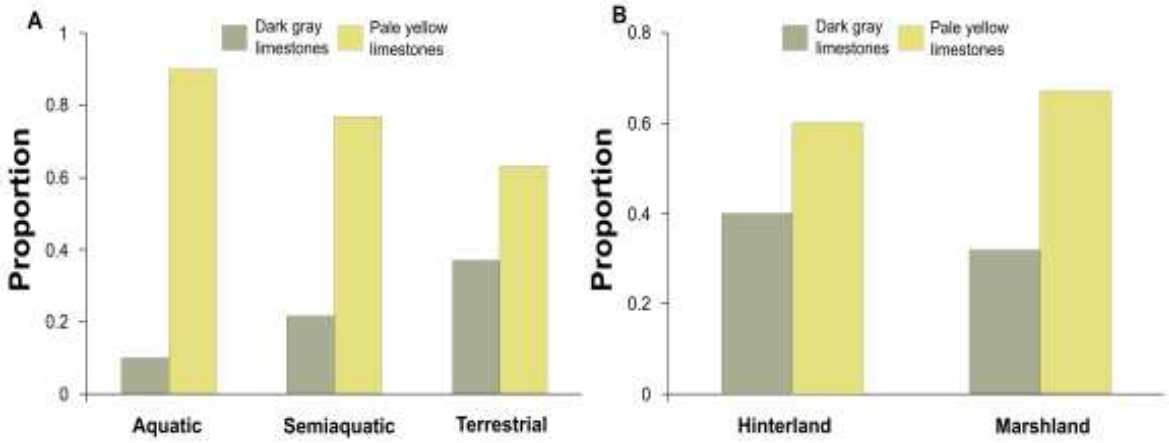

Fig. 10 – Structure of the Crato paleoentomofauna inferred from our database. (A) Different insect habitats identified. (B) Distribution of insects in different environments of the Crato ecosystem.

Our sample supports the Ensifera as the most abundant component of our sample. Overall cricket abundance can indicate both forested and shrubby habitats (McCluney and Sabo, 2014; Anso et al., 2022). Here, all crickets basically belong to the small-medium-sized

families Gryllidae and Baisogryllidae, suggesting that they could inhabit both pre-forested patches and shrublands. Shrub and herbaceous plants are important components of the Nova Olinda Member. Commonly, these plants occur in association with riparian vegetation adapted to wetland conditions (Mohr et al., 2007). This whole scenario indicates the existence of marshes and ponds surrounded by vegetation patches tolerant to climatic seasonality. This marshland would have occurred as a transitional zone between the hinterlands and the lake itself, where the presence of arboreal vegetation was rare. Marshlands also played an important role for terrestrial specimens that spend part of their lives on dry land and part in shallower freshwater such as hemimetabolous insects. Opportunistic insects such as cockroaches certainly visited this zone. Water bugs (e.g. Belostomatidae, Naucoridae) were certainly typical inhabitants of this area along with adult Odonata such as Araripegomphidae, Cretapetaluridae, Gomphaeschnidae, Hemiphlebiidae and Proterogomphidae that took advantage of hydrophilic vegetation to lay eggs near the water surface.

Considering our sample, the proportion of insects recognized as fully aquatic and semiaquatic is extremely higher among insects preserved in pale yellow limestones (Fig. 10 a). Similarly, the proportion of insects assumed to have lived in the marshlands is highest in the pale yellow limestones (Fig. 10 b). Certainly, this proportion was pushed up due to the presence of fully aquatic forms such as immature stages of mayflies and dragonflies, typically documented in pale yellow limestones. Hexagenitidae, Nothomacromiidae, Oligoneuriidae, and Gomphidae-like nymphs are often found on yellowish limestones. Recently, Storari et al. (2021) recovered an autochthonous assemblage with at least 40 Hexagenitidae larvae in the upper part of the Nova Olinda Member, probably corresponding to Besouro ethnostratum of Corecco et al. (2022). The authors classified their finding as a mortality event caused by increased salinity due to the presence of halite pseudomorphs in the overlying and underlying layers. The abundance of aquatic, semiaquatic and terrestrial forms documented in the pale yellow laminites represents a lake filling and expansion of the carbonate facies, expanding the swampy zones and pushing away the well-drained areas (Varejão et al., 2019) (Fig. 11). In this scenario, all sorts of organisms have a higher potential to be washed into the lake. Even terrestrial insects could fall into the water while flying over the lake. The occurrence of freshwater flooded areas likely explains the diversity and better preservation of insects (Bezerra et al. 2021a) found in the yellow slabs. On the other hand, dark gray limestones with insects showing a slightly lower degree of preservation (Bezerra et al. 2021a) and the predominance of landforms suggest a low base-level lake surrounded by dry lands.

Fig. 11 – Illustration of the paleoenvironmental scenario of the marshland habitat, Crato Formation: 1 – Elcanidae; 2 – Baissogryllidae; 3 – Belostomatidae; 4 – Araripegomphidae; 5 – Hexagenitidae adult; 6 – Gryllidae; 7 – Hexagenitidae nymph; 8 – Nothomacromiidae; 9 – *Itajuba sp* (Gnetales); 10 – *Ruffordia goeppertii* Seward (1961); 11 - *Iara iguassu* Fanton *et al.* (2006).

5.4 Trophic diversity of Crato paleoentomofauna

The trophic structure of the Crato biota has been tentatively elucidated by a few studies (Martill et al., 2007; Mendes et al., 2020; Ribeiro et al., 2021a; Kunzmann et al., 2022). Specifically dealing with the Crato paleoentomofauna, Ephemeroptera nymphs are essentially linked to freshwater settings, Hexagenitidae larvae were collectors-gatherers feeding on small particles in the bottom of water bodies. These larvae presumably were an important food source for small aquatic or semiaquatic predators in lentic environments. Notably, Ephemeroptera nymphs are usually associated with Odonata nymphs in Crato *Lagerstätte*. On the other hand, the nymphs of Odonata are voracious predators. The nymphs of the family Nothomacromiidae have powerful fangs and claws used to capture their prey in ambushes in flooded regions. Other notable predators that inhabited the vicinity of the water bodies were the water bugs. In general, water bugs found in the Crato biota were robust with

raptorial forelegs that capture prey among submerged plants. Belostomatidae representatives are the most common water bug, they are large with flat bodies and appendages adapted for grasping a variety of aquatic animals, including other insects.

Many Crato *Lagerstätte* plants have ecological adaptations to wetland conditions. As an example, fossil plants belonging to the genus *Isoetes* (Lycophyta) exhibit a series of modifications that allow them to thrive in periodically submerged, oligotrophic, and stressed environments (Greb et al., 2006). Other specimens with wetland adaptations found in the Crato paleoflora are the herbaceous *Cratolirion bognerianum* (Coiffard et al., 2019), *Cearania heterophylla* Kunzmann et al. (2009) and *Jaguariba wiersemana* (Coiffard et al., 2013). *Klitzschophyllites flabellatus* Mohr et al. (2006) and *Itajuba yansanae* Ricardi-Branco et al. (2013) also showed adaptations to high salinity conditions. All this vegetation must have attracted generalist herbivorous insects such as crickets, grasshoppers, true bugs and beetles to feed on during periods of low water levels in the dry season. Crato paleoentomofauna is characterized by the high number of predatory forms associated with this transitional environment. In these marshy areas, adult Odonata certainly played a significant role in the trophic network. Overall, adult Odonata from the Crato Formation had robust legs capable of grabbing prey in flight.

The diversity of conifer cones suggests the existence of large trees and most conifer fossils are relatively fragmented, indicating that they were transported to the deposition site from a far away area. Most of this vegetation cover provided food, shelter, resting and nesting for many land organisms. Crato paleoentomofauna contains various types of insects adapted to thrive in such vegetation types. Our sample records a series of generalist herbivore specimens such as Cicadellidae, Elcanidae, Gryllidae, Locustopseidae and Lymexylidae. Phytophage insects are represented by hemipterans, including particularly abundant Auchenorrhyncha and probably some hymenopterans. Specialist herbivores feeding on wood logs are represented by termites belonging to the *Meiatermes*-grade. The sawflies Sepulcidae were probably specialized consumers of standing timber. Flower visitors and/or pollen-eating insects were mainly represented by adult wasps such as Sapygidae and Scoliidae, and many Neuroptera such as Osmilidae and Berothidae. Various terrestrial predators are represented by staphylinid beetles, snakeflies, earwigs, and cockroach wasps (Ampulicidae). The raphidiopterans Baissopteridae are certainly key indicators of woodland habitats (Ribeiro et al. 2021a). The neuropterans Chrysopidae and Myrmeleontidae were probably efficient predators in the hinterlands. Parasitoid insects are represented by Hymenoptera, mainly Scoliidae.

5.5 Evidence of plant-insect interaction in the Crato Formation

The plants transformed the terrestrial environment into a highly valuable resource for the herbivore community. In modern ecosystems, plants and insects are continuously interacting in a complex way. These two groups of organisms are intimately associated since insects have several beneficial activities, including defense and pollination while plants provide shelter, oviposition sites and food. There is little differentiation between the insect faunas of the present-day and the Cretaceous. For this reason, insects of the Crato Formation are essential for our understanding of insect evolution. In particular, the age of Crato insects (Late Aptian) coincides with a time at which angiosperms were diversifying and developing complex relationships with insects (Labandeira et al., 1994; Hu et al., 2008).

Crato flora is mainly composed by conifers, genetales, and early angiosperms. Crato plants rarely occur completely articulated and the majority of angiosperms are encountered as isolated leaves or seeds from magnoliids. The evidence of plant–insect interaction in the Crato Formation can be summarized in oviposition, galls, foliar herbivory, leaf mines and skeletonization in leaves. Leaf consumption (herbivory) is the most frequent form of damage recorded in the Crato limestones. This type of interaction was observed in angiosperms and gymnosperms specimens (Braz et al., 2011; Xavier et al., 2014; Santos Filho et al., 2017). These damage types can be associated with the presence of insects belonging to the order Orthoptera. Oviposition observed in Crato plants range from circular to elongate formats and occur preferentially in angiosperms (Xavier et al., 2014; Santos Filho et al., 2017). The oviposition marks can be related to insects belonging to the orders Neuroptera, Diptera, Hymenoptera and mainly Hemiptera. The presence of insect galls is frequently reported in ferns and angiosperm leaves. The occurrence of galls in extant leaves is generally attributed to Cecidomyiidae (Diptera) and Pteromalidae (Hymenoptera) (Banerji, 2004). The skeletonization and leaf mines are recorded in angiosperms leaves in the Crato Formation (Braz et al 2011; Santos Filho et al., 2017). Leaf mines occur with rectilinear, serpentine and occasionally curve formats. Overall, leaf-mining insects belong to Diptera, Lepidoptera, Coleoptera and Hymenoptera.

The interaction between insects and plants is still poorly understood in the Crato Formation. Although under documented so far, it is possible to illustrate that ferns are the most attacked by insects, mainly *Ruffordia goeppertii* (Santos Filho et al., 2017). However, the diversity of damage types in this group of plants is low, generally related to herbivory

margin feeding. The gymnosperms also show a low diversity of damage types. Angiosperms are the group of plants that bear the widest variety of damage morphotypes from different functional feeding groups. This strongly suggests a higher vulnerability of the emerging angiosperms that may have influenced their subsequent evolution and biology.

Overall, the majority damage morphotypes documented in the Crato Formation correspond to herbivory caused by insects with chewing mouthparts. Thus, all marks of insect feeding on plants were probably related to Orthoptera, Coleoptera and Blattodea. The presence of leaf mines can be associated with Diptera and Hymenoptera; oviposition and galling occurrences were probably produced by insect clades belonging to the Diptera, Hemiptera, Hymenoptera, and Neuroptera.

5.6 Comparing Crato paleoentomofauna with other entomofauna from the Early Cretaceous

Considering only the taxonomic literature, insects are the most diverse and abundant group of organisms recorded in the Crato paleoecosystem, with more than 400 species described so far. Crato insects are recognized as terrestrial herbivorous, aquatic herbivores, winged predators, terrestrial omnivores, swimming predators, aquatic detritivorous, pollen and wood eaters, indicating a complex and dynamic environment capable of hosting this fauna. Crato *Lagerstätte* contains a rich neuropteran fauna: about 21% of the insect species described in this unit belong to Neuroptera families. The second most diverse order is the Orthoptera (about 17%) corresponding to crickets and grasshoppers, which would have played a significant role in the local food web. In third place, the Hemiptera make up about 13% of the species, this highly diverse order includes specialist herbivores and aquatic Heteroptera predators. Our PCA analysis shows the Crato paleoentomofauna is strongly influenced by the predatory insects, aquatic and semiaquatic forms (Fig. 12). Therefore, both Odonata and Heteroptera predators represent semiaquatic and aquatic hunters that are a distinctive fraction of this paleoenthomofauna compared to other paleoentomofauna preserved as fossil compressions.

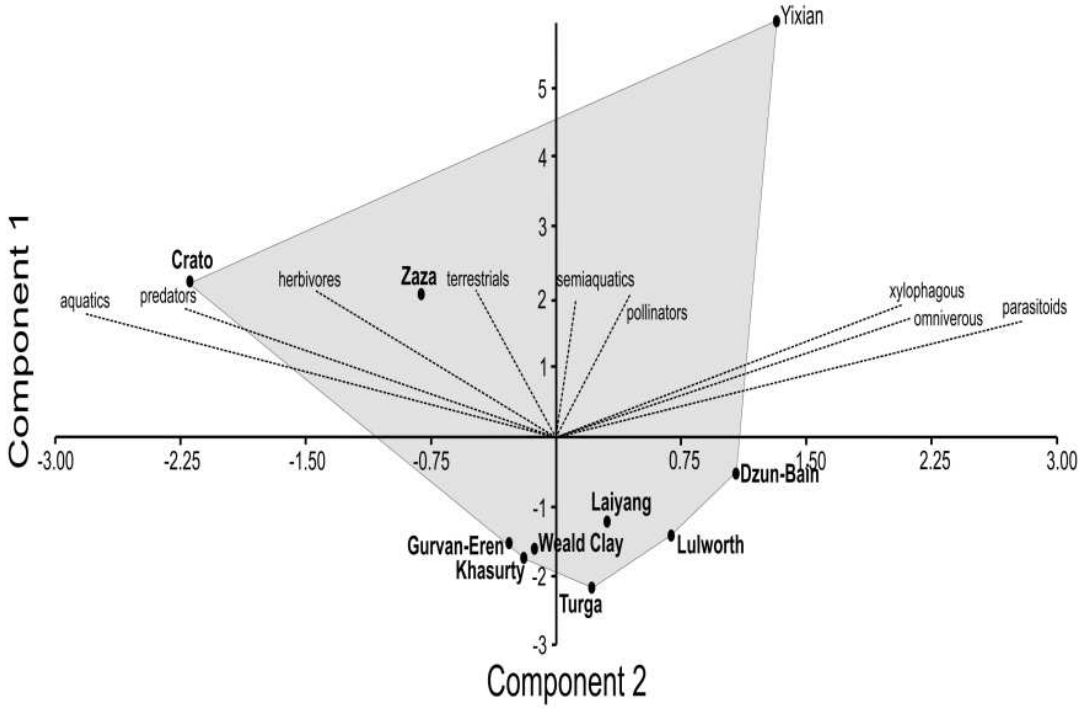

Fig. 12 – Principal component analysis (PCA) for the main Paleoentomofauna of the Early Cretaceous preserved in non-amber assemblages. Principal component 1 (PC1) explains 74.7% of the variance in the data, while PC2 explains 11.3% of the variance.

The Yixian Formation stands out for the diversity, richness, and beauty of fossil insects. This formation is distributed in the northeastern provinces of China and Inner Mongolia, but the majority of fossils come from Liaoning (Zhang et al., 2010). Fossils of this unit belongs to the famous Jehol biota and about 31% of the insects described in Yixian Fm. are placed within Coleoptera. Hymenoptera is also very diverse making up 22% of insect species. Neuroptera and Orthoptera correspond to only 7% and 3% of the Yixian Fm. paleoentomofauna, respectively (Suppl. mat. 5). The Lower Cretaceous deposits of the Siberian Transbaikalia are also rich in fossil assemblages. The Baissa locality of western Transbaikalia belonging to the Zaza Formation stands out for the number of insect species (Makarkin et al., 2012). Coleoptera (22%) and Hymenoptera (19%) are also the dominant insect fossils in the Zaza Formation. Other rich paleoentomofauna preserved as fossil compressions are dominated by terrestrial forms such as those documented in the Gurvan-Eren and Dzun-Bain formations, both from the Aptian of Mongolia; Laiyang Fm. from the Aptian of China; Khasurty locality of the Aptian of Russia; and Lulworth Fm. belonging to the Purbeck succession of southern England, Berriasian in age (Suppl. mat. 5). Distinctly, the

diversity of Coleoptera and Hymenoptera is greatly diminished in Crato paleoentomofauna. As expected, the entomofauna preserved in Early Cretaceous amber also tend to be unbalanced in favor of terrestrial forms (Suppl. mat. 6). However, Diptera appear as the most diverse insects, as observed in the faunas of Jordanian (Albian), Charentese (Late Albian of France) and Lebanese (Barremian) ambers. In contrast, the record of Diptera in the Crato paleoentomofauna is not expressive. Compared to other Early Cretaceous assemblages, the paleoptera richness in the Crato fauna is highly significant, about 18% of the recovered species belong to this Infraclass, which is higher than any other paleoentomofauna of this time interval (Fig. 13).

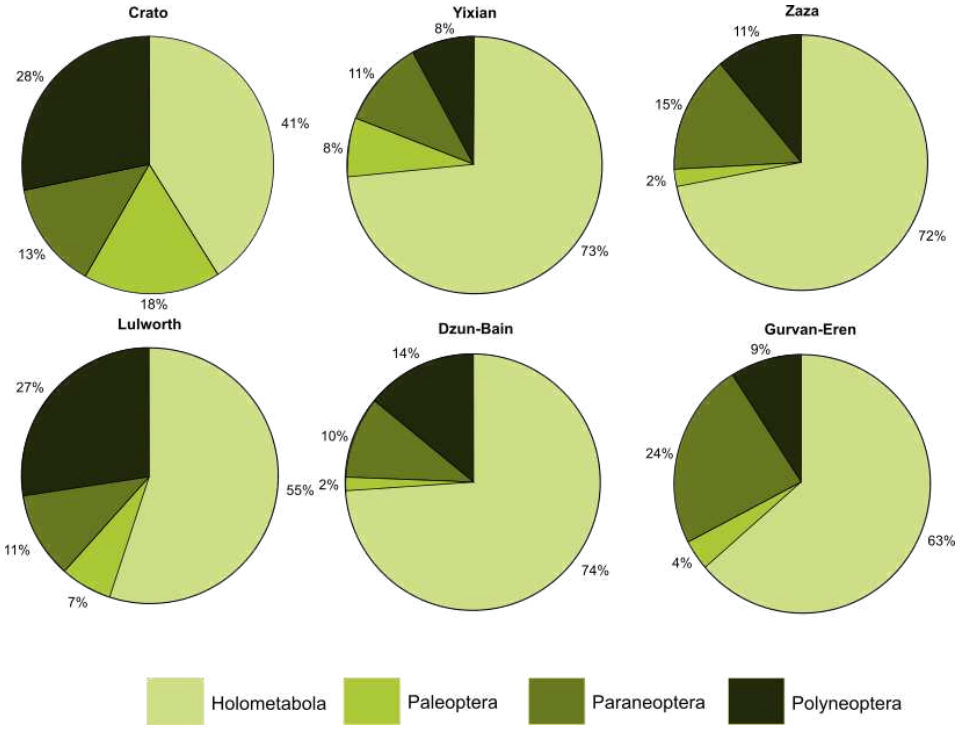

Fig. 13 – Infraclass composition of the Crato paleoentomofauna compared to the main bearing insects deposits of the Early Cretaceous, based on taxonomic literature.

Certainly, there are many beetles, wasps, and flies from the Crato Formation awaiting a formal description. Thus the number of their species is expected to increase in the coming years. An example of this are the recent discoveries of a team of Brazilian researchers that has significantly increased the documentation of dipterans in the Crato Formation (Lamas et al., 2021; Ribeiro et al., 2021b; Carmo et al., 2022; Santos et al., 2023). Even so, it is unlikely to reach the same level as other paleoentomofauna from the Early Cretaceous such as the Yixian and Zaza formations. We assume that the different faunal compositions reflect their ecosystems. Although other Early Cretaceous paleoenthomofauna are also preserved in

lacustrine deposits, the combination of a wetland environment and semi-arid climate that yielded extensive and long-lasting marshes facilitated the accumulation of insects from different niches. Therefore, environmental transformations shaped the uniqueness of the Crato paleoentomofauna. Nevertheless, the explanation for the low number of species within the Coleoptera and Hymenoptera orders in the Crato paleoentomofauna still needs improvement.

6. Conclusion

The paleoentomofauna of the Crato *Lagerstätte* consists of insects from different types of habitats. Terrestrial specimens are the most abundant, while the fully aquatic and semiaquatic ones are less numerous. The paleoentomofauna is preserved in two main macrofacies, a basal dark gray limestone, rich in organic matter, and an upper the Ca-rich pale yellow limestone. Although, taxonomic literature of Crato paleoentomofauna to date shows an entomofauna that was dominated by terrestrial forms, this study describes a high diversity of aquatic and semiaquatic insects, (more so than entomofauna from other Early Cretaceous assemblages). Within the two microfacies, the pale-yellow limestones show a greater quantity of aquatic and semiaquatic forms than the dark gray limestones from the same area, suggesting deposition at different stages and under different conditions. It is thought that the pale-yellow limestones may represent an expansion of water bodies during wetter periods that caused flooding and the formation of extensive wetland and marshes. Examples of insects from the dark gray limestones were found to show a proportionately higher degree of disarticulation together with a higher incidence of examples found in lateral positions rather than dorsoventral positions. It is proposed that this demonstrates a higher degree of reworking before their final deposition and burial. It also strongly suggests a more allochthonous origin of the samples. Evidence presented here also suggests the existence of an ecosystem that can be described as a shallow lacustrine wetland that underwent periodic fluctuations associated within a semi-arid climate subjected to periodic episodes of higher rainfall. From the specimens described, there does not appear to be any significant differences in the composition of the Crato paleoentomofauna during the deposition of the entire unit. The taphonomic differences between the composition of the two distinct macrofacies of limestones described, however, can be explained by climatic oscillations and cycles.

Acknowledgments

We would like to thank Dr. Charlotte R. Williams for her revision of the manuscript, whose comments and insightful suggestions improved our original manuscript. We are also grateful to Dr. Mónica M. Solórzano Kraemer for her detailed comments and constructive suggestions which have greatly helped us to improve our presentation and discussion. This study was financed in part by the Coordenação de Aperfeiçoamento de Pessoal de Nível Superior - Brasil (CAPES). FIB is grateful for his doctorate scholarship (Coordenação de Aperfeiçoamento de Pessoal de Nível Superior, Brasil - CAPES, process 88882. 454892/2019-01).

References

Andersen, S., 2001. Silky lacewings (Neuroptera: Psychopsidae) from the Eocene–Palaeocene transition of Denmark with a review of the fossil record and comments on phylogeny and zoogeography. Insect Syst. Evol. 32, 419–438. https://doi.org/10.1163/187631201X00290

Anderson, E.P., Smith, D.M., 2017. The same picture through different lenses: quantifying the effects of two preservation pathways on Green River Formation insects. Paleobiology 43, 224–247. https://doi.org/10.1017/pab.2016.2

Anso, J., Gasc, A., Bourguet, E., Desutter-Grandcolas, L., Jourdan, H., 2022. Crickets as indicators of ecological succession in tropical systems, New Caledonia. Biotropica 54, 1270–1284. https://doi.org/10.1111/btp.13151

Arai, M., Assine, M.L., 2020. Chronostratigraphic constraints and paleoenvironmental interpretation of the Romualdo Formation (Santana Group, Araripe Basin, Northeastern Brazil) based on palynology. Cretac. Res. 116, 104610. https://doi.org/10.1016/j.cretres.2020.104610

Arai, M., 2014. Aptian/Albian (Early Cretaceous) paleogeography of the South Atlantic: a paleontological perspective. Braz. J. Geol. 44, 339–350. https://doi.org/10.5327/Z2317-4889201400020012

Arribas, M.E., Bustillo, A., Tsige, M., 2004. Lacustrine chalky carbonates: origin, physical properties and diagenesis (Palaeogene of the Madrid Basin, Spain). Sed. Geol. 166, 335–351. https://doi.org/10.1016/j.sedgeo.2004.01.012

Assine, M.L., 2007. Bacia do Araripe. Bol. Geociênc. Petrobras 15, 371–389.

Assine, M.L., Perinotto, J.A., Neumann, V.H., Custódio, M.A., Varejão, F.G., Mescolotti, P.C.,

2014. Sequências deposicionais do Andar Alagoas (Aptiano superior) da Bacia do Araripe, Nordeste do Brasil. Bol. Geociênc. Petrobras 22, 3–28.

Atkinson, D., 1994. Temperature and organism size: a biological law for ectotherms? Adv. Ecol. Res 25, 1–58. https://doi.org/10.1016/S0065-2504(08)60212-3

Azevedo, R.B.R., French, V., Partridge, l., 2002. Temperature modulates epidermal cell size in *Drosophila melanogaster*. J. Insect Physiol. 48, 231–237. https://doi.org/10.1016/s0022-1910(01)00168-8

Banerji, J., 2004. Evidence of insect-plant interactions from the Upper Gondwana Sequence (Lower Cretaceous) in the Rajmahal Basin, India. Gondwana Res. 7, 205–210. https://doi.org/10.1016/S1342-937X(05)70320-8

Barling, N., Martill, D.M., Heads, S.W., Gallien, F., 2015. High fidelity preservation of fossil insects from the Crato Formation (Lower Cretaceous) of Brazil. Cretac. Res. 52, 605–622. https://doi.org/10.1016/j.cretres.2014.05.007

Barling, N., Martill, D.M., Heads, S.W., 2020. A geochemical model for the preservation of insects in the Crato Formation (Lower Cretaceous) of Brazil. Cretac. Res. 116, 104608. https://doi.org/10.1016/j.cretres.2020.104608

Baudin, F., Berthou, P.-Y., 1996. Depositional environments of the organic matter of Aptian-Albian sediments from the Araripe Basin (NE Brazil). Bull. Centres Rech. Explor.-Prod. Elf-Aquitaine 20, 213–227.

Bechly, G., 1997. Dragonflies from the Lower Cretaceous of Brazil. Meganeura 1, 27–28.

Behrensmeyer, A.K., Hill, A., 1980. Fossils in the making: Vertebrate Taphonomy and Paleoecology. Chicago University Press, Chicago, 338 pp.

Behrensmeyer, A.K., 2021. Taphonomy, in: Alderton, D., Elias, S.A. (Eds.), Encyclopedia of Geology Second Edition, Academic Press, 12–22. https://doi.org/10.1016/B978-0-08-102908-4.00120-X

Béthoux, O., Nel, A., 2002. Venation pattern and revision of Orthoptera sensu nov. and sister groups. Phylogeny of Palaeozoic and Mesozoic Orthoptera sensu nov. Zootaxa 96, 1–88. https://doi.org/10.11646/ZOOTAXA.96.1.1

Bezerra, F. I., Da Silva, J.H., Miguel, E.C., Paschoal, A.R., Nascimento Jr., D.R., Freire, P.T.C., Viana, B.C., Mendes, M., 2020. Chemical and mineral comparison of fossil insect

cuticles from Crato *Konservat Lagerstätte*, Lower Cretaceous of Brazil. J. Iber. Geol. 46, 61–76. https://doi.org/10.1007/s41513-020-00119-y

Bezerra, F.I., Solórzano-Kraemer, M.M., Mendes, M., 2021a. Distinct preservational pathways of insects from the Crato Formation, Lower Cretaceous of the Araripe Basin, Brazil. Cretac. Res. 118, 104631. https://doi.org/10.1016/j.cretres.2020.104631

Bezerra, F.I., Agressot, E.V.H., Solórzano-Kraemer, M.M., Freire, P.T.C., Paschoal, A.R., da Silva, J.H., Mendes, M., 2021b. Taphonomic analysis of the paleoentomofauna assemblage from the Cenozoic of the Fonseca Basin, southeastern Brazil. Palaios 36, 182–192. https://doi.org/10.2110/palo.2020.067

Bezerra, F., Da Silva, J., Agressot, E., Freire, P., Viana, B., Mendes, M., 2023. Effects of chemical weathering on the exceptional preservation of mineralized insects from the Crato Formation, Cretaceous of Brazil: Implications for late diagenesis of fine-grained Lagerstätten deposits. Geological Magazine 160, 911–926. https://doi.org/10.1017/S0016756823000043

Braz, F.F., Utida, G, Bernardes-de-Oliveira, M.E.C., Mohr, B.A.R., Wappler, T., 2011. Marcas de atividade de insetos em folhas ninfealeanas eocretáceas da Formação Crato, Bacia do Araripe, Brasil, in: Carvalho, I.S.C., (Ed.), Paleontologia: Cenários de vida. Editora Interciências, Rio de Janeiro, pp. 57–67.

Brenner, G., 1976. Middle Cretaceous floral provinces and early migrations of angiosperms, in: Beck, C.B. (Ed.), Origin and early evolution of angiosperms. Columbia University Press, New York, pp. 23–44.

Brito Neves, B.B., Santos, E.J., Van Schmus, W.R., 2000. Tectonic history of the Borborema Province, northeastern Brazil, in: Cordani, U.G., Milani, E.J., Thomaz Filho, A., Campos, D.A. (Eds.), Tectonic Evolution of South America. Petrobras S.A, Rio de Janeiro, pp. 151–182.

Cardoso, F.M.C., 2010. O grabén da Palestina: contribuição à estratigrafia e estrutura do estágio rifte na Bacia do Araripe, Nordeste do Brasil. Masters dissertation, Universidade Federal do Rio Grande do Norte.

Carmo, D.D.D., Sampronha, S., Santos, C.M.D., Ribeiro, G.C., 2022. Cretaceous Horse flies and their phylogenetic significance (Diptera: Tabanidae). Arthropod Syst. Phylogeny 80, 295–307. https://doi.org/10.3897/asp.80.e86673

Catto, B., Jahnert, R.J., Warren, L.V., Varejão, F.G., Assine, M.L., 2016. The microbial nature

of laminated limestones: lessons from the Upper Aptian, Araripe Basin, Brazil. Sediment. Geol. 341, 304–315. https://doi.org/10.1016/j.sedgeo.2016.05.007

Coiffard, C., Mohr, B.A.R., Bernardes-de-Oliveira, M.E.C., 2013. *Jaguariba wiersemana* gen. nov. et sp. nov., an Early Cretaceous member of crown group Nymphaeales (Nymphaeaceae) from northern Gondwana. Taxon 62, 141–151. https://doi.org/10.1002/tax.621012

Coiffard, C., Kardjilov, N., Manke, I., Bernardes-de-Oliveira, M.E.C., 2019. Fossil evidence of core monocots in the Early Cretaceous. Nat. Plants 5, 691–696. https://doi.org/10.1038/s41477-019-0468-y

Coimbra, J.C., Arai, M., Carreño, A.L., 2002. Biostratigraphy of Lower Cretaceous microfossils from the Araripe basin, Northeastern Brazil. Geobios 35, 687–698. https://doi.org/10.1016/S0016-6995(02)00082-7

Coimbra, J.C., Freire, T.M., 2021. Age of the Post-rift Sequence I from the Araripe Basin, Lower Cretaceous, NE Brazil: implications for spatio-temporal correlation. Rev. Bras. Paleontol. 24, 37–46. https://doi.org/10.4072/rbp.2021.1.03

Colgan, D. J., Cassis, G. Beacham, E. 2003. Setting the molecular phylogenetic framework for the Dermaptera. Insect Syst. Evol. 34, 60–80. https://doi.org/10.1163/187631203788964935

Corecco, L., Bezerra, F.I., Silva Filho, W.F.S., Nascimento Júnior, D.R., da Silva, J.H., Felix, J.L., 2022. Petrological meaning of ethnostratigraphic units: Laminated Limestone of the Crato Formation, Araripe Basin, NE Brazil. Pesqui. em Geocienc. 49, e121139. https://doi.org/10.22456/1807-9806.121139

Darling, D.C., Sharkey, M.J., 1990. Order Hymenoptera. In: Grimaldi, D.A. (ed.), Insects from the Santana Formation, Lower Cretaceous, of Brazil. Bulletin of the American Museum of Natural History, New York, 123–153 pp.

Dias, J.J., Carvalho, I.S., 2020. Remarkable fossil crickets preservation from Crato Formation (Aptian, Araripe Basin), a *Lagerstätten* from Brazil. J. South Am. Earth Sci. 98, 102443. https://doi.org/10.1016/j.jsames.2019.102443

Dias, J.J., Carvalho, I.S. 2022. The role of microbial mats in the exquisite preservation of Aptian insect fossils from the Crato *Lagerstätte*, Brazil. Cretac. Res. 130, 105068. https://doi.org/10.1016/j.cretres.2021.105068

Dodd, J.R., Stanton, R.J., 1990. Paleoecology: Concepts and Applications, second ed. John

Wiley and Sons, New York, 502 pp.

Evans, J.W. 1956. Palaeozoic and Mesozoic Hemiptera. Aust. J. Zool. 4, 165–258.

Finkelstein, D.B., Hay, R.L., Altaner, S.P., 1999. Origin and diagenesis of lacustrine sediments, upper Oligocene Creede Formation, southwestern Colorado. Geol. Soc. Am. Bull. 111, 1175–1191. https://doi.org/10.1130/0016-7606(1999)111<1175:OADOLS>2.3.CO;2

Folk, R.L., Chafetz, H.S., 2000. Bacterially induced microscale and nanoscale carbonate precipitates, in: Riding, R.B., Awramik, S.M. (Eds.), Microbial Sediments. Springer Verlag, Berlin, pp. 40–49.

Fossen, H., Harris, L.B., Cavalcante, C., Archanjo, C.J., Ávila, C.F., 2022. The Patos-Pernambuco shear system of NE Brazil: Partitioned intracontinental transcurrent deformation revealed by enhanced aeromagnetic data. J. Struct. Geol. 158, 104573. https://doi.org/10.1016/j.jsg.2022.104573

Gierlowski-Kordesch, E.H., 2010. Lacustrine carbonates, in: Alonso-Zarza, A.M., Tanner, L.H. (Eds.), Carbonates in Continental Settings: Facies, Environments, and Processes. Elsevier, Amsterdam, pp. 1–102. https://doi.org/10.1016/S0070-4571(09)06101-9

Greb, S.F., DiMichele, W.A., Gastaldo, R.A., 2006. Evolution and importance of wetlands in earth history, in: Greb, S.F., DiMichele, W.A. (Eds.), Wetlands through time. Geological Society of America Special Paper, 1–40. https://doi.org/10.1130/2006.2399(01)

Grimaldi, D.A., Engel, M.S., Krishna, K. 2008. The Species of Isoptera (Insecta) from the Early Cretaceous Crato Formation: A Revision. Am. Mus. Novit., 3626, 1–30.

Guerra-Sommer, M., Siegloch A.M., Degani-Schmidt, I., Scaramuzza dos Santos A.C., Carvalho, I.S., Andrade, J.A.F.G., Freitas, F.I., 2021. Climate change during the deposition of the Aptian Santana Formation (Araripe Basin, Brazil): Preliminary data based on wood signatures. J. South Am. Earth Sci. 111, 103462. https://doi.org/10.1016/j.jsames.2021.103462

Hamilton, K. G. 1990. Homoptera, in: Grimaldi, D. (Ed.), Insects from the Santana Formation, Lower Cretaceous, of Brazil. Bulletin of the American Museum of Natural History, New York, pp. 82–122.

Heimhofer, U., Martill, D.M., 2007. The sedimentology and depositional environment of the Crato Formation, in: Martill, D.M., Bechly, G., Loveridge, R.F. (Eds.), The Crato Fossil Beds of Brazil – Window into an Ancient World. Cambridge University Press, Cambridge, pp. 44–62.

Heimhofer, U., Ariztegui, D., Lenniger, M., Hesselbo, S.P., Martill, D.M., Rios-Netto, A.M., 2010. Deciphering the depositional environment of the laminated Crato fossil beds (Early Cretaceous, Araripe Basin, North-eastern Brazil). Sedimentology 57, 677–694. https://doi.org/10.1111/j.1365-3091.2009.01114.x

Heimhofer, U., Hochuli, P.A., 2010. Early Cretaceous angiosperm pollen from a low-latitude succession (Araripe Basin, NE Brazil). Rev. Palaeobot. Palynol. 161, 105–126 https://doi.org/10.1016/j.revpalbo.2010.03.010

Hu, A., Dilcher, D.L., Jarzen, D.M., Taylor, D.W., 2008. Early steps of angiosperme pollinator coevolution. Proc. Natl. Acad. Sci. U.S.A. 105, 240–245. https://doi.org/10.1073/pnas.0707989105

Ilger, J.M., 2011. Young bivalves on insect wings: a new taphonomic model of the *Konservat-Lagerstätte* Hagen-Vorhalle (early late Carboniferous; Germany). Palaeogeogr. Palaeoclimatol. Palaeoecol. 310, 315–323. https://doi.org/10.1016/j.palaeo.2011.07.023

Iniesto, M., Gutiérrez–Silva, P., Dias, J.J., Carvalho, I.S., Buscalioni, A.D., Lopez–Archilla, A.I., 2021. Soft tissue histology of insect larvae decayed in laboratory experiments using microbial mats: Taphonomic comparison with Cretaceous fossil insects from the exceptionally preserved biota of Araripe, Brazil. Palaeogeogr. Palaeoclimatol. Palaeoecol. 564, 110156. https://doi.org/10.1016/j.palaeo.2020.110156

Klok, C.J., Harrison, J.F., 2013. The temperature size rule in arthropods: Independent of macro-environmental variables but size dependent. Integr. Comp. Biol. 53, 557-570. https://doi.org/10.1093/icb/ict075

Kukalová-Peck, J., 1985. Ephemeroid wing venation based upon new gigantic Carboniferous mayflies and basic morphology, phylogeny, and metamorphosis of pterygote insects (Insecta, Ephemerida). Can. J. Zool. 63, 933–955.

Kunzmann, L., Mohr, B.A.R., Bernar des-de-Oliveira , M.E.C. 2009. *Cearania heterophylla* gen. nov. et sp. nov., a fossil gymnosperm with affinities to the Gnetales from the Early Cr etaceous of northern Gondwana. Rev. Palaeobot. Palynol. 158, 193–212. https://doi.org/10.1016/j.revpalbo.2009.09.001

Kunzmann, L., Coiffard, C., Westerkamp, A.P.A.O., Batista, M.E.P., Uhl, D., Solórzano-Kraemer, M.M., Mendes, M., Nascimento Jr., D.R., Iannuzzi, R., Silva Filho, W.F. 2022. Crato Flora: A 115-Million-Year-Old Window into the Cretaceous World of Brazil, in:

Iannuzzi, R., Rößler, R., Kunzmann, L. (Eds.), Brazilian Paleofloras. Springer, Cham. https://doi.org/10.1007/978-3-319-90913-4_27-1

Labandeira, C.C., Dilcher, D.L., Davis, D.R., Wagner, D.L., 1994. Ninety-seven million years of angiosperm-insect association: paleobiological insights into the meaning of coevolution. Proc. Natl. Acad. Sci. U.S.A. 91, 12278–12282. https://doi.org/10.1073/pnas.91.25.12278

Lamas, C.J.E., Sampronha, S., Ribeiro, G.C., 2021. A new robber fly from the Lower Cretaceous (Aptian) Crato Formation of NE Brazil (Insecta: Diptera: Asilidae). Cretac. Res. 131, 105114. https://doi.org/10.1016/j.cretres.2021.105114

Lee, S.W., 2016. Taxonomic diversity of cockroach assemblages (Blattaria, Insecta) of the Aptian Crato Formation (Cretaceous, NE Brazil). Geol. Carpathica 67, 433–450. https://doi.org/10.1515/geoca-2016-0027

Legendre, P., Legendre, L., 1998. Numerical Ecology Second Edition. Elsevier, Amsterdam, 853 pp.

Lúcio, T., Souza Neto, J.A., Selby, D., 2020. Late Barremian/Early Aptian Re-Os age of the Ipubi Formation black shales: stratigraphic and paleoenvironmental implications for Araripe Basin, northeastern Brazil. J. South Am. Earth Sci. 102:102699. doi:10.1016/j.jsames.2020.102699

Makarkin, V.N., Yang, Q., Peng, Y.Y., Ren, D., 2012. Comparative overview of the neuropteran assemblage of the Lower Cretaceous Yixian Formation (China), with description of a new genus of Psychopsidae (Insecta: Neuroptera). Cretac. Res. 35, 57–68. https://doi.org/10.1016/j.cretres.2011.11.013

Marques, F.O., Nogueira, F.C.C., Bezerra, F.H.R., De Castro, D.L., 2014. The Araripe Basin in NE Brazil: An intracontinental graben inverted to a high-standing horst. Tectonophysics 630, 251–264. https://doi.org/10.1016/j.tecto.2014.05.029

Marramà, G., Kriwet, J., 2017. Principal component and discriminant analyses as powerful tools to support taxonomic identification and their use for functional and phylogenetic signal detection of isolated fossil shark teeth. Plos One 12, e0188806. https://doi.org/doi: 10.1371/journal.pone.0188806

Martill, D.M., Wilby, P., 1993. Stratigraphy, in: Martill D.M. (Ed.), Fossils of the Santana and Crato formations, Brazil. Palaeontological Association, Dorchester, pp. 20–50.

Martill, D.M., Bechly, G., Loveridge, R.F., 2007. The Crato fossil beds of Brazil: window

into an ancient world. Cambridge University Press, Cambridge, 624 pp.

Martill, D.M., Heimhofer, U., 2007. Stratigraphy of the Crato Formation, in: Martill, D.M., Bechly, G., Loveridge, R.F. (Eds.), The Crato Fossil beds of Brazil: Window into an Ancient World. Cambridge University Press, Cambridge, 25–43.

Martínez-Delclòs, X., Briggs, D.E.G., Peñalver, E., 2004. Taphonomy of insects in carbonates and amber. Palaeogeogr. Palaeoclimatol. Palaeoecol. 203, 19–64. https://doi.org/10.1016/S0031-0182(03)00643-6

Martins-Neto, R.G., 2003. Systematics of the Caelifera (Insecta, Orthopteroidea) from the Santana Formation, Araripe Basin (Lower Cretaceous, northeast Brazil), with a description of new genera and species. Acta zool. cracov. 46 (suppl.), 205–228.

Matos, R.M.D., 1992. The Northeast Brazilian rift system. Tectonics 11, 766–791. https://doi.org/10.1029/91TC03092

Matos, R.M.D., 1999. History of the Northeast Brazilian rift system: kinematic implications for the break-up between Brazil and West Africa, in: Cameron, N.R., Bate, R.H., Clure, V.S. (Eds.), The Oil and Gas Habitats of the South Atlantic, Special Publications of the Geological Society of London, pp. 55–73. https://doi.org/10.1144/GSL.SP.1999.153.01.04

McCafferty, W.P., 1990. Ephemeroptera, in: Grimaldi, D.A. (Ed.), Insects from the Santana Formation, Lower Cretaceous, of Brazil. Bulletin of the American Museum of Natural History, New York, pp. 20–50.

McCluney, K.E., Sabo, J.L., 2014. Sensitivity and tolerance of riparian arthropod communities to altered water resources along a drying river. PLoS One, 9, e109276. https://doi.org/10.1371/journal.pone.0109276

Melo, R.M., Guzmán, J., Almeida-Lima, D., Piovesan, E.K., Neumann, V.H.M.L., Sousa, A.J., 2020. New marine data and age accuracy of the Romualdo Formation, Araripe Basin, Brazil. Sci. Rep. 10, 15779. https://doi.org/10.1038/s41598-020-72789-8

Mendes, M., Bezerra, F.I., Adami, K., 2020. Ecosystem structure and trophic network in the Late Early Cretaceous Crato Biome, in: Iannuzzi, R., Röbler, R., Kunzmann, L. (Eds.), Brazilian Paleofloras: From Paleozoic to Holocene. Springer, cham. https://doi.org/10.1007/978-3-319-90913-4_33-1

Menon, F., 2005. New record of Tettigarctidae (Insecta, Hemiptera, Cicadoidea) from the Lower Cretaceous of Brazil. Zootaxa 1087, 53–58.

https://doi.org/10.11646/ZOOTAXA.1087.1.5

Menon, F., Heads, S.W., Martill, D.M., 2005. New Palaeontinidae (Insecta: Cicadomorpha) from the Lower Cretaceous Crato Formation of Brazil. Cretac. Res. 26, 837–844. https://doi.org/10.1016/j.cretres.2005.05.005

Mohr, B.A.R., Kunzmann, L., Bernardes-de-Oliveira, M.E.C., 2006. Reconstruction of the Crato Flora (Northeastern Brazil), a Lower Cretaceous vegetation from Northtern Gondwana, in: Second Palaeontological Congress, Ancient Life and Modern Approaches, Beijing, pp. 13–18.

Mohr, B.A.R., Bernardes-de-Oliveira , M.E.C., Loveridge, R.F., 2007. The macrophyte flora of the Crato Formation, in: Martill, D.M., Bechly, G., Loveridge, R.F. (Eds.), The Crato Fossil Beds of Brazil: Window into an Ancient World. Cambridge University Press, Cambridge, pp. 537–565.

Nascimento Jr., D.R., Silva Filho, W.F., Freire, J.G., Santos, F.H., 2016. Syngenetic and

diagenetic features of evaporite-lutite successions of the Ipubi Formation, Araripe Basin,

Santana do Cariri, NE Brazil. J. South Am. Earth Sci. 72, 315–327.

https://doi.org/10.1016/j.jsames.2016.10.001

Nascimento Jr., D.R., Silva Filho, W.F., Erthal, F., 2023. Crato Lake Deposits. Rocks to Preserve an Extraordinary Fossil *Lagerstätte*, in: Iannuzzi, R., Röbler, R., Kunzmann, L. (Eds.), Brazilian Paleofloras: From Paleozoic to Holocene, Springer, cham. https://doi.org/10.1007/978-3-319-90913-4_28-2

Neumann, V.H.M.L. 1999. Estratigrafía, sedimentologia, geoquímica y diagénesis de los sistemas lacustres Aptienses Albienses de la Cuenca de Araripe (Noreste de Brasil). Ph.D. thesis, Universidad de Barcelona, p 244.

Neumann, V.H., Cabrera, L., 1999. Una nueva propuesta estratigráfica para la tectonosecuencia post-rifte de la Cuenca de Araripe, noreste de Brasil. In: Simpósio Cretáceo Brasileiro 5, Serra Negra, pp. 279–285.

Neumann, V.H., Borrego, A.G., Cabrera, L., Dinod, R., 2003. Organic matter composition and distribution through the Aptian–Albian lacustrine sequences of the Araripe Basin, northeastern Brazil. Int. J. Coal Geol. 54, 21–40. https://doi.org/10.1016/S0166-5162(03)00018-1

Nijhout, H.F. 2003. The control of body size in insects. Dev. Biol. 261, 1–9. https://doi.org/10.1016/S0012-1606(03)00276-8

Osés, G.L., Petri, S., Becker-Kerber, B., Romero, G.R., Rizzutto, M.A., Rodrigues, F., Galante, D., Silva, T.F., Curado, J.F., Rangel, E.C., Ribeiro, R.P., Pacheco, M.L., 2016. Deciphering the preservation of fossil insects: a case study from the Crato Member, Early Cretaceous of Brazil. PeerJ 4, e2756. https://doi.org/10.7717/peerj.2756

Osés, G.L., Petri, S., Voltani, C. G., Prado, G.M.E.M., Galante, D., Rizzutto, M.A., Rudnitzki, I.D., da Silva, E.P., Rodrigues, F., Rangel, E.C., Sucerquia, P.A., Pacheco, M.L.A.F., 2017. Deciphering pyritization-kerogenization gradient for fish soft-tissue preservation. Sci. Rep. 7, 1468. https://doi.org/10.1038/s41598-017-01563-0

Peñalver, E., 2002, Los insectos dípteros del Mioceno del Este de la Península Ibérica; Rubielos de Mora, Ribesalbes y Bicorp Tafonomía y sistemática: Ph.D. thesis, Universitat de València, p 550.

Ponte, F.C., Ponte Filho, F.C., 1996. Geological structure and tectonic evolution of the Araripe Basin. National Department of Mineral Production, Recife, p 68.

Ribeiro, A.C., Ribeiro, G.C., Varejão, F.G., Battirola, L.D., Pessoa, E.M., Simões, M.G., Warren, L.V., Riccomini, C., Poyato-Ariza, F.C. 2021a. Towards an actualistic view of the Crato *Konservat Lagerstätte* paleoenvironment: a new hypothesis as an Early Cretaceous (Aptian) equatorial and semi-arid wetland. Earth Sci. Rev. 216, 103573. https://doi.org/10.1016/j.earscirev.2021.103573

Ribeiro, G.C., Santos, R.R., Santos, D., 2021b. Four new species of the genus *Leptotarsus* Guérin-Méneville, 1831 (Insecta: Diptera: Tipulidae) from the Lower Cretaceous Crato Formation of Brazil. Cretac. Res. 123, 104776. https://doi.org/10.1016/j.cretres.2021.104776

Ricardi-Branco, F., Torres, M., Tavares, S.S., Carvalho, I.S., Tavares, P.G.E., Campos, A.C.A., 2013. *Itajuba yansanae* Gen and SP NOV of Gnetales, Araripe Basin (Albian-Aptian) in Northeast Brazil, in: Zhang, Y., Ray, P. (Eds.), Climate change and regional/local responses. InTech, Rijeka, pp. 187–205.

Salgado-Campos, V.M.J., Carvalho, I.S., Bertolino, L.C., Borghi, L., Rios-Netto, A.M., Araújo, B.C., Souza, D.C., Ferreira, L.O., Bobco, F.E.R., 2022. Unraveling an alkaline lake and a climate change in Northeastern Brazil during the Late Aptian. Sediment. Geol. 10, 106290. https://doi.org/10.1016/j.sedgeo.2022.106290

Santos, F.H., Azevedo, J.M., Nascimento Jr, D.R., Souza, A.C.B., Mendes, M., Bezerra, F.I., Limaverde, S.S., 2017. Análise de fácies e petrografia de uma seção do Membro Crato em Nova Olinda (CE): Contribuições à história deposicional e diagenética do neoaptiano na Bacia do Araripe. Geol. USP - Ser. Cient., 17, 3–18. https://doi.org/10.11606/issn.2316-9095.v17-319

Santos, D., Carvalho, I.S., Ribeiro, G.C., 2023. A cranefly rendezvous: The highest known Mesozoic diversity of Tipulidae (Insecta: Diptera) in the Lower Cretaceous Crato Formation of NE Brazil. Cretac. Res. 142, 105372. https://doi.org/10.1016/j.cretres.2022.105372

Santos, M.F.A., Mattos, I., Mermudes, J.R.M., Scheffler, S.M., Reyes-Castillo, P., 2021. A new passalid fossil (Insecta: Coleoptera) from the Santana Formation (Crato member, Lower Cretaceous), Araripe Basin, NE Brazil: Paleoecological and paleobiogeographic implications. Cretac. Res. 118, 104664. https://doi.org/10.1016/j.cretres.2020.104664

Santos Filho, E.B., Adami-Rodrigues, K., Lima, F.J., Batim, R.A.M., Wappler, T., Saraíva, A.A.F., 2017. Evidence of plant–insect interaction in the Early Cretaceous Flora from the Crato Formation, Araripe Basin, Northeast Brazil. Hist. Biol. 31, 926–937. https://doi.org/10.1080/08912963.2017.1408611

Scaramuzza dos Santos A.C., Guerra-Sommer, M., Degani-Schmidt, I., Siegloch A.M., Carvalho, I.S., Mendonça Filho, J.G., Mendonça, J.O., 2020. Fungus–plant interactions in Aptian Tropical Equatorial Hot arid belt: White rot in araucarian wood from the Crato fossil *Lagerstätte* (Araripe Basin, Brazil). Cretac. Res. 114, 104525. https://doi.org/10.1016/j.cretres.2020.104525

Schuh, R.T., Slater, J.A., 1995. True Bugs of the World (Hemiptera: Heteroptera) – Classification and Natural History. Ithaca, Cornell University Press, 800 pp.

Scotese, C.R., 2014. Atlas of Early Cretaceous Paleogeographic Maps, PALEOMAP Atlas for ArcGIS, Mollweide Projection. PALEOMAP Project, Evanston, IL.

Smith, D.M., 2000, Beetle taphonomy in a recent ephemeral lake in southeastern Arizona. Palaios 15, 152–160. https://doi.org/10.2307/3515501

Solórzano-Kraemer, M.M., Kraemer, A.S., Stebner, F., Bickel, D.J., Rust, J., 2015. Entrapment bias of arthropods in Miocene amber revealed by trapping experiments in a tropical forest in Chiapas, Mexico. PloS One 10, e0118820. https://doi.org/10.1371/journal.pone.0118820

Solórzano-Kraemer, M.M., Delclòs, X., Clapham, M.E., Arillo, A., Peris, D., Jäger, P., Stebner, F., Peñalver, E., 2018. Arthropods in modern resins reveal if amber accurately recorded forest arthropod communities. Proc. Natl. Acad. Sci. U.S.A. 115, 6739–6744. https://doi.org/10.1073/pnas.1802138115

Souza-Lima, W., Silva, R.O., 2018. Aptian–Albian Paleophytogeography and paleoclimatology from Northeastern Brazil sedimentary basins. Rev. Palaeobot. Palynol. 258, 163–189. https://doi.org/10.1016/j.revpalbo.2018.08.003

Storari, A.P., Rodrigues, T., Bantim, R.A.M., Lima, F.J., Saraiva, A.A.F., 2021. Mass mortality events of autochthonous faunas in a Lower Cretaceous Gondwanan *Lagerstätte*. Sci. Rep. 11, 6976. https://doi.org/10.1038/s41598-021-85953-5

Varejão, F.G., Warren, L.V., Simões, M.G., Buatois, L.A., Mángano, M.G., Bahniuk, A.M.R., Assine, M.L., 2021. Mixed siliciclastic-carbonatesedimentation in an evolving epicontinental sea: Aptian record of marginal marine settings in the interior basins of north-eastern Brazil. Sedimentology 68, 2125–2164. https://doi.org/10.1111/sed.12846

Varejão, F.G., Warren, L.V., Simões, M.G., Fürsich, F.T., Matos, S.A., Assine, M.L., 2019. Exceptional preservation of soft tissues by microbial entombment: insights into the taphonomy of the Crato *Konservat-Lagerstätte*. Palaios 34, 331–48. https://doi.org/10.2110/palo.2019.041

Wang, B., Zhang, H., Jarzembowski, E.A., Fang, Y., Zheng, D., 2013. Taphonomic variability of fossil insects: a biostratinomic study of Palaeontinidae and Tettigarctidae (Insecta: Hemiptera) from the Jurassic Daohugou *Lagerstätte*. Palaios 28, 233–242. https://doi.org/10.2110/palo.2012.p12-045r

Warren, L.V., Varejão, F.G., Quaglio, F., Simões, M.G., Fürsich, F.T., Poiré, D.G., Catto, B., Assine, M.L., 2017. Stromatolites from the Aptian Crato Formation, a hypersaline lake system in the Araripe Basin, northeastern Brazil. Fácies 63, 1–19. https://doi.org/10.1007/s10347-016-0484-6

Xavier, S.A.S., Viana, M.S.S., De Souza, E.B., Sousa, M.J.G., 2014. Register of oviposition in a inflorescence from Crato Formation (Aptian), Araripe Basin, Northwest of Brazil. Rev. Geol. 1:67–75.

Zhang, H., Wang, B., Fang, Y., 2010. Evolution of insect diversity in the Jehol Biota. Sci. China Earth Sci. 53, 1908–1917. https://doi.org/10.1007/s11430-010-4098-5

7 CONCLUSÕES E PERSPECTIVAS FUTURAS

O Brasil possui importantes registros de paleoentomofaunas distribuídos por seu território: a de citar alguns depósitos como o Grupo Itararé (Carbonífero da Bacia do Paraná); as formações Taciba e Irati (ambas do Permiano da Bacia do Paraná); a Formação Santa Maria (Triássico da Bacia do Paraná); a Formação Crato (Cretáceo da Bacia do Araripe); a Formação Fonseca (Eoceno-Oligoceno da Bacia de Fonseca) e a Formação Tremembé (Oligoceno da Bacia de Taubaté). Essas unidades contêm associações fossilíferas que são verdadeiras janelas paleobiológicas para compreensão do funcionamento de ecossistemas estabelecidos no passado. Porém, a maioria destes depósitos detém paleoentomofaunas ainda sub-amostradas e pouco estudadas, tanto em termos de número de espécies descritas quanto de signicância paleoecológica e tafonômica. Esta tese buscou caracterizar, em macro e micro escala, os diferentes processos e mecanismos relacionados à preservação excepcional das paleoentomofaunas da Formação Fonseca (Eoceno – Olígoceno de Minas Gerais) e Formação Crato (Cretáceo Inferior do Ceará). Esta pesquisa investigou os aspectos tafonômicos e composição química dos organismos, além de jogar luz sobre o papel da paleoecologia e do paleoambiente no padrão de preservação destas paleoentomofaunas.

A Formação Fonseca reconhecida por seus registros de angiospermas, retem uma entomofauna não igualmente conhecida. Aqui, os insetos fósseis tipicamente escuros preservados numa matriz silte arenítica tiveram seus aspectos fóssil-diagenéticos avaliados. Os resultados das análises revelaram que os insetos escuros representam material carbonáceo preservado via polimerização de biomacromoléculas que resultaram em componentes alifáticos de cadeia longa. Neste caso, o material carbonáceo representa restos da quitina original do próprio inseto, que sofreu transformações químicas durante o processo de diagênese. Mais campanhas de coleta ainda são necessárias para obtenção de uma melhor amostragem para verificação do potencial desta unidade como um depósito do tipo *Lagerstätte* ou não. Além disso, o intervalo de ocorrência da Formação Fonseca ainda é pouco compreendido no Brasil, pois o limite Eoceno-Olígoceno foi um período de aquecimento que precedeu um resfriamento global, a partir do Oligoceno médio. Portanto, futuros estudos sobre a significância paleoecológica da paleoentomofauna da Formação Fonseca são mais do que justificáveis.

Ao contrário da paleoentomofauna de Fonseca, a paleoentomofauna da Formação Crato é mundialmente conhecida, sendo justamente a beleza, abundância e diversidade de

seus insetos fósseis uma das razões dessa unidade ser reconhecida como sítio paleontológico de classe mundial, um depósito do tipo *Konservat Lagerstätte*. Os processos geoquímicos que permitiram a excepcional preservação da paleoentomofauna da Formação Crato ainda permanecem incompletamente compreendidos. No entanto, modelos tafonômicos propostos nos últimos anos melhoraram muito nossa compreensão dos processos fóssil-diagenéticos ocorridos na Formação Crato. A presente tese apresenta muitos achados que ajudaram a construir a atual percepção dos processos tafonômicos reconhecidos na paleoentomofauna da Formação Crato. Aqui, comparando os dois tipos de preservação, os insetos fósseis querogenizados e piritizados, mostrando que os insetos piritizados possuem maior qualidade de preservação do que os insetos querogenizados. Esse resultado é surpreendente, pois, de maneira geral, se espera que os fósseis piritizados possuam menor qualidade de preservação devido ao maior tempo de exposição à decomposição microbiana. Em resumo, o viés tafonômico em direção à maior qualidade dos insetos piritizados é provavelmente a rápida mineralização dos insetos durante a eodiagênese. Posteriormente, os insetos tridimensionais piritizados são oxidados *in situ* e transformados em réplicas de óxidos-hidróxidos de ferro (Hematita e goethita) mais estáveis. Essa oxidação lenta é fundamental para manutenção de atributos paleontológicos (e.g. morfologia) em uma atmosfera oxidante. Nesta tese documentamos três tipos de alterações pós-diagenéticas que afetam a qualidade de preservação dos insetos fósseis da Formação Crato, como insetos com sobreposições de óxido de ferro, insetos associados à formação de dendritos e insetos preservados apenas como uma impressão.

Mais pesquisas ainda são necessárias para estabelecer os controles deposicionais e bioestratinômicos da preservação excepcional da paleoentomofauna da Formação Crato. Embora as reconstruções ambientais tenham sido discutidas, apenas descrições simplistas dos processos que transportaram as carcaças para o local de deposição foram apresentadas (i.e. Menon e Martill, 2007). Falta uma compreensão abrangente do paleoambiente e da ecologia da(s) área(s) de captação da Formação Crato. Uma vez que isso tenha sido alcançado, a verificação do modelo usando experimentação actuo-palaeontológica pode começar.

REFERÊNCIAS

AGASSIZ, Louis. On the fossil fishes found by Mr. Gardner in the Province of Ceará, in the north of Brazil. **The Edinburgh new philosophical journal**, v. 30, p. 82-84, 1841.

AGASSIZ, Louis. Sur quelques poissons fossiles du Brésil. Compte Rendus de l´Academie des Sciences. Paris, v. 18, p. 1007-1015, 1844.

AGUIAR, Robério Boto *et al*. **Pesquisa hidrogeológica em bacias sedimentares no Nordeste brasileiro**. *In*: XVI Congresso Brasileiro de águas subterrâneas e XVII Encontro Nacional de perfuradores de poços. Águas Subterrâneas [S. l.], 2010. Disponível em:https://aguassubterraneas.abas.org/asubterraneas/article/view/22894. Acesso em: 7 set. 2023.

ALEMÃO, Francisco Freire; ALEMÃO, Manoel Freire. **Trabalhos da Commissão scientifica de exploração**. Rio de Janeiro: Typographia Universal de Laemmert, 1862.

ALMEIDA, Fernando Flávio Marques. The System of Continental Rifts Bordering The Santos Basin, Brazil. **Anais da Academia Brasileira de Ciências**, v. 48, p. 15-26, 1976.

ANTONIETTO, Lucas Silveira *et al*. Taxonomy, ontogeny and paleoecology of two species of Harbinia Tsao, 1959 (Crustacea, Ostracoda) from the Santana Formation, lower Cretaceous, Northeastern Brazil. **Journal of Paleontology**, v. 86, p. 659-668, 2012.

ARAI, Mitsuru. Paleogeografia do Atlântico Sul no Aptiano: um novo modelo a partir de dados micropaleontológicos recentes South Atlantic Aptian paleogeography: a new model based on recent Brazilian micropaleontological data. **Boletim de Geociências da Petrobras**, v. 17, p. 331-351, 2009.

ARAI, Mitsuru. **Sucessão das associações de dinoflagelados (Protista, Pyrrhophyta) ao longo das colunas estratigráficas do Cretáceo das bacias da Margem Continental Brasileira: uma análise sob o ponto de vista paleoceanográfico e paleobiogeográfico**. Porto Alegre, Universidade Federal do Rio Grande do Sul. Tese de doutorado, p. 241, 2007.

ARAI, Mitsuru; ASSINE, Mário Luís. Chronostratigraphic constraints and paleoenvironmental interpretation of the Romualdo Formation (Santana Group, Araripe Basin, Northeastern Brazil) based on palynology. **Cretaceous Research**, v. 116, 104610, 2020.

ARAI, Mitsuru. Aptian/Albian (Early Cretaceous) paleogeography of the South Atlantic: a paleontological perspective. **Brazilian Journal of Geology**, v. 44, n. 2, p. 339-350, 2014.

ARAI, Mitsuru; COIMBRA, João Carlos; SILVA-TELLES, Augusto. **Síntese bioestratigráfica da Bacia do Araripe (Nordeste do Brasil)**. *In:* 2º SIMPÓSIO SOBRE A BACIA DO ARARIPE E BACIAS INTERIORES DO NORDESTE, Crato, **Anais** [...]. Atas do simpósio, 2001.

ARAI, Mitsuru; Coimbra João Carlos. **Análise paleoecológica do registro das primeiras ingressões marinhas na Formação Santana (Cretáceo Inferior da Chapada do Araripe)**. *In*: 1° Simpósio sobre a Bacia do Araripe e Bacias Interiores do Nordeste, Crato, **Anais** [...] Atas do simpósio, 1990.

ASSINE, Mário Luís. Araripe basin. **Boletim de Geociências da Petrobras**, v. 15, p. 371-

389, 2007.

ASSINE, Mário Luís. Paleocorrentes e Paleogeografia na Bacia do Araripe, Nordeste do Brasil. **Revista Brasileira de Geociências**, v. 24, n. 4, p. 223-232, 1994.

ASSINE, Mário Luís. Análise estratigráfica da Bacia do Araripe, Nordeste do Brasil. **Revista Brasileira de Geociências**, v. 22, n. 3, p. 289-300, 1992.

ASSINE, Mário Luís *et al.* Comments on paper by M. Arai" Aptian/Albian (Early Cretaceous) paleogeography of the South Atlantic: a paleontological perspective". **Brazilian Journal of Geology**, v. 46, p. 3-7, 2016.

ASSINE, Mário Luís *et al.* Sequências deposicionais do Andar Alagoas (Aptiano superior) da Bacia do Araripe, Nordeste do Brasil. **Boletim de Geociências da Petrobras**, v. 22, p. 3-28, 2014.

BARLING, Nathan; HEADS Sam; MARTILL David. Behavioural impacts on the taphonomy of dragonflies and damselflies (Odonata) from the Lower Cretaceous Crato Formation, Brazil. **Palaeoentomology**, v. 4, p. 141-155. 2021.

BARLING, Nathan; MARTILL, David; HEADS Sam. A geochemical model for the preservation of insects in the Crato Formation (Lower Cretaceous) of Brazil. **Cretaceous Research**, v. 116, 104608, 2020.

BARLING, Nathan *et al*. High fidelity preservation of fossil insects from the Crato Formation (Lower Cretaceous) of Brazil. **Cretaceous Research**, v. 52, p. 605-622, 2015.

BENTO, Ricardo R. França. **Propriedades vibracionais de cristais de seselina por espectroscopias Raman e FT-Raman**. Fortaleza, Universidade Federal do Ceará. Dissertação de Mestrado, 2003.

BERRY, Edward W. A study of the Tertiary floras of the Atlantic and Gulf Coastal Plain. **Proceedings of the American Philosophical Society**, v. 50, p. 301-315, 1911.

BERRY, Edward W. The affinities and distribution of the Lower Eocene flora of southeastern North America. **Proceedings of the American Philosophical Society**, v. 53, p. 129-250, 1914.

BERRY, Edward W. Tertiary plants from Brazil. **Proceedings of the American Philosofical Society**, v. 75, n. 7, p. 565-590, 1935.

BERTHOU, Pierre-Yves. **Critical analysis of the main publications about the stratigraphical framework of the Paleozoic and Mesozoic sedimentary deposits in the Araripe Basin (northeastern Brazil)**. *In*: Boletim do 3° Simpósio sobre o Cretácico do Brasil. UNESP – Campus de Rio Claro/SP, p.123-126, 1994.

BEURLEN, Karl. A geologia da Chapada do Araripe. **Anais da Academia Brasileira de Ciências**, v. 34, n. 3, p. 365-370, 1962.

BEURLEN, Karl. As espécies dos Cassiopinae, nova subfamília dos Turritellidae, no Cretáceo do Brasil. **Arquivos de Geologia**, n. 5, p. 1-44, 1964.

BEURLEN, Karl. Novos equinóides no Cretáceo do Nordeste do Brasil. **Anais da Academia Brasileira de Ciências**, v. 38, n. 3/4, p. 455-464, 1966.

BEURLEN, Karl. As condições ecológicas e faciológicas da Fonnação Santana na Chapada do Araripe (Nordeste do Brasil). **Anais da Academia Brasileira de Ciências**, v. 43, p. 411-415, 1971.

BEZERRA, Francisco Irineudo *et al*. Effects of chemical weathering on the exceptional preservation of mineralized insects from the Crato Formation, Cretaceous of Brazil: implications for late diagenesis of fine-grained Lagerstätten deposits. **Geological Magazine**, v. 160, n. 5, p. 911-926, 2023.

BEZERRA, Francisco Irineudo *et al*. Taphonomic Analysis of the paleoentomofauna assemblage from the Cenozoic of the Fonseca Basin, Southeastern Brazil. **PALAIOS**, v. 36, n. 5, p. 182-192, 2021a.

BEZERRA, Francisco Irineudo; SOLÓRZANO-KRAEMER, Mónica M.; MENDES, Márcio. Distinct preservational pathways of insects from the Crato Formation, Lower Cretaceous of the Araripe Basin, Brazil. **Cretaceous Research**, v. 118, 104631, 2021b.

BEZERRA, Francisco Irineudo *et al*. Chemical and mineral comparison of fossil insect cuticles from Crato *Konservat Lagerstätte*, Lower Cretaceous of Brazil. **Journal of Iberian Geology**, v. 46, p. 61-76, 2020.

BEZERRA, Francisco Irineudo; MENDES, Márcio; DESOUZA, Og. New record of Mastotermitidae from Fonseca Basin, Eocene-Oligocene boundary of southeastern Brazil. **Biologia**, v. 75, p. 1881-1890, 2020.

BIRKS, John. 2008. Paleoecology. *In*: JORGENSEN, Sven Erik; FATH, Brian D. (Org.). **Encyclopedia of Ecology**. Amsterdam: Elsevier, 2008. p. 2623-2634.

BITTENCOURT, Jonathas S. *et al*. O registro fóssil das coberturas sedimentares do Cráton do São Francisco em Minas Gerais. **Geonomos**, v. 23, n.2, p. 39-62, 2015.

BÖGER, Horst. Bildung und gebrauch von begriffen in der paläoökologie. **Lethaia**, v. 3, p. 243-269, 1970.

BRAUN, Oscar Paulo G. Estratigrafia dos sedimentos da parte interior da região nordeste do Brasil (bacias de Tucano-Jatobá, Mirandiba-Araripe). *In*: Divisão de Geologia e Mineralogia Rio de Janeiro, 75 p., 1966.

BRITO NEVES *et al*. 2000. Tectonic history of the Borborema Province. *In*: CORDANI *et al*. (Org..). **Tectonic evolution of South America**. 31st International Geological Congress, Rio de Janeiro, p. 151-182, 2000.

CAMPOS, Diogenes de A.; KELLNER, Alexander. A short note on the first occurence of Tapejaridae in the Crato Member (Aptian), Santana Formation, Araripe basin, Northeast Brazil. **Anais da Academia Brasileira de Ciências**, v. 69, n. 1, p. 83-87, 1997.

CASTRO, David L.; CASTELO BRANCO Raimundo M. Caracterização da arquitetura interna das bacias rifte do Vale do Cariri (NE do Brasil), com base em modelagem gravimétrica 3-D. **Revista Brasileira de Geofísica**, v. 17, p. 129-144, 1999.

CASTRO, Éverton C.; FERREIRA, Juliano. **Aspectos estratigráficos, sedimentares e estruturais dos sedimentos cenozóicos da borda leste do Quadrilátero Ferrífero entre Santa Rita Durão e Fonseca, Minas Gerais**. Ouro Preto, Universidade Federal de Ouro Preto. Trabalho de Graduação, 49 p., 1997.

CLARK, James; KIETZKE, Kenneth K., Paleoecology of the Lower Nodular Zone, Brule Formation, in the Big Badlands of South Dakota. *In*: CLARK, James; BEERBOWER, James R.; KIETZKE, Kenneth K. (Org.) **Oligocene Sedimentation, Stratigraphy, Paleoecology and Paleoclimatology in the Big Badlands of South Dakota.** Chicago: Fieldiana Geology Memoirs. 5, 1967, p. 111-137.

CARVALHO, Ismar de Souza *et al*. The Araripe Geopark (NE Brazil): Discovering the Earth's Past as a Driver of Economic and Social Transformation. **Geoheritag**, v. 13, n. 3, 1-16, 2021.

CARVALHO, Marise Sardenberg S.; SANTOS, Maria Eugênia C.M. Histórico das Pesquisas Paleontológicas na Bacia do Araripe, Nordeste do Brasil. **Anuário do Instituto de Geociências**, v. 28, n. 1, p. 15-34, 2005.

CATTO, Bruno *et al*. The microbial nature of laminated limestones: lessons from the Upper Aptian, Araripe Basin, Brazil. **Sedimentary Geology**, v. 341, p. 304-315, 2016.

CHANG, Hung Kiang; KOWSMANN, Renato O.; FIGUEIREDO, Antônio Manuel F. New concepts on the development of east Brazilian marginal basins. **Episodes**, p. 11, n. 3: p. 194-202, 1988.

CLEMENTS, Frederic E. **Plant Succession: An Analysis of the Development of Vegetation**. Washington, DC: Carnegie Institute of Washington, 1916.

CLEMENTS, Frederic E. Scope and significance of paleo-ecology. **Bulletin of the Geological Society of America**, v. 29, p. 369-374, 1918.

CLOUD, Preston E. Paleoecology: retrospect and prospect. **Journal of Paleontology**, 33, 926-962, 1959.

COIMBRA, João C.; ARAI, Mitsuru; Carreño, Ana L. Biostratigraphy of Lower Cretaceous microfossils from the Araripe basin, Northeastern Brazil. **Geobios**, v. 35, p. 687-698, 2002.

COIMBRA, João Carlos; FREIRE, Tiago Menezes. Age of the Post-Rift Sequence I from the Araripe Basin, Lower Cretaceous, NE Brazil: Implications for spatio-temporal correlation. **Revista Brasileira de Paleontologia**, v. 24, n. 1, p. 37-46, 2021.

CORDANI, Umberto G. *et al*. 1984. Estudo preliminar de integração do Pré-cambriano com os eventos tectônicos das bacias sedimentares brasileiras. Rio de Janeiro: CENPES, p. 63, 1984.

CURVELLO, Walter da Silva. Sobre um vegetal do linhito de Fonseca, Minas Gerais. **Anais da Academia Brasileira Ciências**, v. 27, n. 3, p. 293-296, 1955.

da SILVA, Maria Augusta M. Evaporitos do Cretáceo da Bacia do Araripe: ambientes de deposição e história diagenética. **Boletim de Geosciências da Petrobras**, v. 2, p. 53-63, 1988.

da SILVA, Maria Augusta M. Lower Cretaceous sedimentary sequences in the Araripe Basin. **Revista Brasileira de Geosciências**, v. 16, p. 311-319, 1986.

DELGADO *et al*. Paleometry: a brand new area in Brazilian science. **Materials Research**, v. 17, p. 1434-1441, 2014.

DIAS, Jaime J.; CARVALHO, Ismar S. The role of microbial mats in the exquisite preservation of Aptian insect fossils from the Crato Lagerstätte, Brazil. **Cretaceous Research**, v. 130, 105068, 2022.

DIAS, Jaime J.; CARVALHO, Ismar S. Remarkable fossil crickets preservation from Crato Formation (Aptian, Araripe Basin), a *Lagerstätten* from Brazil. **Journal of South American Earth Sciences**, v. 98, 102443, 2020.

DO CARMO, Dermeval A. *et al*. On the validity of two Lower Cretaceous non-Marine Ostracode Genera: biostratigraphic and paleogeographic implications. **Journal of Paleontology**, v. 82, n. 4, p. 790-799, 2008.

DO CARMO, Dermeval A. *et al*. **Paleoecologia dos Ostracodes não-Marinhos do Cretáceo inferior da Bacia Potiguar, RN, Brasil**. *In*: 5° SIMPÓSIO SOBRE O CRETÁCEO DO BRASIL, **Anais** [...]. v. 19, p. 385-388, 1999.

DO CARMO, Dermeval A. **Taxonomia, paleoecologia e distribuição estratigráfica dos Ostracodes da Formação Alagamar (Cretáceo Inferior), Bacia Potiguar, Brasil**. Porto Alegre, Universidade Federal do Rio Grande do Sul. Tese de Doutorado, p. 156, 1998.

DOLIANITI, Elias. Contribuição à flora pliocênica de Fonseca, Minas Gerais I, *Chondodendron brasiliense* n. sp. **Anais da Academia Brasileira de Ciências**, v. 21, n. 3, p. 239-244, 1949.

DORR, John Van N. **Physiographic, stratigraphic and structural development of the Quadrilatero Ferrifero, Minas Gerais, Brazil**. United States Government printing office, Washington. Geol. Survey Prof. Paper. 110 p., 1969.

DUARTE, Lélia. Restos de Araucariáceas da Formação Santana-membro Crato (Aptiano) NE do Brasil. **Anais da Academia Brasileira de Ciências**, v. 65, n. 4, 358-362, 1993.

DUARTE, Lélia. Sobre uma flor de Bombacaceae, da bacia terciária de Fonseca, MG. **Anais da Academia Brasileira de Ciências**, v. 46, n. 3-4, p. 407-411, 1974.

DUARTE, Lélia; MELLO-FILHA, M.D.C. Flórula cenozóica de Gandarela, MG I. **Anais da Academia Brasileira de Ciências**, v. 52, n. 1, p. 77-91, 1980.

DUNLOP, Jason A.; MARTILL, David M. The first whip spider (Arachnida: Amblypygi) and three new whip scorpions (Arachnida: Thelyphonida) from the Lower Cretaceous Crato Formation of Brazil. **Transactions of the Royal Society of Edinburgh: Earth Sciences**, v. 92, p. 325-334, 2002.

EFREMOV, Ivan. A. Taphonomy; new branch of paleontology. **Pan-American Geologist**, v. 74, p. 81-93, 1940.

EMERSON, Alfred E. A review of the Mastotermitidae (Isoptera), including a new fossil genus from Brazil. **American Museum Novitates**, v. 2236, p.1-46, 1965.

FANTON, Jean Carlo Mari; RICARDI-BRANCO, Fresia; MENDES, Márcio. As paleofloras de Fonseca e Gandarela revisadas e insetos associados: Paleógeno do Sudeste brasileiro, *In*: CARVALHO, Ismar de Souza *et al*. (Org.). **Paleontologia**: Cenários de vida – Paleoclima. Rio de Janeiro: Interciência, 2014. p. 241-253.

FANTON, Jean Carlo Mari. **Reconstruindo as florestas tropicais úmidas do Eoceno–**

Oligoceno do sudeste do Brasil (Bacias de Fonseca e Gandarela, Minas Gerais) com folhas de Fabaceae, Myrtaceae e outras angiospermas: origens da Mata Atlântica. Campinas, Universidade de Campinas. Tese de doutorado, p. 285, 2013.

FANTON, Jean Carlo Mari; RICARDI-BRANCO, Fresia; SILVA, Adalene Moreira. *Terminalia Palaeopubescens* sp. nov. (Combretaceae) da Formação Fonseca (Eoceno/Oligoceno) de Minas Gerais, Brasil: Morfologia foliar, fungos epifilicos associados e paleoclima. **Ameghiniana**, v. 49, n. 3, p. 273-288, 2012.

FIELDING, Sarah; MARTILL, David M.; NAISH, Darren. Solnhofen-style soft-tissue preservation in a new species of turtle from the Crato Formation (Early Cretaceous, Aptian) of North-East Brazil. **Palaentology**, v. 48, n. 6, p. 1301-1310, 2005.

FORBES, Edward. Report on the Mollusca and Radiata of the Aegean Sea, and on their distribution, considered as bearing on Geology. **Report of the British Association for the Advancement of Science**, v. 13, p. 139-207, 1843.

FRANZEN, Lutz; WINDBERGS, Maike. Applications of Raman spectroscopy in skin research — From skin physiology and diagnosis up to risk assessment and dermal drug delivery. **Advanced Drug Delivery Reviews**, v. 89, p. 91-104, 2015.

FREY, Eberhard; MARTILL, David M. A new pterosaur from the Crato Formation (Lower Cretaceous-Aptian) of Brazil. **Neues Jahrbuch für Geologie und Paläontologie. Abhandlungen. Stuttgart**, v. 194, n. 2/3, p. 379-412, 1994.

GALLO DA SILVA, Valéria; AZEVEDO, Sérgio Alex K. Um Dipnoi da Formação Brejo Santo, Eocretáceo da Chapada do Araripe, Ceará, Brasil. **Acta Geológica Leopoldensia**, v. 43, n. 19, p. 43-58, 1996.

GOLDSTEIN, Joseph I.; NEWBURY, Dale E. **Scanning Electron Microscopy and X-Ray Microanalysis- A text for biologist, Materials Scientist and Geologists**. New York: Plenum Press, 1992.

GOLDSTEIN, Joseph I. *et al*. Electron Beam—Specimen Interactions: Interaction Volume. *In*: GOLDSTEIN, Joseph I. *et al*. (Org.). **Scanning Electron Microscopy and X-Ray Microanalysis**. New York: Springer, 2018, p. 1-14.

GORCEIX, Henri. Bacias terciárias d'água doce nos arredores de Ouro Preto - Gandarela e Fonseca - Minas Gerais – Brasil. *In*: Dos Anais da Escola de Minas de Ouro Preto, 3, 1884, Ouro Preto. **Anais** [...]. Minas Gerais: Republicada na Revista da Escola de Minas, 1884. p. 9–16.

GREENWOOD, David R.; e WING, Scott L. Eocene continental climates and latitudinal temperature gradients. **Geology**, v. 23, p. 1044-1048, 1995.

GRIMALDI, David. Insects from the Santana Formation, Lower Cretaceous of Brazil. **Bulletin of the American Museum of Natural History**, v. 195, p. 69-183, 1990.

GRIMALDI, David; MAISEY, John G. 1990. Introduction. *In*: Grimaldi, David A. (Org.). **Insects from the Santana Formation, Lower Cretaceous, of Brazil**. New York: American Museum of Natural History, 1990, p. 5-14.

HASUI, Yociteru. 1998. Evolução Morfotectônica do Sudeste do Brasil, *In*: Congresso Brasileiro de Geologia, 40, Belo Horizonte. **Anais** [...]. Belo Horizonte: SBG/Núcleo Minas

Gerais, 1998, p. 11-31.

HASUI, Yociteru; PONÇANO, Waldir Lopes. 1978. Organização Estrutural e Evolução da Bacia de Taubaté, *In*: Congresso Brasileiro de Geologia, 30, Recife. **Anais** [...]. Recife: SBG, 1978, p. 368-381.

HECKER, R. F.. **Introduction to Paleoecology**. New York: American Elsevier, 1965.

HEDGPETH, Joel W. **Treatise on Marine Ecology and Paleoecology: Vol. One, Ecology**. Baltimore: Geological Society of America, 1957.

HEIMHOFER, Ulrich *et al*. 2010. Deciphering the depositional environment of the laminated Crato fossil beds (Early Cretaceous, Araripe Basin, North-eastern Brazil). **Sedimentology**, v. 57, n. 2, p. 677-694, 2010.

HOLLICK, Arthur; BERRY, Edward W. A late tertiary flora from Bahia, Brazil. **The Johns Hopkins University Studies in Geology**, v. 5, p. 1-137, 1924.

INIESTO, Miguel *et al*. Soft tissue histology of insect larvae decayed in laboratory experiments using microbial mats: taphonomic comparison with Cretaceous fossil insects from the exceptionally preserved biota of Araripe, Brazil. **Palaeogeography, Palaeoclimatology, Palaeoecology**, v. 564, 110156, 2021.

JAPSEN, Peter. *et al*. Episodic burial and exhumation in NE Brazil after opening of the South Atlantic. **Geological Society of America Bulletin**, v. 124, n. 5/6; p. 800–816, 2012.

KELLNER, Alexander; CAMPOS, Diogenes A. The function of the cranial crest and jaws of a unique Pterosaur from the Early Cretaceous of Brazil. **Science**, v. 297, p. 389-392, 2002.

KELLNER, Alexander. Fossilized theropod soft tissue. **Nature**, v. 379, p. 32, 1996.

LAWRENCE, David R. Taphonomy. *In*: **Paleontology**. Encyclopedia of Earth Science. Berlin, Heidelberg: Springer, 1979, p. 793-799.

LAWRENCE, David R. Taphonomy and information losses in fossil communities. **Geological Society of America Bulletin**, v. 79, p. 1315-1330, 1968.

LEAL, Maria Eduarda C.; BRITO, Paulo M. The Ichthyodectiform Cladocyclus gardneri (Actinopteri:Teleostei) from the Crato and Santana Formations, Lower Cretaceous of Araripe basin, North-Eastern Brazil. **Annales de Paleontologie**, v. 90, p. 103-113, 2004.

LIMA, Murilo R.; SALARD-CHEBOLDAEFF, Marguerite. Palynologie des bassins de Gandarela et Fonseca (Eocene de L'Etat de Minas Gerais, Brésil). **Boletim IG-USP**, v.12, p. 33-54, 1981.

LIPSKI, Marlos. **Tectonismo cenozóico no Quadrilátero Ferrífero, Minas Gerais**. Ouro Preto, Universidade Federal de Ouro Preto. Dissertação Mestrado, p. 171, 2002.

LONG, Derek A. **Raman Spectroscopy**. New York: McGraw-Hill, 1977

LÚCIO, Thales; Souza Neto, João A.; Selby, David. Late Barremian/Early Aptian Re-Os age of the Ipubi Formation black shales: stratigraphic and paleoenvironmental implications for Araripe Basin, northeastern Brazil. **Journal of South American Earth Sciences**, v. 102, 102699, 2020.

MAISEY, John G. 1991. **Santana Fossils. An illustrated Atlas**. TFH Publications Inc, 459 p.

MAIZATTO, José R.; PORFIRO, Virgínia. **Estudos preliminares sobre os aspectos bioestratigráficos e paleolimnológicos da bacia terciária do Fonseca –Quadrilátero Ferrífero –Minas Gerais**. *In*: VII Simpósio de Geologia do Centro-Oeste e X Simpósio de Geologia de Minas Gerais. Brasília, **Anais** [...]. Boletim de resumos, 1999.

MAIZATTO, José R.; CASTRO, Paulo T.; PORFIRO, Virgínia. **Aspectos bioestratigráficos, paleolimnológicos e sedimentológicos da bacia terciária de Fonseca –Quadrilátero Ferrífero – Minas Gerais – Brasil, com base na análise palinológica e sedimentar**. *In*: II Encontro Anual da Sociedade Brasileira de Paleontologia. Mafra, **Anais** [...]. Encontro Anual da Sociedade Brasileira de Paleontologia, 2000.

MAIZATTO, José R. **Análise bioestratigráfica, paleoecológica e sedimentológica das bacias terciárias do Gandarela e Fonseca, Quadrilátero Ferrífero, Minas Gerais, com base nos aspectos palinológicos e sedimentares**. Ouro Preto, Universidade Federal de Ouro Preto. Tese de Doutorado, p. 216, 2001.

MAIZATTO, José R., REGALI, Marília S.; CASTRO, Paulo T. **Análise biocronoestratigráfica e paleoclimática das bacias paleógenas e neógenas do Gandarela e Fonseca- Quadrilátero Ferrífero- Minas Gerais, Brasil**. *In*: 12° Simpósio Brasileiro de Paleobotânica e Palinologia. Florianópolis, **Anais** [...]. Boletim de Resumos, 2008.

MALDANIS, Lara *et al*. Heart fossilization is possible and informs the evolution of cardiac outflow tract in vertebrates. **eLife**, v. 5, e14698, 2016.

MALISKA, Ana Maria. **Microscopia Eletrônica de Varredura e Microanálise**. Departamento de Engenharia Mecânica. Universidade Federal de Santa Catarina, 2011.

MANNHEIMER, Walter A. **Microscopia dos Materiais - Uma introdução**. Rio de Janeiro: E-papers Serviços Editoriais, 2002.

MARQUES, Fernando O., *et al*. The Araripe Basin in NE Brazil: an intracontinental graben inverted to a high-standing horst. **Tectonophysics**, v. 630, p. 251-264, 2014.

MARTILL, David M.; LOVERIDGE Robert F.; HEIMHOFER, Ulrich. Dolomite pipes in the Crato Formation fossil lagerstätte (Lower Cretaceous, Aptian), of northeastern Brazil. **Cretaceous Research,** v. 29, n. 1, p. 78-86, 2008.

MARTILL, David M.; HEIMHOFER, Ulrich. Stratigraphy of the Crato Formation. *In*: MARTILL, David M., BECHLY, Günter; LOVERIDGE, Robert F. (Org.). **The Crato Fossil Beds of Brazil – Window into an Ancient World**. Cambridge: Cambridge University Press, 2007. p. 25-43.

MARTILL, David M., BECHLY, Günter; LOVERIDGE, Robert F. **The Crato Fossil Beds of Brazil: window into an ancient world**. Cambridge: Cambridge University Press, 2007a

MARTILL, David M.; LOVERIDGE, Robert F.; HEIMHOFER, Ulrich. Halite pseudomorphs in the Crato Formation (Early Cretaceous, Late AptianeEarly Albian), Araripe Basin, northeast Brazil: further evidence for hypersalinity. **Cretaceous Research**, v. 28, p. 613-620, 2007b.

MARTILL, David M. *et al*. A new crested maniraptoran dinosaur from the Santana Formatiom (Lower Cretaceous) of Brazil. **Journal of Geology Society**, v. 153, n. 5-8, 1996.

MARTILL, David M.; WILBY. Philip. Stratigraphy. *In*: MARTILL, David M. (Org.), **Fossils of the Santana and Crato Formations, Brazil**. London: The Palaeontological Association, 1993. p. 20-50.

MARTINS-NETO, Rafael G. Um novo gênero e duas espécies de Tridactylidae (Insecta, Orthopteridea) na Formação Santana (Cretáceo Inferior do Nordeste do Brasil). **Anais da Academia Brasileira de Ciências**, v. 62, n. 1, p. 51-59, 1990.

MATOS, Renato Marcos D. The Northest Brasilian rift system. **Tectonics**, v. 11, n. 4, p. 776-791, 1992.

MATOS, Renato Marcos D. History of the Northeast Brazilian rift system: kinematic implications for the break-up between Brazil and West Africa. *In*: CAMERON, Nick R. et al. (Org.). **The Oil and Gas Habitats of the South Atlantic**. London: Geological Society of London, 1999, p. 55-73.

MAXWELL, Charles H. Geology and ore deposits of the Alegria District, Minas Gerais, Brazil. U.S. Geological Survey Professional Paper 341-J. p. 1–72, 1972.

MELO, Robbyson Mendes *et al*. New marine data and age accuracy of the Romualdo Formation, Araripe Basin, Brazil. **Scientific Reports**, v. 10, 15779, 2020.

MENDES, Márcio; OLIVEIRA, Francisco Irineudo Bezerra de; LIMAVERDE, Saulo. Um novo gênero e duas novas espécies de Pergidae (Insecta, Hymenoptera) na Formação Fonseca (Bacia de Fonseca, Paleógeno) Minas Gerais, Brasil. **Revista de Geologia**, v. 28, n. 2, p. 27-36, 2015.

MENDES, Márcio; PINTO, Irajá D. The first findings of Blattodea (Insecta, Blattidae) from the Fonseca formation, Oligocene period, Minas Gerais, in the south east of Brazil. **Acta Geologica Leopoldensia**, v. 24, p. 283-290, 2001.

MENON, Federica, MARTILL, David M. 2007. Taphonomy and preservation of Crato Formation arthropods. *In*: MARTILL, David M., BECHLY, Günter; LOVERIDGE, Robert F. (Org.). **The Crato Fossil Beds of Brazil – Window into an Ancient World**. Cambridge: Cambridge University Press, Cambridge, 2007, p. 79-96.

MIRANDA, Tiago S. de. **Caracterização geológica e geomecânica dos depósitos carbonáticos e evaporíticos da Bacia do Araripe, NE Brasil**. Recife, Universidade Federal de Pernambuco. Ttese de doutorado, p. 229, 2015.

MIRANDA, Tiago S. de *et al*. Quantifying aperture, spacing and fracture intensity in a carbonate reservoir analogue: Crato Formation, NE Brazil. **Marine and Petroleum Geology**, v. 97, p. 556-567, 2018.

MIRANDA, Tiago S. de *et al*. Araripe Basin, NE Brazil: A rift basin implanted over a previous pull-apart system? *In*: IV ATLANTIC CONJUGATE MARGIN CONFERENCE. **Anais** [...]. p. 80-82, 2014.

MIRANDA, Tiago S. de *et al*. Aplicação da técnica de scanline à modelagem geológica/geomecânica de sistemas de fraturamento nos depósitos carbonáticos e evaporíticos da Bacia do Araripe, NE do Brasil. **Boletim de Geociências da Petrobras**, v. 20, n. 1/2, p. 305-326, 2012.

MOHR, Barbara A.; RYDIN, Catarina. Trifurcatia £abellata n. gen. n. sp., a putative

monocotyledon angiosperm from the Lower Cretaceous Crato Formation (Brazil). Mitteilungen aus dem Museum Naturkunde. Berlim. **Geowissenschaftlische Reihe**, v. 5, p. 335-344, 2002.

MOHR, Barbara A.; EKLUND, Helena. Araripia florifera, a magnoliid angiosperm from the Lower Cretaceous Crato Formation (Brazil). **Review Palaeobotany and Palynology**, v. 126, p. 279-292, 2003.

NEUMANN, Virginio Henrique M. **Estratigrafía, Sedimentología, Geoquímica y Diagénesis de los Sistemas Lacustres Aptienses-Albienses de la Cuenca de Araripe (Noreste de Brasil)**. Barcelona, Universidade de Barcelona. Tese de Doutorado, p. 244, 1999.

NEUMANN, Virginio Henrique M.; CABRERA, Luis. **Una nueva propuesta estratigráfica para la tectonosecuencia post-rifte de la cuenca de Araripe, nordeste de Brasil**. *In*: V SIMPÓSIO SOBRE O CRETÁCEO DO BRASIL E 1º SIMPÓSIO SOBRE EL CRETÁCICO DE AMÉRICA DEL SUR, Serra Negra. **Anais** [...]. Atas do Simpósio, 1999.

NEUMANN, Virginio Henrique M.; BORREGO, Angeles G.; CABRERA, Luis; DINO, Rodolfo. Organic matter composition and distribution through the Aptian-Albian lacustrine sequences of the Araripe Basin, northeastern Brazil. **International Journal of Coal Geology**, v. 54, p. 21-40, 2003.

NEVES, Sérgio Pacheco *et al*. Timing of crust formation, deposition of supracrustal sequences, and Transamazonian and Brasiliano metamorphism in eastern Borborema Province (NE Brazil): implications for western Gondwana assembly. **Precambrian Research**, v. 149, p. 197-216, 2006.

NOBRE, Geraldo da Silva. **João da Silva Feijó: um naturalista no Ceará**. Fortaleza: Gráfica Editorial Cearense Ltda, 1978.

OLIVEIRA, Alvimir Alves *et al*. **Projeto Chapada do Araripe**. Relatório Final. 5. Recife: DNPM/CPRM, 1979.

OLIVEIRA-E-SILVA, Maria Isabel M. **Flórula da Bacia de Fonseca, Minas Gerais, Brasil**. Rio de Janeiro, Universidade Federal do Rio de Janeiro. Dissertação mestrado, p. 175, 1982.

OSÉS, Gabriel L. *et al*. Deciphering pyritization-kerogenization gradient for fish soft-tissue preservation. **Scientific Reports**, v. 7, p. 1-15, 2017.

OSÉS, Gabriel L. *et al*. Deciphering the preservation of fossil insects: a case study from the Crato Member, Early Cretaceous of Brazil. **PeerJ**, v. 4, e2756, 2016.

RAND, Helmo M. 1983. **Levantamento gravimetrico e magnetometrico da Bacia Araripe**. Relatório interno da PETROBRAS. Caderno de dados e mapas, p. 11, 1983.

RAND, Helmo M.; Manso, Valdir do Amaral 1984. **Levantamento gravimétrico e magnetométrico da Bacia do Araripe**. *In*: CONGRESSO BRASILEIRO DE GEOLOGIA. Anais [...]. Atas do simpósio, 1984.

RASNITSYN, Alexandr P.; MARTÍNEZ-DELCLÓS, Xavier. New Cretaceous Scoliidae (Vespida-Hymenoptera) From the Lower Cretaceous of Spain and Brazil. **Cretaceous Research**, v. 20, p. 767-772, 1999.

REGALI, Marília *et al*. Palinologia dos sedimentos mesocenozóicos do Brasil (I). **Boletim**

Técnico da Petrobrás, v. 17, n. 3, p. 177-191, 1974a.

REGALI, Marília *et al*. Palinologia dos sedimentos mesocenozóicos do Brasil (II). **Boletim Técnico da Petrobrás**, v. 17, n. 4, p. 263-301, 1974b.

RICARDI-BRANCO, Fresia *et al*. Plant accumulations along the Itanhaém River basin, southern coast of São Paulo state, Brazil. **Palaios**, v. 24, p. 416-424, 2009.

RICCOMINI, Claudio. **O rifte continental do sudeste do Brasil**. São Paulo, Universidade de São Paulo. Tese Doutorado, p. 256, 1989.

RICHETTI, Pâmela *et al*. Analogue modelling of basin inversion: the role of oblique kinematics and implications for the Araripe Basin (Brazil). **Solid Earth**, v. 13, p. 1859-1905, 2022.

ROMERO, Edgardo Juan. South American paleofloras. *In*: Goldblatt, Peter (Org.). **Biological relationships between Africa and South America.** New Haven: Yale University press, p. 62-85, 1993.

SAAD, Antônio *et al*. Neoctectônica da Plataforma Brasileira. *In*: SOUZA, Célia Regina G. (Org.). **Quaternário do Brasil**. Ribeirão Preto, Holos Editora, p. 211-230, 2005.

SALA, Oswaldo. O laboratório de espectroscopia vibracional Hans Stammreich na Universidade de São Paulo. **Química Nova**, v. 7, n. 4, p. 320-326, 1984.

SALISBURY, Steven W. *et al*. A new mesosuchian crocodilian from the Lower Cretaceous Crato Formation of north-eastern Brazil. **Palaeontographica, Abteilung A**, v. 270, p. 3-47, 2003.

SANT'ANNA, Lucy G. **Mineralogia das argilas e evolução geológica da Bacia de Fonseca, Minas Gerais**. São Paulo, Universidade de São Paulo. Dissertação de Mestrado, p. 151, 1994.

SANT'ANNA, Lucy G. *et al*. Cenozoic Tectonics of the Fonseca Basin Region, Eastern Quadrilatero Ferrifero, MG, Brazil. **Journal of South American Earth Sience**, v. 10, n. 2-3, p. 275-284, 1997.

SANT'ANNA, Lucy G.; SCHORSCHER, Hans D. Estratigrafia e mineralogia dos depósitos cenozoicos da região da Bacia de Fonseca, Estado de Minas Gerais. **Anais da Academia Brasileira de Ciências**, v. 69, n. 2, p. 211-226, 1997.

SANTOS, Edilton J. *et al*. The Cariris Velhos tectonic event in Northeast Brazil. **Journal of South American Earth Sciences**. v. 21, p. 61-76, 2010.

SARTENAER, Paul. La plongée en scaphandre autonome au service de la Taphonomie, **Bulletin de l'Institut océanographique de Monaco**, v. 1159, p. 14, 1959.

SCHER, Howie D.; MARTIN, Ellen E. Timing and climatic consequences of the opening of Drake passage. **Science**, v. 312, p. 428–430, 2006.

SCHORSCHER, Hans D. **Arcubouço petrográfico e evolução crustal de terrenos pré-cambrianos do sudeste de Minas Gerais: Quadrilátero Ferrífero, Espinhaço Meridional e Dominios Granitos-Gnáissicos adjacentes**. São Paulo, Universidade de São Paulo. Tese de Doutorado, p. 274, 1992.

SCHORSCHER, Hans D. Contribuicão a estratigrafia proterozoica do Quadrilátero Ferrífero. **Anais da Academia Brasileira de Ciências,** v. 52, n. l, p. 195, 1980.

SILVA, Agnelo Leite. **Estratigrafia Física e Deformação do Sistema Lacustre Carbonático Aptiano-Albiano da Bacia do Araripe em Afloramento Selecionados**. Recife, Universidade Federal de Pernambuco. Dissertação de Mestrado, p. 118, 2003.

SILVEIRA, Luís Fernando *et al*. Multiscale characterization of an extensive stromatolites field: a new correlation horizon for the Crato Member, Araripe Basin, Brazil. **Journal of Sedimentary Research,** 2023. doi.org/10.2110/jsr.2022.090

SMALL, Horatio L. Geologia e suprimento de água subterrânea no Ceará e parte do Piauí. **Publicação Inspetoria Obras Contra Secas**, v. 25, p. 1-80, 1913.

SOMMER, Friedrich W. *et al*. Contribuição à paleoflora de Fonseca, Minas Gerais. **Anais da Academia Brasileira de Ciências**, v. 39, n. 3-4, p. 537-538, 1967.

SOUZA, Débora Menezes de *et al*. Ostracodes do Aptiano–Albiano da Bacia do Araripe: Implicações paleoambientais e bioestratigráficas. **Estudos Geológicos**, v.27, n. 1, 2017.

SOUZA, Juliana Ferreira G. *et al*. Provenance analysis of the Araripe intracontinental basin, northeast Brazil – Routes for proto-Atlantic marine incursions in northwest Gondwana. **Sedimentary Geology**, v. 440, 106243, 2022.

STINER, Mary C. Taphonomy. *In*: Pearsall, Deborah M. (Org). **Encyclopedia of archaeology**. New York: Academic press, p. 2113-2119, 2008.

PAIVA, Donald, *et al*. **Introdução à espectroscopia**. Boston: Editora Cengage Learning, 2015.

PINHEIRO, Felipe L. *et al*. Fossilized bacteria in a Cretaceous pterosaur headcrest. **Lethaia**, v. 45, p. 495-499, 2012.

PONTE, Francisco C.; PONTE-FILHO, Francisco C. Caracterização estratigráfica da Formação Abaiara, Cretáceo inferior da Bacia do Araripe. *In*: II Simpósio sobre Bacias Cretáceas Brasileiras. **Anais** [...]. p. 61-64, 1992.

PONTE, Francisco C.; APPI, Ciro J. **Proposta de revisão da coluna litoestratigráfica da Bacia do Araripe**. *In*: Congresso Brasileiro de Geologia, Natal. **Anais** [...]. Atos do Simpósio, 1990.

PONTE, Francisco C.; PONTE-FILHO, Francisco C. Estrutura geológica e evolução tectônica da Bacia do Araripe. Brasil. Departamento Nacional da Produção Mineral, 4° e 10° Distritos Regionais. Delegacias do MME em Pernambuco e Ceará, p. 68, 1996.

PORTO, Sérgio P.; WOOD, D.L. Ruby optical maser as a Raman source. **Journal of the Optical Society of America**, v. 1, p. 139-141, 1962.

UNIVERSITY OF IOWA. Central Microscopy Research Facility. Iowa City: CMRF, 2022. Disponível em: https://cmrf.research.uiowa.edu/scanning-electron-microscopy. Acesso em: 24 abril 2022, 16:52.

VARAJÃO, César Augusto C. *et al*. Estudo da evolução da paisagem do Quadrilátero Ferrífero (Minas Gerais, Brasil) por meio da mensuração das taxas de erosão (^{10}Be) e da

pedogênese. **Revista Brasileira de Ciências do Solo**, v. 33, p. 1409–1425, 2009.

VAREJÃO, Filipe Giovanini *et al*. Marine or freshwater? Accessing the paleoenvironmental parameters of the Caldas Bed, a key marker bed in the Crato Formation (Araripe Basin, NE Brazil). Brazilian Journal of Geology, v. 51, n. 1, e2020009, 2021a.

VAREJÃO, Filipe Giovanini *et al*. Mixed siliciclastic–carbonate sedimentation in an evolving epicontinental sea: Aptian record of marginal marine settings in the interior basins of north-eastern Brazil. **Sedimentology**, v. 68, n. 5, p. 2125-2164, 2021b.

XAVIER, Paulo Henrique. **Preparação de Cerâmicas Nanoestruturadas de Ca3Co4O9 para Aplicação em Dispositivos Termoelétricos**. Alfenas, Universidade Federal de Alfenas. Dissertação de Mestrado, p. 61, 2018.

WALL, David *et al*. The environmental and climatic distribution of dinoflagellate cysts in modern marine sediments from regions in the North and South Atlantic Oceans and adjacent seas. **Marine Micropaleontology**, v. 2, p. 121-200, 1977.

WARREN, Lucas V. *et al*. Stromatolites from the Aptian Crato Formation, a hypersaline lake system in the Araripe Basin, northeastern Brazil. **Facies**, v. 63, n. 3, p. 1-19, 2017.

WILF, Peter *et al*. High plant diversity in Eocene South America: Evidence from Patagonia. **Science**, v. 300, p. 122-125, 2003.

ZACHOS, James C. *et al*. An early cenozoic perspective on greenhouse warming and carboncycle dynamics. **Nature**, v. 451, p. 279-283, 2008.

ZALÁN, Pedro V. Evolução fanerozoica das bacias sedimentares brasileiras. *In*: MANTESSO-NETO, Virginio *et al*. (Org.). **Geologia do Continente Sul-Americano**: evolução da obra de Fernando Flávio Marques de Almeida. São Paulo: Beca editora, p. 595-612, 2004.

ZIEGLER, Alfred M. *et al*. Tracing the tropics across land and sea: Permian to present. **Lethaia**, v. 36, p. 227-254, 2003.

APÊNDICE A - MATERIAL SUPLEMENTAR 2

PCA Analisis

PC	Eigenvalue	% variance
1	135.954	24.719
2	857.951	15.599
3	746.834	13.579
4	666.667	12.121
5	608.434	11.062
6	555.556	10.101
7	34.407	62.558
8	222.222	40.404
9	138.732	25.224

PCA Loadings

	PC 1	PC 2	PC 3	PC 4	PC 5	PC 6	PC 7	PC 8	PC 9
Aaeschnidae	-0.04869	0.3243	0.070782	2,69E-12	0.041144	-6,52E-13	0.069293	7,64E-13	0.029629
Achilidae	0.26989	0.017107	0.014413	-2,43E-13	0.013802	8,87E-13	0.034309	-6,00E-14	0.017022
Ampulicidae	-0.02850	-0.03319	-0.052567	-1,51E-13	-0.21822	0.31623	0.17851	-3,98E-12	0.053323
Anisolabidae	-0.02015	-0.01578	-0.019166	3,55E-13	-0.029877	4,02E-12	-0.30983	0.5	0.26621
Araripegomphidae	-0.04869	0.3243	0.070782	8,26E-13	0.041144	7,23E-13	0.069293	-6,03E-13	0.029629
Araripelocustidae	-0.03307	-0.05245	-0.12542	0.28868	0.19815	-1,82E-12	0.11703	1,46E-12	0.042101
Babinskaiidae	-0.03307	-0.05245	-0.12542	-0.28868	0.19815	2,99E-12	0.11703	5,50E-13	0.042101
Baissogryllidae	-0.03307	-0.05245	-0.12542	0.28868	0.19815	1,29E-12	0.11703	1,21E-12	0.042101
Baissopteridae	-0.01836	-0.01343	-0.015817	-2,35E-13	-0.023202	-9,44E-13	-0.16206	-2,10E-12	-0.80471
Belostomatidae	0.26989	0.017107	0.014413	7,46E-13	0.013802	9,34E-14	0.034309	8,25E-14	0.017022
Berothidae	-0.03307	-0.05245	-0.12542	-0.28868	0.19815	3,80E-12	0.11703	1,25E-12	0.042101
Blattullidae	-0.02850	-0.03319	-0.052567	-8,24E-12	-0.21822	-0.31623	0.17851	3,53E-12	0.053323
Buprestidae	-0.03939	-0.12515	0.32494	3,37E-12	0.06814	2,87E-12	0.087046	3,47E-13	0.034781
Cercopionidae	0.26989	0.017107	0.014413	4,86E-13	0.013802	1,39E-12	0.034309	-2,07E-13	0.017022
Chrysomelidae	-0.03939	-0.12515	0.32494	3,37E-12	0.06814	2,87E-12	0.087046	3,47E-13	0.034781
Cicadellidae	0.26989	0.017107	0.014413	3,90E-13	0.013802	1,28E-12	0.034309	1,37E-13	0.017022
Cicindelidae	-0.03939	-0.12515	0.32494	3,37E-12	0.06814	2,87E-12	0.087046	3,47E-13	0.034781
Cretapetaluridae	-0.04869	0.3243	0.070782	1,88E-12	0.041144	-4,36E-13	0.069293	4,67E-13	0.029629
Ectobiidae	-0.02850	-0.033179	-0.052567	-7,04E-12	-0.21822	-0.31623	0.17851	2,91E-12	0.053323
Elcanidae	-0.033075	-0.052452	-0.12542	0.28868	0.19815	1,96E-13	0.11703	1,40E-12	0.042101
Gelastocoridae	0.26989	0.017107	0.014413	3.42E-17	0.013802	1,39E-12	0.034309	1,68E-13	0.017022
Gomphaeschnidae	-0.048691	0.3243	0.070782	1,88E-12	0.041144	-4,36E-13	0.069293	4,67E-13	0.029629
Gomphidae	-0.048691	0.3243	0.070782	1,90E-12	0.041144	-7,08E-13	0.069293	4,54E-13	0.029629
Gryllidae	-0.033075	-0.052452	-0.12542	0.28868	0.19815	3,15E-13	0.11703	4,90E-13	0.042101
Hemiphlebiidae	-0.048691	0.3243	0.070782	1,88E-12	0.041144	-3,02E-13	0.069293	5,17E-13	0.029629
Hexagenitidae	-0.02015	-0.015782	-0.019166	-1,61E-12	-0.029877	-3,22E-12	-0.30983	-0.5	0.26621
Labiduridae	-0.02015	-0.015782	-0.019166	-9,33E-13	-0.029877	4,57E-12	-0.30983	0.5	0.26621
Lalacidae	0.26989	0.017107	0.014413	3.42E-17	0.013802	1,39E-12	0.034309	1,68E-13	0.017022
Locustopseidae	-0.033075	-0.052452	-0.12542	0.28868	0.19815	1,96E-13	0.11703	1,40E-12	0.042101
Lymexylidae	-0.039392	-0.12515	0.32494	3,37E-12	0.06814	2,87E-12	0.087046	3,47E-13	0.034781
Meiatermes-grade	-0.028504	-0.033179	-0.052567	-7,04E-12	-0.21822	-0.31623	0.17851	2,91E-12	0.053323
Mesoblattinidae	-0.028504	-0.033179	-0.052567	-7,04E-12	-0.21822	-0.31623	0.17851	2,91E-12	0.053323
Mesochrysopidae	-0.033075	-0.052452	-0.12542	-0.28868	0.19815	3,67E-12	0.11703	1,37E-12	0.042101
Mesoserphidae	-0.028504	-0.033179	-0.052567	-1,87E-12	-0.21822	0.31623	0.17851	-4,37E-14	0.053323
Mesoveliidae	0.26989	0.017107	0.014413	4,86E-13	0.013802	1,39E-12	0.034309	-2,07E-13	0.017022
Myerslopiidae	0.26989	0.017107	0.014413	3,90E-13	0.013802	1,28E-12	0.034309	1,37E-13	0.017022

Myrmeleontidae	-0.033075	-0.052452	-0.12542	-0.28868	0.19815	4,20E-12	0.11703	1,73E-12	0.042101
Naucoridae	0.26989	0.017107	0.014413	3,90E-13	0.013802	1,28E-12	0.034309	1,37E-13	0.017022
Nepidae	0.26989	0.017107	0.014413	4,86E-13	0.013802	1,39E-12	0.034309	-2,07E-13	0.017022
Nitidulidae	-0.039392	-0.12515	0.32494	3,37E-12	0.06814	2,87E-12	0.087046	3,47E-13	0.034781
Nothomacromiidae	-0.048691	0.3243	0.070782	1,88E-12	0.041144	-3,02E-13	0.069293	5,17E-13	0.029629
Notonectidae	0.26989	0.017107	0.014413	4,86E-13	0.013802	1,39E-12	0.034309	-2,07E-13	0.017022
Nymphidae	-0.033075	-0.052452	-0.12542	-0.28868	0.19815	4,20E-12	0.11703	1,73E-12	0.042101
Oligoneuriidae	-0.02015	-0.015782	-0.019166	-1,61E-12	-0.029877	-3,22E-12	-0.30983	-0.5	0.26621
Osmilidae	-0.033075	-0.052452	-0.12542	-0.28868	0.19815	3,80E-12	0.11703	1,25E-12	0.042101
Palaeontinidae	0.26989	0.017107	0.014413	3,90E-13	0.013802	1,28E-12	0.034309	1,37E-13	0.017022
Proterogomphidae	-0.048691	0.3243	0.070782	1,88E-12	0.041144	-4,36E-13	0.069293	4,67E-13	0.029629
Sapygidae	-0.028504	-0.033179	-0.052567	-1,87E-12	-0.21822	0.31623	0.17851	-4,37E-14	0.053323
Scarabaeidae	-0.039392	-0.12515	0.32494	3,37E-12	0.06814	2,87E-12	0.087046	3,47E-13	0.034781
Scoliidae	-0.028504	-0.033179	-0.052567	-2,00E-12	-0.21822	0.31623	0.17851	-5,08E-13	0.053323
Sepulcidae	-0.028504	-0.033179	-0.052567	-1,87E-12	-0.21822	0.31623	0.17851	-4,37E-14	0.053323
Staphylinidae	-0.039392	-0.12515	0.32494	3,37E-12	0.06814	2,87E-12	0.087046	3,47E-13	0.034781
Tettigarctidae	0.26989	0.017107	0.014413	3,90E-13	0.013802	1,28E-12	0.034309	1,37E-13	0.017022
Tridactylidae	-0.033075	-0.052452	-0.12542	0.28868	0.19815	3,15E-13	0.11703	4,90E-13	0.042101
Umenocoleidae	-0.028504	-0.033179	-0.052567	-7,04E-12	-0.21822	-0.31623	0.17851	2,91E-12	0.053323

APÊNDICE B - MATERIAL SUPLEMENTAR 3

Insect body area measurement

Body area of Crato insects	Untransformed values		log transformed values		Shapiro Wilk test	
	Mean	SD	Mean	SD	W	p < W
Both macrofacies	83.365	104.597	1.715	0.4023	0.9737	10^{-4}
pale-yellow limestones	83.434	109.518	1.701	0.412	0.9666	10^{-4}
dark-gray limestones	83.176	89.984	1.753	0.3731	0.9807	0.0705

Body area of Crato Heteroptera	Untransformed values		log transformed values		Shapiro Wilk test	
	Mean	SD	Mean	SD	W	p < W
Both macrofacies	296.032	157.416	2.357	0.396	0.7928	10^{-4}
pale-yellow limestones	286.369	161.011	2.328	0.42	0.7998	10^{-4}
dark-gray limestones	346.76	134.588	2.509	0.18	0.9729	0.9194

Body area of Crato Ensifera	Untransformed values		log transformed values		Shapiro Wilk test	
	Mean	SD	Mean	SD	W	p < W
Both macrofacies	52.8421	49.4867	1.6454	0.2351	0.948	0.0001
pale-yellow limestones	53.1514	54.9627	1.6438	0.235	0.92	10^{-4}
dark-gray limestones	52.0858	33.1111	1.6493	0.2385	0.9525	0.1252

Body area of Crato Caelifera	Untransformed values		log transformed values		Shapiro Wilk test	
	Mean	SD	Mean	SD	W	p < W
Both macrofacies	50.75	15.572	1.6872	0.136	0.9262	0.4818
pale-yellow limestones	48.75	22.998	1.6536	0.196	0.9176	0.5238
dark-gray limestones	52.75	5.1234	1.7207	0.041	0.9154	0.5116

Body area of Crato Auchenorrhyncha	Untransformed values		log transformed values		Shapiro Wilk test	
	Mean	SD	Mean	SD	W	p < W
Both macrofacies	27.9787	15.3572	1.3552	0.3267	0.8847	0.0123
pale-yellow limestones	27.6706	14.3344	1.3637	0.3049	0.8791	0.046
dark-gray limestones	28.5562	18.1572	1.3391	0.3862	0.8982	0.2786

Body area of Crato Neuroptera	Untransformed values		log transformed values		Shapiro Wilk test	
	Mean	SD	Mean	SD	W	p < W
Both macrofacies	74.1287	51.93	1.768	0.3125	0.9552	0.374
pale-yellow limestones	65.9136	52.4791	1.6813	0.3739	0.9385	0.503
dark-gray limestones	81.6591	52.5398	1.8473	0.2319	0.7939	0.008

Body area of Crato Odonata	Untransformed values		log transformed values		Shapiro Wilk test	
	Mean	SD	Mean	Mean	W	p < W
pale-yellow limestones	68.5227	39.9523	1.7493	0.2933	0.8911	0.006

Body area of Crato Dermaptera	Untransformed values		log transformed values		Shapiro Wilk test	
	Mean	SD	Mean	Mean	W	p < W
pale-yellow limestones	100.993	55.857	1.9457	0.2951	0.9213	0.457

Body area of Crato Coleoptera	Untransformed values		log transformed values		Shapiro Wilk test	
	Mean	SD	Mean	Mean	SD	Mean
Both macrofacies	44.1557	42.8883	1.4997	0.3587	0.9833	0.9347
pale-yellow limestones	29.96	17.3916	1.3958	0.2898	0.9531	0.4755
dark-gray limestones	76.0962	64.4252	1.7333	0.4069	0.9753	0.9358

Body area of Crato Blattodea	Untransformed values		log transformed values		Shapiro Wilk test	
	Mean	SD	Mean	Mean	SD	Mean
Both macrofacies	67.7461	46.1408	1.7413	0.2834	0.9857	0.2135
pale-yellow limestones	60.9494	37.9117	1.7105	0.2583	0.9847	0.4219
Dark-gray limestones	81.6712	57.6338	1.8045	0.3232	0.9714	0.3817

Body area of Crato Ephemeroptera	Untransformed values		log transformed values		Shapiro Wilk test	
	Mean	SD	Mean	SD	W	p < W

pale-yellow limestones	35.9611	19.5876	1.5007	0.2306	0.9557	0.5209

Body area of Crato Hymenoptera	**Untransformed values**		**log transformed values**		**Shapiro Wilk test**	
	Mean	**SD**	**Mean**	**Mean**	**SD**	**Mean**
Both macrofacies	14.7008	13.9148	1.0303	0.341	0.9198	0.2842
pale-yellow limestones	15.557	15.2237	1.0328	0.3769	0.9096	0.2784
Dark-gray limestones	10.42	0.028	1.0178	0.0011	1	1

APÊNDICE C - MATERIAL SUPLEMENTAR 4

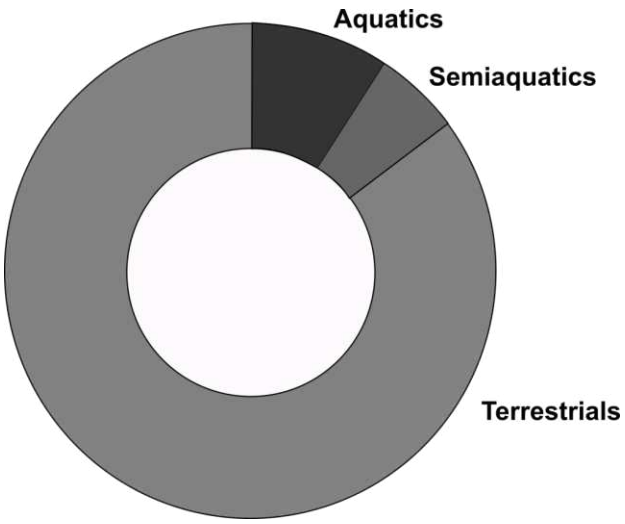

Trophic structure of the Crato paleoentomofauna based on different habitat types identified in our sample.

APÊNDICE D - MATERIAL SUPLEMENTAR 5

Comparison of composition - preserved paleoentomofauna in main non-amber deposits from the Early Cretaceous

	Herbivore	Predator	Xylophage	Omniverous	parasitoids	Pollinators	Aquatic	Semiaquatic	Terrestrial
Crato	127	151	15	26	1	66	18	64	306
Zaza	127	55	27	21	12	144	16	13	383
Dzun-Bain	42	21	35	27	7	52	1	9	175
Gurvan-Eren	27	15	2	8	13	21	10	9	73
Yixian	153	122	59	59	54	171	16	108	459
Laiyang	37	12	4	14	13	54	4	10	131
Turga	32	3	2	4	11	13	2	3	64
Khasurty	30	8	6	8	0	43	5	6	104
Lulworth	24	21	4	41	2	22	1	12	108
Weald Clay	36	39	11	0	4	22	1	25	95

Comparison of Crato paleoentomofauna and the main amber deposits from the Early Cretaceous

	Herbivore	Predator	Xylophage	Omniverous	parasitoids	Pollinators	Aquatic	Semiaquatic	Terrestrial
Crato	127	151	15	26	1	66	18	64	306
Lebanese	46	21	3	16	19	106	0	2	216
Escucha	11	12	1	7	35	35	1	3	110
Charentese	11	13	0	13	2	9	0	3	45
Jordanian	4	3	0	4	1	11	0	2	22

Infraorders distribution of main paleoentomofauna during Early Cretaceous

	Holometabola	Paleoptera	Paraneoptera	Polyneoptera
Crato	167	73	55	114
Zaza	313	11	64	48
Dzun-Bain	142	3	20	27
Gurvan-Eren	70	4	26	10
Yixian	492	51	76	53
Laiyang	119	2	33	12
Turga	55	1	18	0
Khasurty	96	4	12	6
Lulworth	100	12	20	50
Weald Clay	67	29	12	23
Lebanese	155	1	55	17
Escucha	94	0	14	8
Charentese	29	1	11	12
Jordanian	17	1	5	3

PCA analysis - taxonomic literature composition of main paleoentomofauna preserved in non-amber deposits

PC	Eigenvalue	% variance
1	7	74.683
2	1	11.265
3	0.555178	6
4	0.38506	4
5	0.235689	3
6	0.0632666	0.70296
7	0.022581	0.2509
8	0.00285254	0.031695
9	5,02E+00	0.0005583

loadings	PC 1	PC 2	PC 3	PC 4	PC 5	PC 6	PC 7	PC 8	PC 9

Herbivore	0.36772	-0.25408	-0.13862	-0.052498	-0.09032	-0.26255	0.5457	-0.57966	0.25955
Predator	0.32521	-0.39492	0.45871	-0.002479	-0.22948	-0.037344	0.16695	0.60568	0.2812
Xylophage	0.33127	0.36546	-0.12868	-0.16987	-0.60057	0.58508	-0.01581	-0.060609	0.066071
Omniverous	0.29464	0.37454	0.39387	-0.5553	0.54136	0.066528	0.04574	-0.055944	0.081815
parasitoids	0.28952	0.49244	-0.090507	0.66359	0.24275	-0.018981	0.33811	0.22632	0.017625
Pollinators	0.35358	0.07794	-0.48875	-0.11212	0.042714	-0.3865	-0.51968	0.17795	0.40562
Aquatic	0.30961	-0.49936	-0.19636	0.17866	0.44316	0.59205	-0.17542	-0.072661	-0.036554
Semiaquatic	0.34399	0.019961	0.50886	0.34726	-0.15876	-0.18727	-0.49155	-0.3926	-0.21379
Terrestrial	0.37342	-0.08554	-0.23261	-0.23364	-0.05542	-0.21817	0.12335	0.21917	-0.79412

PCA analysis - taxonomic literature comparasion of Crato paleoentomofauna and main amber deposits

PC	Eigenvalue	% variance
1	7	76.041
2	2	17.044
3	0.516922	6
4	0.105427	1

loadings	PC 1	PC 2	PC 3	PC 4
Herbivore	0.3818	0.022674	-0.036232	-0.092308
Predator	0.37476	-0.12221	0.17549	0.005458
Xylophage	0.37921	-0.043034	0.13297	-0.19262
Omniverous	0.35734	0.051175	-0.29153	0.86105
parasitoids	-0.11289	0.6551	0.69402	0.22823
Pollinators	0.20271	0.61741	-0.48224	-0.36196
Aquatic	0.36441	-0.16858	0.2977	-0.13014
Semiaquatic	0.36555	-0.18728	0.24341	-0.10153
Terrestrial	0.34933	0.32594	-0.055933	-0.050872

APÊNDICE E - MATERIAL SUPLEMENTAR 6

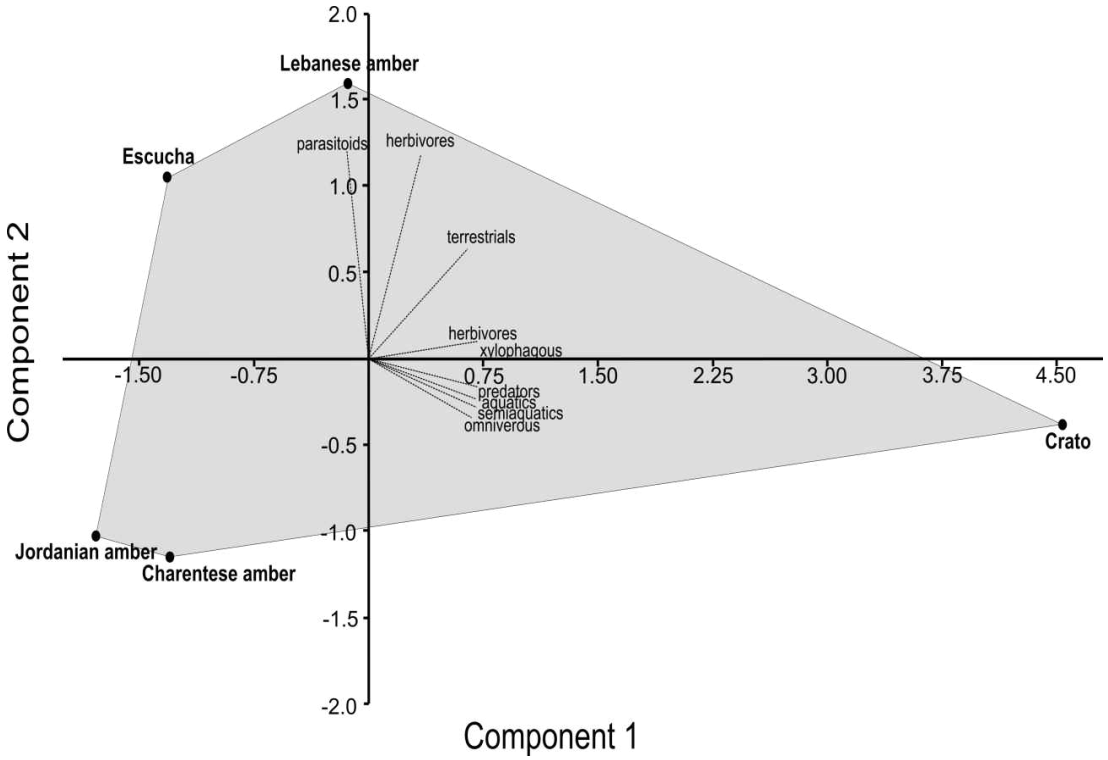

Principal component analysis (PCA) comparing the Crato Paleoentomofauna with the main paleoentomofauna preserved in amber deposits of the Early Cretaceous. Principal component 1 (PC1) explains 76% of the variance in the data, while PC2 explains 17% of the variance.